



**UNIVERSITÀ DI PARMA**

**UNIVERSITA' DEGLI STUDI DI PARMA**

Dottorato di Ricerca in  
“Scienze del Farmaco, delle Biomolecole e dei Prodotti della Salute”

Ciclo XXXIV

# **Novel Adjuvant Strategies to overcome Antimicrobial Resistance**

Coordinatore

Chiar.mo Prof Marco Mor

Tutore:

Chiar.mo Prof Gabriele Costantino

Chiar.mo Prof. Marco Pieroni

Dottoranda: Marialaura Pavone

Anni Accademico 2018/2019 – 2020/2021



## List of Abbreviations

ACN: Acetonitrile

APS: adenosine 5'-phosphosulfate

Boc<sub>2</sub>O: Di-tert-butyl decarbonate

BTA: 1H-benzo[d][1,2,3]triazole (benzotriazole)

CDI: 1,1'-Carbonyldiimidazole

Cpd: compound

DCM: Dichloromethane

DME: dimethoxyethane

DMF: Dimethylformamide

DTNB: 5,5'-Dithiobis(2-nitrobenzoic acid)

*EcSAT*: *E. coli* serine acetyltransferase

EDGs: electron donor groups

eq: equivalent

EtOAc: Ethyl Acetate

EWGs: electron withdrawing groups

FBDD: fragment based drug discovery

HATU: 1-[Bis(dimethylamino)methylene]-1H-1,2,3-triazolo[4,5-b]pyridinium 3-oxid hexafluorophosphate

HTS: High throughput screening

LiOH: lithium hydroxide

MDR: Multidrug Resistant

Mel: iodomethane

MeOH: Methanol

MIC: Minimal inhibitory concentration

MOA: mechanism of action

MTT: 3-(4,5-dimethylthiazol-2-yl)-2,5-diphenyltetrazolium bromide

NaH: sodium hydride

NAS: N-acetylserine

NBD-Cl: 4-Chloro-7-nitrobenzofurazan

NH<sub>4</sub>OH: Ammonium hydroxide

OAS: *O*-Acetylserine

OASS: *O*-Acetylserine sulfhydrylase

on: overnight

PAPS: phosphoadenoside 5'-phosphosulfate  
Pd(PPh<sub>3</sub>)<sub>2</sub>Cl<sub>2</sub>: Bis(triphenylphosphine)palladium(II) dichloride  
Pd(PPh<sub>3</sub>)<sub>4</sub>: Tetrakis(triphenylphosphine)palladium(0)  
PdCl<sub>2</sub>(dppf): 1,1'-Bis(diphenylphosphino)ferrocene dichloropalladium  
PLP: Pyridoxal 5'-phosphate  
RM: reaction mixture  
rt: room temperature  
SAT: Serine acetyltransferase  
SEM-Cl: 2-(Trimethylsilyl)ethoxymethyl chloride  
StOASS: *S. typhimurium* O-Acetylserine sulfhydrylase  
StSAT: *S. typhimurium* serine acetyltransferase  
THF: tetrahydrofuran  
TNB: 5-thio-2-nitrobenzoic acid  
VS: virtual screening  
WHO: World Health Organization



# INDEX

<b>1. Introduction .....</b>	<b>8</b>
<b>1.1. Antimicrobial discovery .....</b>	<b>8</b>
<b>1.2. Antimicrobial resistance and the current antibacterial pipeline. Where are we? .....</b>	<b>9</b>
<b>1.3. Adjuvant strategies .....</b>	<b>12</b>
<b>1.4. Non-essential targets .....</b>	<b>13</b>
<b>1.5. Aim of the project .....</b>	<b>13</b>
<b>2. Cysteine Biosynthesis .....</b>	<b>15</b>
<b>2.1. Sulfur Assimilation Pathway .....</b>	<b>15</b>
<b>2.2. Cysteine Synthase Complex .....</b>	<b>16</b>
<b>3. Serine Acetyltransferase (SAT) Inhibitors.....</b>	<b>20</b>
<b>3.1 Background.....</b>	<b>20</b>
<b>3.2 Exploring the chemical space around N-(5-nitrothiazol-2-yl)-1,2,3-thiadiazole-4-carboxamide.....</b>	<b>22</b>
3.2.1. Aim of the project and first generation of derivatives.....	22
3.2.2. Determination of StSAT Inhibition .....	23
3.2.3. Results and Discussion .....	23
3.2.3.1. First generation of derivatives.....	23
3.2.3.1. Second generation of derivatives .....	26
3.2.4. Chemistry .....	31
3.2.5. Conclusion.....	34
3.2.6. Experimental section .....	35
3.2.6.2. Chemistry.....	35
3.2.6.2. Biology .....	72
<b>3.3. Synthesis of pyrazole derivatives as SAT inhibitors .....</b>	<b>74</b>
3.3.1. Aim of the project .....	74
3.3.2. Results and Discussion .....	75
3.3.3. Chemistry .....	81
3.3.4. Conclusion.....	85

3.3.5. Experimental Section .....	85
<b>4. O-Acetylserine sulfhydrylase (OASS) inhibitors .....</b>	<b>98</b>
<b>4.1. State of the art .....</b>	<b>98</b>
<b>4.2. Exploration of carboxylic acid fragments in the search of novel chemotypes with OASS inhibitory properties .....</b>	<b>100</b>
4.2.1. Background .....	100
4.2.2. Aim of the project .....	102
4.2.3. Results and Discussions.....	103
4.2.4. Biophysical Binding Studies.....	106
4.2.5. Chemistry .....	107
4.2.6. Conclusion.....	109
4.2.7. Experimental section .....	112
<b>4.3. Preliminary chemical investigation on 1H-benzo[d][1,2,3]triazole carboxamide (BTA) as a scaffold for a new series of cysteine biosynthesis inhibitors.....</b>	<b>136</b>
4.3.1. Background .....	136
4.3.2. Preliminary investigation of BTA derivatives mechanism of action (MOA) on the cysteine biosynthesis .....	138
4.3.3. Aim of the project and first round of optimization .....	141
4.3.4. Biological evaluation of the first series of derivatives .....	142
4.3.4.1. Antimicrobial activity.....	142
4.3.4.2. Toxicity.....	143
4.3.4.3. Spectroscopic assay of compounds 165, 170 and 171 .....	144
4.3.5. Second series of optimization .....	147
4.3.6. Chemistry .....	149
4.3.7. Conclusion.....	155
4.3.8. Experimental Section .....	156
4.3.8.2. Chemistry.....	156
4.3.8.2. Biology .....	175
<b>Material and Methods .....</b>	<b>178</b>
<b>References .....</b>	<b>179</b>

# 1. Introduction

## 1.1. Antimicrobial discovery

The discovery of antibiotics has undoubtedly represented one of the most relevant breakthroughs of the 20<sup>th</sup> century. Indeed, infection diseases have been the leading cause of human death for a long time, and the raising of the “*antibiotic era*” has revolutionized modern medicine and the treatment of infections worldwide.<sup>1</sup>

The establishment of the current antibiotic arsenal laid its foundation in the early 1900s, and it is associated to the name of Paul Ehrlich. In 1909, Ehrlich discovered an arsenic derivative active against *Treponema pallidum*, the causative agent of syphilis, starting from the systematic screening of a library containing synthetic compounds inspired by his previous work on dyes for bacteria cells. Subsequently, in 1911, the molecule was commercialized under the name of Salvarsan®. This discovery is associated with Ehrlich’s idea of the “magic bullet”, namely a chemical compound that could be synthesized to exert his activity only on the parasite and not on the host. This concept drove the beginning of the first systemic screening program for drug discovery that brought to the discovery of Salvarsan®.<sup>2,3</sup> Later, Gerhard Domagk, following the Ehrlich work and inspired by dyes used to stain bacterial cells, discovered Prontosil®, a precursor of the active molecule sulfonamide. This antibiotic represents the first sulfa-drugs and also became the first broad-spectrum antimicrobials used in the clinic. However, the event that has changed and most impacted the course of medicine was the serendipitous discovery of Penicillin in 1928 by Alexander Fleming. All these discoveries and the later commercialization of Penicillin in the 1940s led to the so-called “golden age” of antibiotics. The following milestone in antibiotics history was the discovery of streptomycin by Selman Waksman. Moreover, Waksman was also the first to use the word antibiotic to define any small molecule produced by a microbe to destroy other microbes. Waksman developed strategies and techniques to screen soil-dwelling bacteria for the research of metabolites able to inhibit bacterial growth. This system, known as the Waksman platform, led to the discovery of several major antibiotics and antifungals. Indeed, the Waksman platform was also a model to the pharmaceutical industry, allowing the discovery of most of the natural microbial scaffold and more than 20 classes of antimicrobial during the golden age (1940-1970). Most of the antibiotics currently in clinical use were discovered during this period.



However, the rise of antimicrobial resistance (AMR) has affected their effectiveness (Figure 1).<sup>4-6</sup>

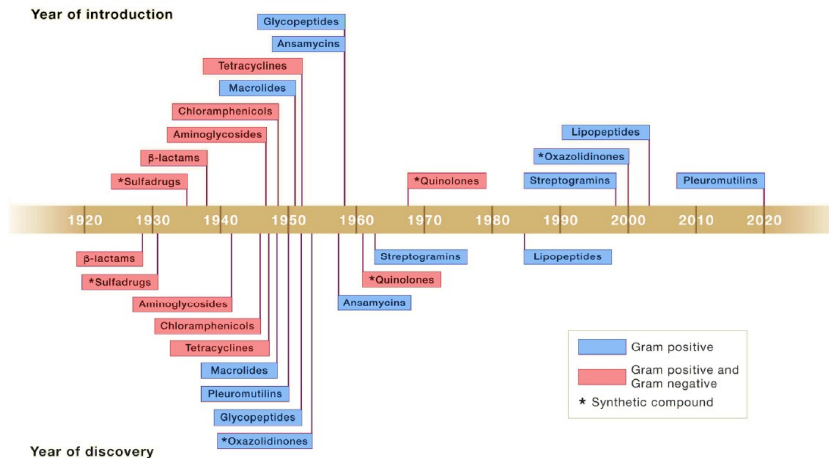


Figure 1. Timeline of antibiotic discovery. Picture adapted from ref.<sup>7</sup>

## 1.2. Antimicrobial resistance and the current antibacterial pipeline. Where are we?

After the 1980s, consistently fewer new antimicrobials were developed and introduced in the market. Thus, the lack of new antibiotics or therapeutic approaches has led to a gap between clinical need and drug innovation.<sup>8</sup> At the same time, resistance to antibiotics increased, mainly due to the overuse and inappropriate use of antibiotics in the medical, animal, and agriculture field. All these factors promote the genetic selection pressure, leading to the emergence of multi-drug-resistant (MDR) bacterial infections in the community. It is interesting to notice that, among all the different classes of medicine developed, antibiotics are the only ones able to fight infections when used systematically, but the regularly used leads to their ineffectiveness.<sup>9</sup>

The first case of resistance came a few years after the approval of penicillin. Indeed, AMR is a natural phenomenon that occurs when bacteria, viruses, fungi, and parasites acquire or develop the ability to survive when exposed to antimicrobials.<sup>10</sup> At this regard, bacteria possess different strategies that can contribute to arise the resistance, and the most important are: (i) inhibiting the intracellular accumulation of the antimicrobials through the upregulation of the efflux pump and downregulation of the

outer membrane, (ii) changing in the drug target, (iii) drug inactivation and (iv) using alternative pathways to bypass the antibiotic action.<sup>11</sup>

While the resistances are increasing, the current antimicrobial pipeline is shrinking, and always fewer treatments are available against the resistant strains. Indeed, one of the last new drugs approved, with a new mechanism of action, was linezolid in 2000, and the last new class of antibiotics discovered was daptomycin in 1986, approved by FDA in 2003.<sup>12</sup> However, it must be noticed that after 2014, a timid improvement in the pipeline was observed (**Figure 2**). In 2019, cefiderocol was introduced on the market, a new siderophore cephalosporin active against carbapenem-resistant Gram-negative bacteria.<sup>13</sup> Whereas, in 2018, lefamulin was the first pleuromutilin antibiotic approved for the treatment of bacterial infections in humans, even though this class of drugs has been known since 1955.<sup>14</sup> According to The Pew Charitable Trusts, 43 new antibiotics are in development as of December 2020. Of them, 13 are currently in Phase 3, 19 had the potential to be active against ESKAPE, and two have new drug applications submitted. Therefore, among the potential drug with an innovative mechanism, none is active against the critical threat pathogens.<sup>15</sup>

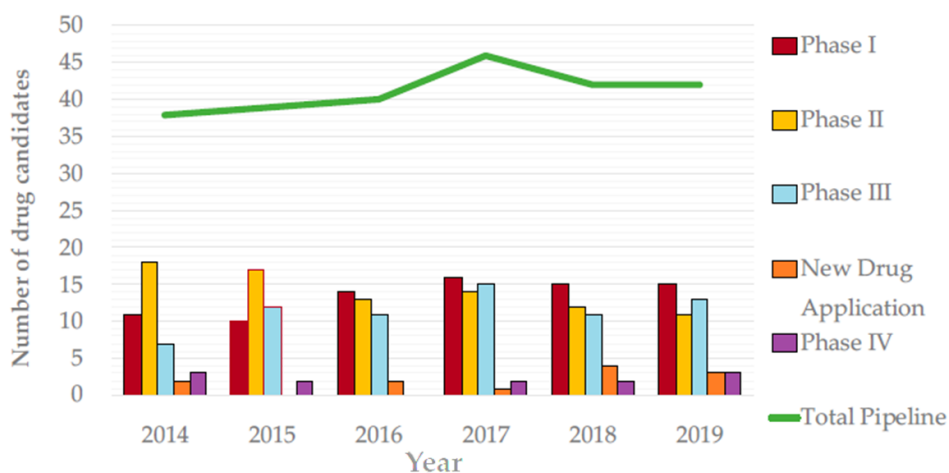


**Figure 2.** Evolution of antibiotics pipeline (in green) and antibiotics currently in development. Picture adapted from ref.<sup>16</sup>

Despite the few molecules developed, a growing number of pathogens have developed resistance against the antibiotic arsenal during the years. Indeed, the World Health Organization (WHO) has included antimicrobial resistance (AMR) in the top 10 major urgent threats to human health.<sup>17</sup> Additionally, in 2017 WHO has also introduced a list of the most critical pathogens, which present a level of resistance considered a real threat to human health,<sup>18</sup> and most of them are Gram-negative bacteria (ESKAPE: *Enterococcus faecium*, *Staphylococcus aureus*, *Klebsiella pneumoniae*, *Acinetobacter baumannii*, *Pseudomonas aeruginosa*, and *Enterobacter* spp.).<sup>19</sup> The current list will be updated in 2022.

It is also important to highlight that the cost of AMR is drastic in both numbers of lives and economically. Every year MDR bacterial strains are responsible for 33000 deaths only in Europe, with an associated cost of approximately € 1.5 billion, due to the expensive healthcare.<sup>20</sup>

Nowadays, it has broadly accepted that AMR is not under control, and it has been estimated that if no urgent action is taken, the number of people who will die due to AMR will increase to 10 million each year by 2050.<sup>21</sup>

Furthermore, bacterial infections caused by MDR bacteria can represent a common complication during viral respiratory tract infections, which could increase the morbidity and mortality of the patients. Indeed, the widespread of SARS-CoV-2 could pose a new concern in regard to the AMR. Patients affected by Covid-19, especially if admitted to the Intensive Care Units (ICU), may present a secondary infection, often caused by MDR bacteria. This scenario has led to extensive use of broad-spectrum antimicrobial drugs since the outbreak of SARS-Cov-2, which could have a deeper impact on the emergence of AMR.<sup>22–26</sup>

The current situation is leading the world in the so-called “resistance era or post-antibiotic era”, where it is difficult to approve new drugs, and it is possible to die due to common infections after minor injuries.<sup>27,28</sup> To avoid this scenario, it is essential to find new strategies to fight the AMR. Besides the different actions promoted by WHO, such as optimizing antibiotic use, improving the global knowledge regarding resistance, and guaranteeing sustainable investment in tackling antimicrobial resistance, the development of new antibiotics is crucial. It is widely accepted that to tackle the MDR bacteria, could be adopted three main strategies:

- (i) the development of new antibiotics to replace the ineffective drugs in the pipeline. Even if this solution may be evident on the one hand, on the other hand, it is always more challenging to reach. Indeed, as already reported,

- most of the current drugs in development did not present a new mechanism of action, and often they are an improved version of the old antibiotics, and many of them already present a mechanism of resistance;
- (ii) screening of alternatives to antibiotics; examples are vaccines, antibodies, probiotics, and bacteriophages. These strategies could serve as preventive or adjunctive therapies in clinics;
  - (iii) or developing new molecules able to extend the lifespan of the antibiotics already approved, such as antibiotics adjuvant.<sup>29</sup>

### 1.3. Adjuvant strategies

The research and the development of new anti-infective drugs with novel mechanisms of action and scaffold seems crucial to avoid the return to the pre-antibiotic era. In this regard, a strategy to preserve and extend the lifetime of the antibiotics arsenal is the use of **antibiotic adjuvants**. To be efficacious, the adjuvant must be administered with the antibiotic. Indeed, antibiotic adjuvants are chemical entities characterized by weak or absent antibiotic activity that, in association with antibiotics, may boost their efficacy against MDR bacterial strains.<sup>30,31</sup> This strategy finds its basis in the concept of combination therapy. Two antibiotics were delivered together in the clinic to obtain an improved therapeutic effect, particularly to reach a synergistic effect. The two antibiotics can hit multiple targets, different steps related to the same biosynthetic pathways, or decrease the efflux.<sup>32</sup> Indeed, it has been widely proved that combination therapy may be a good starting point to kill the bacteria in less time and fight the increasing resistance.<sup>11,33,34</sup>

The combination between antibiotic and adjuvant might show different beneficial effects, such as using a smaller amount of antibiotic, which can lead to fewer toxicity problems, as in the case of colistin, and slow the onset of resistance mechanisms, or reduce the impact on the microbiota.<sup>35</sup> To date, formulations made of antibiotics and adjuvants are already available. The most known is the combination of amoxicillin and clavulanic acid, an inhibitor of  $\beta$ -lactamase, which are enzymes able to break the beta-lactam ring that is a structural feature of the Penicillin as Amoxicillin.<sup>36,37</sup>

Most adjuvants have been developed to be inhibitors of (i) beta-lactamase, (ii) efflux pumps, or (iii) to be outer membrane permeabilizers. Besides these categories, another approach to develop antibiotic potentiators is to block the virulence factors, which are

proteins, genes, and other biomolecules, allowing the microorganisms to cause diseases.<sup>38,39</sup>

## 1.4. Non-essential targets

In the research of new approaches to face the resistance and extend the current antibiotic pipeline, the inhibition of the so-called “non-essential” targets is generating increased interest, especially in the field of basic research. Such targets, mostly responsible for bacterial virulence, are dispensable during the normal bacterial cell cycle (i.e., during *in vitro* growth) but become indispensable during the persistent phase of the infection, when the bacteria have to face harsh conditions inside the host. In such conditions, bacteria require to reprogram their metabolic functions to survive. Hence, interfering with the production of these virulence factors leads to hampering the bacterial capability to establish an efficacious infection and counteract host defense. As such, bacteria become weaker and more susceptible to the antibiotic effect, reducing the possibility of developing resistance since the milder evolutionary pressure.<sup>40,41</sup> Examples of such factors are represented by quorum sensing enhancers, biofilm, and key amino acids such as cysteine, which is a precursor of many detoxifying biomolecules.

## 1.5. Aim of the project

New strategies are needed to tackle down AMR, and especially in academia, different efforts are made to face this challenging situation. The purpose of this thesis work is the research and investigation of new chemical entities able to inhibit novel pharmaceutical targets to develop potential antibiotic adjuvants. To do that, we have focused our attention on unexplored or underexplored “non-essential” targets, in particular metabolic enzymes such as those involved in cysteine biosynthesis. Indeed, strong evidence has proved that suppression or reduction of cysteine biosynthesis lead to a decrease of bacterial fitness and a reduction of virulence.<sup>42–47</sup>

Cysteine is essential to all organisms, and if its biosynthesis can be dispensable during normal growth conditions, it is up-regulated during the persistence phase of the infection in response to starvation and oxidative stress encountered inside the macrophages; therefore, it represents an essential tool for bacteria to respond the action of the host defense.<sup>48</sup> It has been demonstrated that in mutants lacking cysteine

biosynthesis pathway in *Salmonella enterica* serovar Typhimurium, due to the inactivation of cysteine biosynthesis, unpaired oxidative stress can lead to a decrease in antibiotic resistance in both vegetative and swarm cell populations.<sup>49</sup> Therefore, cysteine metabolism is related to different bacteria functions that could play an important role during the infection, like toxin activation, biofilm formation, resistance to oxidative stress, and antibiotics.<sup>50-53</sup> Additionally, bacteria and mammals possess different pathways to synthesize cysteine. In particular, mammals rely on reverse trans-sulfuration from methionine to synthesize cysteine. Therefore, the enzymes involved in the cysteine pathway in bacteria are absent in mammals, making them suitable potential drug targets.

All this evidence justifies our strategy to shed medicinal chemistry efforts on the search for new cysteine biosynthesis inhibitors.

## 2. Cysteine Biosynthesis

Cysteine is the most important sulfur-containing amino acid, especially for bacteria and plants, where it represents the only source of sulfur. Indeed, in microorganisms, cysteine is a precursor of various biomolecules, such as methionine, CoA, biotin, glutathione.<sup>54</sup>

The cysteine pathway is well conserved in different microorganisms, especially in  $\gamma$ -proteobacteria, such as *S. typhimurium* or *H. influenzae*, *M. tuberculosis*, and *E. histolytica*, even though some variations can be observed.<sup>55</sup> The overall process that leads to cysteine biosynthesis involves three main steps: (i) the uptake of sulfate and its reduction to sulfide, (ii) the *O*-acetylation of serine, and (iii) the  $\beta$ -replacement of the *O*-acetylserine acetoxy group to obtain cysteine.<sup>56</sup>

### 2.1. Sulfur Assimilation Pathway

In bacteria, cysteine biosynthesis is carried out by the reductive sulfate assimilation pathway (RSAP), which begins with sulfate transport, present in the environment, inside the cell. Once inside the cell, due to its poor reactivity, the sulfate must be activated by the reduction to bisulfide, a high endergonic process that requires energy. Each mole of cysteine requires one mole of GTP, two moles of ATP, and three moles of NADPH. Firstly, the sulfate is incorporated into ATP, leading to adenosine 5' phosphosulfate (APS) formation. Subsequently, APS kinase phosphorylates APS to 3'-phosphoadenylylsulfate (PAPS). The latter, *via* PAPS reductase action, gives sulfite, which is then reduced to bisulfide. Bisulfide is a toxic compound for the cell, and its concentration must keep between 20 and 160  $\mu\text{M}$ .<sup>57</sup> The bisulfide is incorporated into cysteine *via* the reaction catalyzed by *O*-acetylserine sulfhydrylase (OASS or CysK) and Serine acetyltransferase (SAT or CysE), the last two enzymes involved in the cysteine pathway, which form the cysteine synthase (CS) complex.<sup>58,59</sup>

## 2.2. Cysteine Synthase Complex

In plants and bacteria, serine acetyltransferase (SAT or CysE, encoded by *cysE*) is one of the key enzymes of the cysteine machinery. It catalyzes the rate-limiting step of cysteine biosynthesis,<sup>60</sup> in which an acetyl group from acetyl-CoA (AcCoA) is transferred to the hydroxyl of L-serine to generate a molecule with a better leaving group, *O*-acetylserine (OAS), in a  $\beta$ -elimination reaction. OAS is the direct precursor of cysteine (**Figure 3**), and it spontaneously converts to *N*-acetylserine (NAS), which is the natural inducer of cysteine regulon.<sup>61</sup> From a structure point of view, SAT is a dimer of trimers, characterized by a flexible C-terminal portion, which bound an unusual left-handed parallel  $\beta$ -helix structural domain. This portion is found essential for the function and regulation of SAT. Indeed, In the presence of cysteine, it is responsible for intrasteric inhibition and of binding to OASS-A for the formation of the CS complex.<sup>62</sup> SAT C-terminal sequence binds an active site of OASS-A, and it is responsible for its competitive inhibition.<sup>55,63–66</sup>

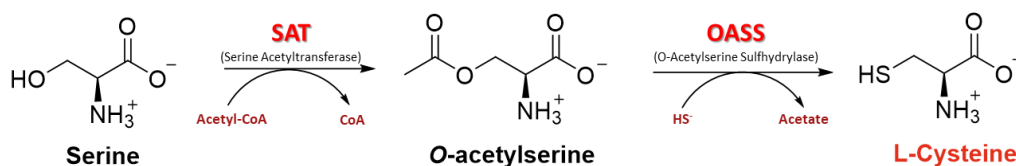


**Figure 3.** The last two steps of cysteine biosynthesis. The formation of the intermediate OAS by SAT and its conversion to L-cysteine by OASS and bisulfite.

The last step of this pathway can be catalyzed by two different enzyme isoforms: *O*-acetylserine sulfidalyse A (OASS-A or CysK, encoded by *cysK*) and *O*-phosohoserine sulfidalyse B (OASS-B or CysM, encoded by *cysM*).<sup>67</sup> In *E. coli*, the two isoforms show a homology of 43%, and they are expressed under different conditions. Indeed, OASS-B is expressed under anaerobic conditions and was demonstrated to be a more promiscuous enzyme, able to accept thiosulfate as a sulfur source, and does not interact with SAT to form the CS complex.<sup>68</sup> Moreover, OASS-B accepts a wider variety of substrates and bulkier ligands, suggesting an active site volume greater than OASS-A. On the contrary, OASS-A is the most abundant isoform expressed under aerobic conditions.<sup>67,69</sup>



Unlike SAT, both the OASS isoforms are dimeric pyridoxal 5'-phosphate (PLP) dependent enzymes, sharing the same Bi-Bi ping pong reaction mechanism (**Figure 4**). Basically, this mechanism is composed of two different half-reactions. The first half-reaction leads to the formation of the  $\alpha$ -aminoacrylate intermediate. First, OAS binds and displaces the Lys, forming a Schiff base with the pyridoxal phosphate. Subsequently, the acetate is released through  $\beta$ -elimination and leads to the  $\alpha$ -aminoacrylate. This intermediate undergoes nucleophilic attack by sulfide (or other sulfur donors, such as thiosulfate) to obtain cysteine, the final product, in the second half-reaction.

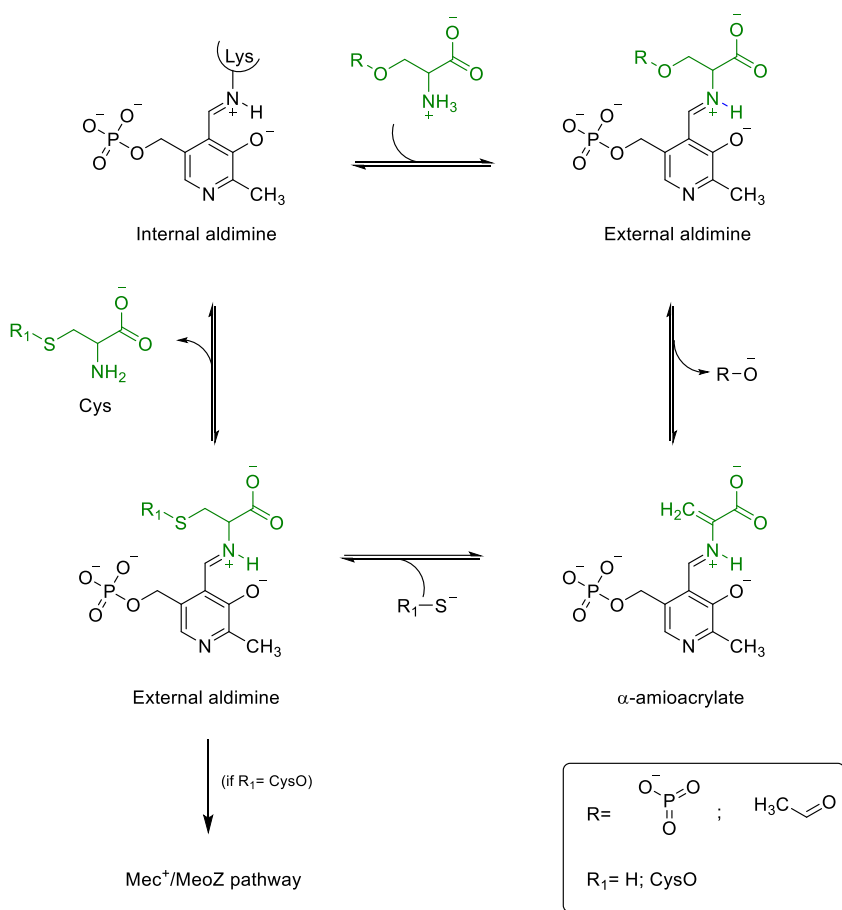


**Figure 4.** General catalytic mechanism of OASS-A/OASS-B. Picture adapted from ref <sup>69</sup>

Regarding the structure of OASS-A/OASS-B, it is a homodimer, with each subunit organized into two different domains and the active sites, each containing a molecule of PLP, facing the solvent. The two domains are flexible and close up upon substrate binding, thus allowing diffusion into the active site only of small molecules and protecting the highly reactive  $\alpha$ -aminoacrylate intermediate from attack by water or other nucleophiles.<sup>69,70</sup>

The overall process of cysteine biosynthesis is highly regulated due to the toxicity that high levels of cysteine might exert on the bacteria cell. Therefore, the production and synthesis of this amino acid inside the cell needs to be fine-tuned. At this regard, three different regulatory mechanisms are present, and CS, OASS, and SAT play a critical role in controlling the cysteine pathway in response to a variation of sulfur availability.

(i) The regulation of gene expression. Under normal physiological conditions, SAT and OASS engage the formation of the CS complex, leading to OAS formation and then to cysteine. Sulfur deficiency results in decreased bisulfide levels, and OAS is accumulated. A high quantity of OAS leads to the dissociation of the CS complex.<sup>71</sup> Furthermore, due to its unstable nature, OAS converts rapidly to NAS, which, as mentioned before, is the natural inducer of the transcription of the cysteine regulon, aiming to increase the expression of genes involved in the cysteine synthesis. On the contrary, bisulfite and thiosulfate act as anti-inducer.

(ii) As previously reported, the downregulation of OASS activity by SAT leads to the OASS-A/SAT complex formation. OAS dissociates the complex by direct competition with SAT for binding to the active site of OASS-A. OAS within the complex is inhibited because its active site is occluded by the C-terminal chain of SAT.

(iii) The last mechanism is the feedback inhibition activity exerted to L-cysteine, the end product of the pathway.<sup>57,72</sup> Indeed, L-cysteine competes with L-serine to the serine binding site of SAT. The binding with cysteine may cause a reduction in affinity for the acetyl-CoA (**Figure 5**).<sup>73</sup>

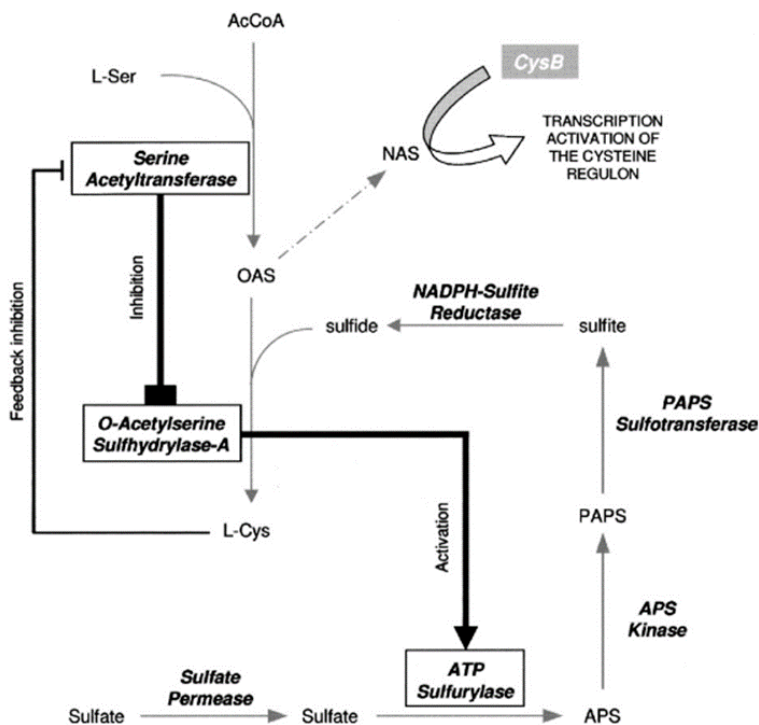


**Figure 5.** General overview of cysteine biosynthesis regulations. Picture adapted from ref <sup>59</sup>

The overall analysis of the cysteine machinery led us to focus our efforts on the identification of novel inhibitors of the two key enzymes of this pathway, SAT and OASS. Therefore, the first part of this thesis is related to the medicinal chemistry efforts for the development of new potential classes of SAT inhibitors. Afterward, the focus will be moved on the research concerning molecules able to inhibit or interact with OASS resulting in the inhibition of cysteine production.

## 3. Serine Acetyltransferase (SAT) Inhibitors

### 3.1 Background

Our research group has a longstanding experience in the research of compounds able to inhibit cysteine biosynthesis in bacteria, focused mainly on the development of *O*-acetylserine sulfhydrylase inhibitors (see 4.1). As explained before, cysteine biosynthetic machinery is composed of two key enzymes, *O*-acetylserine sulfhydrylase (OASS) and serine acetyltransferase (SAT), both essential to finalize the last steps of the synthesis. Taking into account the overall cysteine biosynthesis process, the potentiality of SAT as a promising drug target, and the limited literature available about SAT inhibitors,<sup>74,75</sup> we deemed it was worth focusing our efforts on the research and development of new SAT inhibitors to inhibit cysteine biosynthesis. Indeed, if OASS inhibitors lead to *O*-acetylserine (OAS) accumulation with consequential production of *N*-acetylserine (NAS, the natural inducer of cysteine operon), on the other hand, SAT inhibitors are expected to cause both cysteine and OAS depletion.

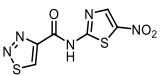
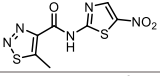
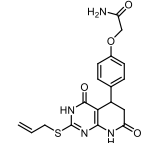
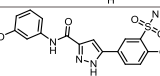
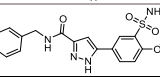
In a first attempt to discover new potential SAT inhibitors, virtual screening (VS), and drug repurposing approach, two different strategies that have become essential tools to identify new hit compounds in drug discovery,<sup>76,77</sup> were combined. A VS was carried out on our in-house library consisting of chemical compounds designed and synthesized to have biological activity on targets other than SAT. This led to the identification of hit compounds characterized by a 2-aminooxazole moiety. The synthesis of new 2-aminooxazole analogues successfully led to molecules with IC<sub>50</sub> values between 1 and 11 μM. Despite the promising enzymatic activity, even the most promising compound could not interfere with bacterial growth.<sup>78</sup>

Therefore, we pursued another approach, and a different virtual screening was conducted using commercial ChemDiv focused anti-infective, antifungal, and antiviral/antibacterial libraries, containing 91,243 compounds and using SAT crystal structures of *E. coli* and *H. influenzae*. Seventy-three compounds showed suitable characteristics to be potential SAT inhibitors. Selected compounds were purchased, and their ability to inhibit SAT was evaluated. Five compounds showed an IC<sub>50</sub> < 100 μM toward StSAT, encouraging enough to carry out a hit-to-lead optimization, especially for two series of structurally related molecules (D319 and D511) (**Table 1**). Along with the enzymatic activity, a preliminary screening of the minimal inhibitory concentrations

(MICs) of the compounds was carried out. Evaluation of the MIC of a potential SAT inhibitor would be misleading if performed under standard bacterial growing conditions since the bacteria might obtain cysteine from the environment. Therefore, a minimal medium broth (LB 20%) with limited amounts of nutrients and deprived of cysteine was used to prove the correlation between inhibition of cysteine biosynthesis and growth inhibitory effects. Among the five tested compounds, only **D319-0482** was found to have a MIC of 64  $\mu\text{g}/\text{mL}$ , whereas the same compound, when tested in a Mueller Hinton Broth (MHB), did not show any measurable MIC even at the highest concentration tested (128  $\mu\text{g}/\text{mL}$ ), as expected.

These preliminary results laid the groundwork for a deeper investigation around both the chemical series of hit compounds in order to define a plausible Structure-Activity Relationship (SAR) and carry out an investigation on the biological properties of the molecules. The D319 series, represented by the hit compounds **D319-0482**, was prioritized for its better performance in the MIC experiments, as reported herein.

**Table 1.** IC<sub>50</sub> values against StSAT and MIC of the Hits derived from Virtual Screening.

ChemDiv code	Structure	IC <sub>50</sub> ( $\mu\text{M}$ )	MIC LB 20% ( $\mu\text{g}/\text{mL}$ )	MIC MHB ( $\mu\text{g}/\text{mL}$ )
D319-0482 (alias compound 1)		48.6 $\pm$ 8	64	>128
D319-0733		47.8 $\pm$ 5	>128	>128
D392-0319		84.1 $\pm$ 5	>128	>128
D511-0060		13.6 $\pm$ 2	>128	>128
D511-0063		52.8 $\pm$ 2	>128	>128

## 3.2 Exploring the chemical space around N-(5-nitrothiazol-2-yl)-1,2,3-thiadiazole-4-carboxamide

### 3.2.1. Aim of the project and first generation of derivatives

**D319-0482**, henceforward called compound **1** (**Figure 6**), was considered a suitable scaffold to pursue our investigation to release effective and potent SAT inhibitors. Compound **1** is characterized by two small heterocycles, a thiadiazole and a 2-amino-5-nitrothiazole ring linked through an amide bond. We deemed it was worthwhile to modify each part of the hit structure, introducing different groups to evaluate the contribution of each portion of the molecule to the overall activity. However, during the first round of investigation, the 2-amino-5-nitrothiazole moiety was kept intact, and modifications to the linker and substitutions of the thiadiazole were carried out. Regarding the replacement of the thiadiazole group, first were introduced other 5-membered heterocycle, and then bulky group with different features and variously substituted. The amide bridge was replaced with a carbamate and urea linker (**Figure 6**).

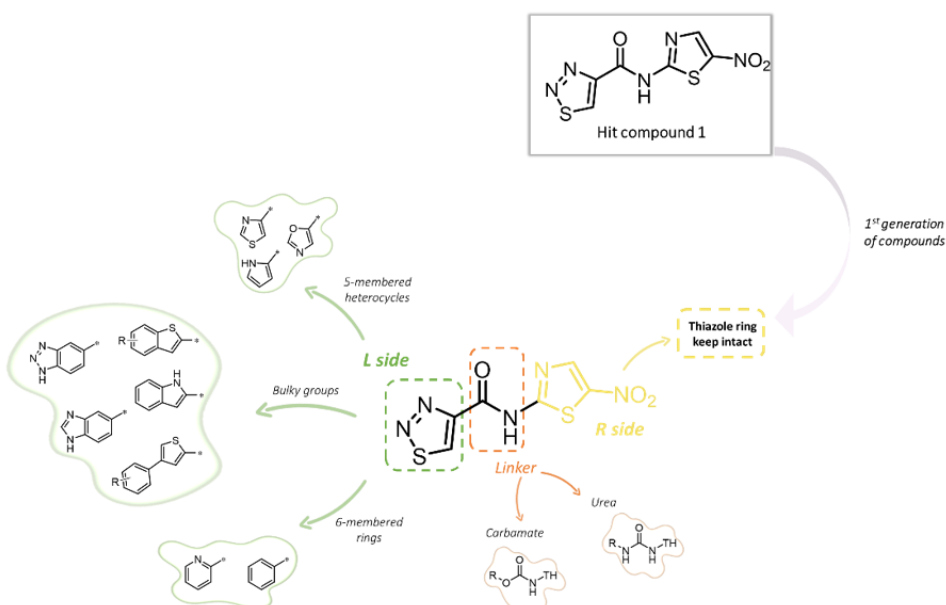


**Figure 6.** Modifications of the hit compound **1** led to the first generation of derivatives.

### 3.2.2. Determination of StSAT Inhibition

The synthesized compounds were evaluated *in vitro* for their ability to inhibit the target enzyme through an indirect assay using Ellman's reagent (5,5'-Dithiobis(2-nitrobenzoic acid or DTNB), a method for quantifying the concentration of thiol groups in solution. During the reaction catalyzed by SAT, the transfer of the acetyl group of acetyl-CoA to serine releases a free thiol CoASH. DTNB has a highly oxidizing disulfide bond, which is stoichiometrically reduced by free thiols, leading to a mixture of disulfide and a molecule of 5-thio-2-nitrobenzoic acid (TNB), a yellow-colored product that can be quantified using a spectrophotometer based on its strong absorbance at 412 nm (Figure 7).<sup>79</sup>

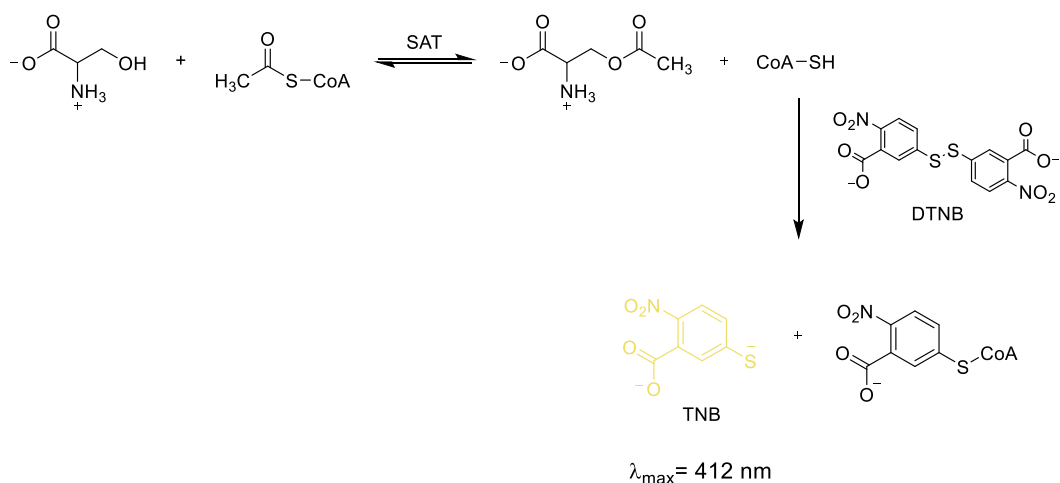


**Figure 7.** Schematic representation of indirect Ellman's assay used to estimate SAT activity.

### 3.2.3. Results and Discussion

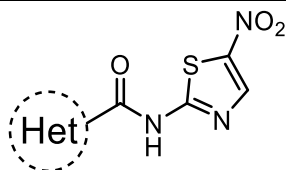
#### 3.2.3.1. First generation of derivatives

The lead compound optimization started with the synthesis of a small set of compound **1** derivatives in order to collect preliminary information about the SAR in relation to their IC<sub>50</sub> (Table 2). At first, the thiadiazole ring was substituted with five-membered heterocycles, like thiazole (**2**), pyrrole (**3**), and oxazole (**4**). Surprisingly, no one of these compounds had an inhibitory activity equal to or greater than the hit compound **1** (**2**,

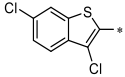
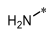
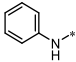
**3, 4**,  $IC_{50} > 100 \mu M$ ). Subsequently, phenyl and 2-pyridine were used as the substituent, but also in this case, no improvement in the activity could be detected (**5, 6**,  $IC_{50} > 100 \mu M$ ). At this point, bulkier steric bicycles were investigated as substituents of the thiadiazole group. In this case, the replacement of the thiadiazole with a group such as benzo[b]thiophene, 4,5,6,7-tetrahydrobenzo[b]thiophene, indole, and benzimidazole led to an appreciable activity (**7**,  $IC_{50} = 18 \pm 2 \mu M$ ; **8**,  $IC_{50} \cong 63 \mu M$ ; **9**,  $IC_{50} = 23 \pm 1 \mu M$ ; **10**,  $IC_{50} \cong 43 \mu M$ ) with the exception of the benzotriazole ring (**11**,  $IC_{50} > 100 \mu M$ ). Taking advantage from the fact that these heterocyclic structures could be further modified, we deemed of interest to explore the activity of substituted benzothiophene analogues. In this regard, a set of derivatives bearing various small functional groups was synthesized. Electron withdrawing groups (EWGs), such as chlorine and fluorine, and an electron donor group (EDG), such as the methyl, were introduced at positions C-3 and C-6 of the scaffold (**12-15**). All the substituents introduced to the benzo[b]thiophene ring were well tolerated, with some of them (**13, 14**) noticeably improving the affinity of the molecule for the enzyme (**12**,  $IC_{50} = 28 \pm 4 \mu M$ ; **13**,  $IC_{50} = 10 \pm 1 \mu M$ ; **14**,  $IC_{50} = 5.2 \pm 0.5 \mu M$ ). The EDG at the C-6 was the only exception, being compound **15** ( $IC_{50} > 100 \mu M$ ) the only derivative with a weaker activity compared to compound **1**. After exploring the impact of derivatives bearing small functional groups, we also investigated the effect of bulkier substituents to obtain molecules with enhanced steric hindrance, which was achieved by adding phenyl substituents at the C-6 of the moiety *via* Suzuki coupling (**16-19**). Introducing *m*-fluorophenol moiety at the C-6 led to a derivative with a considerable increase in inhibitory activity (**16**,  $IC_{50} = 1.5 \pm 0.2 \mu M$ ). On the contrary, the compound bearing the *p*-CF<sub>3</sub>-phenyl ring showed a slight decrease in the activity (**17**,  $IC_{50} = 66 \pm 20 \mu M$ ). Additionally, a noteworthy inhibitory activity was also detected when *p*-fluorophenyl and phenyl rings were used as substituents at the C-6 of the benzo[b]thiophene moiety (**18**,  $IC_{50} \cong 4 \mu M$ ; **19**,  $IC_{50} \cong 5 \mu M$ ). Subsequently, to reduce the rigidity of the structure although preserving its hindrance, the benzo[b]thiophene core was replaced with a thiophene bearing substituted phenyl rings at the C-4 (**20-23**). As for the benzo[b]thiophene derivatives, the presence of *m*-fluorophenyl moiety led to a compound with higher inhibitory activity (**20**,  $IC_{50} = 6 \pm 1 \mu M$ ). On the other hand, substituents such as the *p*-CF<sub>3</sub> and the *m*-CF<sub>3</sub> phenyl were able to confer a similar inhibitory potency (**21**,  $IC_{50} = 28 \pm 4 \mu M$ ; **22**,  $IC_{50} \cong 12 \mu M$ ). Apparently, it could be speculated that five-membered heterocycles are tolerated as long as their hindrance is augmented by the addition of a bulky substituent.



**Table 2:** StSAT Inhibitory activity (IC<sub>50</sub>) and cytotoxicity toward THP-1 cells (CC<sub>50</sub>) of the first generation of compounds.



Cpd	Het	IC <sub>50</sub> (μM)	Cytotoxicity CC <sub>50</sub> (μM)	Cpd	Het	IC <sub>50</sub> (μM)	Cytotoxicity CC <sub>50</sub> (μM)
1		48.6±8	<25	16		1.5 ± 0.2	< 25
2		> 100	N/A	17		66 ± 20	< 25
3		> 100	N/A	18		≅ 4*	< 25
4		> 100	N/A	19		≅ 5*	< 25
5		> 100	N/A	20		6.1 ± 1.2	< 25
6		>100	N/A	21		28 ± 4	< 25
7		18 ± 2	<25	22		≅ 12*	< 25
8		63*	<25	23		≅ 57*	<25
9		23 ± 1	<25	24		>100	N/A
10		≅ 43*	N/A	25		>100	N/A
11		>100	N/A	26		≅ 80*	N/A
12		28 ± 4	< 25	27		>100	N/A
13		10 ± 1	< 25	28		>100	N/A

<b>14</b>		5.2 ± 0.5	< 25	<b>29</b>		101 ± 9	N/A
<b>15</b>	t	> 100	< 25	<b>30</b>		107 ± 14	N/A

\* low-solubility compounds. The IC<sub>50</sub> was calculated in a limited concentration range (usually highest tested concentration lower than or equal to IC<sub>50</sub>), and for this reason, only an estimate is given.

From this first round of modifications, we concluded that the thiadiazole ring could be effectively replaced with other heterocycles, with a particular predilection for sulfurated heterocycles such as benzothiofene and substituted thiophene rings.

In a similar vein, we also synthesized a small set of derivatives where the amide linker between the 2-amino-5-nitrothiazole and the thiadiazole was substituted by two different structural bridges, namely the carbamate and the urea. All of these molecules showed low potency that, together with the strong absorption at 412 nm, didn't allow to calculate accurate IC<sub>50</sub> values (**24**, **25**, **27**, **28**, IC<sub>50</sub> > 100 μM; **26**, IC<sub>50</sub> ≅ 80 μM; **29**, IC<sub>50</sub> = 101±9 μM, **30**, IC<sub>50</sub> = 107±14 μM). Therefore, the investigation of these modifications was suspended.

The nitro group, which possesses a strong EWG nature, has been often associated with toxicity issues, and for this reason, it is usually considered a structural alert in the design of molecules.<sup>80</sup> Considering this, we wanted to evaluate the toxicity of those derivatives with the most encouraging inhibitory activity (**1**, **7–9**, **12–14**, **16–23**). Unfortunately, all of the molecules tested were found to be toxic, including those ranked as the best compounds, namely **14**, **16**, **18**, **19**, and **20**.

### 3.2.3.1. Second generation of derivatives

The information collected through the analysis of the first generation of compounds pushed us to carry out additional modifications with the aim to couple a good inhibitory potency with a favorable toxic profile. Therefore, after investigating modifications to the *L side* of the hit compound, we deemed of interest to perform two kinds of modification at the *R side*: *a*) replacing the 2-amino-5-nitrothiazole moiety with other heterocycles such as pyridine, benzothiazole, and pyridothiazole, to explore the impact on the activity or *b*) maintaining the 2-aminothiazole core but substituting the nitro group at C-5 with other groups such as H, chlorine, methyl, and phenyl (**Figure 8**).

As for the first generation of derivatives, all the compounds were evaluated for the capability to inhibit StSAT, and those with an improved inhibitory profile were tested to assess the cytotoxicity (**Table 3**).

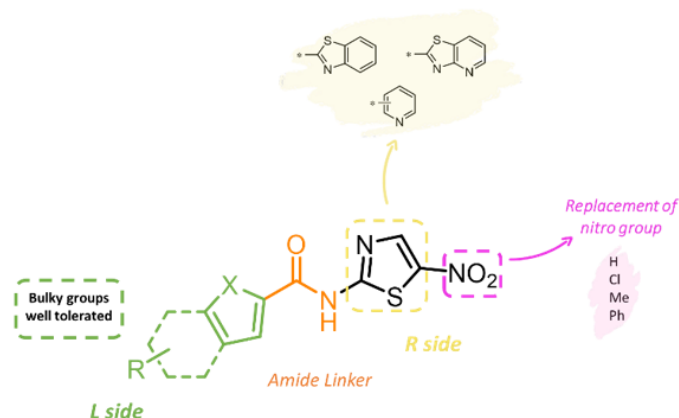


**Figure 8.** Modifications lead to the second generation of derivatives:

Concerning the first attempt, compounds **31** and **32** were prepared. The thiazole ring was integrated into a steric and bulky moiety to increase the structural rigidity to the *R* side of the molecule and evaluate the biological effect of a higher-character  $\pi$ -system. The 2-aminothiazole was condensed to pyridine and phenyl to give 2-aminobenzothiazole and 2-aminopyridothiazole derivatives. Although modified, the aminothiazole ring was maintained in this case, though no improvement in the inhibitory activity could be detected (**31**, **32**,  $IC_{50} > 100 \mu M$ ). In a different setting, the thiazole moiety was substituted with pyridine, but, also in this case, the modification proved to be detrimental. (**33**, **34**,  $IC_{50} > 100 \mu M$ ). This also applied when the thiadiazole was substituted with an indole, which in the previous series (**9**) proved to be efficacious (**35**, **36**,  $IC_{50} > 100 \mu M$ ).

Since the substitution of the 2-amino-5-nitrothiazole with different bulky substituents did not bring any improvement to our purpose, we started to investigate the substitution of the nitro moiety with other functional groups such as H, chlorine, and phenyl.

For these compounds, first, the thiadiazole ring was connected to the 2-aminothiazole, without any functional groups at C-5, through an amide linker to evaluate how this substitution affected the activity (**38**). Then, the thiadiazole was substituted with those heterocycles that, in the first round of modifications, were able to confer good activity. Removal of the nitro group led to a loss of activity when the 2-aminothiazole is linked

to the thiadiazole. Furthermore, replacing the thiadiazole ring with a bulky group on the *L* side of the molecule did not prove beneficial for the enzymatic activity (**38**, **39**,  $IC_{50} > 100 \mu M$ ).

Substitution with the methyl, which is a lipophilic group but with different electronic characteristics compared to the nitro, did not improve the activity compared to the parent compound (**40**,  $IC_{50} > 100 \mu M$ ; **1**,  $IC_{50} = 48.6 \pm 8.43 \mu M$ ). However, this compound did not show appreciable toxicity, with a  $CC_{50} > 200 \mu M$ , which was remarkably higher than that of **1** ( $CC_{50} < 25 \mu M$ ). Encouraged by the lack of toxicity, we decided to repeat some of the substitutions used for modifying compounds **1** to **40**. This led to a series of compounds (**41–59**) with a wide range of biological properties that can be summarized as follows. Regarding the benzo[b]thiophene derivatives, the unsubstituted compound, or the substitution with a methyl group at C-3 or an F at C-6 and Cl at C-3, showed a drop in the inhibitory activity compared to the nitro analogues (**41**,  $IC_{50} > 100 \mu M$ ; **7**,  $IC_{50} = 18 \pm 2 \mu M$ ; **42**,  $IC_{50} > 100 \mu M$ ; **12**,  $IC_{50} = 28 \pm 4 \mu M$ ; **43**,  $IC_{50} > 100 \mu M$ ; **13**,  $IC_{50} = 10 \pm 1 \mu M$ ). On the other hand, Cl at C-6 and C-3 led to a methyl derivate with a very good inhibitory activity comparable to that of the nitro-derivative, although the toxic profile was still inadequate (**44**,  $IC_{50} = 13 \pm 4 \mu M$ ,  $CC_{50} < 25 \mu M$ ; **14**,  $IC_{50} = 5.2 \pm 0.5 \mu M$ ). Surprisingly, the removal of Cl at C-6 brings a derivative with an enhanced toxic profile and only a small decrease in the inhibitory activity (**45**,  $IC_{50} = 65 \pm 9 \mu M$ ;  $CC_{50} > 200 \mu M$ ). The pattern with a 6-phenylbenzo[b]thiophene moiety and a 2-amino-5-methylthiazole (**46–49**) seems to be advantageous to the inhibitory activity. Unexpectedly, the only modification leading to a detrimental effect for the inhibitory activity was that represented by the *m*-fluorophenol moiety as a substituent at C-6, a group that led to one of the most active compounds in the nitro series. Despite these encouraging preliminary results, the introduction of the methyl group on the thiazole ring did not significantly improve the toxicity profile of these derivatives. Surprisingly, **46**, bearing a *p*-CF<sub>3</sub>-phenyl moiety at the C-6, was the only exception that led to a derivate that showed higher cellular viability in the MTT assay, although the activity was concentration-independent in the range from 10 nM to 25  $\mu M$  (**Table 3**). Furthermore, the decoration with substituted phenyl moieties led to only partial inhibition of the enzymatic activity even at the highest concentrations tested, pointing to solubility issues.

With regard to the thiophene derivatives, compounds **51–53**, and **55** showed inhibitory activity of less than 100  $\mu M$ . Compound **51** was the only phenylthiophene derivate that led to remarkable cellular viability, coupled with an appreciable  $IC_{50}$  (**51**,  $IC_{50} \cong 15 \mu M$ ,

CC<sub>50</sub> > 200; **52**, IC<sub>50</sub> ≅ 77 μM, CC<sub>50</sub> < 25; **53**, IC<sub>50</sub> ≅ 50 μM, CC<sub>50</sub> < 25; **54**, IC<sub>50</sub> > 100 μM, CC<sub>50</sub> < 25; **55**, IC<sub>50</sub> ≅ 27 μM).

Among the other bulky substituents used for the 2-amino-5-methylthiazole derivatives, only the indole moiety showed a comparable activity towards the enzyme to compound **1**, allowing low cellular viability (**56**, IC<sub>50</sub> ≅ 43 μM, CC<sub>50</sub> < 25; **57**, IC<sub>50</sub> > 100 μM; **58**, IC<sub>50</sub> = 70±9 μM; **59**, IC<sub>50</sub> > 100 μM). Concerning the N-methylation of the indole, this modification did not lead to any improvement to the activity compared with the N-unsubstituted analogue (**60**, IC<sub>50</sub> = 53±1 μM; **56**, IC<sub>50</sub> ≅ 43 μM).

As mentioned above, the most active compound in the nitro series showed a drop in activity when a methyl substituent was added (**47**, IC<sub>50</sub> > 100 μM; **16**, IC<sub>50</sub> = 1.5 ± 0.2). On the contrary, other compounds in the methyl series have kept an inhibitory activity less than 100 μM, even if higher compared to the nitro analogue (i.e, **14**, IC<sub>50</sub> = 5.2 ± 0.5; **44**, IC<sub>50</sub> = 13 ± 4; **21**, IC<sub>50</sub> = 28 ± 4; **53**, IC<sub>50</sub> ≅ 50; **20**, IC<sub>50</sub> = 6.1 ± 1.2; **55**, IC<sub>50</sub> ≅ 27). Therefore, the SAR related to the nitro derivatives cannot also be applied to the methyl derivatives.

Replacing the nitro group with chlorine, an EWD, or a group such as a phenyl was found to be a suitable solution for the inhibitory properties of the molecule. When the nitro was substituted with the chlorine group, a similar behavior could be noticed as for the methyl substitution. Indeed, the substitution with the thiadiazole led to a derivative with scarce potency (**61**, IC<sub>50</sub> > 100 μM), whereas the substitution with bulky heterocycles groups led to appreciable-affinity compounds (**62**, IC<sub>50</sub> = 22±3 μM; **63**, IC<sub>50</sub> = 19 μM). Unfortunately, the high toxicity of these molecules discouraged the study of further derivatives.

Differently, replacing the nitro with the phenyl moiety, and linking it to the thiadiazole ring, led to a compound with an inhibitory activity < 100 μM (**64**, IC<sub>50</sub> ≅ 67 μM). This may serve as preliminary speculation that also bulky substituent attached to the 2-aminothiazole could improve the activity towards SAT. The inhibitory activity was lost when the phenyl moiety was introduced at the C-4 of the 2-aminothiazole (**65**, IC<sub>50</sub> > 100 μM). The replacement of the thiadiazole moiety with bulky groups, such as indole, benzo[b]thiophene, and 3,6-dichlorobenzo[b]thiophene, still led to compounds with a good activity towards the enzyme. However, as for the chlorine derivatives, these derivatives resulted in being toxic, the only exception being represented by compound **66**, which showed an improvement in the cytotoxicity profile (**66**, IC<sub>50</sub> = 17±5 μM, CC<sub>50</sub> = 87.73; **67**, IC<sub>50</sub> = 25±6 μM; CC<sub>50</sub> = 33.76; **68**, IC<sub>50</sub> = 4.8±0.9 μM, CC<sub>50</sub> < 25). Further investigation will follow to understand whether indole derivatives linked to the 2-amino-5-phenylthiazole ring could allow higher cellular viability.

**Table 3:** StSAT Inhibitory activity (IC<sub>50</sub>) and cytotoxicity toward THP-1 cells (CC<sub>50</sub>) of the second generation of compounds.

Cpd	Structure	IC <sub>50</sub> (μM)	Cytotoxicity CC <sub>50</sub> (μM)	Cpd	Structure	IC <sub>50</sub> (μM)	Cytotoxicity CC <sub>50</sub> (μM)
31		>100	N/A	50		≅ 18*	N/A
32		>100	N/A	51		≅ 15*	>200
33		> 100	N/A	52		≅ 77*	<25
34		> 100	N/A	53		≅ 50*	<25
35		>100	N/A	54		>100	<25
36		> 100	N/A	55		≅ 27*	N/A
37		> 100	N/A	56		≅ 43*	<25
38		> 100	N/A	57		>100	N/A
39		>100	N/A	58		70 ± 9	N/A
40		>100	>200	59		>100	N/A
41		>100	N/A	60		53 ± 1	N/A
42		>100	N/A	61		>100	N/A
43		> 100	N/A	62		22 ± 3	26.3
44		13±4	<25	63		19*	<25
45		65 ± 9	>200	64		67*	<25
46		N.D.*	144.5	65		>100	N/A
47		> 100	<25	66		17±5	87.73

<b>48</b>		$\cong 14^*$	<25	<b>67</b>		$25 \pm 6$	33.76
<b>49</b>		$\cong 42^*$	39.76	<b>68</b>		$4.8 \pm 0.9$	<25

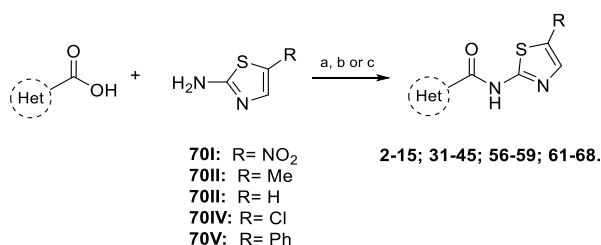
\* low-solubility compounds. The IC<sub>50</sub> was calculated in a limited concentration range (usually highest tested concentration lower than or equal to IC<sub>50</sub>), and for this reason, only an estimate is given.

\*\* the activity was concentration-independent in the range 10 nM and 25  $\mu$ M.

### 3.2.4. Chemistry

The final compounds were obtained through standard amide coupling reaction, starting from the appropriate amine and the carboxylic acids, suitably activated with 1,1'-carbonyldiimidazole (CDI) (**Scheme 1**). When it was impossible to obtain the desired compounds *via* this method, TBTU and EDC were used as the coupling agents, whereas the conversion of the acids to the corresponding acyl chlorides and the subsequent reaction with the 2-amino-5-chlorothiazole allowed the isolation of **62** and **63**, even if in a low yield, likely due to the poor reactivity of the 2-amino-5-chlorothiazole.

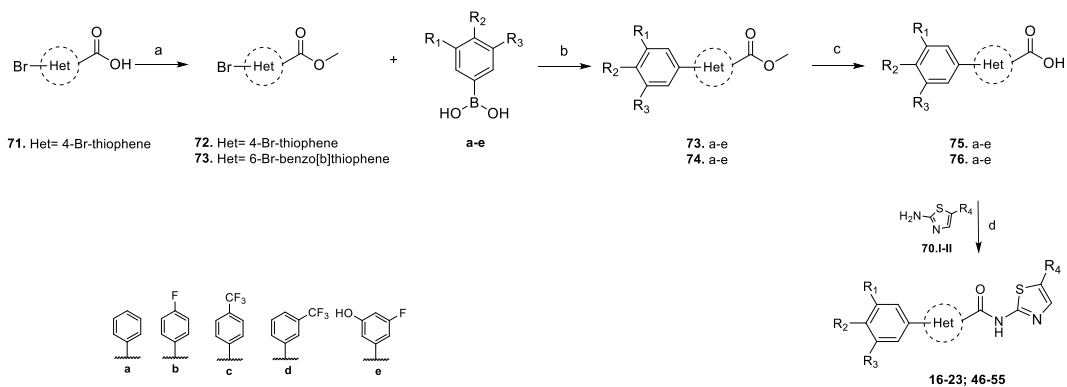
#### Scheme 1.<sup>a,b</sup>



**Scheme 1**<sup>a</sup> *Reagents and conditions:* a) TBTU, EDC, DIPEA, DMAP, DMF dry, rt, 67-5%; b) CDI, DMF dry, rt, on; c) 1) (COCl)<sub>2</sub>, DMF dry, DCM dry, N<sub>2</sub> atm, rt, 4 h; 2) Pyridine, DCM dry, 50 °C, 15 h, 12%. <sup>b</sup> For complete structures, see **Table 2** and **Table 3**.

Thiophene derivatives with an aromatic substituent at C-4 and benzothiophene with an aromatic substituent at C-6 were synthesized *via* Suzuki-Miyaura cross-coupling reaction using XPhos Pd G2 as a catalyst (**Scheme 2**).

### Scheme 2.<sup>a,b</sup>

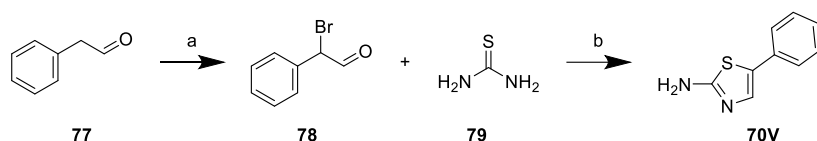


**Scheme 2.** <sup>a</sup>Reagents and conditions: a) CH<sub>3</sub>I, K<sub>2</sub>CO<sub>3</sub>, DMF, rt, 15 h, 70%; b) 1) K<sub>3</sub>PO<sub>4</sub>, THF/H<sub>2</sub>O, N<sub>2</sub> atm, 10 min, 2) XPHOS PdG2, 70 °C, 90 min, 93-47%; c) LiOH, THF/H<sub>2</sub>O/MeOH 3:1:1, r.t, 1-5 h, 100-74%; d) 1) CDI, DMF dry, N<sub>2</sub> atm, rt, 1 h, 2) amine, 70 °C, on, 71-12%. <sup>b</sup>For complete structures, see **Table 2** and **Table 3**.

The majority of the carboxylic acids were commercially available, or in some cases, the methyl esters were purchased and then hydrolyzed, utilizing LiOH in THF/MeOH/H<sub>2</sub>O. All the amines used were purchased, except for the 2-amino-5-phenylthiazole (**70V**), synthesized in two steps starting from phenylacetaldehyde, which was first alpha-brominated, and then reacted with thiourea according to the Hantzsch protocol (**Scheme 3**).



### Scheme 3.<sup>a</sup>



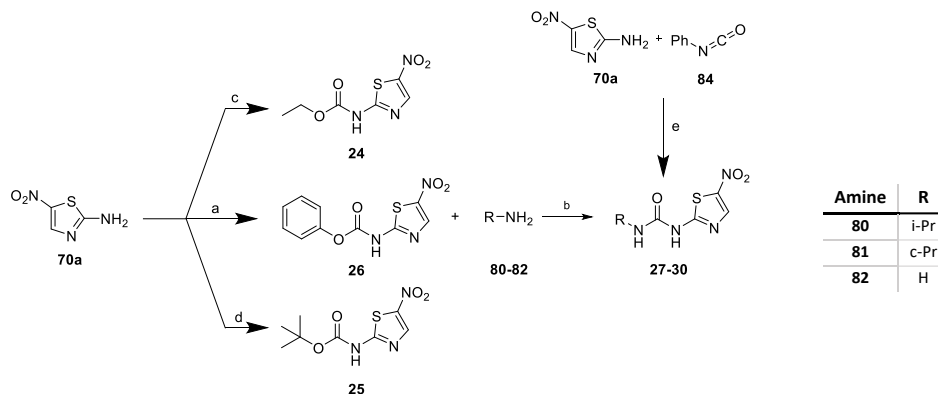
**Scheme 3.**<sup>a</sup> Reagents and conditions: a) Br<sub>2</sub>, DCM, r.t; b) EtOH, reflux, on, 20%.

Compound **30** was synthesized *via* an addition reaction between the 2-amino-5-nitrothiazole and an appropriate isocyanate under an inert atmosphere, using triethylamine as the base and toluene as solvent. Nevertheless, as reported in **Scheme 3**, a different protocol was used to obtain urea **29** and its derivatives **27** and **28**. 2-amino-5-nitrothiazole was first reacted with phenyl chloroformate to obtain the carbamate derivate **26**, which was irradiated in a microwave reactor with the proper aliphatic amine. This procedure proved to be a versatile, rapid, and efficient protocol to obtain a variety of urea derivatives starting from the most common reagents.

Compound **60** was obtained through an *N*-alkylation of **56**, with iodomethane in the presence of sodium hydride in THF.

The chemical structures of the synthesized compounds were confirmed on the basis of their NMR and mass spectra.

### Scheme 4.<sup>a</sup>



**Scheme 4.** <sup>a</sup>Reagents and conditions: a) Phenyl chloroformate, pyridine, DCM dry, 90 min, rt; 86%; b) THF dry, MW (T: 150 °C, Power: 300 W, Time: 20 min, Pressure: 250 PSI); 80-10%; c) Ethyl chloroformate, THF dry, 66 °C, 2h; 31%; d) Boc<sub>2</sub>O, DMAP, Et<sub>3</sub>N, THF dry, r.t., 4,5 h; 58%; Et<sub>3</sub>N, DCM dry, 0 °C - r.t., 15h; 33%.

### 3.2.5. Conclusion

The discovery of hit compound **1** as a promising SAT inhibitor prompted us to carry out a medicinal chemistry campaign to obtain molecules with improved biological properties. Two generations of compounds were synthesized and analyzed to define a preliminary SAR, considering both enzymatic inhibition and toxicity to THP-1 derived macrophages cells.

In general, introducing bulky groups in the *L* side of the molecules was demonstrated to be particularly advantageous for the inhibitory effect of the molecules. Nevertheless, besides the good inhibitory activity shown by some compounds, all those bearing EWGs such as nitro or Cl at the C-5 of the 2-aminothiazole showed high toxicity in MTT assay, even at a concentration of 25 μM. As for the *L* side of the molecule, the introduction of bulky lipophilic substituents, like the phenyl at the C-5 of the 2-aminothiazole, on the other side, appears beneficial regarding the inhibitory activity. This information might lead to further explore the hindrance of the thiadiazole ring to improve the toxic profile of the molecule. Indeed, the indole moiety linked to the 2-amino-5-phenylthiazole (**66**) showed a better cytotoxic profile than the corresponding analogue with a benzo[*b*]thiophene core. Compounds with 2-amino-5-methylthiazole have shown

borderline results, and, surprisingly, the most active compounds within the nitro series resulted inactive when the methyl is used in place of the NO<sub>2</sub> moiety at C-5. Furthermore, unlike **40**, that showed an excellent cytotoxicity profile, most of these derivatives are toxic in the assays used. Only three compounds belonging to the methyl derivatives showed an acceptable toxicity profile (**45**, **46**, **51**) coupled to good inhibitory activity, resulting in the most promising compounds derived from this investigation. From these SAR data, it can be speculated that the combination of the methyl group at the C-5 of the thiazole and appropriate halogen groups on the benzo[b]thiophene or 4-phenylthiophene ring in the *L* side of the molecule led to compounds with excellent cytotoxicity profiles, and as for compound **51**, also an inhibitory activity 3-fold increase compared to the hit compound (**45**, IC<sub>50</sub> = 65±9 μM, CC<sub>50</sub> > 200 μM; **46**, CC<sub>50</sub> = 144.5; **51**, IC<sub>50</sub> ≅ 15 μM, CC<sub>50</sub> > 200).

Considering the few SAT inhibitors reported in the literature and the growing interest in the research of potent inhibitors of such enzyme, the progress achieved in this work and the bulk of information collected might be exploited for the design and synthesis of drug-like SAT inhibitors, as it is currently ongoing in our lab.

### 3.2.6. Experimental section

#### 3.2.6.2. Chemistry

##### General procedure for the amidation reaction

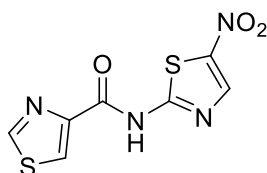
**Method A:** *O*-(Benzotriazol-1-yl)-*N,N,N',N'*-tetramethyluronium tetrafluoroborate (TBTU) (1.00 eq) and *N*-(3-Dimethylaminopropyl)-*N'*-ethylcarbodiimide hydrochloride (EDC HCl) (1.00 eq) were added to a solution of the carboxylic acid (1 eq) in dry DMF (4 mL/mmol) under nitrogen atmosphere. The reaction mixture was stirred at room temperature for 15 minutes, then triethylamine (1.5 eq) and the amine (1.00 eq) were added. The mixture was stirred at the same temperature for 4-12 h. Then, the reaction mixture was extracted with EtOAc (3 X 20 mL), the organic layers were collected, washed with brine (2 X 50 mL), and dried over Na<sub>2</sub>SO<sub>4</sub>. After filtration, the volatiles were removed under vacuum, and the crude material was purified by flash column chromatography eluting with DCM/MeOH. Purification conditions, yields, and analytical data are reported below.

**Method B:** Carbonyldiimidazole (CDI) (1.00 eq) was added to a solution of the proper carboxylic acid (1.00 eq) in dry DMF (2 mL/mmol) under N<sub>2</sub> atmosphere. The reaction

mixture was left stirring for 1 h at room temperature, and then the amine (1.00 eq) was added. The reaction mixture was heated to 70 °C overnight. The reaction was quenched with water and extracted with EtOAc (3 X 20 mL). The organic layers were dried over anhydrous Na<sub>2</sub>SO<sub>4</sub>, filtered, and concentrated under reduced pressure. The crude was purified by flash column chromatography eluting with DCM/MeOH or with trituration. Purification conditions, yields, and analytical data are reported below.

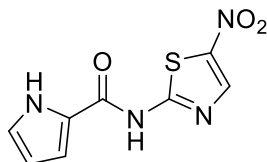
**Method C:** The proper carboxylic acid (1.00 eq) was suspended in anhydrous DCM (6 mL/mmol), and anhydrous DMF (0.06 mL/mmol) under N<sub>2</sub> atmosphere, and then oxalyl chloride (2 M solution in DCM, 2 eq) was added slowly to the stirred suspension. The reaction mixture was stirred at room temperature for 2 h. After this time, the solvent was evaporated under reduced pressure. The crude was re-dissolved in anhydrous DCM (5 mL/mmol). A suspension of 2-amino-5-chlorothiazole (1.00 eq) and pyridine (1.00 eq) in anhydrous DCM (1.2 mL/mmol) was added dropwise, and the reaction mixture was stirred at 50 °C overnight. The reaction was cooled to room temperature, and water was added and extracted with EtOAc (3 X 20 mL<<<). Organic layers were collected, dried over anhydrous Na<sub>2</sub>SO<sub>4</sub>, filtered, and concentrated under reduced pressure. The crude was purified by flash column chromatography (DCM/MeOH) to give the title compounds. Purification conditions, yields, and analytical data are reported below

### N-(5-nitrothiazol-2-yl)thiazole-2-carboxamide (2).



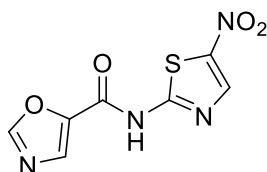
The title compound was obtained as a yellow powder following the **general method B** (yield: 15%). Purification by flash column chromatography using Methanol/Dichloromethane (0.6:99.4). <sup>1</sup>H NMR (300 MHz, DMSO): 8.71 (s, 1H), 8.30 (d, *J* = 2.2 Hz, 1H), 8.22 (d, *J* = 2.4 Hz, 1H). HPLC-ESI-MS analysis: calculated for C<sub>7</sub>H<sub>4</sub>N<sub>4</sub>O<sub>3</sub>S<sub>2</sub>: 255.97; found: 256.23 [M+H<sup>+</sup>].

### N-(5-nitrothiazol-2-yl)-1H-pyrrole-2-carboxamide (3).



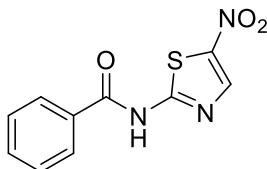
The title compound was obtained as a yellow powder following the **general method B** (yield: 10%). Purification by flash column chromatography using Petroleum Ether/EtOAc (from 85:15 to 70:30). <sup>1</sup>H NMR (400 MHz, DMSO): 13.17 (s, 1H), 12.13 (s, 1H), 8.66 (s, 1H), 7.42 (ddd, *J* = 3.7, 2.4, 1.4 Hz, 1H), 7.17 (td, *J* = 2.8, 1.5 Hz, 1H), 6.25 (dt, *J* = 4.5, 2.3 Hz, 1H). HPLC-ESI-MS analysis: calculated for C<sub>8</sub>H<sub>6</sub>N<sub>4</sub>O<sub>3</sub>S: 238.02; found: 239.13 [M+H<sup>+</sup>].

### N-(5-nitrothiazol-2-yl)oxazole-5-carboxamide (4).



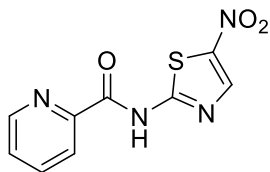
Oxazole-5-carboxylic acid was activated with HATU instead of CDI or TBTU/EDC. Purification by flash column chromatography using DCM/MeOH (99.5:0.5) afforded the product as a light orange powder in 15% yield. <sup>1</sup>H NMR (300 MHz, DMSO): 8.78 (s, 1H), 8.71 (s, 1H), 8.30 (s, 1H). HPLC-ESI-MS analysis: calculated for C<sub>7</sub>H<sub>4</sub>N<sub>4</sub>O<sub>4</sub>S: 239.99; found: 241.00 [M+H<sup>+</sup>].

### N-(5-nitrothiazol-2-yl)benzamide (5)



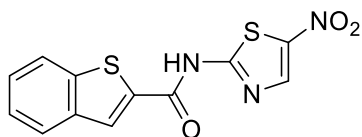
The title compound was obtained as a yellow powder following the **general method A** (yield: 54%). Purification by flash chromatography eluting with DCM/MeOH 98:2. <sup>1</sup>H NMR (300 MHz, DMSO-*d*<sub>6</sub>): δ 13.59 (s, 1H); 8.71 (s, 1H); 8.14-8.11 (m, 2H); 7.70 (t, *J* = 9 Hz, 1H); 7.61 (t, *J* = 6 Hz, 1H). HPLC-ESI-MS analysis: calculated for C<sub>10</sub>H<sub>7</sub>N<sub>3</sub>O<sub>3</sub>S: 249.02; found: 250.02 [M+H<sup>+</sup>].

### N-(5-nitrothiazol-2-yl)picolinamide (6)



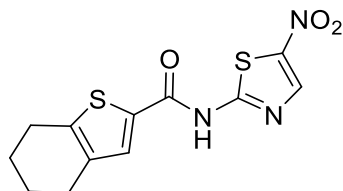
The title compound was obtained as a yellow powder following the **general method A** (yield: 22%). Purification by flash chromatography eluting with DCM/MeOH 98:2.  $^1\text{H}$  NMR (400 MHz, DMSO- $d_6$ ):  $\delta$  13.42 (s, 1H); 8.82-8.81 (m, 1H); 8.73 (s, 1H); 8.23 (d,  $J$  = 7.7 Hz, 1H); 8.15 (t,  $J$  = 7.2 Hz, 1H); 7.83-7.73 (m, 1H). HPLC-ESI-MS analysis: calculated for  $\text{C}_9\text{H}_6\text{N}_4\text{O}_3\text{S}$ : 250.02; found: 251.04 [ $\text{M}+\text{H}^+$ ].

### N-(5-nitrothiazol-2-yl)benzo[b]thiophene-2-carboxamide (7)



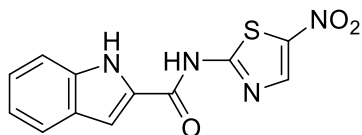
The title compound was obtained as a yellow powder following the **general method A** (yield: 52%). Purification by flash chromatography eluting with DCM/MeOH 95:5.  $^1\text{H}$  NMR (300 MHz, DMSO- $d_6$ ):  $\delta$  8.73 (s, 1H); 8.66 (s, 1H); 8.13-8.04 (m, 2H); 7.59-7.48 (m, 2H). HPLC-ESI-MS analysis: calculated for  $\text{C}_{12}\text{H}_7\text{N}_3\text{O}_3\text{S}_2$ : 304.99; found: 306.20 [ $\text{M}+\text{H}^+$ ].

### N-(5-nitrothiazol-2-yl)-4,5,6,7-tetrahydrobenzo[b]thiophene-2-carboxamide (8)



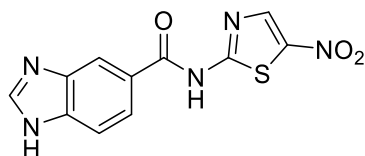
The title compound was obtained as a yellow powder following the **general method A** (yield: 16%). Purification by flash chromatography eluting with Petroleum Ether/EtOAc from 8:2 to 7:3.  $^1\text{H}$  NMR (400 MHz, DMSO- $d_6$ ):  $\delta$  13.56 (s, 1H) 8.87 (s, 1H); 8.00 (s, 1H); 2.80 (m, 2H); 2.61 (m, 2H); 1.79-1.76 (m, 4H).  $^{13}\text{C}$  NMR (100.6 MHz, DMSO): 161.2; 146.1; 143.2; 137.4; 132.1; 25.04; 23.0; 22.5. HPLC-ESI-MS analysis: calculated for  $\text{C}_{12}\text{H}_{11}\text{N}_3\text{O}_3\text{S}_2$ : 309.02; found: 310.13 [ $\text{M}+\text{H}^+$ ].

### N-(5-nitrothiazol-2-yl)-1H-indole-2-carboxamide (9)



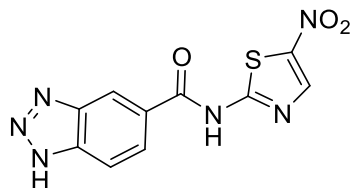
The title compound was obtained as a yellow powder following the **general method A** (yield: 31%). Purification by flash chromatography eluting with DCM/MeOH 99:1.  $^1\text{H}$  NMR (300 MHz, DMSO- $d_6$ ):  $\delta$  13.66 (bs, 1H); 12.10 (s, 1H); 8.72 (s, 1H); 7.77-7.70 (m, 2H); 7.51 (d,  $J = 9$  Hz, 1H); 7.31 (t,  $J = 6$  Hz, 1H); 7.11 (t,  $J = 9$  Hz, 1H). HPLC-ESI-MS analysis: calculated for  $\text{C}_{12}\text{H}_8\text{N}_4\text{O}_3\text{S}$ : 288.03; found: 288.18 [ $\text{M}+\text{H}^+$ ].

### N-(5-nitrothiazol-2-yl)-1H-benzo[d]imidazole-5-carboxamide (10)



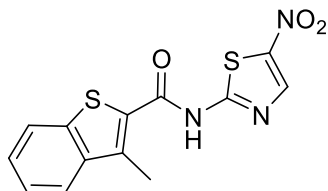
The title compound was obtained as a yellow powder following the **general method A** (yield: 5%). Purification by flash chromatography eluting with DCM/MeOH from 95:5 to 85:15.  $^1\text{H}$  NMR (300 MHz, DMSO- $d_6$ ):  $\delta$  8.72 (s, 1H); 8.54 (s, 1H); 8.45 (s, 1H); 8.00 (dd,  $J_1 = 9$ ,  $J_2 = 3$  Hz, 1H); 7.74 (d,  $J = 9$  Hz, 1H). HPLC-ESI-MS analysis: calculated for  $\text{C}_{11}\text{H}_7\text{N}_5\text{O}_3\text{S}$ : 289.03; found: 288.18 [ $\text{M}+\text{H}^+$ ].

### N-(5-nitrothiazol-2-yl)-1H-benzo[d][1,2,3]triazole-5-carboxamide (11)



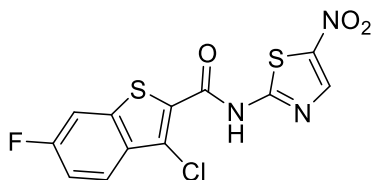
The title compound was obtained as a yellow powder following the **general method B** (yield: 16%). Purification by flash chromatography eluting with DCM/MeOH from 99:1 to 95:5.  $^1\text{H}$  NMR (400 MHz, DMSO- $d_6$ ):  $\delta$  16.16 (bs, 1H) 13.74 (s, 1H); 8.94 (s, 1H); 8.74 (s, 1H); 8.17-7.98 (m, 2H). HPLC-ESI-MS analysis: calculated for  $\text{C}_{10}\text{H}_6\text{N}_6\text{O}_3\text{S}$ : 290.02; found: 291.14 [ $\text{M}+\text{H}^+$ ].

### 3-methyl-N-(5-nitrothiazol-2-yl)benzo[b]thiophene-2-carboxamide (12)



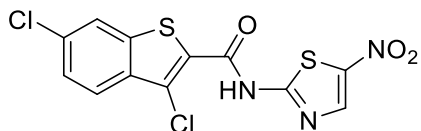
The title compound was obtained as a yellow powder following the **general method B** (yield: 24%). Purification by flash chromatography eluting with 100% DCM.  $^1\text{H}$  NMR (400 MHz,  $\text{DMSO-}d_6$ ):  $\delta$  12.85 (bs, 1H); 8.79 (s, 1H); 8.08 (d,  $J = 7.72$  Hz, 1H); 8.00 (d,  $J = 7.12$  Hz, 1H); 7.57-7.54 (m, 2H); 2.51 (s, 3H). HPLC-ESI-MS analysis: calculated for  $\text{C}_{13}\text{H}_9\text{N}_3\text{O}_3\text{S}_2$ : 319.00; found: 320.26  $[\text{M}+\text{H}^+]$ .

### 3-chloro-6-fluoro-N-(5-nitrothiazol-2-yl)benzo[b]thiophene-2-carboxamide (13)



The title compound was obtained as a yellow powder following the **general method B** (yield: 12%). Purification by flash chromatography eluting with 100 % DCM/MeOH.  $^1\text{H}$  NMR (400 MHz,  $\text{DMSO-}d_6$ ):  $\delta$  8.13 (d,  $J = 8$  Hz, 1H); 8.03-7.99 (m, 1H); 7.59 (d,  $J = 8.4$  Hz, 1H); 7.54-7.49 (m, 1H). HPLC-ESI-MS analysis: calculated for  $\text{C}_{12}\text{H}_5\text{ClFN}_3\text{O}_3\text{S}_2$ : 356.94; found: 358.02  $[\text{M}+\text{H}^+]$ .

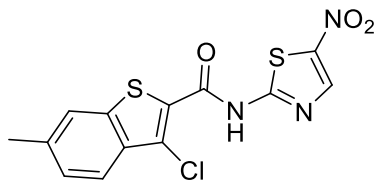
### 3,6-dichloro-N-(5-nitrothiazol-2-yl)benzo[b]thiophene-2-carboxamide (14)



The title compound was obtained as a yellow powder following the **general method B** (yield: 23%). Purification by flash chromatography eluting with 100% DCM.  $^1\text{H}$  NMR (400 MHz,  $\text{DMSO-}d_6$ ):  $\delta$  13.11 (bs, 1H); 8.86 (s, 1H); 8.37 (d,  $J = 1.6$  Hz, 1H); 7.97 (d,  $J = 8.7$  Hz, 1H); 7.64 (dd,  $J_1 = 8.7$ ,  $J_2 = 1.8$ , 1H). HPLC-ESI-MS analysis: calculated for  $\text{C}_{12}\text{H}_5\text{Cl}_2\text{N}_3\text{O}_3\text{S}_2$ : 372.91; found: 374.54  $[\text{M}+\text{H}^+]$ .

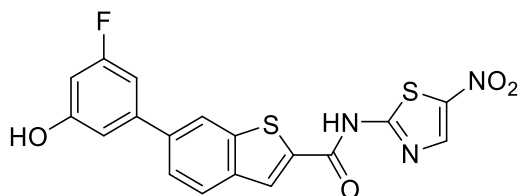


### 3-chloro-6-methyl-N-(5-nitrothiazol-2-yl)benzo[b]thiophene-2-carboxamide (15)



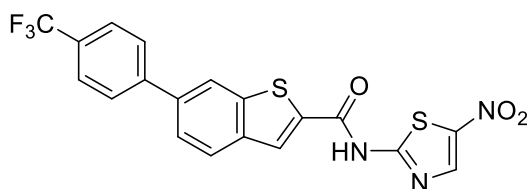
The title compound was obtained as a yellow powder following the **general method B** (yield: 53%). Purification by flash chromatography eluting with 100% DCM.  $^1\text{H}$  NMR (400 MHz,  $\text{DMSO-}d_6$ ):  $\delta$  8.82 (s, 1H); 7.95 (s, 1H); 7.87 (d,  $J = 8.4$  Hz, 1H); 7.46 (d,  $J = 8$  Hz, 1H); 2.50 (s, 3H). HPLC-ESI-MS analysis: calculated for  $\text{C}_{13}\text{H}_8\text{ClN}_3\text{O}_3\text{S}_2$ : 352.97; found: 354.04  $[\text{M}+\text{H}^+]$ .

### 6-(3-fluoro-5-hydroxyphenyl)-N-(5-nitrothiazol-2-yl)benzo[b]thiophene-2-carboxamide (16)



The title compound was obtained as a yellow powder following the **general method B** (yield: 41%). Purification by flash chromatography eluting with DCM/MeOH 99:1.  $^1\text{H}$  NMR (400 MHz,  $\text{DMSO-}d_6$ ):  $\delta$  14.01 (bs, 1H); 10.11 (s, 1H); 8.73 (s, 1H); 8.61 (s, 1H); 8.41 (s, 1H); 8.11 (d,  $J = 8.5$  Hz, 1H); 7.76 (dd,  $J_1 = 8.5$ ,  $J_2 = 1.4$ , 1H); 7.07-7.02 (m, 2H); 6.68-6.58 (m, 1H). HPLC-ESI-MS analysis: calculated for  $\text{C}_{18}\text{H}_{10}\text{FN}_3\text{O}_4\text{S}_2$ : 415.01; found: 416.14  $[\text{M}+\text{H}^+]$ .

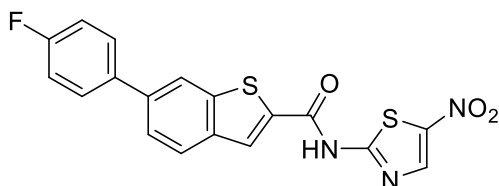
### 6-(4-fluorophenyl)-N-(5-nitrothiazol-2-yl)benzo[b]thiophene-2-carboxamide (17)



The title compound was obtained as a yellow powder following the **general method B** (yield: 45%). Purification by flash chromatography eluting with 100% DCM.  $^1\text{H}$  NMR (400 MHz,  $\text{DMSO-}d_6$ ):  $\delta$  14.00 (bs, 1H); 8.73 (s, 1H); 8.65 (s, 1H); 8.54 (s, 1H); 8.18 (d,  $J$

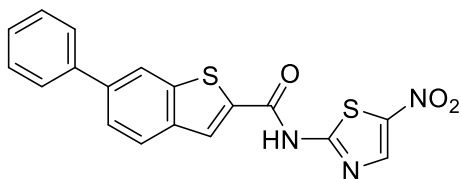
= 8.4 Hz, 1H); 8.03 (d,  $J = 8$  Hz, 2H); 7.89-7.86 (m, 3H). HPLC-ESI-MS analysis: calculated for  $C_{19}H_{10}F_3N_3O_3S_2$ : 449.01; found: 450.53  $[M+H^+]$ .

#### 6-(4-fluorophenyl)-N-(5-nitrothiazol-2-yl)benzo[b]thiophene-2-carboxamide (18)



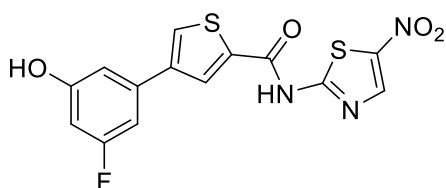
The title compound was obtained as a yellow powder following the **general method B** (yield: 24%). Purification by flash chromatography eluting 100% DCM.  $^1H$  NMR (400 MHz,  $DMSO-d_6$ ):  $\delta$  13.97 (s, 1H); 8.69 (s, 1H); 8.52 (s, 1H); 8.40 (s, 1H); 8.10 (d,  $J = 8.4$  Hz, 1H); 7.87-7.84 (m, 2H); 7.78 (d,  $J = 8.5$  Hz, 1H); 7.37-7.32 (m, 2H). HPLC-ESI-MS analysis: calculated for  $C_{18}H_{10}FN_3O_3S_2$ : 399.01; found: 400.37  $[M+H^+]$ .

#### N-(5-nitrothiazol-2-yl)-6-phenylbenzo[b]thiophene-2-carboxamide (19)



The title compound was obtained as a yellow powder following the **general method B** (yield: 44%). Purification by flash chromatography eluting 100% DCM.  $^1H$  NMR (400 MHz,  $DMSO-d_6$ ):  $\delta$  14.03 (s, 1H); 8.74 (s, 1H); 8.66 (s, 1H); 8.45 (s, 1H); 8.13 (d,  $J = 8.5$  Hz, 1H); 7.86-7.78 (m, 3H); 7.52 (t,  $J = 7.6$  Hz, 2H); 7.43 (t,  $J = 7.2$ , 1H). HR-MS analysis: calculated for  $C_{18}H_{11}N_3O_3S_2$ : 381.02; found: 382.26  $[M+H^+]$ .

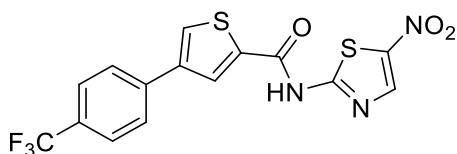
#### 4-(3-fluoro-5-hydroxyphenyl)-N-(5-nitrothiazol-2-yl)thiophene-2-carboxamide (20)



The title compound was obtained as a yellow powder following the **general method B** (yield: 18%). Purification by flash chromatography eluting with DCM/MeOH 99:1.  $^1H$  NMR (600 MHz,  $DMSO-d_6$ ):  $\delta$  13.67 (s, 1H); 10.12 (s, 1H); 8.71 (s, 1H); 8.39 (s, 1H); 7.00-

6.96 (m, 3H); 6.58-6.56 (m, 1H). HPLC-ESI-MS analysis: calculated for  $C_{14}H_8FN_3O_4S_2$ : 364.99; found: 366.21  $[M+H^+]$ .

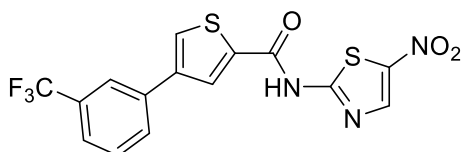
#### **N-(5-nitrothiazol-2-yl)-4-(4-(trifluoromethyl)phenyl)thiophene-2-carboxamide (21)**



The title compound was obtained as a yellow powder following the **general method B** (yield: 24%). Purification by flash chromatography eluting with 100% DCM.  $^1H$  NMR (600 MHz, DMSO- $d_6$ ):  $\delta$  13.73 (s, 1H); 8.86 (s, 1H); 8.73 (s, 1H); 8.59 (s, 1H); 7.96 (d,  $J = 8.2$  Hz, 2H); 7.87 (d,  $J = 8.3$  Hz, 2H); 2.35 (s, 3H). HPLC-ESI-MS analysis: calculated for  $C_{15}H_8F_3N_3O_3S_2$ : 398.99; found: 400.18  $[M+H^+]$ .

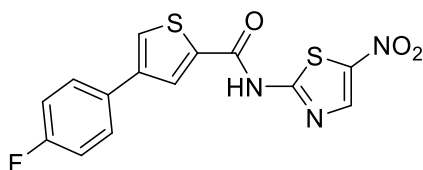
$O-d_6$ ):  $\delta$  13.73 (s, 1H); 8.86 (s, 1H); 8.73 (s, 1H); 8.59 (s, 1H); 7.96 (d,  $J = 8.2$  Hz, 2H); 7.87 (d,  $J = 8.3$  Hz, 2H); 2.35 (s, 3H). HPLC-ESI-MS analysis: calculated for  $C_{15}H_8F_3N_3O_3S_2$ : 398.99; found: 400.18  $[M+H^+]$ .

#### **N-(5-nitrothiazol-2-yl)-4-(3-(trifluoromethyl)phenyl)thiophene-2-carboxamide (22)**



The title compound was obtained as a yellow powder following the **general method B** (yield: 20%). Purification by flash chromatography eluting 100% DCM.  $^1H$  NMR (400 MHz, DMSO- $d_6$ ):  $\delta$  13.68 (s, 1H); 8.86 (s, 1H); 8.73 (s, 1H); 8.60 (s, 1H); 8.07-8.05 (m, 2H); 7.74 (m, 2H). HPLC-ESI-MS analysis: calculated for  $C_{15}H_8F_3N_3O_3S_2$ : 398.995; found: 400.18  $[M+H^+]$ .

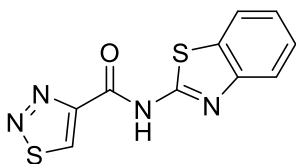
#### **4-(4-fluorophenyl)-N-(5-nitrothiazol-2-yl)thiophene-2-carboxamide (23)**



The title compound was obtained as a yellow powder following the **general method B** (yield: 40%). Purification by flash chromatography eluting with 100% DCM.  $^1H$  NMR (400 MHz, DMSO- $d_6$ ):  $\delta$  13.66 (s, 1H); 8.77 (s, 1H); 8.73 (s, 1H); 8.38 (s, 1H); 7.78 (m,

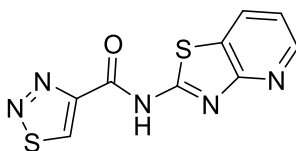
2H); 7.34 (t,  $J = 8.8$  Hz, 1H). HPLC-ESI-MS analysis: calculated for  $C_{14}H_8FN_3O_3S_2$ : 348.99; found: 350.26  $[M+H^+]$ .

### N-(benzo[d]thiazol-2-yl)-1,2,3-thiadiazole-4-carboxamide (31)



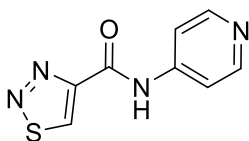
The title compound was obtained as a yellow powder following the **general method B** (yield: 55%). Purification by flash chromatography eluting with DCM/MeOH 98:2.  $^1H$  NMR (300 MHz,  $DMSO-d_6$ ):  $\delta$  10.03 (s, 1H); 8.54 (s, 1H); 8.06 (d,  $J = 9$  Hz, 1H); 7.83 (d,  $J = 9$  Hz, 1H); 7.52-7.47 (m, 1H); 7.40-7.35 (m, 1H). HPLC-ESI-MS analysis: calculated for  $C_{10}H_6N_4OS_2$ : 261.999; found: 263.21  $[M+H^+]$ .

### N-(thiazolo[4,5-b]pyridin-2-yl)-1,2,3-thiadiazole-4-carboxamide (32)



The title compound was obtained as a pink powder following the **general method B** (yield: 3%). Purification by flash chromatography eluting with DCM/MeOH 98:2.  $^1H$  NMR (300 MHz,  $DMSO-d_6$ ):  $\delta$  10.06 (s, 1H); 8.54 (dd,  $J_1 = 6$ ,  $J_2 = 3$  Hz, 1H); 8.21 (dd,  $J_1 = 6$ ,  $J_2 = 3$  Hz, 1H); 7.57-7.52 (m, 1H). HPLC-ESI-MS analysis: calculated for  $C_9H_5N_5OS_2$ : 262.999; found: 264.03  $[M+H^+]$ .

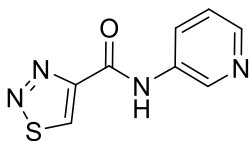
### N-(pyridin-4-yl)-1,2,3-thiadiazole-4-carboxamide (33)



The title compound was obtained as a white powder following the **general method A** (yield: 67%). Purification by flash chromatography eluting with DCM/MeOH from 99:1 to 98:2.  $^1H$  NMR (300 MHz,  $DMSO-d_6$ ):  $\delta$  11.32 (s, 1H); 9.90 (s, 1H); 8.54-8.51 (dd,  $J_1 = 3$ ,  $J_2 = 6$  Hz, 2H); 7.92-7.89 (dd,  $J_1 = 3$ ,  $J_2 = 6$  Hz, 2H).  $^{13}C$  NMR (100.6 MHz,  $DMSO-d_6$ ):  $\delta$

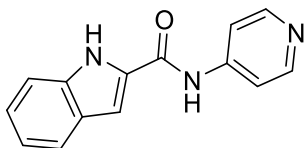
158.7; 157.4; 150.9; 145.7; 144.3; 114.8. HPLC-ESI-MS analysis: calculated for  $C_8H_6N_4OS$ : 206.03; found: 207.23  $[M+H^+]$ .

#### N-(pyridin-3-yl)-1,2,3-thiadiazole-4-carboxamide (34)



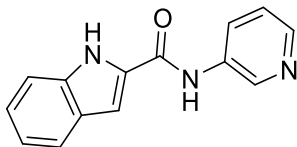
The title compound was obtained as a white powder following the **general method A** (yield: 30%). Purification by flash chromatography eluting with DCM/MeOH from 99.5:0.5 to 98:2.  $^1H$  NMR (400 MHz,  $DMSO-d_6$ ):  $\delta$  11.21 (s, 1H); 9.89 (s, 1H); 9.05 (s, 1H); 8.37-8.27 (m, 2H); 7.45-7.42 (m, 1H).  $^{13}C$  NMR (100.6 MHz,  $DMSO-d_6$ ):  $\delta$  158.2; 157.6; 145.6; 143.9; 142.9; 135.5; 128.3; 124.1. HPLC-ESI-MS analysis: calculated for  $C_8H_6N_4OS$ : 206.03; found: 207.23  $[M+H^+]$ .

#### N-(pyridin-4-yl)-1H-indole-2-carboxamide (35)



The title compound was obtained as a slightly yellow powder following the **general method A** (yield: 58%). Purification by flash chromatography eluting with DCM/MeOH 98:2.  $^1H$  NMR (300 MHz,  $DMSO-d_6$ ):  $\delta$  11.87 (s, 1H); 10.55 (m, 1H); 8.50 (d,  $J = 6$  Hz, 2H); 7.83-7.81 (m, 2H); 7.72-7.70 (d,  $J = 6$  Hz, 1H); 7.50-7.45 (m, 2H); 7.26 (t,  $J = 6$  Hz, 1H); 7.09 (t,  $J = 6$  Hz, 1H).  $^{13}C$  NMR (100.6 MHz,  $DMSO-d_6$ ):  $\delta$  160.94; 150.82; 146.24; 137.60; 131.16; 127.35; 124.76; 122.46; 120.59; 114.24; 112.95; 105.42. HPLC-ESI-MS analysis: calculated for  $C_{14}H_{11}N_3O$ : 237.09; found: 238.25  $[M+H^+]$ .

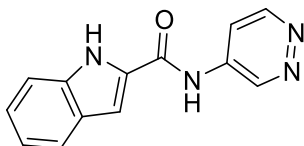
#### N-(pyridin-3-yl)-1H-indole-2-carboxamide (36)



The title compound was obtained as a white powder following the **general method A** (yield: 46%). Purification by flash chromatography eluting with DCM/MeOH from

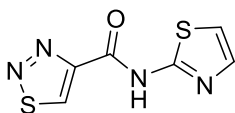
99.5:0.5 to 98:2.  $^1\text{H}$  NMR (300 MHz,  $\text{DMSO-}d_6$ ):  $\delta$  10.48 (s, 1H); 8.31 (d,  $J = 6$  Hz, 1H); 8.22 (d,  $J = 9$  Hz, 1H); 7.70 (d,  $J = 9$  Hz, 2H); 7.50-7.40 (m, 4H); 7.24 (t,  $J = 9$  Hz, 1H); 7.08 (t,  $J = 9$  Hz, 1H).  $^{13}\text{C}$  NMR (100.6 MHz,  $\text{DMSO-}d_6$ ):  $\delta$  160.6; 144.9; 142.1; 137.4; 136.1; 131.3; 127.8; 127.4; 124.6; 124.2; 122.3; 120.6; 112.9; 104.9. HPLC-ESI-MS analysis: calculated for  $\text{C}_{14}\text{H}_{11}\text{N}_3\text{O}$ : 237.09; found: 238.18  $[\text{M}+\text{H}^+]$ .

### N-(pyridazin-4-yl)-1H-indole-2-carboxamide (37)



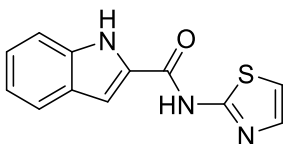
The title compound was obtained as a slightly yellow powder following the **general method A** (yield: 46%). Purification by flash chromatography eluting with DCM/MeOH from 99.5:0.5 to 98:2.  $^1\text{H}$  NMR (400 MHz,  $\text{DMSO-}d_6$ ):  $\delta$  11.95 (s, 1H); 10.79 (s, 1H); 9.57 (s, 1H); 9.10 (d,  $J = 5.8$  Hz, 1H); 8.14 (d,  $J = 3.3$  Hz, 1H); 7.74 (d,  $J = 8.1$  Hz, 1H); 7.63-7.42 (m, 2H); 7.28 (t,  $J = 7.6$  Hz, 1H); 7.11 (t,  $J = 7.4$  Hz, 1H).  $^{13}\text{C}$  NMR (100.6 MHz,  $\text{DMSO-}d_6$ ):  $\delta$  160.6; 144.9; 142.1; 137.4; 136.1; 131.3; 127.8; 127.4; 124.6; 124.2; 122.3; 120.6; 112.9; 104.9. HPLC-ESI-MS analysis: calculated for  $\text{C}_{13}\text{H}_{10}\text{N}_4\text{O}$ : 238.09; found: 239.19  $[\text{M}+\text{H}^+]$ .

### N-(thiazol-2-yl)-1,2,3-thiadiazole-4-carboxamide (38)



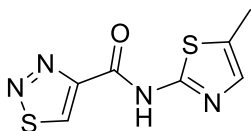
The title compound was obtained as a white powder following the **general method B** (yield: 49%). Purification by flash chromatography eluting with DCM/MeOH 99.9:0.1.  $^1\text{H}$  NMR (300 MHz,  $\text{DMSO-}d_6$ ):  $\delta$  13.05 (s, 1H); 9.99 (s, 1H); 7.61 (d,  $J = 3$  Hz, 1H); 7.37 (d,  $J = 3$  Hz, 1H). HPLC-ESI-MS analysis: calculated for  $\text{C}_6\text{H}_4\text{N}_4\text{OS}_2$ : 211.98; found: 213.15  $[\text{M}+\text{H}^+]$ .

### N-(thiazol-2-yl)-1H-indole-2-carboxamide (39)



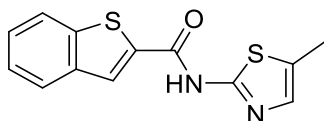
The title compound was obtained as a white powder following the **general method B** (yield: 15%). Purification by flash chromatography eluting with Petroleum Ether/EtOAc from 9:1 to 6:4.  $^1\text{H}$  NMR (400 MHz,  $\text{DMSO-}d_6$ ):  $\delta$  12.71 (bs, 1H); 11.91 (s, 1H); 7.70-7.65 (m, 2H); 7.58 (d,  $J = 3.5$  Hz, 1H); 7.48 (d,  $J = 8.2$  Hz, 1H); 7.30-7.25 (m, 2H); 7.09 (t,  $J = 7.4$  Hz, 1H). HPLC-ESI-MS analysis: calculated for  $\text{C}_{12}\text{H}_9\text{N}_3\text{OS}$ : 243.05; found: 244.18  $[\text{M}+\text{H}^+]$ .

#### **N-(5-methylthiazol-2-yl)-1,2,3-thiadiazole-4-carboxamide (40)**



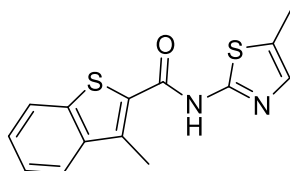
The title compound was obtained as a white powder following the **general method A** (yield: 16%). Purification by flash chromatography eluting with DCM/MeOH 99:1.  $^1\text{H}$  NMR (300 MHz,  $\text{DMSO-}d_6$ ):  $\delta$  9.85 (s, 1H); 7.23 (s, 1H); 8.45 (s, 1H); 2.37 (s, 1H). HPLC-ESI-MS analysis: calculated for  $\text{C}_7\text{H}_6\text{N}_4\text{OS}_2$ : 225.998; found: 227.15  $[\text{M}+\text{H}^+]$ .

#### **N-(5-methylthiazol-2-yl)benzo[b]thiophene-2-carboxamide (41)**



The title compound was obtained as a white powder following the **general method B** (yield: 20%). Purification by flash chromatography eluting with DCM/MeOH 99:1 to 95:5.  $^1\text{H}$  NMR (400 MHz,  $\text{DMSO-}d_6$ ):  $\delta$  12.85 (s, 1H); 8.49 (s, 1H); 8.08 (d,  $J = 8$  Hz, 1H); 8.00 (d,  $J = 7.6$  Hz, 1H); 7.53-7.45 (m, 2H); 7.24 (s, 1H); 2.38 (s, 3H). HPLC-ESI-MS analysis: calculated for  $\text{C}_{13}\text{H}_{10}\text{N}_2\text{OS}_2$ : 274.02; found: 275.25  $[\text{M}+\text{H}^+]$ .

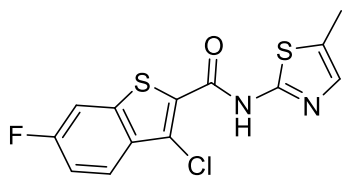
#### **3-methyl-N-(5-methylthiazol-2-yl)benzo[b]thiophene-2-carboxamide (42)**



The title compound was obtained as a slightly yellow powder following the **general method B** (yield: 21%). Purification by flash chromatography eluting with 100% DCM/MeOH.  $^1\text{H}$  NMR (400 MHz,  $\text{DMSO-}d_6$ ):  $\delta$  12.67 (s, 1H); 7.99 (d,  $J = 6.8$  Hz, 1H); 7.92

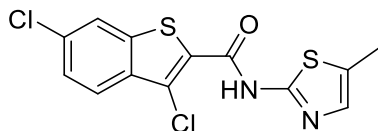
(d,  $J = 7.2$  Hz, 1H); 7.50-7.47 (m, 2H); 7.20 (s, 1H); 2.76 (s, 3H); 2.34 (s, 3H). HPLC-ESI-MS analysis: calculated for:  $C_{14}H_{12}N_2OS_2$ : 288.04; found: 289.12  $[M+H^+]$ .

### 3-chloro-6-fluoro-N-(5-methylthiazol-2-yl)benzo[b]thiophene-2-carboxamide (43)



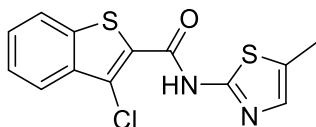
The title compound was obtained as a yellow powder following the **general method B** (yield: 18%). Purification by flash chromatography eluting with DCM/EtOAc from 8:2 to 7:2.  $^1H$  NMR (400 MHz,  $DMSO-d_6$ ):  $\delta$  10.33 (s, 1H); 7.93-7.90 (m, 1H); 7.59 (d,  $J = 8.4$  Hz, 1H); 7.33-7.29 (m, 1H); 7.18 (s, 1H); 2.45 (s, 3H). HPLC-ESI-MS analysis: calculated for  $C_{13}H_8ClFN_2OS_2$ : 325.98; found: 327.13  $[M+H^+]$ .

### 3,6-dichloro-N-(5-methylthiazol-2-yl)benzo[b]thiophene-2-carboxamide (44)



The title compound was obtained as a yellow powder following the **general method B** (yield: 40%). Purification by flash chromatography eluting with DCM/MeOH 99:1.  $^1H$  NMR (400 MHz,  $DMSO-d_6$ ): 12.99 (bs, 1H); 8.29 (d,  $J=1.6$ , 1H); 7.91 (d,  $J=8.7$ , 1H); 7.61 (dd,  $J_1 = 8.7$ ,  $J_2 = 1.9$  Hz, 1H); 7.24 (d,  $J = 1.6$  Hz, 1H); 2.33 (s, 3H). HPLC-ESI-MS analysis: calculated for  $C_{13}H_8Cl_2N_2OS_2$ : 341.95; found: 343.08  $[M+H^+]$ .

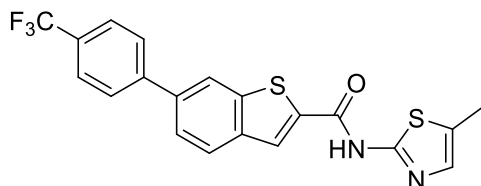
### 3-chloro-N-(5-methylthiazol-2-yl)benzo[b]thiophene-2-carboxamide (45)



The title compound was obtained as a yellow powder following the **general method A** (yield: 21%). Purification by flash chromatography eluting with Petroleum Ether/EtOAc from 8:2 to 6:4.  $^1H$  NMR (600 MHz,  $DMSO-d_6$ ):  $\delta$  12.88 (bs, 1H); 8.08 (d,  $J = 7.0$  Hz, 1H); 7.92 (m, 1H); 7.62-7.55 (m, 2H); 7.22 (d,  $J = 1.3$  Hz, 1H); 2.32 (s, 3H). HPLC-ESI-MS analysis: calculated for  $C_{13}H_9ClN_2OS_2$ : 307.98; found: 309.10  $[M+H^+]$ .

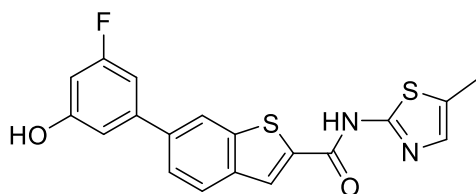


**N-(5-methylthiazol-2-yl)-6-(4-(trifluoromethyl)phenyl)benzo[b]thiophene-2-carboxamide (46)**



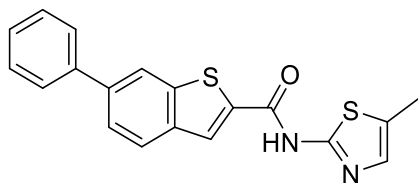
The title compound was obtained as a white powder following the **general method B** (yield: 66%). Purification by trituration with MeOH.  $^1\text{H}$  NMR (600 MHz, DMSO):  $\delta$  12.86 (s, 1H); 8.49 (s, 1H); 8.11 (d,  $J = 8.4$  Hz; 2H); 8.02 (d,  $J = 8.1$  Hz, 2H); 7.86-7.83 (m, 3H); 7.25 (s, 1H); 2.37 (s, 3H). HR-MS analysis: calculated for  $\text{C}_{20}\text{H}_{13}\text{F}_3\text{N}_2\text{OS}_2$ : 418.04; found: 419.19  $[\text{M}+\text{H}^+]$ .

**6-(3-fluoro-5-hydroxyphenyl)-N-(5-methylthiazol-2-yl)benzo[b]thiophene-2-carboxamide (47)**



The title compound was obtained as a pale brown powder following the **general method B** (yield: 71%). Purification by trituration with DCM and Diethyl Ether.  $^1\text{H}$  NMR (400 MHz, DMSO- $d_6$ ):  $\delta$  10.16 (bs, 1H); 8.50 (s, 1H); 8.37 (s, 1H); 8.05 (d,  $J = 8.4$  Hz, 1H); 7.73 (d,  $J_1 = 8.4$ ;  $J_2 = 1.4$  Hz, 1H); 7.26 (s, 1H); 7.07-7.02 (m, 2H); 6.63 (dt,  $J_1 = 10.7$ ;  $J_2 = 2.0$  Hz, 1H); 2.38 (s, 3H). HPLC-ESI-MS analysis: calculated for  $\text{C}_{19}\text{H}_{13}\text{FN}_2\text{O}_2\text{S}_2$ : 384.04; found: 385.31  $[\text{M}+\text{H}^+]$ .

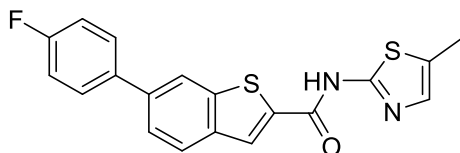
**N-(5-methylthiazol-2-yl)-6-phenylbenzo[b]thiophene-2-carboxamide (48)**



The title compound was obtained as a slightly yellow powder following the **general method B** (yield: 64%). Purification by flash chromatography eluting with DCM/MeOH

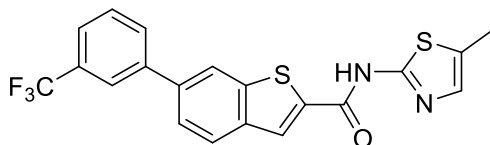
99:1.  $^1\text{H}$  NMR (600 MHz,  $\text{DMSO-}d_6$ ):  $\delta$  12.84 (s, 1H); 8.39 (s, 1H); 8.06-(d,  $J = 8.0$  Hz, 1H); 7.80-7.79 (m, 3H); 7.51 (m, 2H); 7.41 (t,  $J = 7.3$  Hz, 1H); 7.24 (s, 1H); 2.38 (s, 3H). HPLC-ESI-MS analysis: calculated for  $\text{C}_{19}\text{H}_{14}\text{N}_2\text{OS}_2$ : 350.45; found: 351.14 [ $\text{M}+\text{H}^+$ ].

#### 5-methylthiazol-2-yl 6-(4-fluorophenyl)benzo[b]thiophene-2-carboxylate (49)



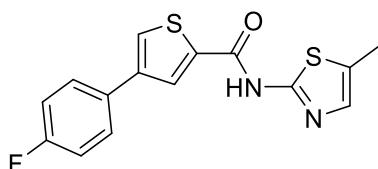
The title compound was obtained as a white yellow powder following the **general method B** (yield: 22%). Purification by flash chromatography eluting with DCM/MeOH 99:1.  $^1\text{H}$  NMR (600 MHz,  $\text{DMSO-}d_6$ ):  $\delta$  12.88 (s, 1H); 8.48 (s, 1H); 8.37 (s, 1H); 8.05 (d,  $J = 8.5$  Hz, 1H); 7.88–7.81 (m, 2H); 7.76 (dd,  $J_1 = 8.3$ ,  $J_2 = 1.3$  Hz, 1H); 7.35-7.32 (m, 2H); 7.23 (s, 1H); 2.37 (s, 3H). HPLC-ESI-MS analysis: calculated for  $\text{C}_{19}\text{H}_{13}\text{FN}_2\text{OS}_2$ : 368.06; found: 369.17 [ $\text{M}+\text{H}^+$ ].

#### N-(5-methylthiazol-2-yl)-6-(3-(trifluoromethyl)phenyl)benzo[b]thiophene-2-carboxamide (50)



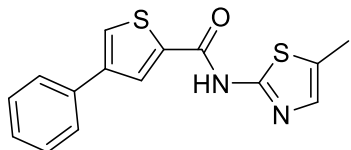
The title compound was obtained as a slightly yellow powder following the **general method B** (yield: 18%). Purification by flash chromatography eluting with DCM/MeOH 99:1.  $^1\text{H}$  NMR (400 MHz,  $\text{DMSO-}d_6$ ):  $\delta$  12.86 (s, 1H); 8.53-8.51 (m, 2H); 8.19-8.06 (m, 3H); 7.88 (d,  $J = 8.4$  Hz, 1H); 7.82–7.71 (m, 2H); 7.25 (s, 1H); 2.38 (s, 3H). HPLC-ESI-MS analysis: calculated for  $\text{C}_{20}\text{H}_{13}\text{F}_3\text{N}_2\text{OS}_2$ : 418.04; found: 419.21 [ $\text{M}+\text{H}^+$ ].

#### 4-(4-fluorophenyl)-N-(5-methylthiazol-2-yl)thiophene-2-carboxamide (51)



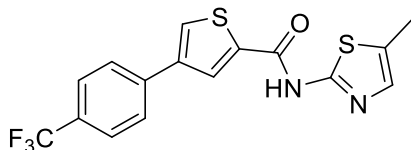
The title compound was obtained as a white powder following the **general method B** (yield: 62%). Purification by flash chromatography eluting with Petroleum Ether/EtOAc 80:20.  $^1\text{H}$  NMR (300 MHz,  $\text{DMSO-}d_6$ ):  $\delta$  12.54 (bs, 1H); 8.66 (s, 1H); 8.24 (s, 1H); 7.79-7.75 (m, 2H); 7.35-7.29 (m, 2H); 7.23 (s, 1H); 2.38 (s, 1H). HPLC-ESI-MS analysis: calculated for  $\text{C}_{15}\text{H}_{11}\text{FN}_2\text{OS}_2$ : 318.03; found: 319.19  $[\text{M}+\text{H}^+]$ .

#### **N-(5-methylthiazol-2-yl)-4-phenylthiophene-2-carboxamide (52)**



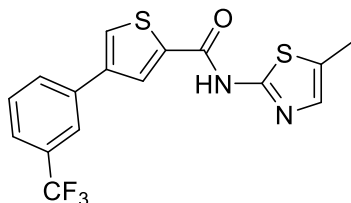
The title compound was obtained as a light yellow powder following the **general method B** (yield: 68%). Purification by flash chromatography eluting with 100% DCM.  $^1\text{H}$  NMR (600 MHz,  $\text{CDCl}_3$ ):  $\delta$  12.03 (s, 1H); 7.96 (m, 1H); 7.77 (m, 1H); 7.54-7.48 (m, 2H); 7.43-7.36 (m, 2H); 7.33-7.30 (m, 1H); 6.99 (s, 1H); 2.32 (s, 3H). HPLC-ESI-MS analysis: calculated for  $\text{C}_{15}\text{H}_{12}\text{N}_2\text{OS}_2$ : 300.04; found: 301.10  $[\text{M}+\text{H}^+]$ .

#### **N-(5-methylthiazol-2-yl)-4-(4-(trifluoromethyl)phenyl)thiophene-2-carboxamide (53)**



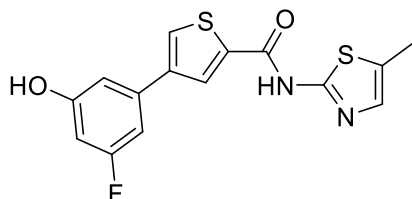
The title compound was obtained as a yellow powder following the **general method B** (yield: 50%). Purification by flash chromatography eluting with 100% DCM.  $^1\text{H}$  NMR (600 MHz,  $\text{CDCl}_3$ ):  $\delta$  11.69 (s, 1H); 7.99 (d,  $J = 1.5$  Hz, 1H); 7.81 (d,  $J = 1.4$ , 1H); 7.66 (d,  $J = 8.2$  Hz, 2H); 7.62 (d,  $J = 8.2$  Hz, 2H); 7.01 (d,  $J = 1.2$  Hz, 1H); 2.35 (s, 3H). HR-MS analysis: calculated for  $\text{C}_{16}\text{H}_{11}\text{F}_3\text{N}_2\text{OS}_2$ : 368.03; found: 369.17  $[\text{M}+\text{H}^+]$ .

#### **N-(5-methylthiazol-2-yl)-4-(3-(trifluoromethyl)phenyl)thiophene-2-carboxamide (54)**



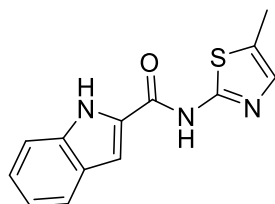
The title compound was obtained as a white powder following the **general method B** (yield: 50%). Purification by flash chromatography eluting with Petroleum Ether/EtOAc 80:20.  $^1\text{H NMR}$  (400 MHz,  $\text{DMSO-}d_6$ ):  $\delta$  12.53 (s, 1H); 8.78 (s, 1H); 8.48 (s, 1H); 8.07-8.05 (m, 2H); 7.73-7.72 (m, 2H); 7.24 (s, 1H); 2.38 (s, 3H). HPLC-ESI-MS analysis: calculated for  $\text{C}_{16}\text{H}_{11}\text{F}_3\text{N}_2\text{O}_5$ : 368.02; found: 369.17  $[\text{M}+\text{H}^+]$ .

#### 4-(3-fluoro-5-hydroxyphenyl)-N-(5-methylthiazol-2-yl)thiophene-2-carboxamide (55)



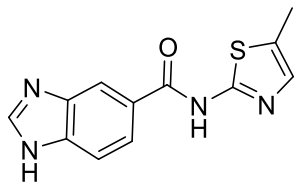
The title compound was obtained as a slightly yellow powder following the **general method B** (yield: 25%). Purification by flash chromatography eluting with DCM/MeOH 99:1.  $^1\text{H NMR}$  (600 MHz,  $\text{DMSO-}d_6$ ):  $\delta$  12.50 (s, 1H); 10.10 (s, 1H); 8.65 (s, 1H); 8.26 (s, 1H); 7.23 (s, 1H); 7.03-6.94 (m, 2H); 6.56-6.57 (dt,  $J_1 = 10.7$ ;  $J_2 = 2.2$  Hz; 2H); 2.37 (s, 3H). HPLC-ESI-MS analysis: calculated for  $\text{C}_{15}\text{H}_{11}\text{FN}_2\text{O}_2\text{S}_2$ : 334.02; found: 335.14  $[\text{M}+\text{H}^+]$ .

#### N-(5-methylthiazol-2-yl)-1H-indole-2-carboxamide (56)



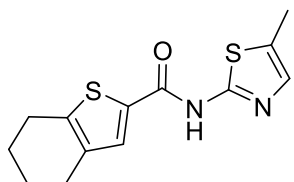
The title compound was obtained as a white powder following the **general method B** (yield: 24%). Purification by flash chromatography eluting with DCM/MeOH from 99:1 to 95:5.  $^1\text{H NMR}$  (300 MHz,  $\text{DMSO-}d_6$ ):  $\delta$  12.50 (s, 1H); 11.89 (s, 1H); 7.68-7.62 (m, 2H); 7.48 (d,  $J = 9$  Hz, 1H); 7.27-7.23 (m, 2H); 7.10-7.05 (m, 1H); 2.39 (s, 3H). HPLC-ESI-MS analysis: calculated for  $\text{C}_{13}\text{H}_{11}\text{N}_3\text{O}_2\text{S}$ : 257.06; found: 258.17  $[\text{M}+\text{H}^+]$ .

### N-(5-methylthiazol-2-yl)-1H-benzo[d]imidazole-5-carboxamide (57)



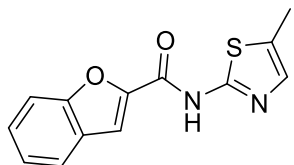
The title compound was obtained as a slightly yellow powder following the **general method B** (yield: 20%). Purification by flash chromatography eluting with DCM/MeOH from 99:1 to 95:5.  $^1\text{H}$  NMR (400 MHz,  $\text{DMSO-}d_6$ ):  $\delta$  12.88-12.77 (m, 1H); 12.37 (s, 1H); 8.50-8.33 (m, 2H); 7.96 (t,  $J = 8.8$  Hz, 1H); 7.76-7.63 (m, 1H); 7.22 (s, 1H); 2.39 (s, 3H). HPLC-ESI-MS analysis: calculated for  $\text{C}_{12}\text{H}_{10}\text{N}_4\text{OS}$ : 258.06; found: 259.24  $[\text{M}+\text{H}^+]$ .

### N-(5-methylthiazol-2-yl)-4,5,6,7-tetrahydrobenzo[b]thiophene-2-carboxamide (58)



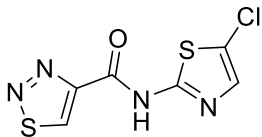
The title compound was obtained as a slightly yellow powder following the **general method B** (yield: 70%). Purification by flash chromatography eluting with DCM/MeOH 99.5:0.5.  $^1\text{H}$  NMR (600 MHz,  $\text{DMSO-}d_6$ ):  $\delta$  12.33 (s, 1H); 7.86 (s, 1H); 7.18 (s, 1H); 2.76 (t,  $J = 6.0$  Hz, 2H); 2.58 (t,  $J = 6.0$  Hz, 2H); 2.35 (s, 3H); 1.83-1.68 (m, 4H). HPLC-ESI-MS analysis: calculated for  $\text{C}_{13}\text{H}_{14}\text{N}_2\text{OS}$ : 278.05; found: 279.290  $[\text{M}+\text{H}^+]$ .

### N-(5-methylthiazol-2-yl)benzofuran-2-carboxamide (59)



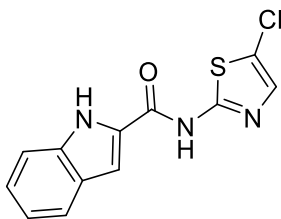
The title compound was obtained as a slightly yellow powder following the **general method B** (yield: 31%). Purification by flash chromatography eluting with Petroleum Ether/EtOAc 8:2.  $^1\text{H}$  NMR (400 MHz,  $\text{CDCl}_3$ ):  $\delta$  11.85 (s, 1H); 7.75 (d,  $J = 7.6$  Hz, 1H); 7.70 (s, 1H); 7.50-7.49 (m, 1H); 7.37-7.36 (m, 1H); 7.28-7.26 (m, 1H); 2.49 (s, 3H). HPLC-ESI-MS analysis: calculated for  $\text{C}_{13}\text{H}_{10}\text{N}_2\text{O}_2\text{S}$ : 258.05; found: 259.11  $[\text{M}+\text{H}^+]$ .

### N-(5-chlorothiazol-2-yl)-1,2,3-thiadiazole-4-carboxamide (61)



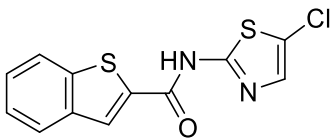
The title compound was obtained as a yellow powder following the **general method A** (yield: 6%). Purification by flash chromatography eluting with DCM/MeOH 98:2.  $^1\text{H}$  NMR (400 MHz, DMSO- $d_6$ ):  $\delta$  13.36 (s, 1H); 10.02 (s, 1H); 7.66 (s, 1H). HPLC-ESI-MS analysis: calculated for  $\text{C}_6\text{H}_3\text{ClN}_4\text{OS}_2$ : 245.94; found: 247.13  $[\text{M}+\text{H}^+]$ .

### N-(5-chlorothiazol-2-yl)-1H-indole-2-carboxamide (62)



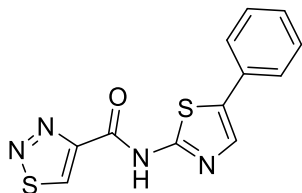
The title compound was obtained as a slightly yellow powder following the **general method C** (yield: 12%). Purification by flash column chromatography eluting with DCM/MeOH 99:1.  $^1\text{H}$  NMR (600 MHz, DMSO- $d_6$ ):  $\delta$  12.93 (s, 1H); 11.94 (s, 1H); 7.68 (d,  $J = 8.0$  Hz, 1H); 7.66 (s, 1H); 7.47 (t,  $J = 7.5$  Hz, 1H); 7.27 (t,  $J = 7.5$  Hz, 1H); 7.09 (t,  $J = 7.4$  Hz, 1H). HPLC-ESI-MS analysis: calculated for  $\text{C}_{12}\text{H}_8\text{ClN}_3\text{OS}$ : 277.01; found: 278.28  $[\text{M}+\text{H}^+]$ .

### N-(5-chlorothiazol-2-yl)benzo[b]thiophene-2-carboxamide (63)



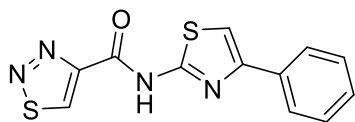
The title compound was obtained as a slightly yellow powder following the **general method C** (yield: 12%). Purification by flash chromatography eluting with 100% DCM and then DCM/MeOH 99:1.  $^1\text{H}$  NMR (400 MHz,  $\text{CDCl}_3$ ):  $\delta$  10.75 (s, 1H); 8.03 (s, 1H); 7.96-7.92 (m, 2H); 7.54-7.49 (m, 2H); 7.27 (s, 1H). HPLC-ESI-MS analysis: calculated for  $\text{C}_{12}\text{H}_7\text{ClN}_2\text{OS}_2$ : 293.97; found: 295.05  $[\text{M}+\text{H}^+]$ .

#### N-(5-phenylthiazol-2-yl)-1,2,3-thiadiazole-4-carboxamide (64)



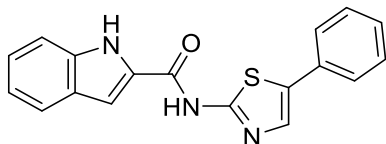
The title compound was obtained as a yellow powder following the **general method B** (yield: 12%). Purification by flash chromatography eluting with DCM/MeOH 99.5:0.5.  $^1\text{H}$  NMR (400 MHz, DMSO- $d_6$ ):  $\delta$  13.16 (s, 1H); 10.01 (s, 1H); 8.02 (s, 1H); 7.69 (d,  $J$  = 7.2 Hz, 2H); 7.46 (t,  $J$  = 7.2 Hz, 2H); 7.34 (t,  $J$  = 7.2 Hz, 1H).  $^{13}\text{C}$  NMR (100.6 MHz, DMSO):  $\delta$  161.8; 158.9; 147.3; 144.1; 142.5; 131.8; 129.7; 128.3; 126.6; 126.3. HR-MS analysis: calculated for  $\text{C}_{12}\text{H}_8\text{N}_4\text{OS}_2$ : 288.01; found: 289.25  $[\text{M}+\text{H}^+]$ .

#### N-(4-phenylthiazol-2-yl)-1,2,3-thiadiazole-4-carboxamide (65)



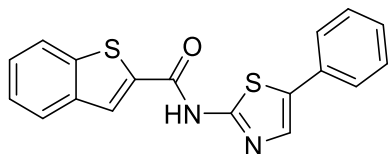
The title compound was obtained as a white powder following the **general method B** (yield: 23%). Purification by flash chromatography eluting with DCM/MeOH 99.9:0.1.  $^1\text{H}$  NMR (300 MHz, DMSO- $d_6$ ):  $\delta$  10.06 (s, 1H); 7.97-7.94 (m, 2H); 7.76 (s, 1H); 7.46 (bt,  $J$  = 6 Hz, 2H); 7.34 (bt,  $J$  = 6 Hz, 1H). HPLC-ESI-MS analysis: calculated for  $\text{C}_{12}\text{H}_8\text{N}_4\text{OS}_2$ : 288.01; found: 289.12  $[\text{M}+\text{H}^+]$ .

#### N-(5-phenylthiazol-2-yl)-1H-indole-2-carboxamide (66)



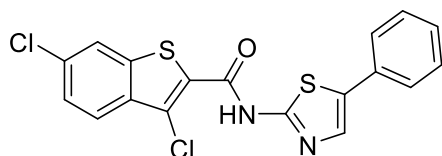
The title compound was obtained as a yellow powder following the **general method B** (yield: 25%). Purification by trituration with DCM and Diethyl Ether.  $^1\text{H}$  NMR (400 MHz, DMSO- $d_6$ ):  $\delta$  12.75 (s, 1H); 11.91 (s, 1H); 7.98 (s, 1H); 7.70-7.63 (m, 4H); 7.50-7.43 (m, 3H); 7.35-7.26 (m, 2H); 7.10 (t,  $J$  = 7.6 Hz, 1H). HPLC-ESI-MS analysis: calculated for  $\text{C}_{18}\text{H}_{13}\text{N}_3\text{OS}$ : 319.08; found: 320.26  $[\text{M}+\text{H}^+]$ .

### N-(5-phenylthiazol-2-yl)benzo[b]thiophene-2-carboxamide (67)



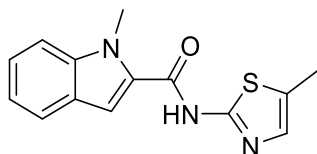
The title compound was obtained as a yellow powder following the **general method B** (yield: 30%). Purification by trituration with DCM.  $^1\text{H NMR}$  (600 MHz,  $\text{DMSO-}d_6$ ):  $\delta$  13.08 (s, 1H); 8.53 (s, 1H); 8.05 (d,  $J = 7.9$  Hz, 1H); 7.98 (d,  $J = 7.9$  Hz, 1H); 7.96 (s, 1H); 7.62 (dd,  $J_1 = 8.2$ ,  $J_2 = 1.0$  Hz, 2H); 7.52-7.47 (m, 1H); 7.46-7.43 (m, 1H); 7.41 (t,  $J = 7.8$ , 2H); 7.29 (t,  $J = 7.4$ , 1H). HPLC-ESI-MS analysis: calculated for  $\text{C}_{18}\text{H}_{12}\text{N}_2\text{OS}_2$ : 336.04; found: 337.34  $[\text{M}+\text{H}^+]$ .

### 3,6-dichloro-N-(5-phenylthiazol-2-yl)benzo[b]thiophene-2-carboxamide (68)



The title compound was obtained as a yellow powder following the **general method B** (yield: 30%). EtOAc and MeOH were added to the reaction mixture; after few minutes a precipitate occurred, and it was filtered off.  $^1\text{H NMR}$  (400 MHz,  $\text{DMSO-}d_6$ ):  $\delta$  13.36 (bs, 1H); 8.31 (s, 1H); 8.02 (s, 1H); 7.94 (d,  $J = 8.7$  Hz, 2H); 7.68 (d,  $J = 7.4$  Hz, 2H); 7.62 (dd,  $J_1 = 8.7$ ,  $J_2 = 1.6$  Hz, 1H); 7.46 (t,  $J = 7.6$  Hz, 2H); 7.36 (t,  $J = 7.3$  Hz, 1H). HPLC-ESI-MS analysis: calculated for  $\text{C}_{18}\text{H}_{10}\text{Cl}_2\text{N}_2\text{OS}_2$ : 403.96; found: 405.09  $[\text{M}+\text{H}^+]$ .

### Synthetic procedure to obtain 1-methyl-N-(5-methylthiazol-2-yl)-1H-indole-2-carboxamide (60)



NaH (2.00 eq) was added to a well-stirred solution of **56** (20 mg, 1.00 eq) in THF at 0 °C. The reaction was left stirred at room temperature for 1 h. After this time, the solution was cooled to 0 °C, and  $\text{CH}_3\text{I}$  (2.00 eq) was added dropwise. The reaction mixture was stirred at room temperature until the complete consumption of the starting material.



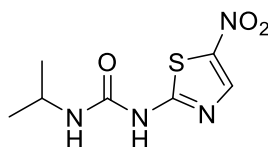
Then it was cooled to 0 °C and quenched with NH<sub>4</sub>Cl, and extracted with EtOAc (3 X 10 mL). The organic layers were collected, dried over anhydrous Na<sub>2</sub>SO<sub>4</sub>, filtered, and concentrated under reduced pressure. The crude was purified by flash column chromatography (Petroleum Ether/Ethyl Acetate from 7:3 to 5:5) to give the title compound as a yellow powder (yield: 70%). <sup>1</sup>H NMR (600 MHz, DMSO-*d*<sub>6</sub>): δ 11.49 (s, 1H); 7.61 (d, *J* = 8.0 Hz, 1H); 7.45 (d, *J* = 8.2 Hz, 1H); 7.25 (s, 1H); 7.8 (t, *J* = 7.9 Hz, 1H); 7.14-7.11 (m, 1H); 7.02 (t, *J* = 7.5 Hz, 1H); 3.78 (s, 3H); 2.28 (s, 3H). HPLC-ESI-MS analysis: calculated for C<sub>14</sub>H<sub>13</sub>N<sub>3</sub>OS: 271.08; found: 272.23 [M+H<sup>+</sup>].

### General procedure for the synthesis of urea derivatives

**Method A:** In a microwave tube, carbamate **26** (1.00 eq) and the aliphatic amine (1.5 eq) were dissolved in THF, and the reaction mixture was heated in a microwave reactor with the following parameters: 150 °C, 25 minutes, 300W, 250 psi, power max: off. At the end of the irradiation, water was added to the reaction mixture, and it was extracted with EtOAc (3 X 20 mL). The crude was purified by flash column chromatography (DCM/MeOH) to give the title compounds. Purification conditions, yields, and analytical data are reported below.

**Method B:** To a cold solution (0 °C) of phenyl isocyanate (82 mg, 0.69 mmol) in anhydrous DCM (2.90 mL/mmol) under N<sub>2</sub> atmosphere were added 5-nitrothiazole (100 mg, 0.69 mmol) and TEA (0.287 mL, 2.07 mmol). The reaction mixture was stirred at room temperature. After the complete consumption of the starting material, the reaction was poured into ice, and water was added. The aqueous phase was extracted with DCM (3 X 20 mL), and the organic layers were dried over anhydrous Na<sub>2</sub>SO<sub>4</sub>, filtered, and concentrated under reduced pressure. The crude material was purified by flash column chromatography. Purification conditions, yields, and analytical data are reported below.

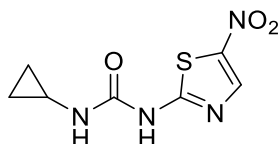
#### 1-isopropyl-3-(5-nitrothiazol-2-yl)urea (**27**)



The title compound was obtained as a yellow powder following the **general method A** (yield: 80%). Purification by flash column chromatography eluting with DCM/MeOH 99:1. <sup>1</sup>H NMR (400 MHz, DMSO-*d*<sub>6</sub>): δ 11.29 (s, 1H); 8.50 (s, 1H); 6.71 (d, *J* = 6 Hz, 1H);

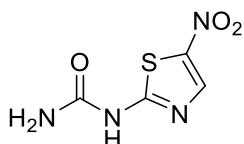
3.85-3.77 (m, 1H); 1.14 (d,  $J = 6.4$  Hz, 6H).  $^{13}\text{C}$  NMR (100.6 MHz,  $\text{DMSO-}d_6$ ):  $\delta$  164.7; 153.0; 144.0; 141.2; 42.4; 22.9. HR-MS analysis: calculated for  $\text{C}_7\text{H}_{10}\text{N}_4\text{O}_3\text{S}$ : 230.04; found: 231.18 [ $\text{M}+\text{H}^+$ ].

### 1-cyclopropyl-3-(5-nitrothiazol-2-yl)urea (28)



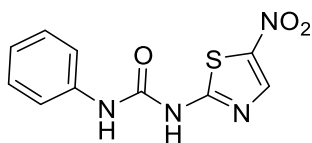
The title compound was obtained as a yellow powder following the **general method A** (yield: 48%). Purification by flash column chromatography eluting with 100% of DCM and then DCM/MeOH 99.5:0.5.  $^1\text{H}$  NMR (400 MHz,  $\text{DMSO-}d_6$ ):  $\delta$  11.43 (s, 1H); 8.51 (s, 1H); 7.03 (s, 1H); 2.64-2.60 (m, 1H); 0.72-0.68 (m, 2H); 0.52-0.48 (m, 2 H).  $^{13}\text{C}$  NMR (100.6 MHz,  $\text{DMSO-}d_6$ ):  $\delta$  164.7; 154.9; 143.8; 141.3; 23.0; 6.7. HR-MS analysis: calculated for  $\text{C}_7\text{H}_8\text{N}_4\text{O}_3\text{S}$ : 228.03; found: 229.23 [ $\text{M}+\text{H}^+$ ].

### 1-(5-nitrothiazol-2-yl)urea (29)



The title compound was obtained as a yellow powder following the **general method A** (yield: 35%). 1<sup>st</sup> Irradiation cycle: 10 min, 150 °C; 2<sup>nd</sup> Irradiation cycle: 10 min, 150 °C. Purification by flash column chromatography eluting with Petroleum Ether/ EtOAc 6:4.  $^1\text{H}$  NMR (400 MHz,  $\text{DMSO-}d_6$ ):  $\delta$  11.55 (s, 1H); 8.51 (s, 1H); 7.16 (bs, 2H).  $^{13}\text{C}$  NMR (100.6 MHz,  $\text{DMSO-}d_6$ ):  $\delta$  164.7; 154.4; 143.7; 141.2. HPLC-ESI-MS analysis: calculated for  $\text{C}_4\text{H}_4\text{N}_4\text{O}_3\text{S}$ : 188.00; found: 189.19 [ $\text{M}+\text{H}^+$ ].

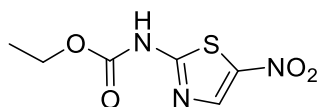
### Synthetic procedure to obtain 1-(5-nitrothiazol-2-yl)-3-phenylurea (30)



The title compound was obtained as an orange powder following the **general method B** (yield: 10%). Purification by flash column chromatography eluting with DCM/MeOH

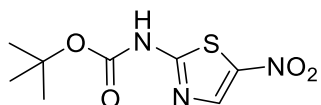
98:2.  $^1\text{H}$  NMR (300 MHz,  $\text{DMSO-}d_6$ ):  $\delta$  9.26 (s, 1H); 8.55 (s, 1H); 7.53 (d,  $J = 9$  Hz, 2H); 7.37 (t,  $J = 9$  Hz, 2H); 7.07 (t,  $J = 9$  Hz, 1H). HPLC-ESI-MS analysis: calculated for  $\text{C}_{10}\text{H}_8\text{N}_4\text{O}_3\text{S}$ : 264.03; found: 265.04  $[\text{M}+\text{H}^+]$ .

### Ethyl (5-nitrothiazol-2-yl)carbamate (24)



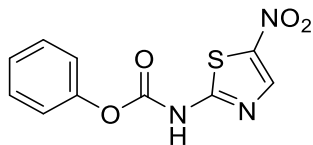
2-amino-5-nitrothiazole (**70 I**) (250 mg, 1.72 mmol) was dissolved in THF, and then Ethyl Chloroformate (202 mg, 1.86 mmol) was added. The reaction mixture was refluxed overnight. The solvent was evaporated under reduced pressure, and the crude was purified by flash column chromatography (Petroleum Ether/EtOAc from 85:15 to 80:20) to give the title compound as a white powder (yield: 31%).  $^1\text{H}$  NMR (400 MHz,  $\text{DMSO-}d_6$ ):  $\delta$  12.85 (s, 1H); 8.56 (s, 1H); 4.29 (q,  $J = 7.1$  Hz, 2H); 1.29 (t,  $J = 7.1$  Hz, 3H).  $^{13}\text{C}$  NMR (100.6 MHz,  $\text{CDCl}_3$ ):  $\delta$  164.6; 152.9; 143.3; 140.1; 63.9; 14.4. HPLC-ESI-MS analysis: calculated for  $\text{C}_6\text{H}_7\text{N}_3\text{O}_4\text{S}$ : 217.02; found: 218.07  $[\text{M}+\text{H}^+]$ .

### Synthetic procedure to obtain Tert-butyl (5-nitrothiazol-2-yl)carbamate (25)



2-amino-5-nitrothiazole (**70 I**) (500 mg, 3.44 mmol), DMAP (3.43 mg, 0.028 mmol), di-tert-butyl dicarbonate (826 mg, 3.78 mmol), TEA (0.16 mL/mmol) were suspended in anhydrous THF (0.5 mL/mmol). The reaction mixture was stirred at room temperature overnight. Then, DCM was added, and the reaction mixture was washed with 0.1 N aq. HCl, and water. The organic layer was dried over anhydrous  $\text{Na}_2\text{SO}_4$ , filtered, and concentrated under reduced pressure. The crude was purified by flash column chromatography (Petroleum Ether/EtOAc 7:3) to give the title compound as an orange powder (yield: 58%).  $^1\text{H}$  NMR (400 MHz,  $\text{DMSO-}d_6$ ):  $\delta$  12.58 (bs, 1H); 8.53 (s, 1H); 1.56 (s, 9H).  $^{13}\text{C}$  NMR (100.6 MHz,  $\text{CDCl}_3$ ):  $\delta$  164.8; 153.2; 143.8; 142.1; 83.7; 28.2. HR-MS analysis: calculated for  $\text{C}_8\text{H}_{11}\text{N}_3\text{O}_4\text{S}$ : 245.01; found: 246.11  $[\text{M}+\text{H}^+]$ .

## Synthetic procedure to obtain Phenyl (5-nitrothiazol-2-yl)carbamate (26)



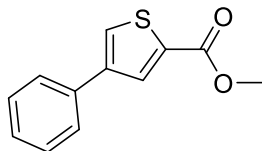
2-amino-5-nitrothiazole (**70 I**) (400 mg, 2.76 mmol) and pyridine (0.267 mL, 3.31 mmol) were dissolved in anhydrous DCM (1mL/mmol), and then phenyl chloroformate (518 mg, 3.31) was added dropwise under N<sub>2</sub> atmosphere at 0 °C. The reaction mixture was stirred at room temperature for 90 minutes.

After the consumption of starting material, water was added to the reaction mixture, and it was extracted with EtOAc (3 X 20 mL). Organic layers were collected, dried over anhydrous Na<sub>2</sub>SO<sub>4</sub>, filtered, and concentrated under reduced pressure. The crude was purified by flash column chromatography (Petroleum Ether/EtOAc 8:2) to give the title compound as a yellow powder (yield: 52%). <sup>1</sup>H NMR (400 MHz, DMSO-*d*<sub>6</sub>): δ 13.41 (s, 1H); 8.63 (s, 1H); 7.48-7.46 (m, 2H); 7.34-7.31 (m, 3H). <sup>13</sup>C NMR (100.6 MHz, DMSO): 164.64; 153.12; 150.31; 143.62; 142.76; 130.19; 126.96; 122.12. HR-MS analysis: calculated for C<sub>10</sub>H<sub>7</sub>N<sub>3</sub>O<sub>4</sub>S: 265.01; found: 266.11 [M+H<sup>+</sup>].

## General procedure for the Suzuki-Miyaura Cross-Coupling Reaction

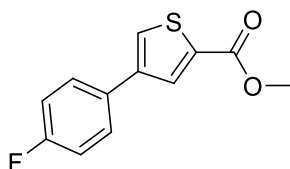
To a solution of methyl 4-bromothiophene-2-carboxylate (**72**) or methyl 6-bromobenzo[*b*]thiophene-2-carboxylate (**73**) (1.00 eq) in THF/H<sub>2</sub>O (3:1, 10 mL/mmol) were added the appropriate boronic acid or ester (1.5 eq) and potassium phosphate tribasic (2.00 eq). The mixture was stirred under a nitrogen atmosphere for 10 minutes. After this time, X-Phos Pd G2 (0.15 eq) was added, and the reaction mixture was stirred at 70 °C for 2 hours. After cooling to room temperature, the reaction mixture was filtered through a plug of celite. The filtrate was concentrated under reduced pressure, and the residue was extracted with EtOAc (3 X 20 mL), dried over anhydrous Na<sub>2</sub>SO<sub>4</sub>, filtered, and concentrated under reduced pressure. The crude was purified by flash column chromatography eluting with Petroleum Ether/EtOAc. Purification conditions, yields, and analytical data are reported in the supporting information.

### Methyl 4-phenylthiophene-2-carboxylate (73 a)



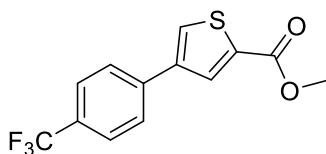
Purification by flash column chromatography eluting with Petroleum Ether/EtOAc from 99:1 to 98:2 allowed the isolation of the product as a white powder (yield: 64%).  $^1\text{H}$  NMR (400 MHz,  $\text{CDCl}_3$ ):  $\delta$  8.11 (d,  $J = 1.5$  Hz, 1H); 7.68 (d,  $J = 1.5$  Hz, 1H); 7.61 (d,  $J = 7.3$  Hz, 2H); 7.44 (t,  $J = 7.6$  Hz, 2H); 7.35 (d,  $J = 7.4$  Hz, 1H); 3.84 (s, 3H).

### Methyl 4-(4-fluorophenyl)thiophene-2-carboxylate (73 b)



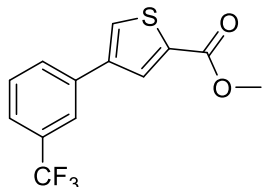
Purification by flash column chromatography eluting with Petroleum Ether/EtOAc 99:1 allowed the isolation of the product as a white powder (yield: 93%).  $^1\text{H}$  NMR (300 MHz,  $\text{DMSO}-d_6$ ):  $\delta$  8.26 (d,  $J = 1.8$  Hz, 1H); 8.23 (d,  $J = 1.5$  Hz, 1H); 7.86-7.82 (m, 2H); 7.29-7.24 (m, 2H); 3.86 (s, 3H).

### Methyl 4-(4-(trifluoromethyl)phenyl)thiophene-2-carboxylate (73 c)



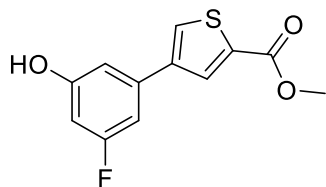
Purification by flash column chromatography eluting with Petroleum Ether/EtOAc 99:1 allowed the isolation of the product (yield: 47%).  $^1\text{H}$  NMR (400 MHz,  $\text{DMSO}-d_6$ ):  $\delta$  8.47 (d,  $J = 1.8$  Hz, 1H); 8.23 (d,  $J = 1.5$  Hz, 1H); 7.86-7.82 (m, 2H); 7.29-7.24 (m, 2H); 3.86 (s, 3H).

### Methyl 4-(3-(trifluoromethyl)phenyl)thiophene-2-carboxylate (73 d)



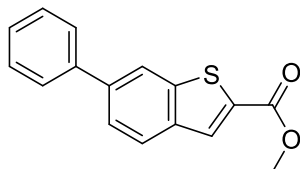
Purification by flash column chromatography eluting with Petroleum Ether/EtOAc 98:2 allowed the isolation of the product (yield: 65%).  $^1\text{H NMR}$  (300 MHz,  $\text{DMSO-}d_6$ ):  $\delta$  8.49 (d,  $J = 1.5$  Hz, 1H); 8.39 (d,  $J = 1.5$  Hz, 1H); 8.15-8.11 (m, 2H); 7.71-7.64 (m, 2H); 3.86 (s, 3H).

### Methyl 4-(3-fluoro-5-hydroxyphenyl)thiophene-2-carboxylate (73 e)



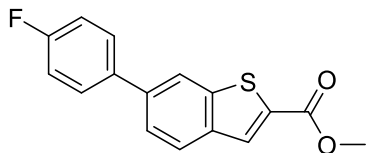
Purification by flash column chromatography eluting with Petroleum Ether/EtOAc 90:10 allowed the isolation of the product (yield: 78%).  $^1\text{H NMR}$  (300 MHz,  $\text{DMSO-}d_6$ ):  $\delta$  10.06 (s, 1H); 8.28 (d,  $J = 1.8$  Hz, 1H); 8.16 (d,  $J = 1.5$  Hz, 1H); 7.10-7.06 (m, 1H); 6.98-6.97 (m, 1H); 6.57-6.53 (m, 1H); 3.85 (s, 3H).

### Methyl 6-phenylbenzo[b]thiophene-2-carboxylate (74 a)



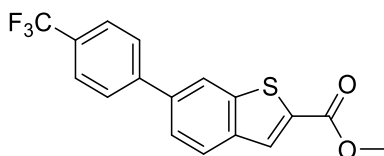
Purification by flash column chromatography eluting with Petroleum Ether/EtOAc 90:10 allowed the isolation of the product (yield: 57%).  $^1\text{H NMR}$  (600 MHz,  $\text{DMSO-}d_6$ ):  $\delta$  8.40 (s, 1H), 8.24 (s, 1H); 8.11 (d,  $J = 8.4$  Hz, 1H); 7.81-7.78 (m, 3H); 7.51 (t,  $J = 7.6$  Hz, 2H); 7.41 (t,  $J = 7.4$  Hz, 1H); 3.90 (s, 3H).

### Methyl 6-(4-fluorophenyl)benzo[b]thiophene-2-carboxylate (74 b)



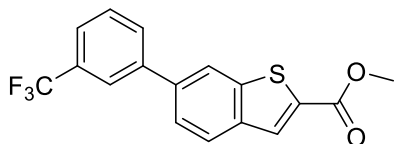
Purification by flash column chromatography eluting with Petroleum Ether/EtOAc 90:10 allowed the isolation of the product (yield: 76%).  $^1\text{H NMR}$  (600 MHz,  $\text{DMSO-}d_6$ ):  $\delta$  8.39 (s, 1H); 8.24 (s, 1H); 8.10 (d,  $J = 8.5$  Hz, 1H); 7.85-7.82 (m, 2H); 7.78 (dd,  $J_1 = 8.4$ ,  $J_2 = 1.6$  Hz, 1H); 7.36-7.32 (m, 2H); 3.90 (s, 3H).

### Methyl 6-(4-(trifluoromethyl)phenyl)benzo[b]thiophene-2-carboxylate (74 c)



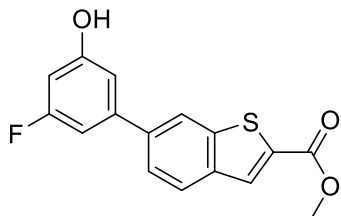
Purification by Combiflash<sup>®</sup> eluting with Petroleum Ether/EtOAc allowed the isolation of the product (yield: 87%).  $^1\text{H NMR}$  (400 MHz,  $\text{DMSO-}d_6$ ):  $\delta$  8.50 (s, 1H); 8.26 (s, 1H); 8.16 (d,  $J = 8.4$  Hz, 1H); 8.02 (d,  $J = 8$  Hz, 2H); 7.87-7.785 (m, 3H); 3.91 (s, 3H).

### Methyl 6-(3-(trifluoromethyl)phenyl)benzo[b]thiophene-2-carboxylate (74 d)



Purification by flash column chromatography eluting with Petroleum Ether/EtOAc 95:5 allowed the isolation of the product (yield: 78%).  $^1\text{H NMR}$  (600 MHz,  $\text{DMSO-}d_6$ ):  $\delta$  8.53 (s, 1H); 8.26 (s, 1H), 8.17-8.09 (m, 3H); 7.88 (d,  $J = 8.3$  Hz, 1H); 7.78-7.73 (m, 2H); 7.54-7.49 (m, 2H); 3.91 (s, 3H).

### Methyl 6-(3-fluoro-5-hydroxyphenyl)benzo[b]thiophene-2-carboxylate (74 e)

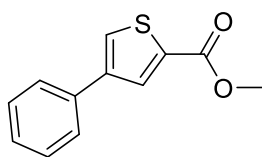


Purification by Combiflash<sup>®</sup> eluting with Petroleum Ether/EtOAc allowed the isolation of the product as a brown powder (yield: 88%). <sup>1</sup>H NMR (400 MHz, DMSO-*d*<sub>6</sub>): δ 8.38 (s, 1H); 8.24 (s, 1H); 8.11 (d, *J* = 8.4 Hz, 1H); 7.76 (d, *J* = 8.4 Hz, 1H); 7.07 (d, *J* = 10 Hz, 1H); 7.00 (s, 1H); 6.63 (d, *J* = 10.4 Hz, 1H); 2.51 (s, 3H).

### General procedure for the hydrolysis of the carboxylic esters

LiOH (4.00 eq) was added to a solution of the proper carboxylic ester (1.00 eq) in THF/MeOH/H<sub>2</sub>O (3:1:1), and the reaction mixture was stirred at room temperature for 2 hours. 1 N aq.HCl was added to the mixture until acid pH. When a precipitate occurs, it was filtered off. Otherwise, the mixture was extracted with EtOAc (4 X 10 mL), and the organic layers were dried over anhydrous Na<sub>2</sub>SO<sub>4</sub>, filtered, and concentrated under reduced pressure. The product was used in the next step without further purification. Yields and analytical data are reported below.

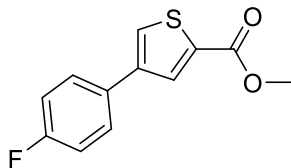
### Methyl 4-phenylthiophene-2-carboxylate (73 a)



Purification by flash column chromatography eluting with Petroleum Ether/EtOAc from 99:1 to 98:2 allowed the isolation of the product as a white powder (yield: 64%). <sup>1</sup>H NMR (400 MHz, CDCl<sub>3</sub>): δ 8.11 (d, *J* = 1.5 Hz, 1H); 7.68 (d, *J* = 1.5 Hz, 1H); 7.61 (d, *J* = 7.3 Hz, 2H); 7.44 (t, *J* = 7.6 Hz, 2H); 7.35 (d, *J* = 7.4 Hz, 1H); 3.84 (s, 3H).

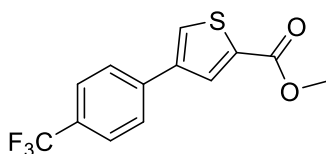


### Methyl 4-(4-fluorophenyl)thiophene-2-carboxylate (73 b)



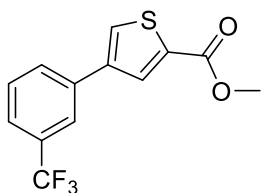
Purification by flash column chromatography eluting with Petroleum Ether/EtOAc 99:1 allowed the isolation of the product as a white powder (yield: 93%).  $^1\text{H NMR}$  (300 MHz,  $\text{DMSO-}d_6$ ):  $\delta$  8.26 (d,  $J = 1.8$  Hz, 1H); 8.23 (d,  $J = 1.5$  Hz, 1H); 7.86-7.82 (m, 2H); 7.29-7.24 (m, 2H); 3.86 (s, 3H).

### Methyl 4-(4-(trifluoromethyl)phenyl)thiophene-2-carboxylate (73 c)



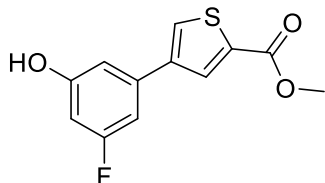
Purification by flash column chromatography eluting with Petroleum Ether/EtOAc 99:1 allowed the isolation of the product (yield: 47%).  $^1\text{H NMR}$  (400 MHz,  $\text{DMSO-}d_6$ ):  $\delta$  8.47 (d,  $J = 1.8$  Hz, 1H); 8.23 (d,  $J = 1.5$  Hz, 1H); 7.86-7.82 (m, 2H); 7.29-7.24 (m, 2H); 3.86 (s, 3H).

### Methyl 4-(3-(trifluoromethyl)phenyl)thiophene-2-carboxylate (73 d)



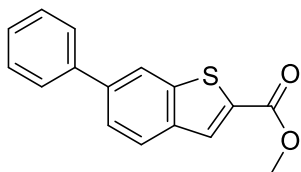
Purification by flash column chromatography eluting with Petroleum Ether/EtOAc 98:2 allowed the isolation of the product (yield: 65%).  $^1\text{H NMR}$  (300 MHz,  $\text{DMSO-}d_6$ ):  $\delta$  8.49 (d,  $J = 1.5$  Hz, 1H); 8.39 (d,  $J = 1.5$  Hz, 1H); 8.15-8.11 (m, 2H); 7.71-7.64 (m, 2H); 3.86 (s, 3H).

### Methyl 4-(3-fluoro-5-hydroxyphenyl)thiophene-2-carboxylate (73 d)



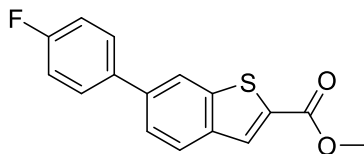
Purification by flash column chromatography eluting with Petroleum Ether/EtOAc 90:10 allowed the isolation of the product (yield: 78%).  $^1\text{H}$  NMR (300 MHz,  $\text{DMSO-}d_6$ ):  $\delta$  10.06 (s, 1H); 8.28 (d,  $J = 1.8$  Hz, 1H); 8.16 (d,  $J = 1.5$  Hz, 1H); 7.10-7.06 (m, 1H); 6.98-6.97 (m, 1H); 6.57-6.53 (m, 1H); 3.85 (s, 3H).

### Methyl 6-phenylbenzo[b]thiophene-2-carboxylate (74 a)



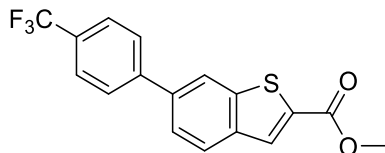
Purification by flash column chromatography eluting with Petroleum Ether/EtOAc 90:10 allowed the isolation of the product (yield: 57%).  $^1\text{H}$  NMR (600 MHz,  $\text{DMSO-}d_6$ ):  $\delta$  8.40 (s, 1H), 8.24 (s, 1H); 8.11 (d,  $J = 8.4$  Hz, 1H); 7.81-7.78 (m, 3H); 7.51 (t,  $J = 7.6$  Hz, 2H); 7.41 (t,  $J = 7.4$  Hz, 1H); 3.90 (s, 3H).

### Methyl 6-(4-fluorophenyl)benzo[b]thiophene-2-carboxylate (74 b)



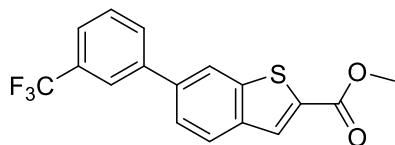
Purification by flash column chromatography eluting with Petroleum Ether/EtOAc 90:10 allowed the isolation of the product (yield: 76%).  $^1\text{H}$  NMR (600 MHz,  $\text{DMSO-}d_6$ ):  $\delta$  8.39 (s, 1H); 8.24 (s, 1H); 8.10 (d,  $J = 8.5$  Hz, 1H); 7.85-7.82 (m, 2H); 7.78 (dd,  $J_1 = 8.4$ ,  $J_2 = 1.6$  Hz, 1H); 7.36-7.32 (m, 2H); 3.90 (s, 3H).

**Methyl 6-(4-(trifluoromethyl)phenyl)benzo[b]thiophene-2-carboxylate (74 c)**



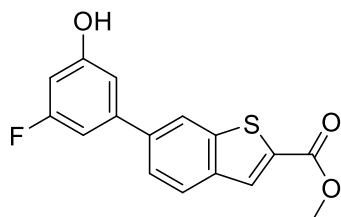
Purification by Combiflash® eluting with Petroleum Ether/EtOAc allowed the isolation of the product (yield: 87%). <sup>1</sup>H NMR (400 MHz, DMSO-*d*<sub>6</sub>): δ 8.50 (s, 1H); 8.26 (s, 1H); 8.16 (d, *J* = 8.4 Hz, 1H); 8.02 (d, *J* = 8 Hz, 2H); 7.87-7.7.85 (m, 3H); 3.91 (s, 3H).

**Methyl 6-(3-(trifluoromethyl)phenyl)benzo[b]thiophene-2-carboxylate (74 d)**



Purification by flash column chromatography eluting with Petroleum Ether/EtOAc 95:5 allowed the isolation of the product (yield: 78%). <sup>1</sup>H NMR (600 MHz, DMSO-*d*<sub>6</sub>): δ 8.53(s, 1H); 8.26 (s, 1H), 8.17-8.09 (m, 3H); 7.88 (d, *J* = 8.3 Hz, 1H); 7.78-7.73 (m, 2H); 7.54–7.49 (m, 2H); 3.91 (s, 3H).

**Methyl 6-(3-fluoro-5-hydroxyphenyl)benzo[b]thiophene-2-carboxylate (74 e)**

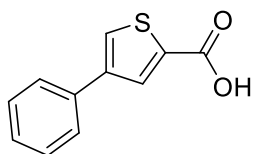


Purification by Combiflash® eluting with Petroleum Ether/EtOAc allowed the isolation of the product as a brown powder (yield: 88%). <sup>1</sup>H NMR (400 MHz, DMSO-*d*<sub>6</sub>): δ 8.38 (s, 1H); 8.24 (s, 1H); 8.11 (d, *J* = 8.4 Hz, 1H); 7.76 (d, *J* = 8.4 Hz, 1H); 7.07 (d, *J* = 10 Hz, 1H); 7.00 (s, 1H); 6.63 (d, *J* = 10.4 Hz, 1H); 2.51 (s, 3H).

## Compounds obtained *via* a hydrolysis reaction

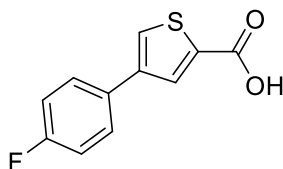
LiOH (4.00 eq) was added to a solution of the proper carboxylic ester (1.00 eq) in THF/MeOH/H<sub>2</sub>O (3:1:1), and the reaction mixture was stirred at room temperature for 2 hours. 1 N aq. HCl was added to the mixture until acid pH. When a precipitate occurred, it was filtered off. Otherwise, the mixture was extracted with EtOAc (x4), and the organic layers were dried over anhydrous Na<sub>2</sub>SO<sub>4</sub>, filtered, and concentrated under reduced pressure. The product was used in the next step without further purification. Yields and analytical data are reported below.

### 4-phenylthiophene-2-carboxylic acid (75 a)



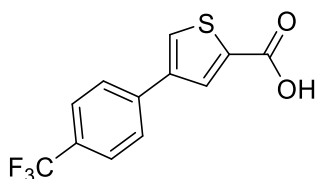
Yield: 35%. <sup>1</sup>H NMR (600 MHz, DMSO-*d*<sub>6</sub>): δ 13.22 (bs, 1H); 8.19 (s, 1H); 8.13 (s, 1H); 7.75 (d, *J* = 7.4 Hz, 2H); 7.43 (t, *J* = 7.7, Hz 2H); 7.33 (t, *J* = 7.3 Hz, 1H).

### 4-(4-fluorophenyl)thiophene-2-carboxylic acid (75 b)



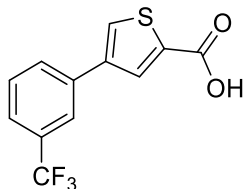
Yield: 74%. <sup>1</sup>H NMR (300 MHz, DMSO-*d*<sub>6</sub>): δ 13.40 (bs, 1H); 8.35 (d, *J* = 1.8 Hz, 1H); 8.28 (d, *J* = 1.5 Hz, 1H); 7.89-7.86 (m, 2H); 7.32-7.46 (m, 2H).

### 4-(4-(trifluoromethyl)phenyl)thiophene-2-carboxylic acid (75 c)



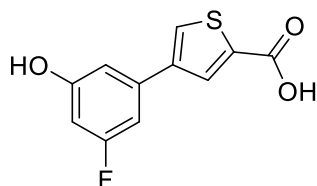
Yield: 78%. <sup>1</sup>H NMR (600 MHz, DMSO-*d*<sub>6</sub>): δ 13.27 (bs, 1H); 8.37 (d, *J* = 1.6 Hz, 1H); 8.20 (d, *J* = 1.6 Hz, 1H); 7.78 (d, *J* = 8.1 Hz, 2H); 7.76 (d, *J* = 8.2 Hz, 2H).

**4-(3-(trifluoromethyl)phenyl)thiophene-2-carboxylic acid (75 d)**



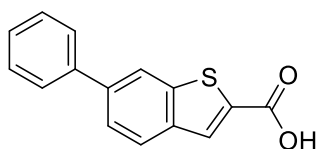
Yield: 63%.  $^1\text{H NMR}$  (300 MHz,  $\text{DMSO-}d_6$ ):  $\delta$  13.33 (bs, 1H); 8.42 (d,  $J = 1.8$  Hz, 1H); 8.27 (d,  $J = 1.8$  Hz, 1H); 8.13-8.09 (m, 2H); 7.69-7.66 (m, 2H).

**4-(3-fluoro-5-hydroxyphenyl)thiophene-2-carboxylic acid (75 e)**



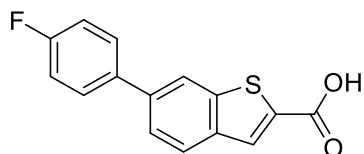
Yield: 87%.  $^1\text{H NMR}$  (300 MHz,  $\text{DMSO-}d_6$ ):  $\delta$  13.18 (bs, 1H); 10.05 (s, 1H); 8.21 (d,  $J = 1.8$  Hz, 1H); 8.05 (d,  $J = 1.5$  Hz, 1H); 7.08-7.03 (m, 1H); 6.95 (t,  $J = 1.8$  Hz, 1H); 6.56-6.51 (m, 1H).

**6-phenylbenzo[b]thiophene-2-carboxylic acid (76 a)**



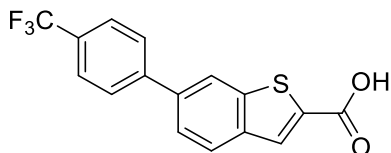
Quantitative yield.  $^1\text{H NMR}$  (600 MHz,  $\text{DMSO-}d_6$ ):  $\delta$  13.49 (bs, 1H); 8.39-8.36 (m, 1H); 8.14 (s, 1H); 8.08 (d,  $J = 8.3$  Hz, 1H); 7.79-7.77 (m, 3H); 7.54-7.49 (m, 2H), 7.42-7.40 (m, 1H)

**6-(4-fluorophenyl)benzo[b]thiophene-2-carboxylic acid (76 b)**



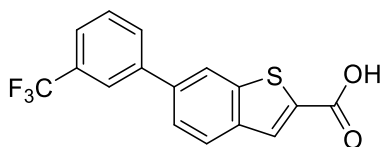
Yield: 92%.  $^1\text{H}$  NMR (400 MHz,  $\text{DMSO-}d_6$ ):  $\delta$  13.49 (bs, 1H); 8.36 (s, 1H); 8.13 (s, 1H); 8.08 (d,  $J = 8.4$  Hz, 1H); 7.85–7.81 (m, 2H); 7.77 (dd,  $J_1 = 8.4$ ,  $J_2 = 1.2$  Hz, 1H); 7.36–7.32 (m, 2H).

**6-(4-(trifluoromethyl)phenyl)benzo[b]thiophene-2-carboxylic acid (76 c)**



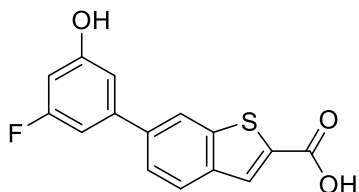
Yield: 60%.  $^1\text{H}$  NMR (600 MHz,  $\text{DMSO-}d_6$ ):  $\delta$  8.47 (s, 1H); 8.14–8.11 (m, 2H); 8.02 (d,  $J = 8.1$  Hz, 1H); 7.86–7.83 (m, 3H).

**6-(3-(trifluoromethyl)phenyl)benzo[b]thiophene-2-carboxylic acid (76 d)**



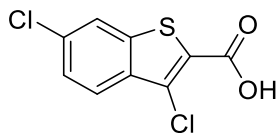
Yield: 76%.  $^1\text{H}$  NMR (400 MHz,  $\text{DMSO-}d_6$ ):  $\delta$  8.28 (s, 1H); 8.07 (m, 2H); 7.90 (d,  $J = 8.3$  Hz, 1H); 7.75–7.66 (m, 3H); 7.53 (s, 1H).

**6-(3-fluoro-5-hydroxyphenyl)benzo[b]thiophene-2-carboxylic acid (76 e)**



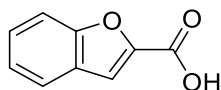
Yield: 44%; brown powder.  $^1\text{H}$  NMR (400 MHz,  $\text{DMSO-}d_6$ ):  $\delta$  13.51 (bs, 1H); 10.11 (s, 1H); 8.35 (s, 1H); 8.14 (s, 1H); 8.07 (d,  $J = 8.5$  Hz, 1H); 7.73 (d,  $J = 8.5$  Hz, 1H); 7.05 (d,  $J = 10.0$  Hz, 1H); 6.61 (d,  $J = 10.7$  Hz, 1H).

**3,6-dichlorobenzo[b]thiophene-2-carboxylic acid (83)**



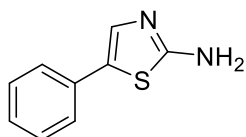
Quantitative yield. White powder.  $^1\text{H}$  NMR (400 MHz, DMSO):  $\delta$  14.01 (bs, 1H); 8.33 (d,  $J = 1.8$  Hz, 1H); 7.95 (d,  $J = 8.7$  Hz, 1H); 7.63 (dd,  $J_1 = 8.7$ ,  $J_2 = 1.9$  Hz, 1H).

### Benzofuran-2-carboxylic acid (84)



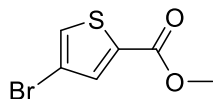
Quantitative yield.  $^1\text{H}$  NMR (300 MHz, DMSO- $d_6$ ):  $\delta$  13.79 (bs, 1H); 7.81-7.80 (m, 1H); 7.72-7.67 (m, 2H); 7.53-7.48 (m, 1H); 7.38-7.33 (m, 1H).

### Synthetic procedure to obtain 5-phenylthiazol-2-amine (70 V)



To a solution of phenylacetaldehyde (2.0 g, 16.65 mmol) in DCM (1 mL/mmol), a solution of  $\text{Br}_2$  (0.854 mL, 16.65 mmol) in DCM (0.6 mL/mmol) was added dropwise. After consumption of the starting material according to TLC, the solvent was removed in vacuo, having care not to heat the bath more than 20 °C to prevent the evaporation of the brominated compound. Without further purification, the red crude oil obtained was quickly reacted with thiourea (2.38 g, 31.32 mmol) in absolute ethanol (1 mL/mmol) at reflux overnight. The mix was recrystallized with 30% MeOH in water to obtain the title compound as a pale-yellow powder (yield: 20%).  $^1\text{H}$  NMR (400 MHz, DMSO- $d_6$ ):  $\delta$  7.42-7.39 (m, 3H); 7.33 (t,  $J = 7.6$  Hz, 2H); 7.20-7.16 (m, 1H); 7.13 (s, 2H). HR-MS analysis: calculated for  $\text{C}_9\text{H}_8\text{N}_2\text{S}$ : 176.04; found: 177.21 [ $\text{M}+\text{H}^+$ ].

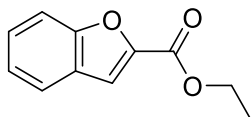
### Synthetic procedure to obtain Methyl 4-bromothiophene-2-carboxylate (72)



A mixture of 4-bromothiophene-2-carboxylic acid (500 mg, 2.42 mmol),  $\text{K}_2\text{CO}_3$  (700 mg, 5.07 mmol), and  $\text{CH}_3\text{I}$  (0.451 mL, 1.25 mmol) in DMF (2 mL/mmol) was stirred at room temperature overnight. Water was added to the reaction mixture, and it was extracted with EtOAc (3 X 30 mL). The organic layers were dried over anhydrous  $\text{Na}_2\text{SO}_4$ , filtered,

and concentrated under reduced pressure. The product was used in the next step without further purification (yield: 70%).  $^1\text{H NMR}$  (400 MHz,  $\text{CDCl}_3$ ):  $\delta$  7.71 (s, 1H); 7.47 (s, 1H); 3.20 (s, 3H).

### Synthetic procedure to obtain Ethyl benzofuran-2-carboxylate (85)



Ethyl bromoacetate (470 mg, 2.87 mmol) and  $\text{K}_2\text{CO}_3$  (792 mg, 5.73 mmol) were added to a solution of Salicylaldehyde (0.300 mL, 2.87 mmol) in dry DMF. The reaction mixture was stirred at 130 °C until the complete consumption of the starting material.  $\text{H}_2\text{O}$  was added to the reaction mixture, and it was extracted with EtOAc (3 X 30 mL). The organic layers were dried over anhydrous  $\text{Na}_2\text{SO}_4$ , filtered, and concentrated under reduced pressure. The crude was purified by flash column chromatography (Petroleum Ether/Diethyl Ether 98:2) to give the title compound (yield: 35 %).  $^1\text{H NMR}$  (400 MHz,  $\text{CDCl}_3$ ):  $\delta$  7.70 (d,  $J = 8.0$  Hz, 1H); 7.61 (d,  $J = 8.4$  Hz, 1H); 7.54 (s, 1H); 7.4 -7.43(m, 1H); 7.32-7.29 (m, 1H); 4.47 (q,  $J = 7.2$  Hz, 2H); 1.44 (t,  $J = 7.2$  Hz, 3H).

### 3.2.6.2. Biology

#### Activity assay

SAT was expressed recombinantly in *E. coli* using published methods.<sup>81</sup>

The concentration of SAT was 70 nM, the buffer was 20 mM sodium phosphate, 85 mM NaCl, and 1 mM EDTA, pH 7.0. The compounds were first screened at a fixed 100  $\mu\text{M}$  concentration. Only those compounds showing a residual activity lower than 50 % were subjected to further assays to calculate the  $\text{IC}_{50}$  values. Compounds bearing a nitrogroup, i.e. all the first generation compounds, strongly absorb at 412 nm, thus making the determination of the inhibitory activity problematic. The use of 3 mm-pathlength cuvettes allowed to mitigate the issue, but in some cases the range of inhibitor concentrations tested was limited. Some of the compounds, especially those with the thiadiazole ring substituted by larger and more hydrophobic groups, showed low solubility in the assay buffer at pH 7.0. For these compounds only data at low



compound concentrations ( $\leq IC_{50}$ ) were used for the fitting and this affected the accuracy of the estimated  $IC_{50}$ . For this reason the  $IC_{50}$  values of these inhibitors are given as an estimate ( $\cong$ ) without the error.

### **Cytotoxicity assay and $CC_{50}$ determination. Cell culture**

Human monocytes THP-1 cells were grown in suspension in RPMI 1640 (Euroclone, Italy) supplemented with 1% Sodium Pyruvate 100mM (Life Technologies, USA), 0.5% Gentamicin 10mg/mL (Sigma Aldrich, USA), 0.1% 2-Mercaptoethanol 50mM (Life Technologies, USA), Glucose (0,25 g/mL) and 10% Fetal Bovine Serum (FBS; Euroclone, Italy).

THP-1 cells were seeded in 24-well plates (Sarstedt, Germany) in the presence of 100ng/mL of phorbol 12-myristate 13-acetate (PMA; Sigma-Aldrich, USA) for 72 hours to allow the cells to differentiate into macrophages.

### **Cytotoxicity assay (MTT assay)**

MTT assay has been used to assess the cytotoxicity of synthesized compounds in THP-derived macrophages by evaluating the ability of mitochondrial succinate dehydrogenase to catalyze the enzymatic reduction of yellow water-soluble 3-[4,5-dimethylthiazole-2-yl]-2,5-diphenyltetrazolium bromide (MTT; Sigma Aldrich, USA) to insoluble purple formazan, index of cell viability. Differentiated macrophages were treated with synthesized compounds at increasing concentrations (25  $\mu$ M, 50  $\mu$ M, 100  $\mu$ M, and 200  $\mu$ M; all compounds were tested as a triplicate) for 72 hours. 20 mM compounds solutions in DMSO were prepared, and consequentially diluted to obtain a final concentration up to 200  $\mu$ M, corresponding to 1% v/v of DMSO. Afterwards, cells were incubated with a solution of 1mg/mL of MTT dissolved in RPMI 1640, supplemented with 5% FBS, at 37°C, 5% CO<sub>2</sub> for 2 hours in dark. The solution was then removed, and resulting formazan crystals were dissolved in 0,2 mL DMSO under shaking for 10 minutes. Finally, absorbance was measured on an aliquot of 0.15mL at a wavelength of 570 nm using an absorbance microplate reader (Spark® Tecan, Switzerland).<sup>82</sup>

### 3.3. Synthesis of pyrazole derivatives as SAT inhibitors

#### 3.3.1. Aim of the project

As previously reported (see 3.1), along with compound **1**, the virtual screening on ChemiDiv libraries reported another interesting chemical series of hit compounds for SAT inhibition, namely **D511-0063**, with comparable  $IC_{50}$  to that of compound **1** (**D511-0063**,  $IC_{50} = 52.8 \pm 2 \mu M$ ; **1**  $IC_{50} = 48.6 \pm 8 \mu M$ ), and **D511-0060**, the most active inhibitor of the series (**D511-0060**,  $IC_{50} = 13.6 \pm 2 \mu M$ ), although, no measurable MIC was detected for these compounds when tested against *E. coli* (**Table 1** and **Figure 9**). The lack of activity in the bacteria cell might be attributed to different causes, like cell defense mechanisms such as efflux pump or the poor propensity to penetrate the cellular membrane, although the latter hypothesis is more likely when Gram-negative bacteria are considered.<sup>83–85</sup> Regardless, the two hits show an appreciable  $IC_{50}$ , and we deemed of interest to explore further the potential of this chemical series.

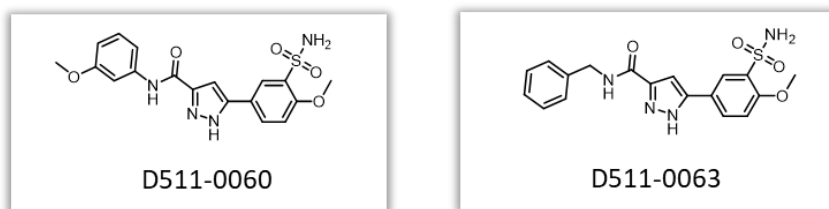


**Figure 9.** Chemical structure of compounds **D511-0060** and **D511-0063**

As for compound **1**, we first resynthesized the hit compounds and then prepared a small set of derivatives to explore the SAR through biochemical investigation.

First, a general protocol for synthesizing the hit compounds was set up, as reported in **Scheme 5**, then a small set of 8 derivatives was easily obtained. **D511-0060** and **D511-0063** present the same structural features with a central pyrazole core and a phenyl sulfonamide moiety at the C-5 of the heterocycle. Moreover, the pyrazole ring presents an amide bond at the C-3. The hit compounds differed only for the aromatic portion linked to the amide, a 3-methoxyphenyl ring for **D511-0060** and a benzyl moiety for **D511-0063**.

For this preliminary SAR investigation, the arylsulfonamide motif was kept intact as considered an essential part of the molecule since present in both the hits with a similar  $IC_{50}$ . We then focused our attention on the moiety connected to the amide bond, since both compounds showed activity towards the target enzyme. Small modifications (p-methoxyphenyl) and more drastic ones, such as the introduction of methyl piperazine to evaluate the presence of an aliphatic portion and a tertiary amide, were introduced. Also, the pyrazole was first N-methylated to evaluate if this position is prone to further substitutions and subsequently replaced with an isoxazole ring. Both the heterocycles contain a pyridine-like N, but the pyrazole 1-NH is replaced with an oxygen atom in the isoxazole ring, which lacks of a hydrogen bond donor (**Figure 10**).<sup>86,87</sup>

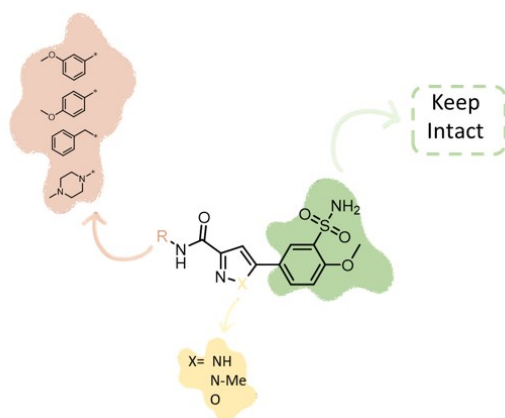


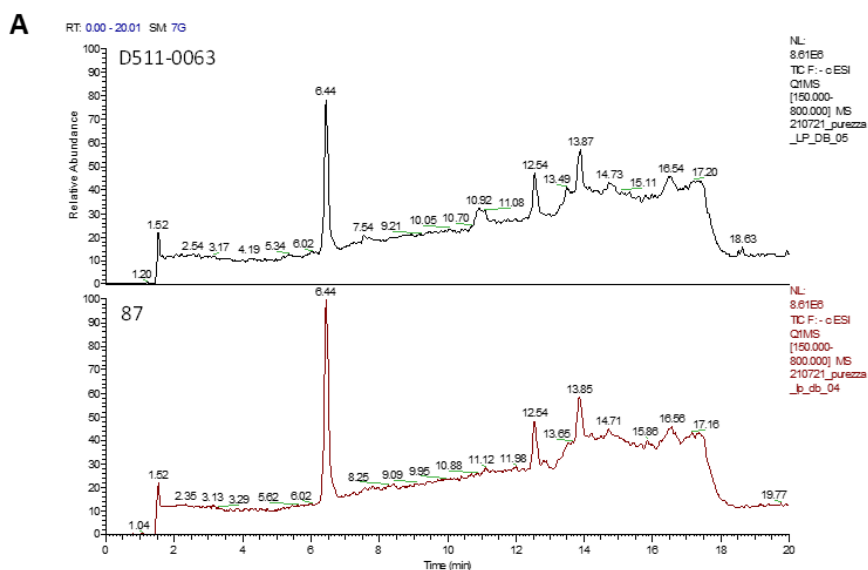
**Figure 10.** Modifications of the hit compounds.

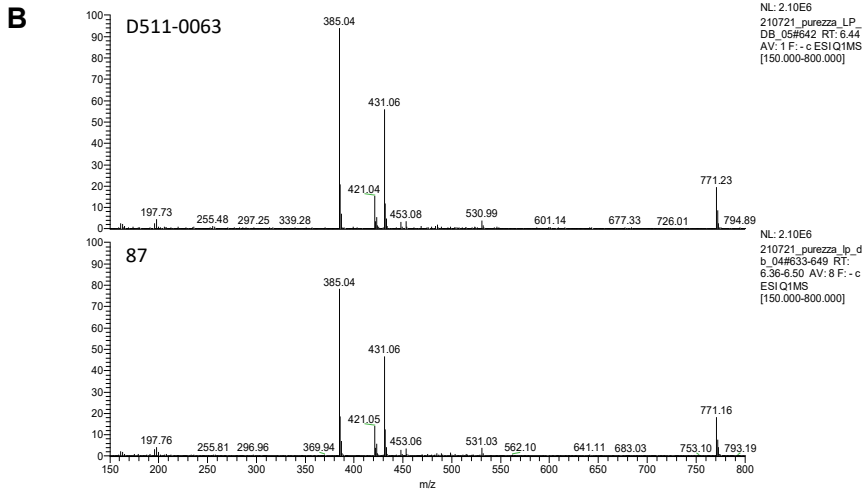
### 3.3.2. Results and Discussion

The resynthesized compounds (**86** and **87**) and the few analogues were evaluated for their inhibitory activity towards *StSAT*, following the procedure already reported in this chapter (see 3.2.2.) (**Table 4**). Out of all the compounds prepared, only compound **87** showed a hint of appreciable  $IC_{50}$  ranging between 62 and 118  $\mu\text{M}$ , a value comparable with that of the commercial sample (**D511-063**,  $IC_{50} = 52.8 \pm 2 \mu\text{M}$ ). The observed fluctuation in the  $IC_{50}$  value for the synthetic compound may be ascribed to the low solubility of the compound in the assay conditions at concentrations higher than 50  $\mu\text{M}$ . In the case of compound **86**, we found out an  $IC_{50} = 276 \mu\text{M}$ , a value remarkably

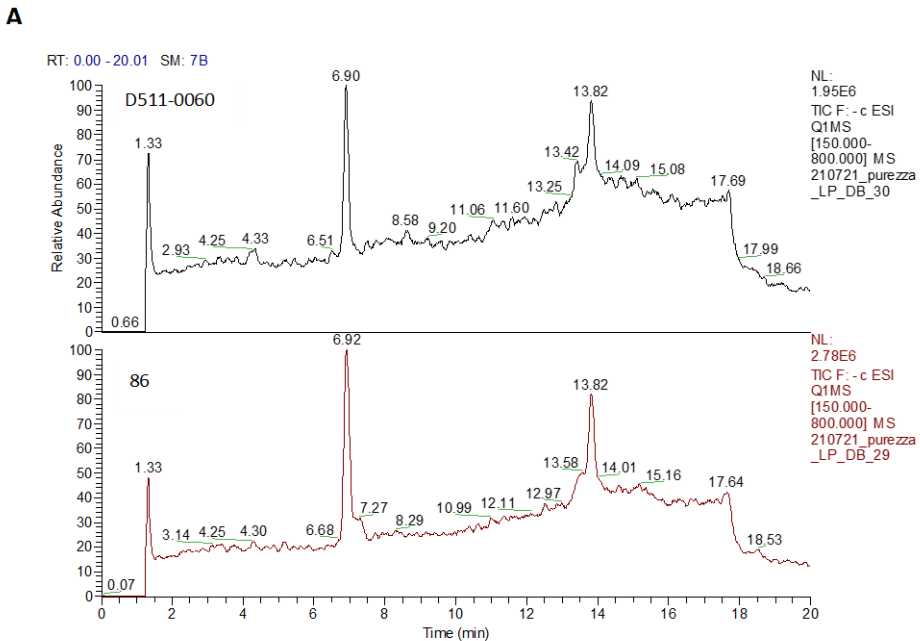
higher than that of the commercial sample (**D511-060**,  $IC_{50} = 13.6 \pm 2 \mu M$ ), as already reported by us. Upon repetition of the experiment, obtaining the same values, we try to investigate the reason of this ambiguous result. It is quite common that hit compounds from chemical libraries, upon resynthesis, give discordant results. The reason of this behavior might be generally ascribed to the presence of impurities; therefore, we set up a series of experiments to evaluate the purity of the commercial and resynthesized samples.

At this regard, HPLC analysis was performed for the resynthesized compounds **86** and **87** to complete their characterization and assess the matching with the commercial batches. Since it would be supposed that the compounds were the same entities, no difference should be detected in the HPLC analysis. First, both the synthesized compounds and the commercial batches were analyzed individually. Compound **87** and **D511-0063** showed the same retention time (6.44 min) and also the same mass spectrum (**Figure 11**). The same similarities were observed for **86** and **D511-0060** (**Figure 12**), although a negligible difference of 0.02 min was detected in the retention time of the peaks. Considering the inconsequential difference and the same mass spectrum, we can assume that the compounds are the same entity.





**Figure 11.** A) Full Scan HPLC Trace in Negative Ion Mode (ESI<sup>-</sup>) of a 10  $\mu$ M solution in MeOH + 0.1% DMSO of each analyte; 12-minute LC-gradient. B) Mass spectrum of peak at RT = 6.44 min.



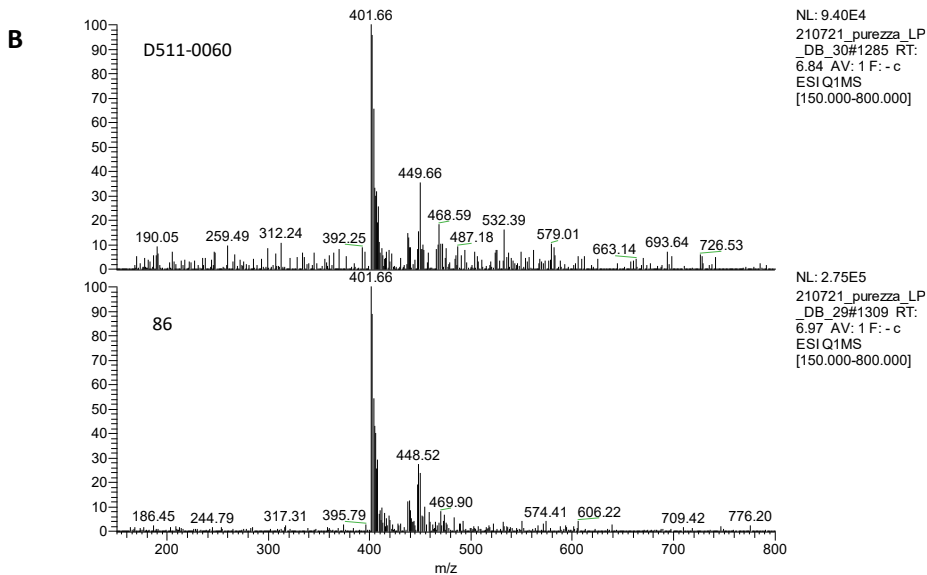


**Figure 12.** A) Full Scan HPLC Trace in Negative Ion Mode (ESI<sup>-</sup>) of a 10  $\mu$ M solution in MeOH + 0.1% DMSO of each analyte; 12-minute LC-gradient. B) Mass spectrum of peak at RT = 6.90 and 6.92 min.

Then, as additional proof of their matching, a mixture of the synthetic compound and the corresponding commercial sample was analyzed. As it is reported in **Figure 13**, when injected, the chromatogram profile of both the solutions with **86+D511-0060** and **87+D511-0063** showed one peak, respectively. Moreover, no significant impurities were detected in both synthesized and commercial compounds.

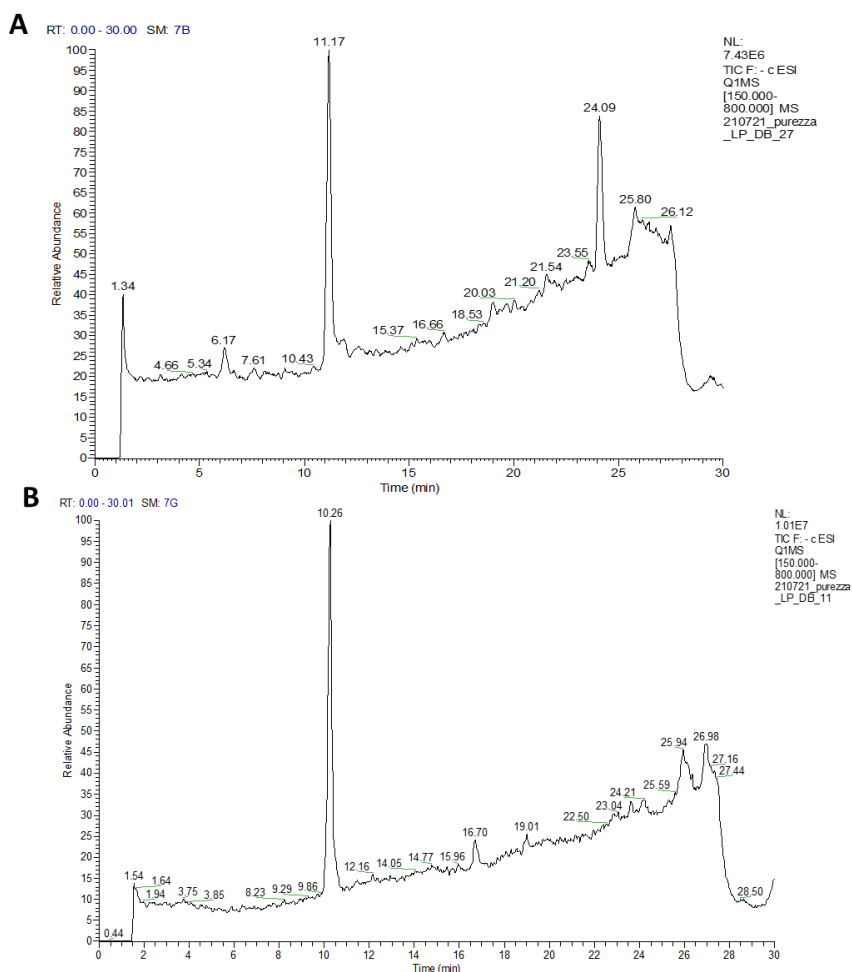


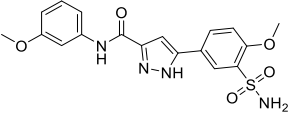
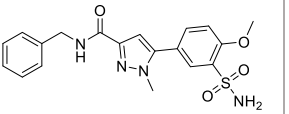
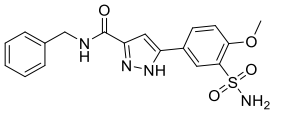
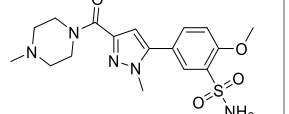
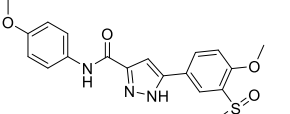
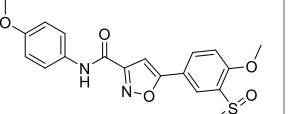
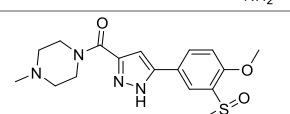
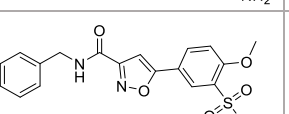
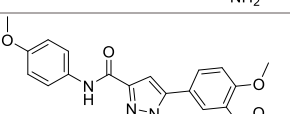
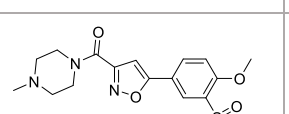
**Figure 13.** Full Scan HPLC Trace in Negative Ion Mode (ESI<sup>-</sup>) of a 10  $\mu$ M solution in MeOH + 0.1% DMSO of A) D511-060+86 and B) D511-063+87; 25 min-LC-gradient.

After confirmation of the structure of the molecules, and the absence of impurities, at least according to the standard analytical methods, we speculated that the physical status of the molecule might be important for interacting with the enzyme. When compound **86** is tested utilizing a stock solution freshly prepared (10 mM), that is the conditions reported above, the  $IC_{50}$  is 276  $\mu$ M. However, when a sample coming from a frozen stock solution (10 mM) is used, an  $IC_{50}$  of 39  $\mu$ M was calculated, a value similar to that of the commercial sample (**86**,  $IC_{50}$  = 39  $\mu$ M; **D511-060**,  $IC_{50}$  = 13.6 $\pm$ 2  $\mu$ M). This evidence might lead to the speculation that the compound solubility may be affected by freeze-thaw procedures, and the compound forms colloidal particles that may act

as aggregators affecting the potency of the inhibition determined. After an accurate literature search,<sup>88–92</sup> we found out that one of the most common mechanisms reported for false-positive hits is the colloidal aggregation of small molecules. This phenomenon is concentration-dependent, then it occurs at a specific concentration called critical aggregation concentration (CAC). The formation of the colloidal aggregate may non specifically bind proteins or sequester protein targets,<sup>93–95</sup> and as a consequence, they showed activity towards the targets. This observation surely needs deeper investigations to be confirmed, however, these odd results made it difficult to consider these molecules as valuable hit compounds for further development, and the investigation was then stopped.

Regarding the analogues **88–95**, no one showed an improvement in the inhibitory activity (**Table 4**).

**Table 4.** : StSAT Inhibitory activity (IC<sub>50</sub>)

Cpd	Compound	IC <sub>50</sub> (μM)	Cpd	Compound	IC <sub>50</sub> (μM)
<b>86</b>		39-276	<b>91</b>		≅1100*
<b>87</b>		≅62-118*	<b>92</b>		>1000
<b>88</b>		≅ 650	<b>93</b>		> 100*
<b>89</b>		> 500	<b>94</b>		≅320
<b>90</b>		≅370*	<b>95</b>		> 500

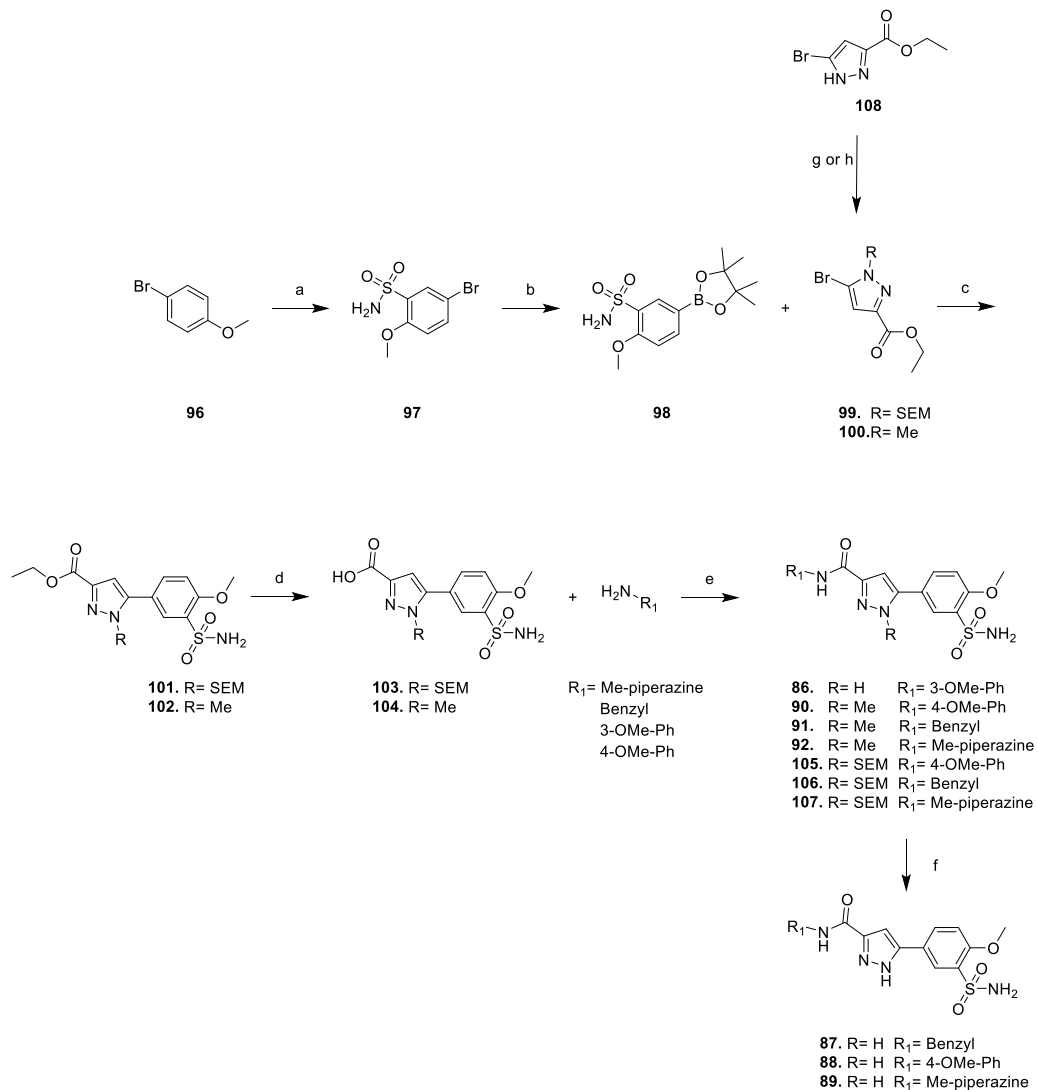
\* low-solubility compounds. The IC<sub>50</sub> was calculated in a limited concentration range (usually highest tested concentration lower than or equal to IC<sub>50</sub>), and for this reason, only an estimate is given.



### 3.3.3. Chemistry

The final compounds characterized by a pyrazole core were synthesized according to the synthetic route reported in **Scheme 5**. Compound **97** was obtained in two subsequent steps, the *in situ* formation of 5-bromo-2-methoxybenzenesulfonyl chloride, *via* chlorosulfonation of 4-bromoanisole (**96**), and the following aminolysis using aqueous ammonium hydroxide solution (30%) in dioxane. Then, two sequential Suzuki Murayama cross-coupling reactions were performed to obtain the intermediates **101** and **102**. **97** was converted in the corresponding boronate ester using bis(pinacolato)diboron, KOAc as the base, and PdCl<sub>2</sub>(dppf) as the catalyst, a classical procedure to obtain boronic derivatives.<sup>96</sup> The corresponding boronic ester **98** was reacted with the pyrazole **99** or **100**, using Tetrakis(triphenylphosphine)palladium as the catalyst and Na<sub>2</sub>CO<sub>3</sub> 2M solution as the base. The first attempt to obtain intermediate **101** was carried out starting from the commercially available compound **108**, with an unprotected NH. Different combinations of Pd catalyst and base were used in order to isolate the desired intermediate, but all failed in allowing the formation of the product. The subsequent *N*-protection of the commercial pyrazole **108** with 2-(Trimethylsilyl)ethoxymethyl chloride (SEM-Cl) and its reaction with **98** (step c, **Scheme 5**) allowed to afford the desired intermediate compound **101**. Likely, considering the pK<sub>a</sub> value of pyrazole NH (pK<sub>a</sub> = 14.21), under the standard condition of the Suzuki coupling, the unprotected pyrazole **108** existed mainly in its deprotonated form. This condition might have an important role in the decreased reactivity during the reaction,<sup>97</sup> which can be easily corrected using a protecting group such as SEM-Cl.

**Scheme 5.**



**Scheme 5. Reagents and conditions:** a) 1. HOSO<sub>2</sub>Cl, CHCl<sub>3</sub>, r.t.; 2. NH<sub>4</sub>OH, dioxane, rt; 80%; b) Bis(pinacolato)diboron, KOAc, PdCl<sub>2</sub>(dppf), 1,4-Dioxane, reflux, on; 80%; c) Tetrakis, Na<sub>2</sub>CO<sub>3</sub> 2M, THF, reflux, on, 55-90%; d) LiOH, THF/H<sub>2</sub>O, reflux, 80-91%; e) CDI, DMF, 70 °C, on, 33-55%; f) 4 N aq. HCl, EtOH, on, 20-85%; g) SEM-Cl, DIPEA, DCM, r.t., on, 80%; h) MeI, K<sub>2</sub>CO<sub>3</sub>, DMF, r.t, on, 70%.

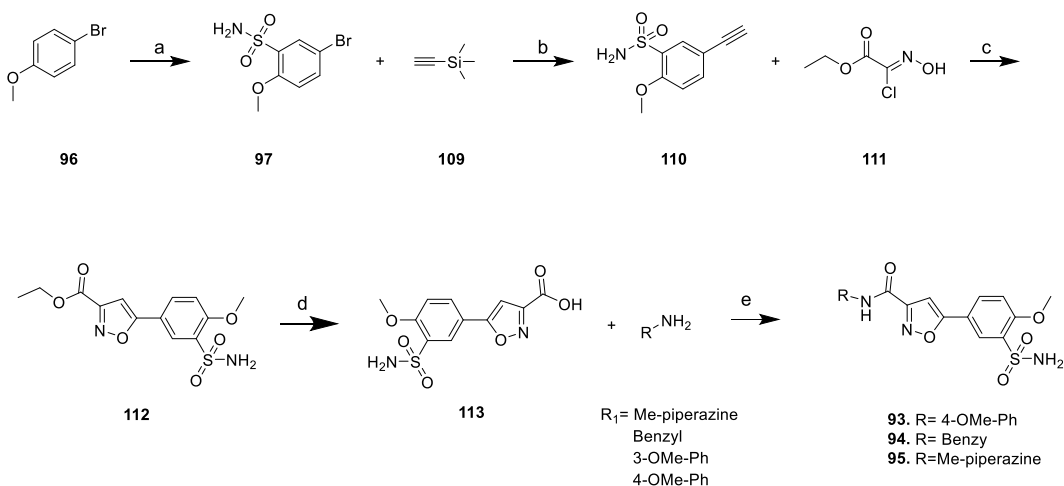
The carboxylic ester **101** and **102** were hydrolyzed to the corresponding carboxylic acid, using LiOH in THF/H<sub>2</sub>O. The subsequent acidification of the reaction mixture allowed the formation of a precipitate corresponding to the desired carboxylic acid, which was

filtered off and used in the next step without further purification. The acid must be added carefully, as an excess of acid may lead to the SEM-deprotection of the pyrazole, as occurred during the synthesis of the final compound **86**. Then, the carboxylic acids were activated with CDI and reacted with the proper amine in an amidation reaction. The SEM-deprotection of the pyrazole intermediates **105**, **106**, and **107**, using acid conditions in ethanol, afforded the final compounds **87-89**.

The *N*-methylation of the pyrazole **108** was achieved through an *N*-alkylation reaction with iodomethane in the presence of NaH in THF.

The synthesis of the isoxazole derivatives (**93-95**) required a slightly different protocol from that described above, and it is reported in **Scheme 6**. The reaction started with a Sonogashira coupling of the synthesized compound **97** with (trimethylsilyl)acetylene **109** to generate the intermediate alkyne **110**. Sonogashira reaction is performed with a palladium catalyst, a copper(I) cocatalyst, and an amine base. In the case of step b, the reaction conditions needed to be set up in regard to the catalyst, eq of TEA, solvent, and temperature, as summarized in **Table 5**. Using Pd(PPh<sub>3</sub>)<sub>2</sub>Cl<sub>2</sub> as palladium did not allow to isolate the intermediate, even with different equivalents of TEA, temperature, and solvent. A different Pd catalyst, Tetrakis(triphenylphosphine)palladium, with ten equivalents of TEA, in 1,4-dioxane at reflux, allowed to obtain the product in good yield (65%) (**Table 5**, entry 3).

**Scheme 6.**



**Scheme 6.** <sup>a</sup> Reagents and conditions: a) 1. HOSO<sub>2</sub>Cl, CHCl<sub>3</sub>, r.t; 2. NH<sub>4</sub>OH, dioxane, rt; on, 80%; b) 1. CuI, Pd(PPh<sub>3</sub>)<sub>4</sub>, TEA, N<sub>2</sub>, 70 °C; 2. K<sub>2</sub>CO<sub>3</sub>, MeOH; 65%; c) Na<sub>2</sub>CO<sub>3</sub>; ACN dry, r.t, 72 h; 85%; d) LiOH, THF/H<sub>2</sub>O, reflux; 90%; e) CDI, DMF, 70 °C, on; 56-33%.

**Table 5.** Conditions used for the Sonogashira reaction, step b Scheme 5.

	Palladium	Copper	TEA	Solvent	Temperature
<b>1</b>	Pd(PPh <sub>3</sub> ) <sub>2</sub> Cl <sub>2</sub> (0.1 eq)	CuI	10 eq	1,4-Dioxane	50°C, on
<b>2</b>	Pd(PPh <sub>3</sub> ) <sub>2</sub> Cl <sub>2</sub> (0.05 eq)	CuI	15 eq	Neat	70°C, on
<b>3</b>	Tetrakis (0.1 eq)	CuI	10 eq	1,4-Dioxane	reflux, on

The following cycloaddition of ethyl chlorooximidoacetate **111** to the alkyne **110** afforded the arylisoxazole-3-carboxylic ethyl ester **112** in excellent yield (85%). This step also required to be set up regarding the equivalent of **111**, the base, and the solvent, as reported in **Table 6**. The best conditions were granted by reacting compound **110** with 3 equivalent of **111**, using NaHCO<sub>3</sub> as the base and ANC as the solvent. The reaction takes 84 hours till the consumption of the starting material to obtain the product in a high yield.

**Table 6.** Conditions used for the cycloaddition reaction, step c Scheme 6.

	Eq of <b>111</b>	Base	Solvent
<b>1</b>	2	TEA (2 eq)	THF dry
<b>2</b>	3	TEA (3eq)	THF dry
<b>3</b>	2.5	Na <sub>2</sub> CO <sub>3</sub>	THF/H <sub>2</sub> O (1:1)
<b>4</b>	3	NaHCO <sub>3</sub>	ACN dry

Hydrolysis of **112** followed by an amide coupling reaction of the resulting carboxylic acid **113** and the proper amine gave the final compounds **93-95**, using analog conditions to the pyrazole derivatives already described in this chapter.

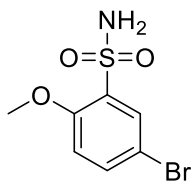
### 3.3.4. Conclusion

The VS on ChemDiv libraries disclosed five potential SAT inhibitors. The principal aim of this project was to resynthesize two of the five compounds identified as promising new scaffolds against the target enzyme. The synthetic route was set up, and a few modifications were introduced to the scaffold to obtain preliminary information about the SAR. Unexpectedly, some discrepancies were found when the synthetic compounds were biochemically evaluated. Additionally, no one derivatives showed increased inhibitory activity towards SAT. Indeed, **86** showed a comparable  $IC_{50}$  to that of the commercial batch only if a frozen stock of **86** was used during the assays (**86**,  $IC_{50} = 39 \mu\text{M}$ ; **D511-060**,  $IC_{50} = 13.6 \pm 2 \mu\text{M}$ ).

Once ascertained the fact that the compounds synthesized were the same as the commercial molecules, we could only speculate that impurities from the synthesis, such as the content of a small amount of metals, hard to detect unless a deeper analysis is conducted, which is behind the scope of this thesis, might be the cause of the discrepancies detected. On the other hand, the hit compounds might act as a colloidal aggregator, leading to false positives (the so-called “compound interference”) in the biochemical assays, which are unavoidable in most virtual and High-Throughput screening assays formats, and, even in this case, further assays are needed to shed light on this aspect.

### 3.3.5. Experimental Section

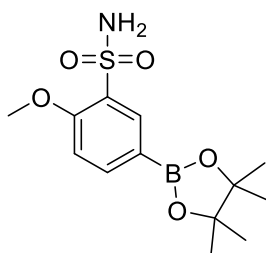
#### 5-bromo-2-methoxybenzenesulfonamide (97)



Chlorosulfonic acid (1 mL, 16.04 mmol) was added dropwise to a cold solution (0 °C) of 4-bromoanisole (500mg, 2.67 mmol) in  $\text{CH}_3\text{Cl}$ . The reaction mixture was stirred at 0 °C for 1 hour and then at room temperature for 4 hours. After this time, ice was added to the reaction mixture, and it was extracted with  $\text{CH}_3\text{Cl}$  (X3). The organic layers were dried over anhydrous  $\text{Na}_2\text{SO}_4$ , filtered, and concentrated under reduced pressure to afford 5-bromo-2-methoxybenzenesulfonyl chloride as a slightly grey powder. Subsequently, the arylsulfonyl chloride was dissolved in 1,4-dioxane and cooled to 0 °C,

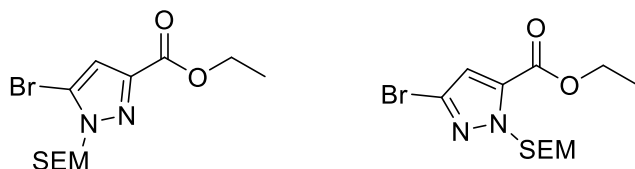
then an aqueous solution of  $\text{NH}_4\text{OH}$  (30% w/w) was added. The reaction mixture was stirred at room temperature overnight. The insoluble material was filtered off and washed with water. The organic layer was extracted with EtOAc (X3), dried over anhydrous  $\text{Na}_2\text{SO}_4$ , filtered, and concentrated under reduced pressure to afford the title compound as a white powder (yield: 80%). The product was used in the next step without further purification.  $^1\text{H}$  NMR (600 MHz,  $\text{DMSO}-d_6$ ):  $\delta$  7.79 – 7.79 (m, 1H); 7.76 – 7.74 (m, 1H); 7.25 (s, 2H); 7.20 (d,  $J = 8.8$  Hz, 1H); 3.90 (s, 3H).

### 2-methoxy-5-(4,4,5,5-tetramethyl-1,3,2-dioxaborolan-2-yl)benzenesulfonamide (98)



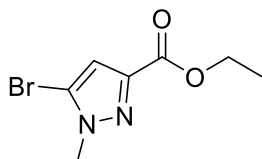
5-bromo-2-methoxybenzenesulfonamide (300 mg, 1.13 mmol), bis(pinacolato)diboron (429 mg, 1.69 mmol), and KOAc (442 mg, 4.5 mmol) were dissolved in anhydrous 1,4-dioxane, the  $\text{PdCl}_2(\text{dppf})$  (82 mg, 0.11 mmol) was added under  $\text{N}_2$  atmosphere. After bubbling  $\text{N}_2$  for 15 minutes, the reaction mixture was heated to reflux for 2 hours. The reaction mixture was cooled to room temperature and filtered through a plug of celite. The crude material was purified by flash column chromatography eluting with Petroleum Ether/EtOAc from 7:3 to 1:1 to afford the title compound as a white powder (yield: 80%).  $^1\text{H}$  NMR (400 MHz,  $\text{DMSO}-d_6$ ):  $\delta$  8.05 (d,  $J = 1.6$  Hz, 1H); 7.84 (dd,  $J_1 = 8.3$ ,  $J_2 = 1.7$  Hz, 1H); 7.22 (d,  $J = 8.4$  Hz, 1H); 7.11 (s, 2H); 3.93 (s, 3H); 1.30 (s, 12H).

### Ethyl 5-bromo-1-((2-(trimethylsilyl)ethoxy)methyl)-1H-pyrazole-3-carboxylate and ethyl 3-bromo-1-((2-(trimethylsilyl)ethoxy)methyl)-1H-pyrazole-5-carboxylate (99)



2-(Trimethylsilyl)ethoxymethyl chloride (121  $\mu$ L, 0.68 mmol) was added to a mixture of ethyl 5-bromo-1H-pyrazole-3-carboxylate (100 mg, 0.46 mmol) and DIPEA (240  $\mu$ L, 1.38 mmol) in DCM 0  $^{\circ}$ C. Then, the reaction mixture was stirred at room temperature overnight. DCM was added, and the mixture was washed with saturated aqueous.  $\text{NaHCO}_3$  and water. The organic phase was dried over anhydrous  $\text{Na}_2\text{SO}_4$ , filtered, and concentrated under reduced pressure to obtain the desired compound as a mixture of two regioisomers (yield: 80%).  $^1\text{H}$  NMR of majority species (400 MHz,  $\text{CDCl}_3$ ):  $\delta$  6.90 (s, 2H); 5.58 (s, 2H); 4.43 (d,  $J = 7.1$  Hz, 2H); 3.65 (t,  $J = 8.0$  Hz, 2H); 1.41 (q,  $J = 7.1$  Hz, 2H); 2.99 (s, 3H); 1.35 (t,  $J = 7.1$  Hz, 3H) 0.92 (t,  $J = 8.2$  Hz, 2H); -0.01 (s, 9H).

### Ethyl 5-bromo-1-methyl-1H-pyrazole-3-carboxylate (100)

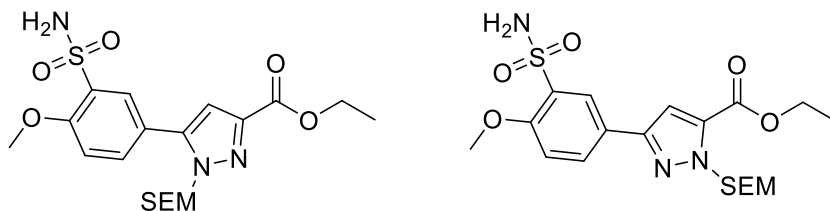


Sodium hydride 60 % dispersion in mineral oil (12 mg, 0.30 mmol) was dissolved in THF (0.8 mL), and the corresponding suspension was cooled to 0  $^{\circ}$ C, subsequently a solution of ethyl 5-bromo-1H-pyrazole-3-carboxylate (50 mg, 0.3 mmol) in THF (0.5 mL) was added. The reaction mixture was warmed to 25 $^{\circ}$ C and stirred at the same temperature for 1 hour. After this time, iodomethane (21  $\mu$ L, 0.35 mmol) was added. The reaction was stirred at room temperature for 3 hours. The mixture was cooled to 0  $^{\circ}$ C and quenched with an  $\text{NH}_4\text{Cl}$  saturated solution added dropwise. The reaction mixture was extracted with EtOAc (X3), dried over anhydrous  $\text{Na}_2\text{SO}_4$ , filtered, and concentrated under reduced pressure to afford 5-the title compound as a white powder (yield: 70%). The product was used in the next step without further purification.  $^1\text{H}$  NMR (400 MHz,  $\text{CDCl}_3$ ):  $\delta$  6.83 (s, 1H); 4.40 (q,  $J = 7.1$  Hz, 2H); 3.96 (s, 3H); 1.39 (t,  $J = 7.1$ , 3H).

## General procedure for the Suzuki-Miyaura Cross-Coupling Reaction

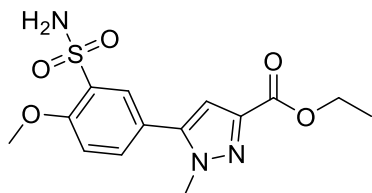
Compound **99** or compound **100** (1 eq), compound **98** (1.2 eq), and a solution of sodium carbonate 2 M (3 eq) were dissolved in anhydrous THF and stirred for 10 minutes under N<sub>2</sub> atmosphere. Then, tetrakis(triphenylphosphine)palladium(0) (0.10 eq) was added, and the reaction mixture was heated to reflux overnight. The mixture was cooled to room temperature and filtered through a plug of celite. The crude material was purified by flash by flash column chromatography eluting with DCM/MeOH. Purification methods, yields, and analytical data are reported below.

### Ethyl 5-(4-methoxy-3-sulfamoylphenyl)-1-((2-(trimethylsilyl)ethoxy)methyl)-1H-pyrazole-3-carboxylate and Ethyl 3-(4-methoxy-3-sulfamoylphenyl)-1-((2-(trimethylsilyl)ethoxy)methyl)-1H-pyrazole-5-carboxylate (**101**)



The compound was obtained as a mixture of the two regioisomer (yield: 55%). Purification by flash chromatography eluting with DCM/MeOH 99:1. <sup>1</sup>H NMR of majority species (400 MHz, CDCl<sub>3</sub>): δ 19 (d, *J* = 1.9 Hz, 1H); 7.91 (dd, *J*<sub>1</sub> = 8.6, *J*<sub>2</sub> = 1.9 Hz, 1H); 7.17 (d, *J* = 8.7 Hz, 1H); 6.94 (s, 1H); 5.49 (s, 2H); 5.21 (s, 2H); 4.45 (d, *J* = 7.1 Hz, 2H); 4.10 (s, 3H); 3.78 (d, *J* = 8.7 Hz, 1H); 1.43 (t, *J* = 7.1 Hz, 3H); 0.97 (t, *J* = 8.4 Hz, 2H); 0.01 (s, 1H).

### Ethyl 5-(4-methoxy-3-sulfamoylphenyl)-1-methyl-1H-pyrazole-3-carboxylate (**102**)



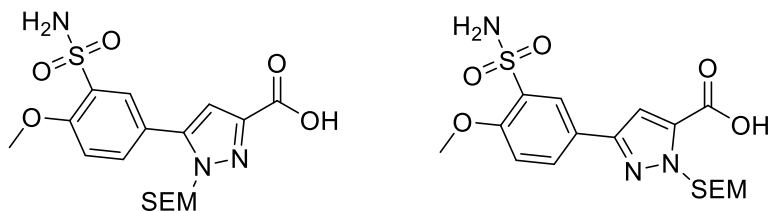
Purification by flash chromatography eluting with DCM/MeOH from 99.5:0.5 to 98:2 (yield: 90%). <sup>1</sup>H NMR (400 MHz, CDCl<sub>3</sub>): δ 7.98 (d, *J* = 2.3 Hz, 1H); 7.18 (d, *J* = 8.6 Hz, 1H); 6.63 (s, 1H); 5.23 (s, 2H); 4.45 (d, *J* = 7.1 Hz, 2H); 3.96 (s, 3H); 1.81 (t, *J* = 7.1 Hz, 3H).



## General procedure for the hydrolysis of the carboxylic esters

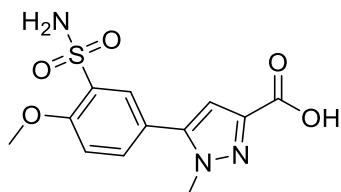
LiOH (8.00 eq) was added to a solution of the proper carboxylic ester (1.00 eq) in THF/H<sub>2</sub>O (1:1), and the reaction mixture was stirred at room temperature for 2 hours. 1 N aq. HCl was added to the mixture until acid pH. When a precipitate occurs, it was filtered off. Otherwise, the mixture was extracted with EtOAc (x4), and the organic layers were dried over anhydrous Na<sub>2</sub>SO<sub>4</sub>, filtered, and concentrated under reduced pressure. The product was used in the next step without further purification. Yields and analytical data are reported below.

### 5-(4-methoxy-3-sulfamoylphenyl)-1-((2-(trimethylsilyl)ethoxy)methyl)-1H-pyrazole-3-carboxylic acid and 3-(4-methoxy-3-sulfamoylphenyl)-1-((2-(trimethylsilyl)ethoxy)methyl)-1H-pyrazole-5-carboxylic acid (103)



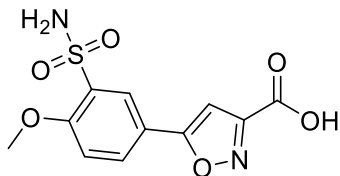
The title compound was obtained as a yellow powder as a mixture of two regioisomers (yield: 80%). <sup>1</sup>H NMR (400 MHz, DMSO-*d*<sub>6</sub>): δ 13.61 (s, 1H); 12.91 (s, 1H); 8.26 (s, 1H); 8.05 (d, *J* = 8.5 Hz, 1H); 8.01 (s, 1H); 7.86 (d, *J* = 8.6 Hz, 1H); 7.38 – 7.35 (m, 2H); 7.28 (d, *J* = 8.7 Hz, 1H); 7.21 (s, 2H); 7.16 (s, 2H); 6.92 (s, 1H); 5.81 (s, 2H); 5.45 (s, 2H); 3.97 (s, 3H); 3.95 (s, 3H); 3.66 – 3.59 (m, 4H); 0.89 – 0.81 (m, 4H); -0.04 (s, 9H); -0.08 (s, 9H).

### 5-(4-methoxy-3-sulfamoylphenyl)-1-methyl-1H-pyrazole-3-carboxylic acid (104)



The title compound was obtained as a slightly yellow powder (yield: 91%). <sup>1</sup>H NMR (400 MHz, DMSO): δ 12.72 (bs, 1H); 7.81 (m, 2H); 7.36 (d, *J* = 8.6 Hz, 1H); 7.25 (s, 2H); 6.81 (s, 1H); 3.98 (s, 3H); 3.89 (s, 3H).

### 5-(4-methoxy-3-sulfamoylphenyl)isoxazole-3-carboxylic acid (113)

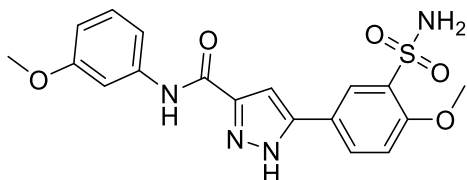


The title compound was obtained as a slightly yellow powder (yield: 90%).  $^1\text{H}$  NMR (400 MHz,  $\text{DMSO-}d_6$ ):  $\delta$  8.21 (d,  $J = 2.3$  Hz, 1H); 8.16 (dd,  $J_1 = 8.7$ ,  $J_2 = 2.3$  Hz, 1H); 7.40 (d,  $J = 8.8$  Hz, 1H); 7.36 (s, 1H); 7.31 (s, 2H); 3.99 (s, 3H).

### General procedure for the amidation reaction

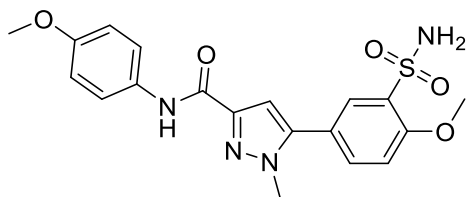
Carbonyldiimidazole (CDI) (1.00 eq) was added to a solution of the proper carboxylic acid (1.00 eq) in dry DMF (2 mL/mmol) under  $\text{N}_2$  atmosphere. The reaction mixture was left stirring for 1h at room temperature, and then the amine (1.00 eq) was added. The reaction mixture was heated to 70 °C overnight. The reaction was quenched with water and extracted with EtOAc (x3). The organic layers were dried over anhydrous  $\text{Na}_2\text{SO}_4$ , filtered, and concentrated under reduced pressure. The crude was purified by flash column chromatography eluting with DCM/MeOH. Purification conditions, yields, and analytical data are reported below.

### 5-(4-methoxy-3-sulfamoylphenyl)-N-(3-methoxyphenyl)-1H-pyrazole-3-carboxamide 86



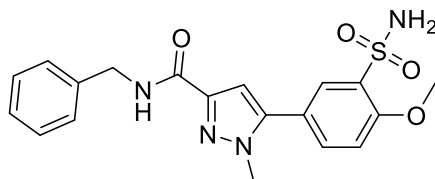
Purification by flash column chromatography eluting with DCM/MeOH from 95:5 to 90:10 allowed the isolation of the product as a white powder (yield: 35%).  $^1\text{H}$  NMR (400 MHz,  $\text{DMSO-}d_6$ ):  $\delta$  13.86 (s, 1H); 8.21 (d,  $J = 1.9$  Hz, 1H); 8.03 (d,  $J = 7.9$  Hz, 1H); 7.52 – 7.26 (m, 5H); 7.19 (s, 2H); 6.70 (s, 1H); 3.96 (s, 3H); 3.77 (s, 3H). HPLC-ESI-MS analysis: calculated for  $\text{C}_{18}\text{H}_{18}\text{N}_4\text{O}_4\text{S}$ : 402.10; found: 401.66 [ $\text{M-H}^+$ ].

**5-(4-methoxy-3-sulfamoylphenyl)-N-(4-methoxyphenyl)-1-methyl-1H-pyrazole-3-carboxamide (90)**



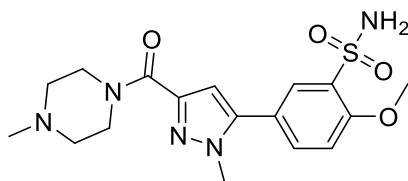
Purification by trituration with DCM and diethyl ether allowed the isolation of the product as a white powder (yield: 45%).  $^1\text{H NMR}$  (400 MHz,  $\text{DMSO-}d_6$ ):  $\delta$  9.99 (s, 1H); 7.87 (d,  $J = 2.1$  Hz, 1H); 7.85 – 7.82 (m, 1H); 7.73 (bd,  $J = 9.0$  Hz, 2H); 7.38 (d,  $J = 8.6$  Hz, 1H); 7.26 (s, 2H); 6.92 – 6.89 (m, 3H); 3.99 (s, 3H); 3.95 (s, 3H); 3.75 (s, 3H). HPLC-ESI-MS analysis: calculated for  $\text{C}_{19}\text{H}_{20}\text{N}_4\text{O}_5\text{S}$ : 416.12; found: 417.27 [ $\text{M}+\text{H}^+$ ].

**N-benzyl-5-(4-methoxy-3-sulfamoylphenyl)-1-methyl-1H-pyrazole-3-carboxamide (91)**



Purification by trituration with DCM and diethyl ether allowed the isolation of the product as a white powder (yield: 45%).  $^1\text{H NMR}$  (400 MHz,  $\text{DMSO-}d_6$ ):  $\delta$  8.74 (s, 1H); 7.84 – 7.79 (m, 2H); 7.38 – 7.32 (m, 5H); 7.25 (m, 3H); 6.78 (s, 1H); 4.44 (d,  $J=5.8$ , 1H); 3.98 (s, 3H); 3.90 (s, 3H). HPLC-ESI-MS analysis: calculated for  $\text{C}_{19}\text{H}_{20}\text{N}_4\text{O}_4\text{S}$ : 400.12; found: 401.26 [ $\text{M}+\text{H}^+$ ].

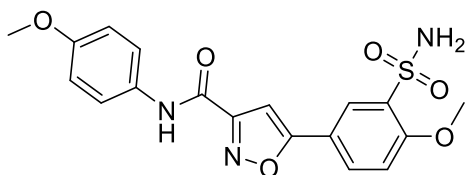
**2-methoxy-5-(1-methyl-3-(4-methylpiperazine-1-carbonyl)-1H-pyrazol-5-yl)benzenesulfonamide (92)**



Purification by flash column chromatography eluting with DCM/MeOH from 97:3 to 92:8 allowed the isolation of the product as a white powder (yield: 45%).  $^1\text{H NMR}$  (400

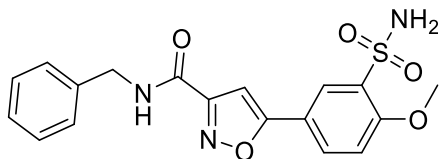
MHz, DMSO-*d*<sub>6</sub>):  $\delta$  7.83 – 7.79 (m, 2H); 7.36 (d, *J* = 8.3 Hz, 1H); 7.24 (s, 2H); 6.67 (s, 1H); 6.78 (s, 1H); 3.98 (s, 3H); 3.93 (m, 2H); 3.87 (s, 3H); 3.62 (m, 2H); 2.34 (s, 4H); 2.21 (s, 3H). HPLC-ESI-MS analysis: calculated for C<sub>17</sub>H<sub>23</sub>N<sub>5</sub>O<sub>4</sub>S: 393.15; found: 394.27 [M+H<sup>+</sup>].

**5-(4-methoxy-3-sulfamoylphenyl)-N-(4-methoxyphenyl)isoxazole-3-carboxamide (93)**



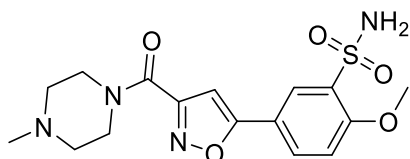
Purification by trituration with DCM and EtOAc allowed the isolation of the product as a slightly yellow powder (yield: 56%). <sup>1</sup>H NMR (400 MHz, DMSO-*d*<sub>6</sub>):  $\delta$  10.63 (s, 1H); 8.24 (d, *J* = 2.2 Hz, 1H); 8.20 (dd, *J*<sub>1</sub> = 8.6, *J*<sub>2</sub> = 2.3 Hz, 1H); 7.63 – 7.69 (m, 2H); 7.46 (s, 1H); 7.43 (d, *J* = 8.8 Hz, 1H); 7.31 (s, 2H); 6.98 – 6.93 (m, 2H); 4.01 (m, 2H); 3.76 (s, 3H). <sup>13</sup>C NMR (100.6 MHz, DMSO):  $\delta$  169.8; 160.6; 158.2; 157.2; 156.5; 132.6; 132.1; 131.5; 125.3; 122.6; 118.7; 114.4; 100.0; 57.1; 55.7. HPLC-ESI-MS analysis: calculated for C<sub>18</sub>H<sub>17</sub>N<sub>3</sub>O<sub>6</sub>S: 403.08; found: 404.29 [M+H<sup>+</sup>].

**N-benzyl-5-(4-methoxy-3-sulfamoylphenyl)isoxazole-3-carboxamide (94)**



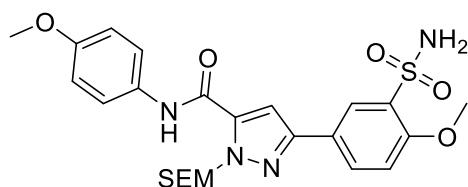
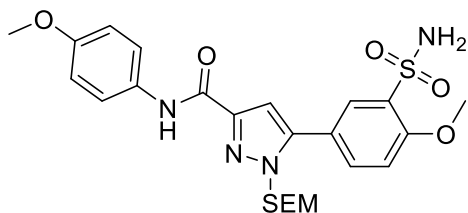
Purification by trituration with DCM and EtOAc allowed the isolation of the product as a slightly yellow powder (yield: 56%). <sup>1</sup>H NMR (400 MHz, DMSO-*d*<sub>6</sub>):  $\delta$  9.40 (t, *J* = 6.2 Hz, 1H); 8.21 (d, *J* = 2.3 Hz, 1H); 8.17 (dd, *J*<sub>1</sub> = 8.6, *J*<sub>2</sub> = 2.3 Hz, 1H); 7.41 (d, *J* = 8.8 Hz, 1H); 7.38 (s, 1H); 7.46 (s, 1H); 7.35 – 7.33 (m, 4H); 7.31 (s, 2H); 7.28 – 7.24 (m, 1H); 4.48 (d, *J* = 6.2 Hz, 2H); 4.00 (s, 3H). <sup>13</sup>C NMR (100.6 MHz, DMSO-*d*<sub>6</sub>):  $\delta$  169.7; 160.2; 158.9; 158.2; 139.4; 132.5; 132.1; 128.8; 127.8; 127.4; 125.3; 118.7; 114.3; 99.8; 55.1. HPLC-ESI-MS analysis: calculated for C<sub>18</sub>H<sub>17</sub>N<sub>3</sub>O<sub>5</sub>S: 387.09; found: 388.11 [M+H<sup>+</sup>].

**2-methoxy-5-(3-(4-methylpiperazine-1-carbonyl)isoxazol-5-yl)benzenesulfonamide (95)**



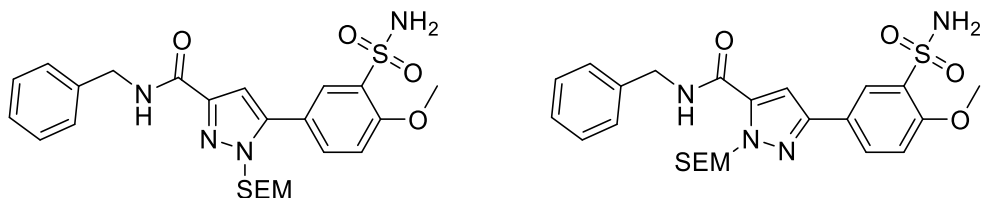
Purification by flash column chromatography eluting with DCM/MeOH from 97:3 to 92:8 allowed the isolation of the product as a white powder (yield: 33%). <sup>1</sup>H NMR (400 MHz, DMSO-*d*<sub>6</sub>): δ 8.21 (d, *J* = 2.2 Hz, 1H); 8.14 (d, *J*<sub>1</sub> = 8.7, *J*<sub>2</sub> = 2.3 Hz, 1H); 7.41 (d, *J* = 8.8 Hz, 1H); 7.30 (s, 2H); 7.27 (s, 1H); 4.00 (m, 3H); 3.68 – 3.58 (m, 4H); 2.39 – 2.33 (m, 4H); 2.22 (s, 3H). HPLC-ESI-MS analysis: calculated for C<sub>16</sub>H<sub>20</sub>N<sub>4</sub>O<sub>5</sub>S: 380.12; found: 381.28 [M+H<sup>+</sup>].

**5-(4-methoxy-3-sulfamoylphenyl)-N-(4-methoxyphenyl)-1-((2-(trimethylsilyl)ethoxy)methyl)-1H-pyrazole-3-carboxamide and 3-(4-methoxy-3-sulfamoylphenyl)-N-(4-methoxyphenyl)-1-((2-(trimethylsilyl)ethoxy)methyl)-1H-pyrazole-5-carboxamide (105)**



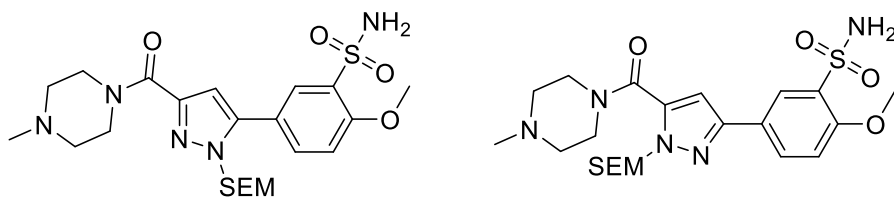
Purification by flash column chromatography eluting with DCM/MeOH from 99.05:3 to 99:1 allowed the isolation of the product as a mixture of the two regioisomers (white powder; yield: 33%). <sup>1</sup>H NMR (400 MHz, DMSO-*d*<sub>6</sub>): δ 10.30 (s, 1H); 10.02 (s, 1H); 8.24 (d, *J* = 1.8 Hz, 1H); 8.04 – 8.02 (m, 2H); 7.89 (d, *J* = 8.6 Hz, 1H); 7.72 (d, *J* = 8.9 Hz, 2H); 7.65 (d, *J* = 8.9 Hz, 2H); 7.52 (s, 1H); 7.38 (d, *J* = 8.6 Hz, 1H); 7.34 (d, *J* = 8.7 Hz, 1H); 7.23 (s, 2H); 7.18 (s, 2H); 5.85 (s, 2H); 5.49 (s, 2H); 3.98 (s, 3H); 3.96 (s, 3H); 3.76 (s, 3H); 3.75 (s, 3H); 3.66 (t, *J* = 8.1 Hz, 2H); 3.60 (t, *J* = 8.1 Hz, 2H); 0.91 – 0.80 (m, 4H); -0.03 (s, 9H); -0.09 (s, 9H).

**N-benzyl-5-(4-methoxy-3-sulfamoylphenyl)-1-((2-(trimethylsilyl)ethoxy)methyl)-1H-pyrazole-3-carboxamide and N-benzyl-3-(4-methoxy-3-sulfamoylphenyl)-1-((2-(trimethylsilyl)ethoxy)methyl)-1H-pyrazole-5-carboxamide (106)**



Purification by flash column chromatography eluting with DCM/MeOH from 99.5:0.5 to 99:1 allowed the isolation of the product as a mixture of the two regioisomers (yield: 55%). <sup>1</sup>H NMR (400 MHz, DMSO-*d*<sub>6</sub>): δ 9.18 (t, *J* = 6.0 Hz, 2H); 8.82 (t, *J* = 6.3 Hz, 2H); 8.18 (d, *J* = 2.3 Hz, 1H); 8.01 (d, *J* = 2.3 Hz, 1H); 7.97 (dd, *J*<sub>1</sub> = 8.6, *J*<sub>2</sub> = 2.3 Hz, 1H); 7.86 (dd, *J*<sub>1</sub> = 8.6, *J*<sub>2</sub> = 2.3 Hz, 1H); 7.41 (s, 1H); 7.38 (s, 1H); 7.37 – 7.30 (m, 11H); 7.29 – 7.21 (m, 4H); 7.19 (s, 4H); 7.18 (s, 2H); 6.89 (s, 1H); 5.85 (s, 2H); 4.47 (t, *J* = 6.4 Hz, 4H); 3.97 (s, 3H); 3.95 (s, 3H); 3.76 (s, 3H); 3.75 (s, 3H); 3.66 (t, *J* = 8.1 Hz, 2H); 3.58 (t, *J* = 7.9 Hz, 2H); 0.89 – 0.79 (m, 4H); -0.05 (s, 9H); -0.08 (s, 9H).

**2-methoxy-5-(3-(4-methylpiperazine-1-carbonyl)-1-((2-(trimethylsilyl)ethoxy)methyl)-1H-pyrazol-5-yl)benzenesulfonamide and 2-methoxy-5-(5-(4-methylpiperazine-1-carbonyl)-1-((2-(trimethylsilyl)ethoxy)methyl)-1H-pyrazol-3-yl)benzenesulfonamide (107)**

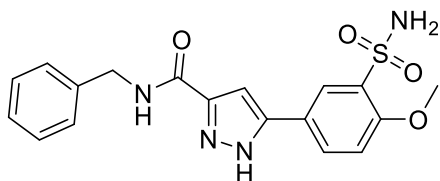


Purification by flash column chromatography eluting with DCM/MeOH from 99:1 to 96:4 allowed the isolation of the product as a mixture of the two regioisomers (yield: 43%). <sup>1</sup>H NMR of majority species (400 MHz, DMSO-*d*<sub>6</sub>): δ 8.23 (s, 1H); 8.02 (d, *J* = 7.1 Hz, 1H); 7.28 (d, *J* = 8.3 Hz, 1H); 7.14 (s, 2H); 6.89 (s, 1H); 5.85 (s, 2H); (d, *J* = 2.3 Hz, 1H); 7.97 (dd, *J*<sub>1</sub> = 8.6, *J*<sub>2</sub> = 2.3 Hz, 1H); 7.86 (dd, *J*<sub>1</sub> = 8.6, *J*<sub>2</sub> = 2.3 Hz, 1H); 7.41 (s, 1H); 7.38 (s, 1H); 7.37 – 7.30 (m, 11H); 7.29 – 7.21 (m, 4H); 7.19 (s, 4H); 7.18 (s, 2H); 6.89 (s, 1H); 5.85 (s, 2H); 3.95 (s, 3H); 3.65 – 3.54 (m, 6H); 2.36 (s, 4H); 2.22 (s, 2H); 0.86 – 0.82 (m, 2H); -0.05 (s, 9H).

## General procedure for the SEM deprotection

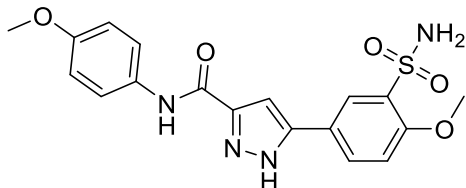
The proper SEM-derivate (1 eq) was dissolved in EtOH, then 4 N aq.HCl was added. The reaction mixture was stirred at room temperature overnight. NaOH 1 N was added to the reaction mixture, and when a precipitate occurred, it was filtered off; otherwise, the mixture was extracted with EtOAc. Purification conditions, yields, and analytical data are reported below.

### N-benzyl-5-(4-methoxy-3-sulfamoylphenyl)-1H-pyrazole-3-carboxamide (87)



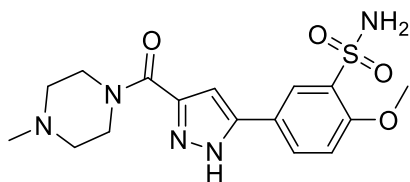
Purification by trituration with EtOAc and DCM allowed the isolation of the product as a white powder (yield: 35%).  $^1\text{H}$  NMR (400 MHz,  $\text{DMSO-}d_6$ ):  $\delta$  13.96 (s, 1H); 9.03 (s, 1H); 8.17 (d,  $J = 2.1$  Hz, 1H); 7.98 (dd,  $J_1 = 8.6$ ,  $J_2 = 2.1$  Hz, 1H); 7.34 – 7.29 (m, 5H); 7.27 – 7.28 (m, 1H); 7.16 (s, 1H); 4.46 (d,  $J = 6.0$  Hz, 2H); 3.95 (s, 3H). HPLC-ESI-MS analysis: calculated for  $\text{C}_{18}\text{H}_{18}\text{N}_4\text{O}_4\text{S}$ : 386.10; found: 385.04  $[\text{M-H}^+]$ .

### 5-(4-methoxy-3-sulfamoylphenyl)-N-(4-methoxyphenyl)-1H-pyrazole-3-carboxamide (88)



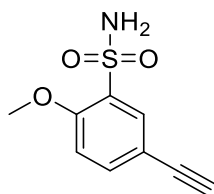
White powder (yield: 85%).  $^1\text{H}$  NMR (400 MHz,  $\text{DMSO-}d_6$ ):  $\delta$  13.83 (s, 1H); 10.06 (s, 1H); 8.21 (s, 1H); 8.02 (d,  $J = 8.1$  Hz, 1H); 7.70 (d,  $J = 8.2$  Hz, 1H); 7.33 (d,  $J = 8.5$  Hz, 2H); 7.18 (s, 2H); 6.94 (d,  $J = 8.4$  Hz, 1H); 3.96 (m, 3H); 3.76 (s, 3H). HPLC-ESI-MS analysis: calculated for  $\text{C}_{18}\text{H}_{18}\text{N}_4\text{O}_5\text{S}$ : 402.10; found: 401.09  $[\text{M-H}^+]$ .

**2-methoxy-5-(3-(4-methylpiperazine-1-carbonyl)-1H-pyrazol-5-yl)benzenesulfonamide (89)**



Purification by flash column chromatography eluting with DCM/MeOH from 95:5 to 90:10 allowed the isolation of the product (yield: 20%). <sup>1</sup>H NMR (400 MHz, DMSO-*d*<sub>6</sub>): δ 13.65 (s, 1H); 8.18 (d, *J* = 2.1 Hz, 1H); 8.00 (dd, *J*<sub>1</sub> = 8.6, *J*<sub>2</sub> = 2.2 Hz, 1H); 7.30 (d, *J* = 8.7 Hz, 1H); 7.17 (s, 2H); 6.97 (s, 1H); 7.16 (s, 1H); 3.95 (s, 3H); 3.84 (m, 2H); 3.64 (m, 2H); 2.37 – 2.34 (m, 4H); 2.21 (s, 3H). HPLC-ESI-MS analysis: calculated for C<sub>16</sub>H<sub>21</sub>N<sub>5</sub>O<sub>4</sub>S: 379.13; found: 380.27 [M+H<sup>+</sup>].

**5-ethynyl-2-methoxybenzenesulfonamide (110)**

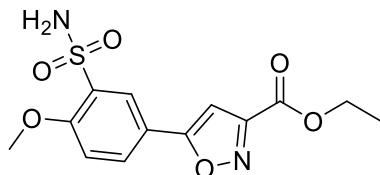


**LP275** (50mg, 0.19 mmol) was dissolved in anhydrous 1,4-dioxane, then tetrakis(triphenylphosphine)palladium(0) (22mg, 0.019 mmol), CuI (4 mg, 0.019 mmol), and TEA (0.265 mL, 1.19 mmol) were added under argon atmosphere. Subsequently, TMS acetylene was added. The reaction mixture was heated to reflux. After the consumption of the starting material according to TLC, EtOAc was added to the reaction mixture, and it was filtered through a plug of celite, then the organic phase was extracted with EtOAc (x3). The organic layers were dried over anhydrous Na<sub>2</sub>SO<sub>4</sub>, filtered, and concentrated under reduced pressure. The corresponding crude material was dissolved in MeOH, and potassium carbonate (51 mg, 0.38 mmol) was added. The reaction mixture was stirred at room temperature for 2 hours. The solvent was evaporated, and the crude material was extracted with EtOAc (X3). The organic layers were dried over anhydrous Na<sub>2</sub>SO<sub>4</sub>, filtered, and concentrated under reduced pressure. The crude material was purified by flash column chromatography eluting with Petroleum Ether/EtOAc 60:40 to afford the title compound as a yellow powder (yield:



65%).  $^1\text{H}$  NMR (400 MHz,  $\text{CDCl}_3$ ):  $\delta$  8.06 (d,  $J = 2.5$  Hz, 1H); 7.66 (dd,  $J_1 = 8.7$ ,  $J_2 = 2.5$  Hz, 1H); 6.97 (d,  $J = 8.8$  Hz, 1H); 5.08 (s, 2H); 4.06 (s, 1H); 4.03 (s, 3H).

### Ethyl 5-(4-methoxy-3-sulfamoylphenyl)isoxazole-3-carboxylate(112)



Ethyl 2-chloro-2-(hydroxyimino)acetate (40 mg, 0.27 mmol), sodium bicarbonate (23mg, 0.27) and **LP295** (20 mg, 0.09 mmol) were dissolved in anhydrous ACN. The reaction mixture was stirred at room temperature for 72 hours. Water was added to the reaction mixture, and it was extracted with EtOAc (X3). The organic layers were dried over anhydrous  $\text{Na}_2\text{SO}_4$ , filtered, and concentrated under reduced pressure. The crude material was purified by flash column chromatography eluting with Petroleum Ether/EtOAc 60:40 to afford the title compound as a slightly yellow powder (yield: 80%).  $^1\text{H}$  NMR (400 MHz,  $\text{DMSO}-d_6$ ):  $\delta$  8.24 – 8.18 (m, 2H); 7.51 (s, 1H); 7.42 (d,  $J = 8.7$  Hz, 1H); 7.31 (s, 2H); 4.41 (q,  $J = 7.1$  Hz, 2H); 2.99 (s, 3H); 1.35 (t,  $J = 7.1$  Hz, 3H).

## 4. O-Acetylserine sulfhydrylase (OASS) inhibitors

### 4.1. State of the art

The discovery of molecules as cysteine inhibitors started from the evidence that SAT is the physiological inhibitor of OASS. Indeed, a study conducted in *H. influenzae* shows that the last five amino acids present in the SAT C-terminal chain play a crucial role in the inhibition of OASS.<sup>98</sup> In particular, the carboxylic moiety of the Ile267, the last amino acid of the C-terminal chain, is essential for the interaction between SAT and OASS.<sup>99</sup> Starting from this evidence, the efforts of our research group in the development of cysteine inhibitors culminated with the development of **UPAR415**, which, to our knowledge, is the most potent synthetic OASS inhibitor known so far (**Figure 14**). Indeed, the analysis of a small pentapeptides library led to the disclosure of molecules with an affinity toward the enzyme in a micromolar range. The chemical issues usually showed to the peptides, such as the low stability and low bioavailability, prompted us to use these molecules as a template for the development of the first non-peptidic OASS inhibitor.<sup>43,100</sup> The carboxylic acid moiety was kept intact due to the pivotal role for the activity, and this moiety was linked to an alkyl chain through a suitable spacer such as a cyclopropane. The alkyl moiety mimics the isoleucine side chain, and the spacer was used to block the chain and the carboxylic acid in the favorable *trans* configuration. Compound **A** was found to be the most active of these cyclopropane inhibitors, with a  $K_d$  towards OASS-A of 1.45  $\mu\text{M}$ . Despite the promising activity, this compound suffered from several drawbacks, like harsh synthesis, being highly volatile, and poor chemical stability in the stock solution used in the biological assays. With the aim to bypass these issues and find new molecules able to inhibit both the OASS isoforms, the vinyl moiety of compound **A** was embodied into a phenyl ring (compound **B**). The *trans* configuration was retained. Structure-Activity Relationship study led to the optimization of compound **B** and the discovery of the most potent OASS inhibitor known so far, namely **UPAR415**.<sup>101</sup> This compound showed a  $K_d$  in the nanomolar range toward both the OASS isoforms, ensuring the complete inhibition of cysteine biosynthesis. Despite the potent activity of **UPAR415** *in vitro*, **UPAR415** was virtually inactive in the cellular assay, although we have demonstrated that this compound acts as an adjuvant when used in combination with colistin, a last resort antibiotic that acts by disrupting the bacterial membranes.<sup>102,103</sup> However, it seems there is a lack of correlation between the remarkable affinity towards the enzyme and the high

concentrations used in the cellular assay, leading to the speculation that this compound likely suffers from poor cellular penetrability, limiting its potential use as an antibacterial adjuvant.

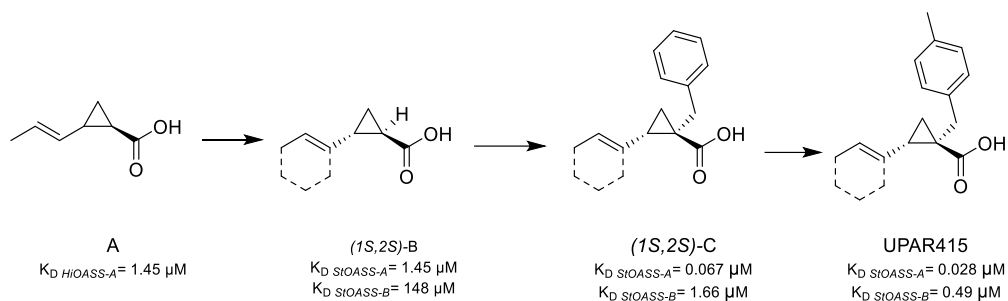
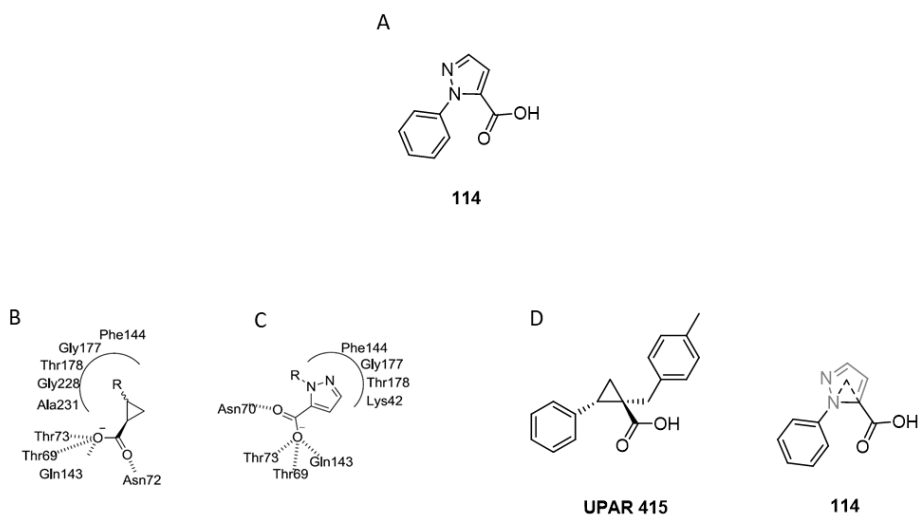


**Figure 14.** Expansion of cyclopropane scaffold.

## 4.2. Exploration of carboxylic acid fragments in the search of novel chemotypes with OASS inhibitory properties

### 4.2.1. Background

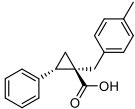
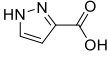
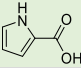
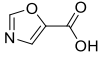
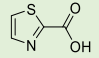
Despite excellent inhibitory activity towards the OASS enzyme, **UPAR415** showed only modest activity in the cellular assay. Therefore its structure was used as the template in a scaffold hopping approach to identify new chemical entities that may enhance the permeability of the membrane and bypass the synthetic challenges of the cyclopropane ring. Taking in mind the SAR information acquired so far about the cyclopropane derivatives, keeping the carboxylic acid portion intact was considered essential due to the pivotal role this moiety plays in inhibitory activity. Among the different potential molecules identified, compound **114** was selected for biochemical evaluation on the target enzyme (**Figure 15 A**). Indeed, this compound showed a binding pattern with the OASS backbone similar to **UPAR415** (**Figure 15, B, and C**). Furthermore, it was possible to envisage a structural similarity of a compound with a cyclopropane core and the identified compound **115** (**figure 15 D**).



**Figure 15.** (A) Chemical structure of compound **114** (B) Interactions of StOASS-A with the cyclopropane (C) and compound **114**. (D) Visual comparison of the structure of **UPAR415** and compound **114**.

Compound **114** showed a 50% inhibition of OASS-A activity at 1mM, a result encouraging enough to suggest further investigation. A small set of analogues was synthesized, and both the N-1 and the N-2 positions of the pyrazole were substituted to identify which position was the most prone to be substituted. Surprisingly, despite the different electronic characters of the substituents introduced (EDG or EWG) on the pyrazole scaffold, the most active derivate was the unsubstituted 1-H-pyrazole-5-carboxylic acid (compound **115**). This fragment showed a 90% inhibition at 1mM and a  $K_d$  of 122  $\mu$ M on OASS-A and a higher  $K_d$  of  $272 \pm 10 \mu$ M towards OASS-B, in compliance with the general trend. This result prompted us to evaluate the activity of other 5-membered heterocycles bearing carboxylic acid function. As it is reported in **Table 7**, compound **116** and compound **118** showed increased inhibitory activity compared to compound **115**.<sup>104</sup>

**Table 7.** Activity of compounds **115-118**.

Cpd	Structure	MW (g/mol)	$K_d$ OASS-A ( $\mu$ M)	$K_d$ OASS-B ( $\mu$ M)	LE (OASS-A) <sup>a</sup> kcal/mol/HA	LE (OASS-B) <sup>a</sup> kcal/mol/HA	ClogP <sup>b</sup>	TPSA <sup>b</sup>
UPAR 415		266.33	0.03	0.049	0.52	0.50	3.60	37.30
<b>115</b>		112.09	122 $\pm$ 5	272 $\pm$ 10	0.67	0.61	0.13	65.98
<b>116</b>		111.1	59 $\pm$ 11	465 $\pm$ 50	0.72	0.60	0.66	53.09
<b>117</b>		113.07	120 $\pm$ 12	548 $\pm$ 59	0.67	0.60	0.04	63.33
<b>118</b>		129.14	52 $\pm$ 6	338 $\pm$ 14	0.74	0.60	0.17	50.19

<sup>a</sup>LE=(1.37/HA). pIC<sub>50</sub> where HA refers to heavy atoms.

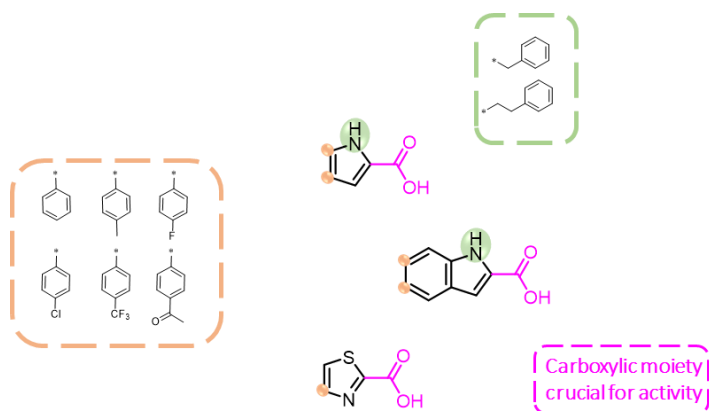
<sup>b</sup>ClogP and TPSA were calculated using molinspiration website (<http://www.molinspiration.com/>).

### 4.2.2. Aim of the project

Many molecules have been developed following a fragment-based drug design (FBDD) approach, which has assumed an important role in target-based drug discovery.<sup>105</sup> The aim of FBDD is to generate potent small-molecule compounds working around small fragments which are characterized by low molecular weight, simple chemical structure, easiness of synthesis, and a low but encouraging binding affinity towards the target.<sup>106,107</sup>

Compounds **116** and **118**, with a two-fold increase of the  $K_d$  towards OASS-A compared to the pyrazole **115**, although not standard fragments, embodied all the characteristics to represent suitable fragment-like derivatives to work on the analysis of the inhibitory activity showed by the 5-membered heterocycles tested, leads us to speculate that compounds bearing carboxylic acid moiety at the C-2 may bring to derivatives with an improved  $K_d$  (**Table 7**). Considering this, the carboxylic moiety in position C-2 was kept during the first round of optimization.

With only this hint in hand, the project went on expanding the fragments with the aim of improving their affinity towards *StOASS*. Compounds **116** and **118** were used as plausible templates for this optimization. During this preliminary round of modifications, lipophilic substituents, such as substituted phenyl rings, were introduced to enlarge the fragments. The pyrrole derivatives were synthesized bearing the lipophilic substituents in two positions, namely at the C-4 and C-5. On the contrary, the thiazole derivatives were synthesized with substituents at the C-4. Additionally, to be seen as a modification of the pyrrole ring, we deemed of interest also to synthesize indole-2-carboxylic acid analogues. In this case, the pyrrole fragment is embodied in a more rigid and bulky structure, and valuable hints might be obtained regarding the activity of the molecule inside the pocket. As for the pyrrole, indole derivatives were synthesized bearing substituents in two positions, at C-5 and C-6. The phenyl moiety introduced in the structure of the acid fragments was decorated with small EWGs or EDGs, arbitrarily introduced in the *para* position in this first series of modifications. Furthermore, a small set of N-substituted pyrrole and indole derivatives was synthesized to evaluate whether the capability of donating H-bond of these moieties might affect the activity of the compounds (**Figure 16**).

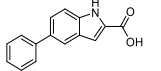
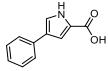
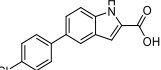
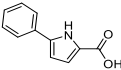
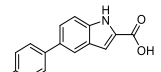
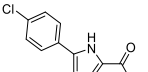
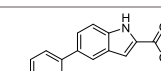
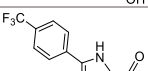
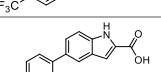
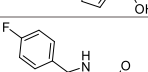
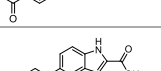
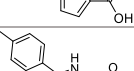
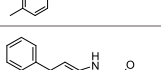
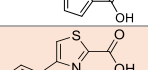
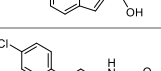
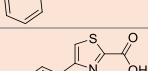
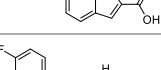
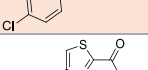
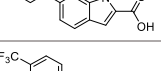
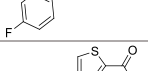
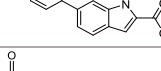
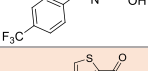
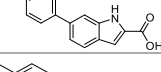
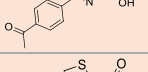
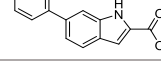
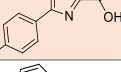
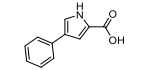
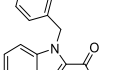


**Figure 16.** Fragment modifications.

### 4.2.3. Results and Discussions

The straightforward synthetic route established to synthesize the fragment derivatives (**Scheme 7** and **8**) allowed us to obtain a variously substituted set of molecules. Three fragments bearing a carboxylic moiety on the C-2 with a pyrrole, thiazole, or indole core were chosen as a starting point for the fragment optimization. Moreover, a phenyl appendage, suitably substituted with EWGs (F, Cl, CF<sub>3</sub>, COMe) and EDG (Me) in the *para* position, was introduced on each heterocyclic fragment. This way, the designed compounds have an MW ranking between 187 and 305 Da and a ClogP between 3 and 5, allowing the placement of additional moieties to optimize the hit discovery process. The binding affinity of the analogues was evaluated through fluorimetric titration (**Table 8**). Quite unexpectedly, the large majority of the attempts to expand the structure of the fragments were unsuccessful, as most of the compounds synthesized did not bind the enzyme. In particular, none of the pyrrole and indole derivatives substituted with a phenyl ring was able to interact with the OASS isoforms. A weak affinity for the enzyme could be detected for four of the six thiazole derivatives (**142**, **143**, **146**, **147**), although only toward the OASS-A isoforms. In any case, none of these derivatives was found to be more affine than the original fragment compound **118**.

**Table 8.** Dissociation constants of the synthesized compound determined for *StOASS-A* and *StOASS-B*

Cpd	Structure	Fluorescence $K_D$ ( $\mu\text{M}$ )		Cpd	Structure	Fluorescence $K_D$ ( $\mu\text{M}$ )	
		OASS-A	OASS-B			OASS-A	OASS-B
119		N.b.*	N.b.	136		N.b.	N.b.
120		N.b.	N.b.	137		N.b.	N.b.
121		N.b.	N.b.	138		N.b.	N.b.
122		N.b.	N.b.	139		N.b.	N.b.
123		N.b.	N.b.	140		N.b.	N.b.
124		N.b.	N.b.	141		N.b.	N.b.
125		N.b.	N.b.	142		396±47	>600
126		N.b.	N.b.	143		230±19	N.b.
127		N.b.	N.b.	144		N.b.	N.b.
128		N.b.	N.b.	145		N.b.	N.b.
129		N.b.	N.b.	146		197±7	N.b.
130		N.b.	N.b.	147		140±37	N.b.
131		N.b.	N.b.	148		N.b.	N.b.
132		N.b.	N.b.	149		N.b.	N.b.



Cpd	Structure	Fluorescence $K_D$ ( $\mu\text{M}$ )		Cpd	Structure	Fluorescence $K_D$ ( $\mu\text{M}$ )	
		OASS-A	OASS-B			OASS-A	OASS-B
<b>133</b>		N.b.	N.b.	<b>150</b>		5.0±0.6	20.2±0.4
<b>134</b>		N.b.	N.b.	<b>151</b>		116±9	6.7±0.4
<b>135</b>		N.b.	N.b.				

\*N.b= No binding

Despite the small number of active compounds and the range of the activity that cannot be considered promising, a rough SAR can be proposed concerning the phenyl attached at the C-4. Thiazole bearing the unsubstituted phenyl moiety showed the highest  $K_d$  of the set (**142**,  $K_d$  OASS-A = 396±47 $\mu\text{M}$ ). Introducing small groups on the phenyl moiety increase the activity, with a better propensity for EDGs. Indeed, the *p*-methyl moiety led to the most active compound of the series (**147**,  $K_d$  OASS-A = 140±37). Among the EWGs tested, chlorine and acetoxy groups are able to interact with the enzyme despite showing a weaker binding affinity compared to **147** (**143**,  $K_d$  OASS-A 230±19  $\mu\text{M}$ ; **146**,  $K_d$  OASS-A = 197±7  $\mu\text{M}$ ). Its replacement with other EWGs such as trifluoromethyl (**145**), a group widely used in medicinal chemistry to replace the methyl, is detrimental to the binding affinity, as well as substitution with fluorine, likely due to their electronegative effect.

These modifications all led to a set of compounds inactive on the OASS-B isoform and with a weak activity on the OASS-A.

Concerning the substitution of the pyrrole and indole nitrogen, a phenyl ring was introduced with methylene and an ethylene bridge. The latter leads to derivatives with less structural rigidity, which may allow a favorable binding pose of the molecule inside the pocket, and thus an improved binding affinity.

Whereas the indole derivatives **148** and **149** did not show any activity, the pyrrole analogues **150** and **151** showed a binding affinity that deserves further attention. N-benzyl derivative **150** showed a  $K_d$  of 5.0±0.6  $\mu\text{M}$  to OASS-A and a  $K_d$  of 20.2±0.4  $\mu\text{M}$  towards OASS-B. Considering the small size, the low ClogP, and the easiness of

synthesis, **150** holds promise for further amelioration. Likely ways of intervention might be the spacer and the phenyl ring, which could be further modified, either through the addition of substituents or through its substitution with other heterocyclic rings. Regardless, also considering the activity of hit compound **114** and considering the small, but still detectable, affinity of the thiazole derivatives, the most important information disclosed after this first round of modification is that a hint of activity is obtained when the H-bond donor character of the fragment nitrogen is abolished. Concerning compound **151**, it seems the affinity to OASS-A is significantly reduced (23-fold decrease) when an ethylene carbon spacer was added between the phenyl and the pyrrole core (**150**,  $K_d$  OASS-A =  $5.0 \pm 0.6$   $\mu$ M; **151**  $K_d$  OASS-A =  $116 \pm 9$   $\mu$ M). However, this modification led to an improved activity toward OASS-B compared to **150**, with a  $K_d$  OASS-B of  $6.7 \pm 0.4$   $\mu$ M. To our experience, this is the first time that a compound is more affine to the OASS-B isoform than the OASS-A, or at least with this difference in the experimental  $K_d$ . Despite the block of both the isoforms is desirable in case of infection, however blocking the inducible isoform might add further selectivity to the action of a potential drug and avoid the raise of resistance. In addition, this compound could be used to develop selective OASS-B inhibitors and represents a valuable chemical probe to gain insights into the difference between the two isoforms of the enzyme.

#### 4.2.4. Biophysical Binding Studies

The synthesized fragments were biochemically evaluated on both the recombinant OASS isoforms to determine the binding affinity. The dissociation constant of the derivatives was measured by a fluorimetric method. This method allows the direct determination of the dissociation constant by exploiting the increase in the fluorescence emission of the cofactor PLP upon ligand binding at the active site. Indeed, when the ligand binds the OASS an increased fluorescence emission of the PLP cofactor at 505 nm occurs upon excitation at the 412 nm (**Figure 17**).<sup>66</sup>

Measurements were carried out on solutions containing 1  $\mu$ M OASS in 100 mM Hepes pH 7, and triturated with increasing concentrations of compounds at 20 °C.

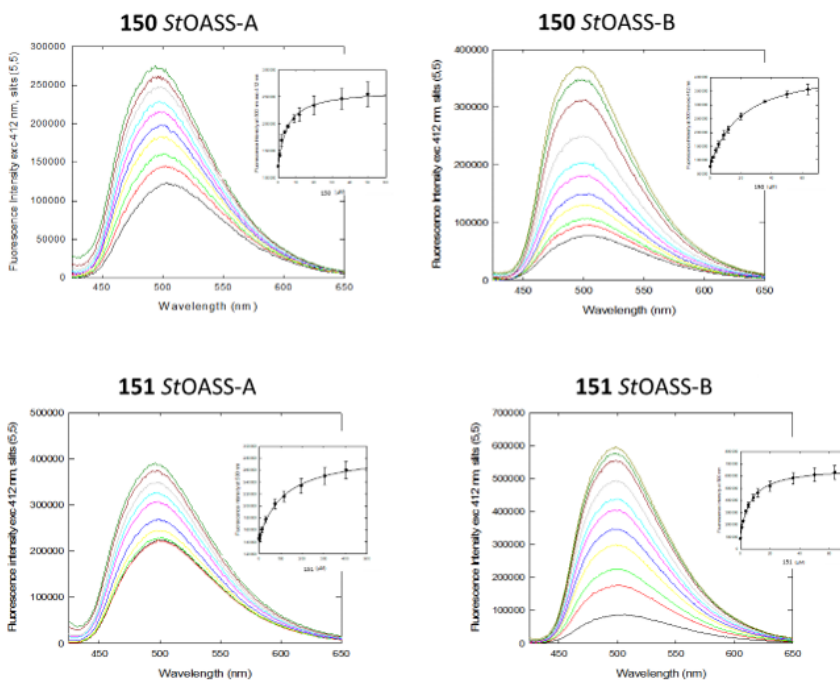
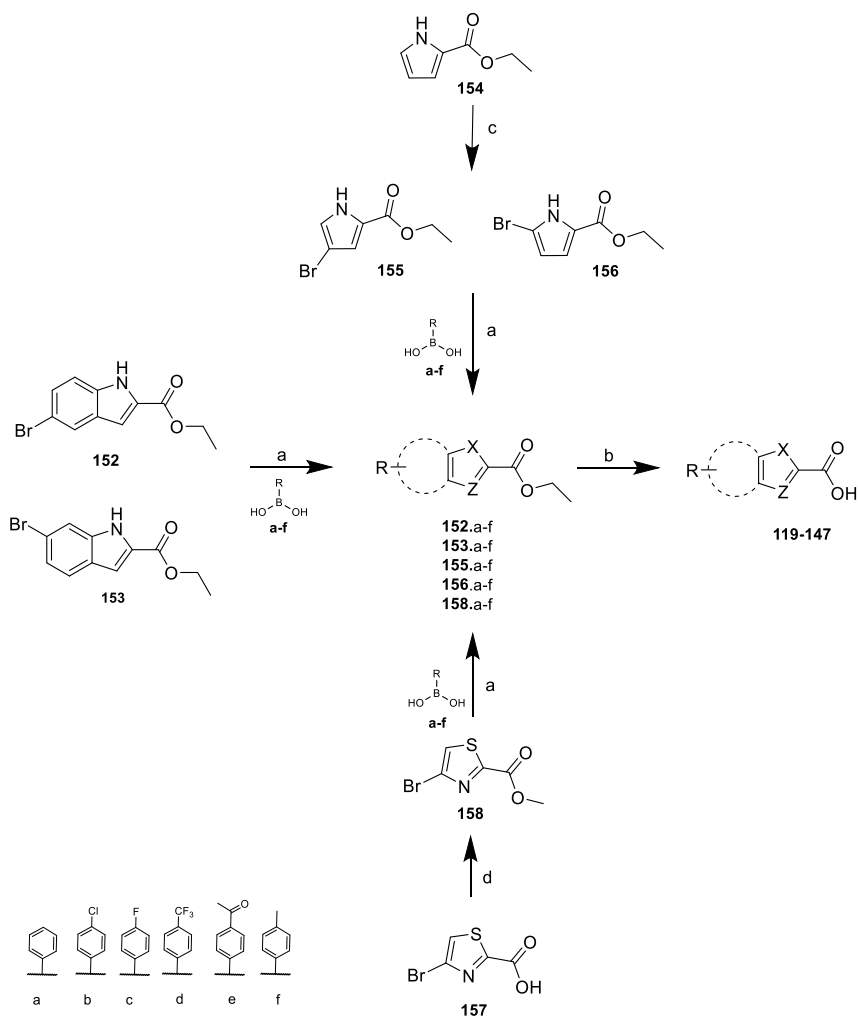


**Figure 17.** Binding of **150** and **151** to StOASS-A (A and C) and StOASS-B (B and D) as probe by the increase in the fluorescence emission of the cofactor PLP.

#### 4.2.5. Chemistry

The final compounds were obtained using a versatile and straightforward protocol, which allowed the synthesis of a series of carboxylic acid fragments with different cores and consisted of two main steps. The phenyl substituents were introduced on the scaffold *via* the Suzuki-Miyaura cross-coupling reaction. The indole, pyrrole, or thiazole bromo derivatives (**152**, **153**, **155**, **156**, **158**) were reacted with various boronic acids in a mixture of THF/H<sub>2</sub>O, using tripotassium phosphate as the base and XPhos PdG2 as the catalyst. The reaction allowed us to afford the desired intermediates in 2-3 hours and in a good yield (40-81%). Then the corresponding carboxylic ester intermediates were hydrolyzed to the final carboxylic acid compounds (**Scheme 7**). The ethyl 5-bromo-1H-indole-2-carboxylate **152** and the ethyl 6-bromo-1H-indole-2-carboxylate **153** were commercially available. The thiophene analogues **158** was obtained from the commercially available 4-bromothiophene-2-carboxylic acid *via* prior conversion of its

**Scheme 7.** *a*; *b*

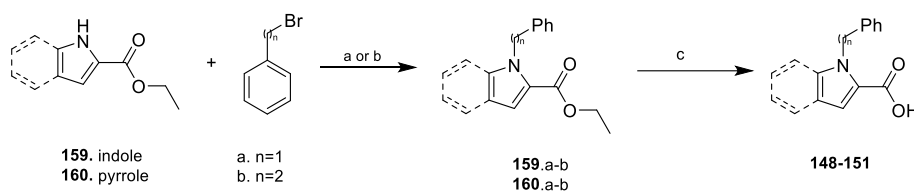


**Scheme 7.** *a* Reagents and conditions. (a)  $K_3PO_4$ , X-Phos Pd G2, THF/ $H_2O$ ,  $70^\circ C$ , 2h, 40-81%; (b) LiOH, THF/ $H_2O$ , reflux, 2-12 h, 40-92%; (c) NBS, THF/MeOH, r.t., 40-38%; d)  $CH_3I$ ,  $K_2CO_3$ , DMF, r.t., on, 90%. *b* For complete structure, see **Table 8**.

methyl ester by reaction with iodomethane in DMF. Subsequently, the obtained methyl ester **158** was submitted to the Suzuki-Miyaura cross-coupling reaction. Regarding the pyrrole derivatives, ethyl 1H-pyrrole-2-carboxylate was purchased, and the subsequent bromination with N-Bromosuccinimide (NBS) allowed the isolation of both the bromo derivatives **155** and **156**, which could be easily separated with flash chromatography according to a protocol already reported in the literature.<sup>108,109</sup>

The N-substituted derivatives (**148-151**) were obtained in two steps. First, the commercially available ethyl 1H-indole-2-carboxylate (**159**) or ethyl 1H-pyrrole-2-carboxylate (**160**) was alkylated with the proper bromo derivative (a or b) in the presence of a suitable base. Then the esters were hydrolyzed to afford the desired final compounds (**Scheme 8**).

### Scheme 8.



**Scheme 8.** <sup>a</sup> Reagents and conditions. pyrrole derivatives: (a): NaH, DMF, r.t.; 45-85%; indole derivatives: (b) Cs<sub>2</sub>CO<sub>3</sub>, ACN, 60°C, o.n., 40-92%; (c) LiOH, THF/ H<sub>2</sub>O, reflux, 2-12 h, 68-87%.

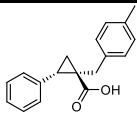
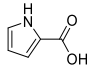
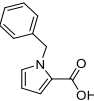
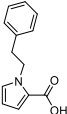
<sup>b</sup> For complete structure, see **Table 8**

### 4.2.6. Conclusion

A large set of compounds was synthesized, taking inspiration from the identified fragment compounds **116** and **118**. Although most derivatives did not show activity towards the enzyme, a hint of SAR can be drafted. Embodying the pyrrole core in a bulky and rigid structure as the indole ring is detrimental to the activity. Moreover, the length of the spacer between the pyrrole ring and the phenyl substituent may affect the selectivity towards OASS isoforms. Indeed, increasing the length of the spacer seems to shift the affinity of the compound towards the OASS-B. It may be concluded that a short spacer is suitable for a compound with an appreciable binding affinity

towards both the isoforms, and further optimizations are needed to refine the SAR of this promising fragment. Additionally, we can speculate that the improved activity showed to **151** towards OASS-B may be attributed to the different sizes of the active site between the two isoforms. At this regard, it is worthwhile to remember that OASS-B active site is bigger than that of OASS-A.<sup>42,101,110</sup> The flexibility of the ethyl chain may lead to a better posing of the compound in the binding pocket, resulting in an increased affinity. Following this rationale, this might explain the drop of the activity toward OASS-A. The N-substituted pyrrole **150** is the most active compound of the series, with a remarkable improvement in the  $K_d$  compared to compound **116**, the 1H-pyrrole-2-carboxylic acid. Indeed, the affinity toward OASS-A was 12-fold increased and 23-fold to OASS-B (**116**,  $K_{d\text{ OASS-A}} = 59 \pm 11 \mu\text{M}$ ,  $K_{d\text{ OASS-B}} = 465 \pm 50 \mu\text{M}$ ; **150**,  $K_{d\text{ OASS-A}} = 5.0 \pm 0.6 \mu\text{M}$ ,  $K_{d\text{ OASS-B}} = 20.2 \pm 0.4 \mu\text{M}$ ) (Table 9).

**Table 9.** Activity of compounds **UPAR415**, **116**, **150** and **151**.

Cpd	Structure	MW (g/mol)	$K_d$ OASS-A ( $\mu\text{M}$ )	$K_d$ OASS-B ( $\mu\text{M}$ )	LE (OASS-A) <sup>a</sup> kcal/mol/HA	LE (OASS-B) <sup>a</sup> kcal/mol/HA	ClogP <sup>b</sup>	TPSA <sup>b</sup>
<b>UPAR 415</b>		266.33	0.03	0.049	0.52	0.50	3.60	37.30
<b>116</b>		111.1	59 ± 11	465 ± 50	0.72	0.60	0.66	53.09
<b>150</b>		201.22	5.0 ± 0.6	20.2 ± 0.4	0.49	0.44	2.54	42.33
<b>151</b>		215.25	116 ± 9	6.7 ± 0.4	0.34	0.45	2.54	41.23

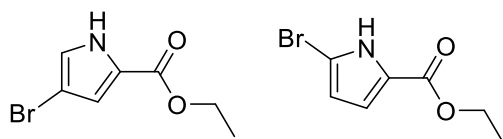
<sup>a</sup>LE=(1.37/HA). pIC<sub>50</sub> where HA refers to heavy atoms.

<sup>b</sup>ClogP and TPSA were calculated using molinspiration website (<http://www.molinspiration.com/>).

Also, the thiazole derivatives showed some appreciable activity, despite being considerably less affine than the original fragment **114** and then hit compounds **150** and **151**. Also, for these derivatives, a few SAR considerations could be drafted based on the substituents at the phenyl ring attached at C-4. In conclusion, despite the large majority of the compounds prepared did not have activity toward the enzymes, **150** and **151** offer can be considered intriguing derivatives to start a second round of modifications, in the hope to improve affinity and shed light on the active site of the OASS-A and OASS-B enzymes corroborate this information.

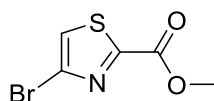
#### 44.2.7. Experimental section

##### Synthetic procedure to obtain Ethyl 4-bromo-1H-pyrrole-2-carboxylate (155) and Ethyl 5-bromo-1H-pyrrole-2-carboxylate (156)



Ethyl 1H-pyrrole-2-carboxylate (150 mg, 1.07 mmol) was dissolved in THF/H<sub>2</sub>O (2/1, 5 mL/mmol). Then, the solution was cooled at 0°C, and N-bromosuccinimide (211 mg, 1.18 mmol) was added portion-wise over 2 hours. The reaction mixture was stirred at room temperature for 4 h. After this time, water was added to the reaction mixture, and it was extracted with EtOAc (3 X 20 mL), then the organic layers were dried over anhydrous Na<sub>2</sub>SO<sub>4</sub>, filtered, and concentrated under reduced pressure. The crude was purified by flash column chromatography eluting with Petroleum Ether/EtOAc to afford the title compounds. Ethyl 5-bromo-1H-pyrrole-2-carboxylate (yield: 40%). <sup>1</sup>H NMR (400 MHz, CDCl<sub>3</sub>): δ 9.32 (s, 1H); 6.93 (dd, *J*<sub>1</sub> = 3.8, *J*<sub>2</sub> = 2.7 Hz, 1H); 6.22 (dd, *J*<sub>1</sub> = 3.8, *J*<sub>2</sub> = 2.6 Hz, 1H); 4.33 (q, *J* = 7.1 Hz, 2H); 1.36 (t, *J* = 7.1 Hz, 3H). Ethyl 4-bromo-1H-pyrrole-2-carboxylate (yield: 35%). <sup>1</sup>H NMR (400 MHz, CDCl<sub>3</sub>): δ 9.40 (s, 1H); 6.82 (dd, *J*<sub>1</sub> = 3.0, *J*<sub>2</sub> = 1.6 Hz, 1H); 6.89 (dd, *J*<sub>1</sub> = 2.6, *J*<sub>2</sub> = 1.6 Hz, 1H); 4.32 (q, *J* = 7.1 Hz, 2H); 1.35 (t, *J* = 7.1 Hz, 3H). Spectra data were consistent with those reported in literature.<sup>108,109</sup>

##### Synthetic procedure to obtain Methyl 4-bromothiazole-2-carboxylate (158)



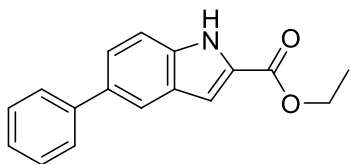
A mixture of 4-bromothiazole-2-carboxylic acid (500 mg, 2.42 mmol), K<sub>2</sub>CO<sub>3</sub> (700 mg, 5.07 mmol), and CH<sub>3</sub>I (0.451 mL, 1.25 mmol) in DMF (2 mL/mmol) was stirred at room temperature overnight. Water was added to the reaction mixture, and it was extracted with EtOAc (3 X 30 mL). The organic layers were dried over anhydrous Na<sub>2</sub>SO<sub>4</sub>, filtered, and concentrated under reduced pressure. The product was used in the next step without further purification (yield: 70%). <sup>1</sup>H NMR (400 MHz, CDCl<sub>3</sub>): δ 7.55 (s, 1H); 4.02 (s, 3H).



## General procedure for the Suzuki-Miyaura Cross-Coupling Reaction

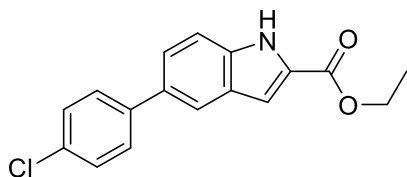
To a solution of the proper Bromo derivatives (1.00 eq) in THF/H<sub>2</sub>O (3:1, 10 mL/mmol) were added the appropriate boronic acid or ester (1.5 eq) and potassium phosphate tribasic (2.00 eq). The mixture was stirred under a nitrogen atmosphere for 10 minutes. After this time, X-Phos Pd G2 (0.15 eq) was added, and the reaction mixture was stirred at 70°C for 2 hours. After cooling to room temperature, the reaction mixture was filtered through a plug of celite. The filtrate was concentrated under reduced pressure, and the residue was extracted with EtOAc (3 X 25 mL), dried over anhydrous Na<sub>2</sub>SO<sub>4</sub>, filtered, and concentrated under reduced pressure. The crude was purified by flash column chromatography eluting with Petroleum Ether/EtOAc. Purification conditions, yields, and analytical data are reported below.

### Ethyl 5-phenyl-1H-indole-2-carboxylate (152 a)



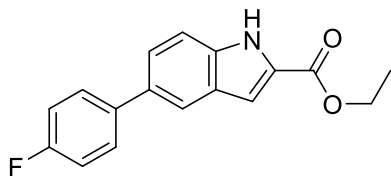
Purification by flash column chromatography eluting with Petroleum Ether/EtOAc 90:10 afforded the product as a orange powder (yield: 81%). <sup>1</sup>H NMR (400 MHz, CDCl<sub>3</sub>): δ 8.97 (s, 1H); 7.90 – 7.88 (m, 1H); 7.66 – 7.63 (m, 2H); 7.59 (dd, *J* = 8.6, 1.7 Hz, 1H); 7.50 - 7.43 (m, 3H); 7.37 - 7.31 (m, 1H); 7.28 – 7.27 (m, 1H); 4.49 (q, *J* = 7.1 Hz, 2H); 1.44 (t, *J* = 7.1, 3H).

### Ethyl 5-(4-chlorophenyl)-1H-indole-2-carboxylate (152 b)



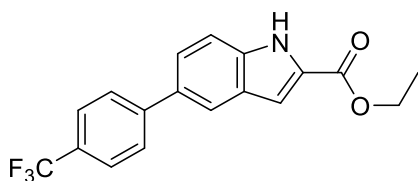
Purification by flash column chromatography eluting with Petroleum Ether/EtOAc 90:10 afforded the product as a yellow powder (yield: 74%). <sup>1</sup>H NMR (400 MHz, CDCl<sub>3</sub>): δ 9.01 (s, 1H); 7.87 – 7.84 (m, 1H); 7.57 – 7.52 (m, 3H); 7.48 – 7.47 (m, 1H); 7.42 - 7.39 (m, 1H); 7.27 - 7.26 (m, 1H); 4.44 (q, *J* = 7.1 Hz, 2H); 1.44 (t, *J* = 7.1, 3H).

### Ethyl 5-(4-fluorophenyl)-1H-indole-2-carboxylate (152 c)



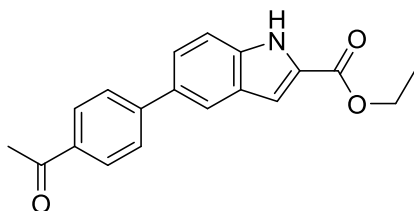
Purification by flash column chromatography eluting with Petroleum Ether/EtOAc 90:10 afforded the product as a light brown powder (yield: 77%).  $^1\text{H}$  NMR (400 MHz,  $\text{CDCl}_3$ ):  $\delta$  8.96 (s, 1H); 7.84 – 7.82 (m, 1H); 7.60 – 7.56 (m, 2H); 7.53 (dd,  $J_1 = 8.6, 1.7$  Hz, 1H); 7.49 - 7.47 (m, 1H); 7.27 - 7.26 (m, 1H); 7.16 – 7.11 (m, 2H); 4.44 (q,  $J = 7.1$  Hz, 2H); 1.44 (t,  $J = 7.1$  Hz, 3H).

### Ethyl 5-(4-(trifluoromethyl)phenyl)-1H-indole-2-carboxylate (152 d)



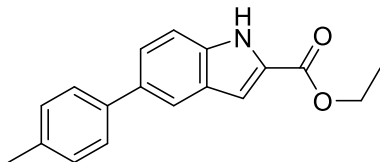
Purification by flash column chromatography eluting with Petroleum Ether/EtOAc from 95:5 to 90:10 afforded the product as a yellow powder (yield: 60%).  $^1\text{H}$  NMR (400 MHz,  $\text{DMSO}-d_6$ ):  $\delta$  12.04 (s, 1H); 8.07 – 8.03 (m, 1H); 7.92 (d,  $J = 8.1$  Hz, 1H); 7.80 (d,  $J = 8.3$  Hz, 2H); 7.66 (dd,  $J_1 = 8.7, 1.8$  Hz, 1H); 7.25 – 7.24 (m, 1H); 4.37 (q,  $J = 7.1$  Hz, 2H); 1.37 (t,  $J = 7.1$  Hz, 3H).

### Ethyl 5-(4-acetylphenyl)-1H-indole-2-carboxylate (152 e)



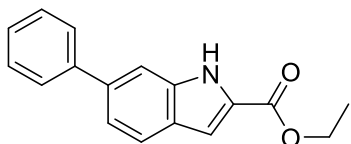
Purification by flash column chromatography eluting with Petroleum Ether/EtOAc 90:10 afforded the product as a yellow powder (yield: 39%).  $^1\text{H}$  NMR (400 MHz,  $\text{CDCl}_3$ ):  $\delta$  8.95 (s, 1H); 8.05 – 8.03 (m, 2H); 7.97 – 7.93 (m, 1H); 7.75 – 7.22 (m, 2H); 7.62 (dd,  $J_1 = 8.6, 1.8$  Hz, 1H); 7.54 – 7.49 (m, 1H); 7.28 - 7.29 (m, 1H); 4.44 (q,  $J = 7.1$  Hz, 2H); 2.65 (s, 3H); 1.44 (t,  $J = 7.1$  Hz, 3H).

**Ethyl 5-(p-tolyl)-1H-indole-2-carboxylate (152 f)**



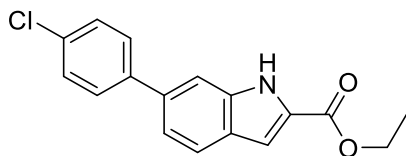
Purification by flash column chromatography eluting with Petroleum Ether/EtOAc from 96:4 to 94:6 afforded the product as a pale yellow powder (yield: 74%). <sup>1</sup>H NMR (400 MHz, DMSO-*d*<sub>6</sub>): δ 11.92 (s, 1H); 7.91 – 7.89 (m, 1H); 7.59 – 7.50 (m, 4H); 7.29 (d, *J* = 7.9 Hz, 2H); 7.18 - 7.17 (m, 1H); 4.36 (q, *J* = 7.1 Hz, 2H); 2.35 (s, 3H); 1.36 (t, *J* = 7.1 Hz, 3H).

**Ethyl 6-phenyl-1H-indole-2-carboxylate (153 a)**



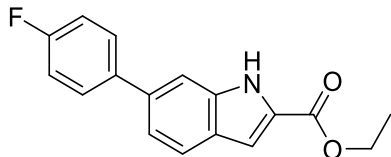
Purification by flash column chromatography eluting with Petroleum Ether/EtOAc 90:10 afforded the product as a white powder (yield: 67%). <sup>1</sup>H NMR (400 MHz, DMSO-*d*<sub>6</sub>): δ 11.97 (s, 1H); 7.75 (d, *J* = 8.4 Hz, 1H); 7.69 – 7.66 (m, 3H); 7.49 (t, *J* = 7.6 Hz, 2H); 7.42 - 7.35 (m, 2H); 7.19 (s, 1H); 4.36 (q, *J* = 7.1 Hz, 2H); 1.36 (t, *J* = 7.1 Hz, 3H).

**Ethyl 6-(4-chlorophenyl)-1H-indole-2-carboxylate (153 b)**



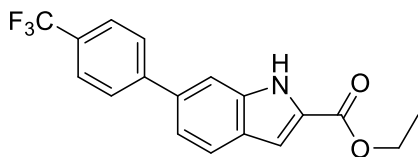
Purification by flash column chromatography eluting with Petroleum Ether/EtOAc 95:5 afforded the product as a pale yellow powder (yield: 71%). <sup>1</sup>H NMR (400 MHz, DMSO-*d*<sub>6</sub>): δ 12.00 (s, 1H); 7.76 (d, *J* = 8.4 Hz, 1H); 7.72 – 7.69 (m, 2H); 7.68 - 7.65 (m, 1H); 7.55 – 7.52 (m, 2H); 7.40 (dd, *J* = 8.4, 1.6 Hz, 1H); 7.19 – 7.18 (m, 1H); 4.36 (q, *J* = 7.1 Hz, 2H); 1.36 (t, *J* = 7.1 Hz, 3H).

### Ethyl 6-(4-fluorophenyl)-1H-indole-2-carboxylate (153 c)



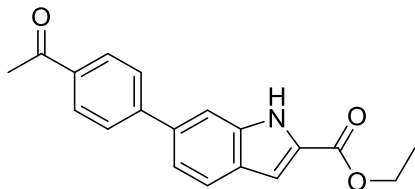
Purification by flash column chromatography eluting with Petroleum Ether/EtOAc from 96:4 to 92:8 afforded the product as a white powder (yield:67 %).  $^1\text{H}$  NMR (400 MHz,  $\text{CDCl}_3$ ):  $\delta$  8.92 (s, 1H); 7.74 (d,  $J$  = 8.4 Hz, 1H); 7.62 – 7.57 (m, 2H); 7.57 - 7.54 (m, 1H); 7.36 (dd,  $J$  = 8.4, 1.6 Hz, 1H); 7.25 – 7.24 (m, 1H); 7.18 – 7.12 (m, 2H); 4.43 (q,  $J$  = 7.1 Hz, 2H); 1.43 (t,  $J$  = 7.1 Hz, 3H).

### Ethyl 6-(4-(trifluoromethyl)phenyl)-1H-indole-2-carboxylate (153 d)



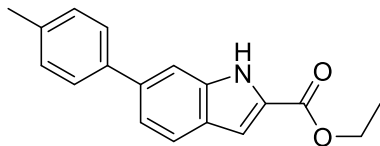
Purification by flash column chromatography eluting with Petroleum Ether/EtOAc 95:5 afforded the product as a pale yellow powder (yield: 78%).  $^1\text{H}$  NMR (400 MHz,  $\text{CDCl}_3$ ):  $\delta$  8.90 (s, 1H); 7.72 -7.63 (m, 6H); 7.57 – 7.55 (m, 1H); 7.34 (dd,  $J$  = 8.4, 1.6 Hz, 1H); 4.36 (q,  $J$  = 7.1 Hz, 2H); 1.36 (t,  $J$  = 7.1 Hz, 3H).

### Ethyl 6-(4-acetylphenyl)-1H-indole-2-carboxylate (153 e)



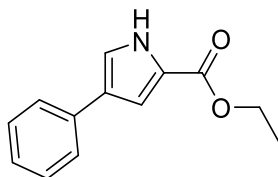
Purification by flash column chromatography eluting with Petroleum Ether/EtOAc 95:5 afforded the product as a white powder (yield: 39%).  $^1\text{H}$  NMR (400 MHz,  $\text{DMSO}-d_6$ ):  $\delta$  12.06 (s, 1H); 8.07 (d,  $J$  = 8.5 Hz, 2H); 7.84 (d,  $J$  = 8.5 Hz, 2H); 7.79 (d,  $J$  = 8.4 Hz, 1H); 7.76 (s, 1H); 7.48 (dd,  $J$  = 8.4, 1.6 Hz, 1H); 7.21– 7.20 (m, 1H); 4.37 (q,  $J$  = 7.1 Hz, 2H); 2.36 (s, 3H); 1.36 (t,  $J$  = 7.1 Hz, 3H).

### Ethyl 6-(p-tolyl)-1H-indole-2-carboxylate (153 f)



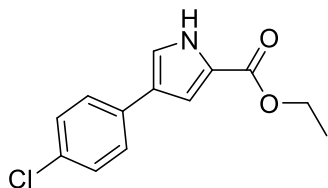
Purification by flash column chromatography eluting with Petroleum Ether/EtOAc from 97:3 to 96:4 afforded the product as a pale yellow powder (yield: 62%). <sup>1</sup>H NMR (400 MHz, DMSO-*d*<sub>6</sub>): δ 11.93 (s, 1H); 7.73 (d, *J* = 8.4 Hz, 1H); 7.64 (s, 1H); 7.57 (d, *J* = 8.1 Hz, 2H); 7.38 (dd, *J* = 8.4, 1.6 Hz, 1H); 7.29 (d, *J* = 7.9 Hz, 2H); 4.36 (q, *J* = 7.1 Hz, 2H); 2.36 (s, 3H); 1.36 (t, *J* = 7.1 Hz, 3H).

### Ethyl 4-phenyl-1H-pyrrole-2-carboxylate (155 a)



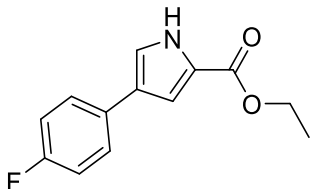
Purification by flash column chromatography eluting with Petroleum Ether/EtOAc from 98:2 to 95:5 afforded the product as a yellow powder (yield: 74%). <sup>1</sup>H NMR (400 MHz, DMSO-*d*<sub>6</sub>): δ 12.02 (s, 1H); 7.63 - 7.61 (m, 2H); 7.50 - 7.49 (m, 1H); 7.35 - 7.31 (m, 2H); 7.19 - 7.15 (m, 2H); 4.26 (q, *J* = 7.1 Hz, 2H); 1.30 (t, *J* = 7.1 Hz, 3H).

### Ethyl 4-(4-chlorophenyl)-1H-pyrrole-2-carboxylate (155 b)



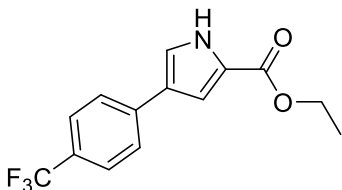
Purification by flash column chromatography eluting with Petroleum Ether/EtOAc from 97:3 to 92:8 afforded the product as a yellow powder (yield: 50%). <sup>1</sup>H NMR (400 MHz, DMSO-*d*<sub>6</sub>): δ 12.08 (s, 1H); 7.66 (d, *J* = 8.4 Hz, 2H); 7.56 - 7.55 (m, 1H); 7.36 (d, *J* = 8.4 Hz, 2H); 7.19 - 7.18 (m, 1H); 4.27 (q, *J* = 7.1 Hz, 2H); 1.31 (t, *J* = 7.1 Hz, 3H).

### Ethyl 4-(4-fluorophenyl)-1H-pyrrole-2-carboxylate (155 c)



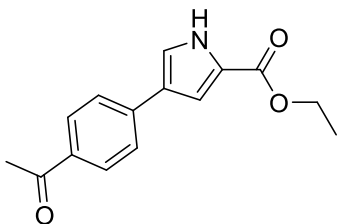
Purification by flash column chromatography eluting with Petroleum Ether/EtOAc from 97:3 to 90:10 afforded the product as a yellow powder (yield: 52%).  $^1\text{H}$  NMR (400 MHz,  $\text{CDCl}_3$ ):  $\delta$  9.17 (s, 1H); 7.49 - 7.44 (m, 2H); 7.17 - 7.16 (m, 1H); 7.14 - 7.13 (m, 1H); 7.08 - 7.02 (m, 2H); 4.35 (q,  $J = 7.1$  Hz, 2H); 1.38 (t,  $J = 7.1$  Hz, 3H).

### Ethyl 4-(4-(trifluoromethyl)phenyl)-1H-pyrrole-2-carboxylate (155 d)



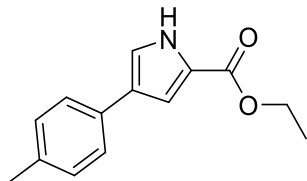
Purification by flash column chromatography eluting with Petroleum Ether/EtOAc from 97:3 to 90:10 afforded the product as a yellow powder (yield: 61%).  $^1\text{H}$  NMR (400 MHz,  $\text{DMSO}-d_6$ ):  $\delta$  12.20 (s, 1H); 7.86 (d,  $J = 8.1$  Hz, 2H); 7.67 - 7.64 (m, 3H); 7.28 (t,  $J = 5.8$  Hz, 1H); 4.27 (q,  $J = 7.1$  Hz, 2H); 1.31 (t,  $J = 7.1$  Hz, 3H).

### Ethyl 4-(4-acetylphenyl)-1H-pyrrole-2-carboxylate (155 e)



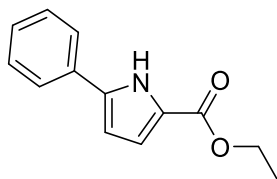
Purification by flash column chromatography eluting with Petroleum Ether/EtOAc from 97:3 to 95:5 afforded the product as a yellow powder (yield: 55%).  $^1\text{H}$  NMR (400 MHz,  $\text{DMSO}-d_6$ ):  $\delta$  12.21 (s, 1H); 7.91 (d,  $J = 8.5$  Hz, 2H); 7.79 (d,  $J = 8.5$  Hz, 2H); 7.69 - 7.68 (m, 1H); 7.31 - 7.28 (m, 1H); 4.28 (q,  $J = 7.1$  Hz, 2H); 2.57 (s, 3H); 1.31 (t,  $J = 7.1$  Hz, 3H).

### Ethyl 4-(p-tolyl)-1H-pyrrole-2-carboxylate (155 f)



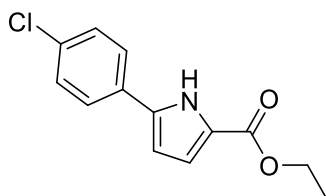
Purification by flash column chromatography eluting with Petroleum Ether/EtOAc from 97:3 to 95:5 afforded the product as a yellow powder (yield: 35%).  $^1\text{H}$  NMR (400 MHz, DMSO- $d_6$ ):  $\delta$  11.97 (s, 1H); 7.50 (d,  $J$  = 8.1 Hz, 2H); 7.44 (dd,  $J$  = 3.1, 1.8 Hz, 1H); 7.15 – 7.12 (m, 3H); 4.25 (q,  $J$  = 7.1 Hz, 2H); 2.28 (s, 3H); 1.30 (t,  $J$  = 7.1 Hz, 3H).

### Ethyl 5-phenyl-1H-pyrrole-2-carboxylate (156 a)



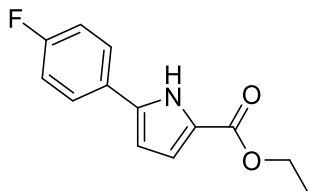
Purification by flash column chromatography eluting with Petroleum Ether/EtOAc from 96:4 to 94:6 afforded the product as a yellow powder (yield: 64%).  $^1\text{H}$  NMR (400 MHz, DMSO- $d_6$ ):  $\delta$  12.06 (s, 1H); 7.85 - 7.83 (m, 2H); 7.40 – 7.37 (m, 2H); 7.29 – 7.25 (m, 1H); 6.85 (dd,  $J$  = 3.8, 2.3 Hz, 1H); 6.64 (dd,  $J$  = 3.8, 2.5 Hz, 1H); 4.26 (q,  $J$  = 7.1 Hz, 2H); 1.30 (t,  $J$  = 7.1 Hz, 3H).

### Ethyl 5-(4-chlorophenyl)-1H-pyrrole-2-carboxylate (156 b)



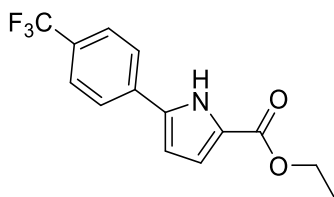
Purification by flash column chromatography eluting with Petroleum Ether/EtOAc from 98:2 to 94:6 afforded the product as a light yellow powder (yield: 65%).  $^1\text{H}$  NMR (400 MHz, DMSO- $d_6$ ): 12.14 (s, 1H); 7.90 – 7.87 (m, 2H); 7.47 - 43 (m, 2H); 6.86 (dd,  $J$  = 3.8, 2.1 Hz, 1H); 6.68 (dd,  $J$  = 3.8, 2.3 Hz, 1H); 4.27 (q,  $J$  = 7.1 Hz, 2H); 1.31 (t,  $J$  = 7.1 Hz, 3H).

### Ethyl 5-(4-fluorophenyl)-1H-pyrrole-2-carboxylate (156 c)



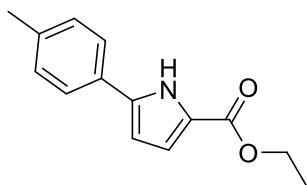
Purification by flash column chromatography eluting with Petroleum Ether/EtOAc from 97:3 to 90:10 afforded the product as a slightly yellow powder (yield: 70%).  $^1\text{H}$  NMR (400 MHz,  $\text{DMSO-}d_6$ ):  $\delta$  12.08 (s, 1H); 7.92 - 7.87 (m, 2H); 7.26 – 7.20 (m, 2H); 6.85 (dd,  $J = 3.8, 2.3$  Hz, 1H); 6.62 (dd,  $J = 3.8, 2.5$  Hz, 1H); 4.27 (q,  $J = 7.1$  Hz, 2H); 1.30 (t,  $J = 7.1$  Hz, 3H).

### Ethyl 5-(4-(trifluoromethyl)phenyl)-1H-pyrrole-2-carboxylate (156 d)



Purification by flash column chromatography eluting with Petroleum Ether/EtOAc from 98:2 to 94:6 afforded the product as a slightly yellow powder (yield: 61%).  $^1\text{H}$  NMR (400 MHz,  $\text{DMSO-}d_6$ ):  $\delta$  12.33 (s, 1H); 8.09 (d,  $J = 8.2$  Hz, 2H); 7.74 (d,  $J = 8.3$  Hz, 2H); 6.91 – 6.89 (m, 1H); 6.82 – 6.81 (m, 1H); 4.29 (q,  $J = 7.1$  Hz, 2H); 1.32 (t,  $J = 7.1$  Hz, 3H).

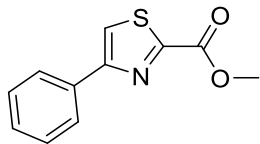
### Ethyl 5-(p-tolyl)-1H-pyrrole-2-carboxylate (156 f)



Purification by flash column chromatography eluting with Petroleum Ether/EtOAc from 98:2 to 94:6 afforded the product as an orange powder (yield: 79%).  $^1\text{H}$  NMR (400 MHz,  $\text{DMSO-}d_6$ ):  $\delta$  11.98 (s, 1H); 7.74 (d,  $J = 8.2$  Hz, 2H); 7.20 (d,  $J = 8.0$  Hz, 2H); 6.85 – 6.83 (m, 1H); 6.59 – 6.58 (m, 1H); 4.26 (q,  $J = 7.1$  Hz, 2H); 2.32 (s, 3H); 1.30 (t,  $J = 7.1$  Hz, 3H).

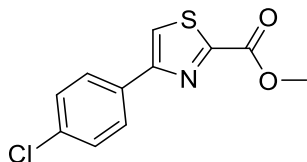


### Methyl 4-phenylthiazole-2-carboxylate (158 a)



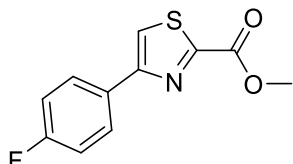
Purification by flash column chromatography eluting with Petroleum Ether/EtOAc 95:5 afforded the product (yield: 72%).  $^1\text{H NMR}$  (400 MHz,  $\text{DMSO-}d_6$ ):  $\delta$  8.55 (s, 1H); 8.03 – 8.00 (m, 2H); 7.52 – 7.48 (m, 2H); 7.44 – 7.40 (m, 1H); 3.96 (s, 3H).

### Methyl 4-(4-chlorophenyl)thiazole-2-carboxylate (158 b)



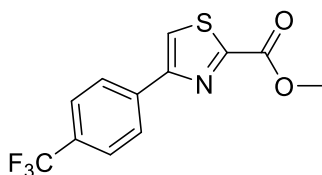
Purification by flash column chromatography eluting with Petroleum Ether/EtOAc 95:5 afforded the product as yellow powder (yield: 38%).  $^1\text{H NMR}$  (400 MHz,  $\text{CDCl}_3$ ):  $\delta$  7.91 – 7.88 (m, 2H); 7.75 (s, 1H); 7.43 – 7.40 (m, 2H); 4.05 (s, 3H).

### Methyl 4-(4-fluorophenyl)thiazole-2-carboxylate LPA64 (158 c)



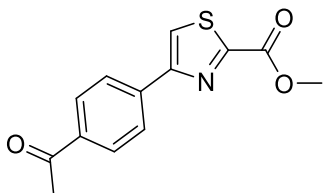
Purification by flash column chromatography eluting with Petroleum Ether/EtOAc 95:5 afforded the product (yield: 80%).  $^1\text{H NMR}$  (400 MHz,  $\text{CDCl}_3$ ):  $\delta$  7.96 – 7.90 (m, 1H); 7.70 (s, 1H); 7.17 – 7.09 (m, 2H); 4.04 (s, 3H).

### Methyl 4-(4-(trifluoromethyl)phenyl)thiazole-2-carboxylate (158 d)



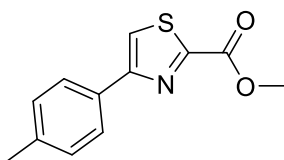
Purification by flash column chromatography eluting with Petroleum Ether/EtOAc 95:5 afforded the product as light yellow powder (yield: 67%).  $^1\text{H NMR}$  (400 MHz,  $\text{CDCl}_3$ ):  $\delta$  8.08 (d,  $J = 8.1$  Hz, 2H); 7.87 (s, 1H); 7.70 (d,  $J = 8.2$  Hz, 2H); 4.06 (s, 3H).

#### Methyl 4-(4-acetylphenyl)thiazole-2-carboxylate (158 e)



Purification by flash column chromatography eluting with Petroleum Ether/EtOAc 95:5 afforded the product (yield: 85%).  $^1\text{H NMR}$  (400 MHz,  $\text{CDCl}_3$ ):  $\delta$  8.08 – 8.02 (m, 4H); 7.89 (s, 1H); 4.06 (s, 3H); 2.64 (s, 3H).

#### Methyl 4-(p-tolyl)thiazole-2-carboxylate (158 f)

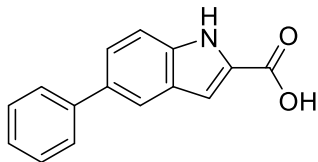


Purification by flash column chromatography eluting with Petroleum Ether/EtOAc 95:5 afforded the product as yellow powder (yield: 73%).  $^1\text{H NMR}$  (400 MHz,  $\text{CDCl}_3$ ):  $\delta$  7.84 (d,  $J = 8.2$  Hz, 2H); 7.24 (s, 1H); 7.24 (m, 2H); 4.03 (s, 3H); 2.39 (s, 3H).

#### General procedure for the hydrolysis of the carboxylic esters

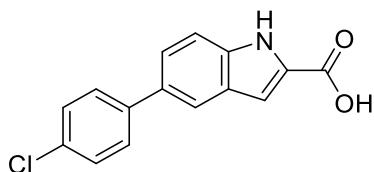
LiOH (8.00 eq) was added to a solution of the proper carboxylic ester (1.00 eq) in THF/ $\text{H}_2\text{O}$  (1:1), and the reaction mixture was stirred at reflux 2-12 hours. 1 N aq. HCl was added to the mixture until acid pH. When a precipitate occurred, it was filtered off. Otherwise, the mixture was extracted with EtOAc (x4), and the organic layers were dried over anhydrous  $\text{Na}_2\text{SO}_4$ , filtered, and concentrated under reduced pressure. Purifications, conditions, yields, and analytical data are reported below.

### 5-phenyl-1H-indole-2-carboxylic acid (119)



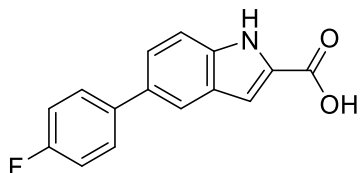
Purification by flash column chromatography eluting with DCM/MeOH 95:5 afforded the product as a yellow powder (yield: 97%). <sup>1</sup>H NMR (400 MHz, DMSO-*d*<sub>6</sub>): δ 11.81 (s, 1H); 7.92 (s, 1H); 7.68 (m, 2H); 7.57 (dd, *J* = 8.6, 1.7 Hz, 1H); 7.52 (d, *J* = 8.6 Hz, 1H); 7.48 – 7.44 (m, 2H); 7.34 – 7.30 (m, 1H); 7.15 – 7.14 (m, 1H). HPLC-ESI-MS analysis: calculated for C<sub>15</sub>H<sub>11</sub>NO<sub>2</sub>: 237.08; found: 238.12 [M+H<sup>+</sup>].

### 5-(4-chlorophenyl)-1H-indole-2-carboxylic acid (120)



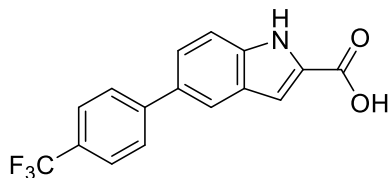
Purification by flash column chromatography eluting with DCM/MeOH 95:5 afforded the product as a brown powder (yield: 33%). <sup>1</sup>H NMR (400 MHz, MeOD): δ 7.75 (t, *J* = 1.2 Hz, 1H); 7.55 – 7.50 (m, 2H); 7.41 (d, *J* = 1.2 Hz, 1H); 7.33 – 7.29 (m, 2H); 7.06 (s, 1H). HPLC-ESI-MS analysis: calculated for C<sub>15</sub>H<sub>10</sub>ClNO<sub>2</sub>: 271.04; found: 272.29 [M+H<sup>+</sup>].

### 5-(4-fluorophenyl)-1H-indole-2-carboxylic acid (121)



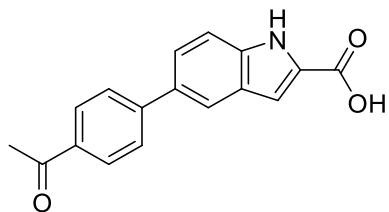
Purification by flash column chromatography eluting with DCM/MeOH/Acetic acid 96.9:3:0.1 afforded the product as a brown powder (yield: 52%). <sup>1</sup>H NMR (400 MHz, DMSO-*d*<sub>6</sub>): δ 13.05 (bs, 1H); 11.86 (s, 1H); 7.95 (s, 1H); 7.78 – 7.72 (m, 2H); 7.61 – 7.53 (m, 2H); 7.37 – 7.29 (m, 2H); 7.18 (d, *J* = 1.6 Hz, 1H). HPLC-ESI-MS analysis: calculated for C<sub>15</sub>H<sub>10</sub>FNO<sub>2</sub>: 271.04; found: 272.16 [M+H<sup>+</sup>].

### 5-(4-(trifluoromethyl)phenyl)-1H-indole-2-carboxylic acid (122)



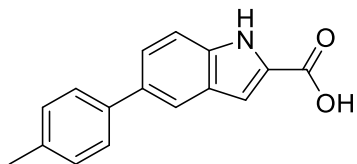
Purification by flash column chromatography eluting with DCM/MeOH/Acetic acid 97.9:2:0.1 afforded the product as a brown powder (yield: 68%).  $^1\text{H}$  NMR (400 MHz, DMSO- $d_6$ ):  $\delta$  13.06 (bs, 1H); 11.91 (s, 1H); 8.04 (s, 1H); 7.92 (d,  $J$  = 8.2 Hz, 2H); 7.80 (d,  $J$  = 8.3 Hz, 2H); 7.64 (dd,  $J$  = 8.7, 1.6 Hz, 1H); 7.56 (d,  $J$  = 8.6 Hz, 1H); 7.18 (d,  $J$  = 1.2 Hz, 1H). HPLC-ESI-MS analysis: calculated for  $\text{C}_{16}\text{H}_{10}\text{F}_3\text{NO}_2$ : 305.07; found: 306.33 [ $\text{M}+\text{H}^+$ ].

### 5-(4-acetylphenyl)-1H-indole-2-carboxylic acid (123)



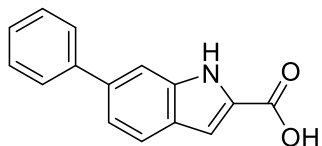
Trituration with diethyl ether afforded the product as a brown powder (yield: 55%).  $^1\text{H}$  NMR (400 MHz, DMSO- $d_6$ ):  $\delta$  11.81 (s, 1H); 8.07 – 8.00 (m, 3H); 7.85 (d,  $J$  = 8.4 Hz, 2H); 7.64 (d,  $J$  = 8.7 Hz, 1H); 7.55 (d,  $J$  = 8.7 Hz, 1H); 7.13 (s, 1H); 2.62 (s, 3H). HPLC-ESI-MS analysis: calculated for  $\text{C}_{17}\text{H}_{13}\text{NO}_3$ : 279.09; found: 280.36 [ $\text{M}+\text{H}^+$ ].

### 5-(p-tolyl)-1H-indole-2-carboxylic acid (124)



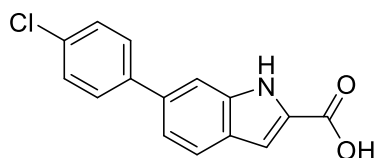
Pale yellow powder (yield: 82%).  $^1\text{H}$  NMR (400 MHz, DMSO- $d_6$ ):  $\delta$  11.79 (s, 1H); 7.89 (s, 1H); 7.58 – 7.49 (m, 4H); 7.26 (d,  $J$  = 8.0 Hz, 2H); 7.14 (d,  $J$  = 1.7 Hz, 1H); 2.62 (s, 3H). HPLC-ESI-MS analysis: calculated for  $\text{C}_{16}\text{H}_{13}\text{NO}_3$ : 251.09; found: 252.24 [ $\text{M}+\text{H}^+$ ].

### 6-phenyl-1H-indole-2-carboxylic acid (125)



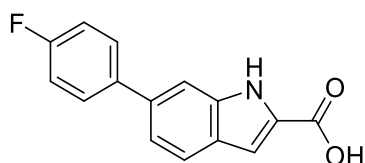
Purification by flash column chromatography eluting with DCM/MeOH/Acetic acid 96.9:3:0.1 afforded the product as a pale yellow powder (yield: 68%). <sup>1</sup>H NMR (400 MHz, MeOD): δ 7.71 – 7.65 (m, 4H); 7.47 – 7.41 (m, 2H); 7.37 (dd, *J* = 8.4, 1.6 Hz, 1H); 7.35 – 7.28 (m, 1H); 7.18 (d, *J* = 0.9 Hz, 1H). HPLC-ESI-MS analysis: calculated for C<sub>16</sub>H<sub>11</sub>NO<sub>2</sub>: 237.08; found: 238.25 [M+H<sup>+</sup>].

### 6-(4-chlorophenyl)-1H-indole-2-carboxylic acid (126)



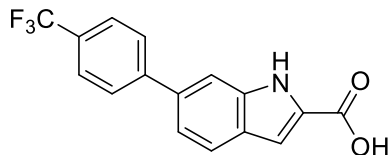
Purification by flash column chromatography eluting with DCM/MeOH/Acetic acid 9.95:3:0.05 afforded the product as a grey powder (yield: 90%). <sup>1</sup>H NMR (400 MHz, DMSO-*d*<sub>6</sub>): δ 12.96 (s, 1H); 11.87 (s, 1H); 7.74 (d, *J* = 8.4 Hz, 1H); 7.72 – 7.68 (m, 2H); 7.64 (m, 1H); 7.57 – 7.50 (m, 2H); 7.38 (dd, *J* = 8.4, 1.6 Hz, 1H); 7.12 (d, *J* = 1.3 Hz, 1H). HPLC-ESI-MS analysis: calculated for C<sub>15</sub>H<sub>10</sub>ClNO<sub>2</sub>: 271.04; found: 272.10[M+H<sup>+</sup>].

### 6-(4-fluorophenyl)-1H-indole-2-carboxylic acid (127)



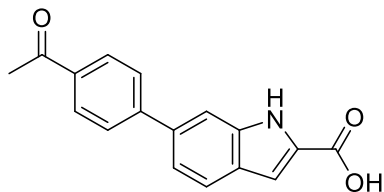
Purification by flash column chromatography eluting with DCM/MeOH/Acetic acid 96.95:3:0.05 afforded the product as a pale yellow powder (yield: 76%). <sup>1</sup>H NMR (400 MHz, MeOD): δ 7.71 – 7.62 (m, 4H); 7.33 (dd, *J* = 8.4, 1.6 Hz, 1H); 7.20 – 7.13 (m, 1H). HPLC-ESI-MS analysis: calculated for C<sub>15</sub>H<sub>10</sub>FNO<sub>2</sub>: 255.07; found: 256.28 [M+H<sup>+</sup>].

### 6-(4-(trifluoromethyl)phenyl)-1H-indole-2-carboxylic acid (128)



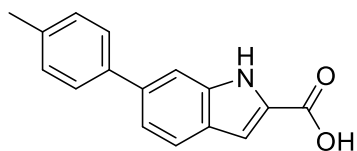
Purification by flash column chromatography eluting with DCM/MeOH/Acetic acid 97.95:3:0.05 afforded the product as a grey powder (yield: 60%).  $^1\text{H}$  NMR (400 MHz, MeOD):  $\delta$  7.86(d,  $J$  = 8.2 Hz, 1H); 7.76 – 7.72 (m, 4H); 7.42 (dd,  $J$  = 8.5, 1.5 Hz, 1H); 7.19 (s, 1H). HPLC-ESI-MS analysis: calculated for  $\text{C}_{16}\text{H}_{10}\text{F}_3\text{NO}_2$ : 305.07, found: 306.33  $[\text{M}+\text{H}^+]$ .

### 6-(4-acetylphenyl)-1H-indole-2-carboxylic acid (129)



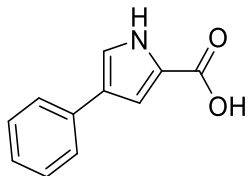
Yellow powder (yield: 78%).  $^1\text{H}$  NMR (400 MHz,  $\text{DMSO}-d_6$ ):  $\delta$  13.03 (s, 1H); 11.93 (s, 1H); 8.06 (d,  $J$  = 8.4 Hz, 2H); 7.84 (d,  $J$  = 8.4 Hz, 1H); 7.78 (d,  $J$  = 8.4 Hz, 1H); 7.74 (s, 1H); 7.47 (dd,  $J$  = 8.4, 1.6 Hz, 1H); 7.14 (d,  $J$  = 1.3 Hz, 1H); 2.63 (s, 3H). HPLC-ESI-MS analysis: calculated for  $\text{C}_{17}\text{H}_{13}\text{NO}_3$ : 279.09; found: 280.29  $[\text{M}+\text{H}^+]$ .

### 6-(p-tolyl)-1H-indole-2-carboxylic acid (130)



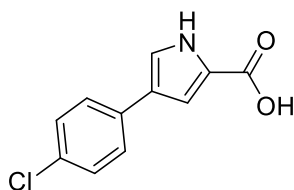
Light gray powder (yield: 91%).  $^1\text{H}$  NMR (400 MHz,  $\text{DMSO}-d_6$ ):  $\delta$  11.65 (s, 1H); 7.68 (d,  $J$  = 8.4 Hz, 1H); 7.62 (s, 1H); 7.56 (d,  $J$  = 8.1 Hz, 1H); 7.34 (dd,  $J$  = 8.4, 1.6 Hz, 1H); 7.28 (d,  $J$  = 7.94 Hz, 2H); 7.03 (s, 1H); 2.35 (s, 3H). HPLC-ESI-MS analysis: calculated for  $\text{C}_{16}\text{H}_{13}\text{NO}_3$ : 251.09; found: 252.30  $[\text{M}+\text{H}^+]$ .

#### 4-phenyl-1H-pyrrole-2-carboxylic acid (131)



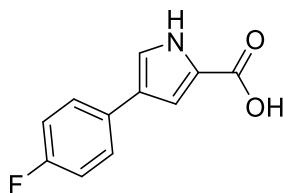
Yellow powder (yield: 45%).  $^1\text{H}$  NMR (400 MHz, MeOD):  $\delta$  7.55 – 7.52 (m, 2H); 7.37 – 7.29 (m, 3H); 7.18 – 7.13 (m, 2H). HPLC-ESI-MS analysis: calculated for  $\text{C}_{11}\text{H}_9\text{NO}_2$ : 187.06; found: 188.25  $[\text{M}+\text{H}^+]$ .

#### 4-(4-chlorophenyl)-1H-pyrrole-2-carboxylic acid (132)



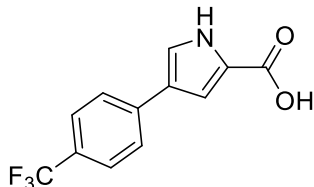
Slightly pink powder (yield: 90%).  $^1\text{H}$  NMR (400 MHz,  $\text{DMSO}-d_6$ ):  $\delta$  12.40 (bs, 1H); 11.95 (s, 1H); 7.66 – 7.62 (m, 2H); 7.49 (dd,  $J = 3.1, 1.8$  Hz, 1H); 7.38 – 7.34 (m, 2H); 7.49 (dd,  $J = 2.4, 1.8$  Hz, 1H). HPLC-ESI-MS analysis: calculated for  $\text{C}_{11}\text{H}_8\text{ClNO}_2$ : 221.02; found: 222.17  $[\text{M}+\text{H}^+]$ .

#### 4-(4-fluorophenyl)-1H-pyrrole-2-carboxylic acid (133)



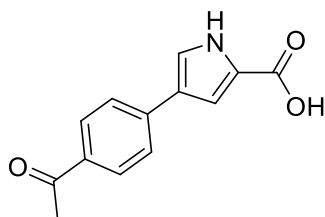
Brown powder (yield: 97%).  $^1\text{H}$  NMR (400 MHz,  $\text{DMSO}-d_6$ ):  $\delta$  12.35 (bs, 1H); 11.89 (s, 1H); 7.67 – 7.61 (m, 2H); 7.34 (dd,  $J = 3.0, 1.8$  Hz, 1H); 7.18 – 7.11 (m, 2H); 7.10 – 7.09 (m, 1H). HPLC-ESI-MS analysis: calculated for  $\text{C}_{11}\text{H}_8\text{FNO}_2$ : 205.05; found: 206.22  $[\text{M}+\text{H}^+]$ .

#### 4-(4-(trifluoromethyl)phenyl)-1H-pyrrole-2-carboxylic acid (134)



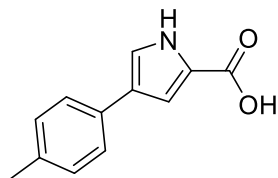
Yellow powder (yield:70%).  $^1\text{H NMR}$  (400 MHz, MeOD):  $\delta$  7.63 (d,  $J = 8.1$  Hz, 2H); 7.50 (d,  $J = 8.2$  Hz, 2H); 7.34 (d,  $J = 1.7$  Hz, 1H); 7.15 (d,  $J = 1.7$  Hz, 2H). HPLC-ESI-MS analysis: calculated for  $\text{C}_{12}\text{H}_8\text{F}_3\text{NO}_2$ : 255.05; found: 256.28  $[\text{M}+\text{H}^+]$ .

#### 4-(4-acetylphenyl)-1H-pyrrole-2-carboxylic acid (135)



Purification by flash column chromatography eluting with DCM/MeOH 97:3 afforded the product as a yellow powder (yield: 49%).  $^1\text{H NMR}$  (400 MHz,  $\text{DMSO}-d_6$ ):  $\delta$  12.05 (s, 1H); 7.91 (d,  $J = 8.1$  Hz, 2H); 7.77 (d,  $J = 8.0$  Hz, 2H); 7.62 (s, 1H); 7.23 (s, 1H); 2.56 (s, 3H). HPLC-ESI-MS analysis: calculated for  $\text{C}_{13}\text{H}_{11}\text{NO}_2$ : 229.09, found: 230.18  $[\text{M}+\text{H}^+]$ .

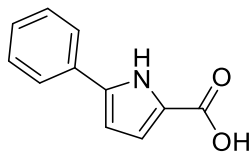
#### 4-(p-tolyl)-1H-pyrrole-2-carboxylic acid (136)



Yellow powder (yield: 65%).  $^1\text{H NMR}$  (400 MHz,  $\text{DMSO}-d_6$ ):  $\delta$  12.35 (s, 1H); 11.82 (s, 1H); 7.49 (d,  $J = 8.1$  Hz, 2H); 7.39 (dd,  $J = 3.0, 1.8$  Hz, 1H); 7.13 (d,  $J = 7.9$  Hz, 2H); 7.07 – 7.06 (m, 1H); 2.28 (s, 3H). HPLC-ESI-MS analysis: calculated for  $\text{C}_{12}\text{H}_{11}\text{NO}_2$ : 201.08; found: 202.24  $[\text{M}+\text{H}^+]$ .

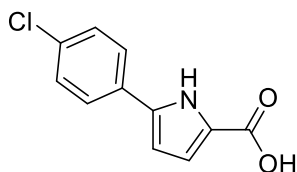


### 5-phenyl-1H-pyrrole-2-carboxylic acid (137)



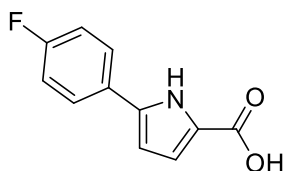
Purple powder (yield: 80%).  $^1\text{H}$  NMR (400 MHz, MeOD):  $\delta$  7.60 – 7.58 (m, 2H); 7.29 (t,  $J$  = 7.7, 1H); 7.16 (m, 1H); 6.81 (d,  $J$  = 3.8 Hz, 1H); 6.44 (d,  $J$  = 3.8 Hz, 1H). HPLC-ESI-MS analysis: calculated for  $\text{C}_{11}\text{H}_9\text{NO}_2$ : 187.06; found: 188.25  $[\text{M}+\text{H}^+]$ .

### 5-(4-chlorophenyl)-1H-pyrrole-2-carboxylic acid (138)



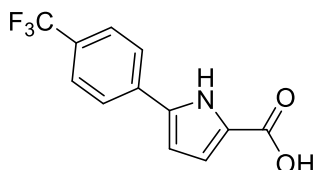
Slightly purple powder (yield: 50%).  $^1\text{H}$  NMR (400 MHz, MeOD):  $\delta$  7.60 – 7.56 (m, 2H); 7.30 – 7.27 (m, 2H); 6.81 (d,  $J$  = 3.9 Hz, 1H); 6.46 (d,  $J$  = 3.9 Hz, 1H). HPLC-ESI-MS analysis: calculated for  $\text{C}_{11}\text{H}_8\text{ClNO}_2$ : 221.02; found: 222.10  $[\text{M}+\text{H}^+]$ .

### 5-(4-fluorophenyl)-1H-pyrrole-2-carboxylic acid (139)



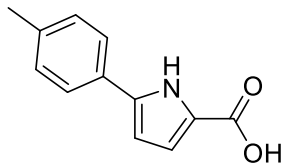
Purple powder (yield: 80%).  $^1\text{H}$  NMR (400 MHz,  $\text{DMSO}-d_6$ ):  $\delta$  11.97 (s, 1H); 7.92 – 7.85 (m, 2H); 7.25 – 7.19 (m, 2H); 6.80 (dd,  $J$  = 3.7, 1.8 Hz, 1H); 6.59 (dd,  $J$  = 3.7, 2.1 Hz, 1H). HPLC-ESI-MS analysis: calculated for  $\text{C}_{11}\text{H}_8\text{FNO}_2$ : 205.05; found: 206.22  $[\text{M}+\text{H}^+]$ .

### 5-(4-(trifluoromethyl)phenyl)-1H-pyrrole-2-carboxylic acid (140)



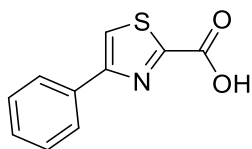
Slightly pink powder (yield:61%).  $^1\text{H}$  NMR (400 MHz, MeOD):  $\delta$  7.78 (d,  $J$  = 8.1, 2H); 7.58 (d,  $J$  = 8.2 Hz, 2H); 6.84 (d,  $J$  = 3.9 Hz, 1H); 6.59 (d,  $J$  = 3.9 Hz, 1H). HPLC-ESI-MS analysis: calculated for  $\text{C}_{12}\text{H}_8\text{F}_3\text{NO}_2$ :255.05; found: 256.21  $[\text{M}+\text{H}^+]$ .

#### 5-(p-tolyl)-1H-pyrrole-2-carboxylic acid (141)



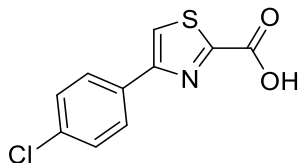
Purification by flash column chromatography eluting with DCM/MeOH 97:3: afforded the product as a purple powder (yield: 40%).  $^1\text{H}$  NMR (400 MHz, MeOD):  $\delta$  7.49 – 7.45 (m, 2H); 7.11 (d,  $J$  = 7.9 Hz, 2H); 6.80 (d,  $J$  = 3.8 Hz, 2H); 6.39 (d,  $J$  = 3.8 Hz, 2H); 2.25 (s, 3H). HPLC-ESI-MS analysis: calculated for  $\text{C}_{12}\text{H}_{11}\text{NO}_2$ : 201.08, found: 202.24  $[\text{M}+\text{H}^+]$ .

#### 4-phenylthiazole-2-carboxylic acid (142)



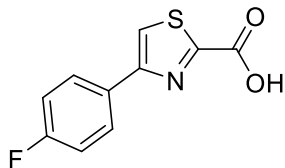
Slightly yellow powder (yield: 48%).  $^1\text{H}$  NMR (400 MHz,  $\text{DMSO}-d_6$ ):  $\delta$  8.05 (s, 1H); 7.95 (d,  $J$  = 7.0 Hz, 2H); 7.44 (t,  $J$  = 7.1 Hz, 2H); 7.34 (t,  $J$  = 7.2 Hz, 1H).  $^{13}\text{C}$  NMR (100.6 MHz,  $\text{DMSO}$ ): 171.8; 162.2; 155.0; 134.9; 129.1; 128.32; 126.7; 118.12. HPLC-ESI-MS analysis: calculated for  $\text{C}_{10}\text{H}_7\text{NO}_2\text{S}$ : 205.02; found: 206.03 $[\text{M}+\text{H}^+]$ .

#### 4-(4-chlorophenyl)thiazole-2-carboxylic acid (143)



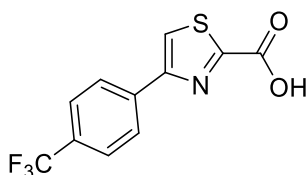
Cream powder (yield: 67%).  $^1\text{H}$  NMR (400 MHz,  $\text{DMSO}-d_6$ ):  $\delta$  8.68 (s, 1H); 8.16 (d,  $J$  = 8.5 Hz, 2H); 8.08 (d,  $J$  = 8.6 Hz, 2H); 2.63 (s, 3H).  $^{13}\text{C}$  NMR (100.6 MHz,  $\text{DMSO}$ ):  $\delta$  170.8; 161.8; 153.93; 133.8; 132.9; 129.18; 128.4; 119.05. HPLC-ESI-MS analysis: calculated for  $\text{C}_{10}\text{H}_6\text{ClNO}_2\text{S}$ : 238.98; found: 240.02  $[\text{M}+\text{H}^+]$ .

#### 4-(4-fluorophenyl)thiazole-2-carboxylic acid (144)



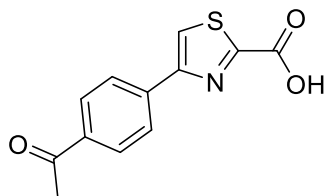
Light yellow powder (yield: 54%).  $^1\text{H NMR}$  (400 MHz,  $\text{DMSO-}d_6$ ):  $\delta$  14.09 (bs, 1H); 8.08 – 8.03 (m, 2H); 7.36 – 7.30 (m, 2H). HPLC-ESI-MS analysis: calculated for  $\text{C}_{10}\text{H}_6\text{FNO}_2\text{S}$ : 223.01; found: 224.19  $[\text{M}+\text{H}^+]$ .

#### 4-(4-(trifluoromethyl)phenyl)thiazole-2-carboxylic acid (145)



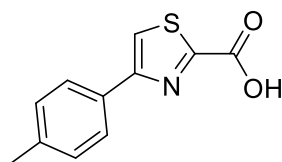
Slightly yellow powder (yield: 84%).  $^1\text{H NMR}$  (400 MHz, MeOD):  $\delta$  8.36 (s, 1H); 8.23 (d,  $J$  = 8.2 Hz, 2H); 7.78 (d,  $J$  = 8.2 Hz, 2H). HPLC-ESI-MS analysis: calculated for  $\text{C}_{11}\text{H}_6\text{F}_3\text{NO}_2\text{S}$ : 273.00; found: 274.24  $[\text{M}+\text{H}^+]$ .

#### 4-(4-acetylphenyl)thiazole-2-carboxylic acid (146)



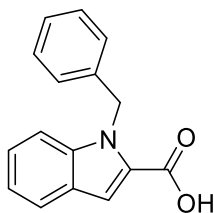
Light brown powder (yield: 30%).  $^1\text{H NMR}$  (400 MHz,  $\text{DMSO-}d_6$ ):  $\delta$  8.68 (s, 1H); 8.16 (d,  $J$  = 8.5 Hz, 2H); 8.08 (d,  $J$  = 8.6 Hz, 2H); 2.63 (s, 3H). HPLC-ESI-MS analysis: calculated for  $\text{C}_{12}\text{H}_9\text{NO}_3\text{S}$ : 247.03; found: 248.27  $[\text{M}+\text{H}^+]$ .

#### 4-(p-tolyl)thiazole-2-carboxylic acid (147)



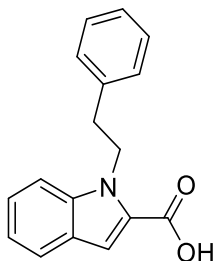
Purification by flash column chromatography eluting with DCM/MeOH/Acetic acid 96,95:3:0,05 afforded the product as light yellow powder (yield: 84%).  $^1\text{H}$  NMR (400 MHz, DMSO- $d_6$ ):  $\delta$  7.95 (s, 1H); 7.84 (d,  $J$  = 7.7 Hz, 2H); 7.24 (d,  $J$  = 7.3 Hz, 2H); 2.34 (s, 1H). HPLC-ESI-MS analysis: calculated for  $\text{C}_{11}\text{H}_9\text{NO}_2\text{S}$ : 219.04; found: 220.21  $[\text{M}+\text{H}^+]$ .

#### 1-benzyl-1H-indole-2-carboxylic acid (148)



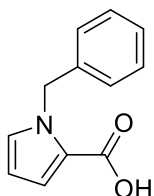
Slightly yellow powder (yield: 66%).  $^1\text{H}$  NMR (400 MHz, DMSO- $d_6$ ):  $\delta$  7.71 (d,  $J$  = 7.9 Hz, 1H); 7.53 (dd,  $J$  = 8.5, 0.7 Hz, 1H); 7.32 (d,  $J$  = 0.7 Hz, 1H); 7.31 – 7.18 (m, 4H); 7.15 – 7.11 (m, 1H); 7.04 – 7.02 (m, 1H); 5.89 (s, 2H). HPLC-ESI-MS analysis: calculated for  $\text{C}_{16}\text{H}_{13}\text{NO}_2$ : 251.09; found: 252.30  $[\text{M}+\text{H}^+]$ .

#### 1-phenethyl-1H-indole-2-carboxylic acid (149)



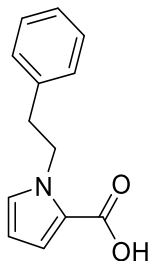
Yellow powder (yield: 90%).  $^1\text{H}$  NMR (400 MHz, DMSO- $d_6$ ):  $\delta$  12.87 (bs, 1H); 7.67 (d,  $J$  = 7.9 Hz, 1H); 7.55 (d,  $J$  = 8.5 Hz, 1H); 7.31 – 7.18 (m, 7H); 7.12 – 7.08 (m, 1H); 4.79 – 4.75 (m, 2H); 2.99 – 2.96 (m, 2H). HPLC-ESI-MS analysis: calculated for  $\text{C}_{17}\text{H}_{15}\text{NO}_2$ : 265.11; found: 266.30  $[\text{M}+\text{H}^+]$ .

#### 1-benzyl-1H-pyrrole-2-carboxylic acid (150)



Purification by flash column chromatography eluting with DCM/MeOH 97:3 afforded the product as a white powder (yield: 68%).  $^1\text{H}$  NMR (400 MHz,  $\text{DMSO-}d_6$ ):  $\delta$  12.12 (bs, 1H); 7.32 – 7.28 (m, 2H); 7.26 – 7.21 (m, 2H); 7.09 – 7.07 (m, 2H); 6.86 (dd,  $J_1 = 3.9$ ,  $J_2 = 1.8$  Hz, 1H); 6.15 (dd,  $J_1 = 3.9$ ,  $J_2 = 2.6$  Hz, 1H); 5.56 (s, 3H).  $^{13}\text{C}$  NMR (100.6 MHz, DMSO):  $\delta$  162.3; 139.7; 129.9; 128.9; 127.6; 127.1; 122.6; 118.4; 108.5; 51.3. HPLC-ESI-MS analysis: calculated for  $\text{C}_{12}\text{H}_{12}\text{NO}_2$ : 201.07; found: 202.24  $[\text{M}+\text{H}^+]$ .

### 1-phenethyl-1H-pyrrole-2-carboxylic acid (151)

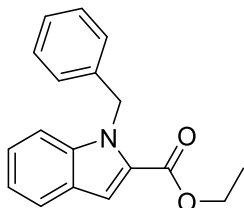


Yellow powder (yield: 87%).  $^1\text{H}$  NMR (400 MHz,  $\text{DMSO-}d_6$ ):  $\delta$  12.15 (s, 1H); 7.28 (t,  $J = 7.3$  Hz, 2H); 7.24 – 7.14 (m, 3H); 6.97 – 6.96 (m, 1H); 6.82 – 6.81 (m, 1H); 6.03 – 6.01 (m, 1H); 4.48 (t,  $J = 7.6$  Hz, 2H); 2.97 (t,  $J = 7.5$  Hz, 2H).  $^{13}\text{C}$  NMR (100.6 MHz, DMSO):  $\delta$  170.8; 161.8; 153.93; 133.8; 132.9; 129.18; 128.4; 119.05. HPLC-ESI-MS analysis: calculated for  $\text{C}_{13}\text{H}_{13}\text{NO}_2$ : 215.09; found: 216.18  $[\text{M}+\text{H}^+]$ .

### Synthetic procedure to obtain compounds 159 a and 159 b

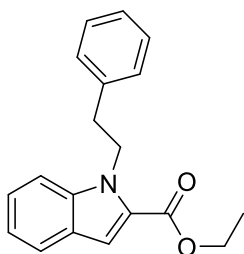
Ethyl 1H-indole-2-carboxylate (50 mg, 0.26 mmol) was dissolved in acetonitrile (7 mL/mmol), the cesium carbonate (127 mg, 0.39 mmol) was added, and the reaction mixture was left stirring for 15 minutes at room temperature. Subsequently, benzyl bromide or (2-bromoethyl)benzene (1.5 eq) was added, and the reaction mixture was heated to reflux and stirred overnight. After this time, the reaction mixture was concentrated *in vacuo*, and the resulting crude material was dissolved in EtOAc. The organic phase was washed with water, dried over anhydrous  $\text{Na}_2\text{SO}_4$ , filtered, and concentrated under reduced pressure. The crude was purified by flash column chromatography eluting with Petroleum Ether/EtOAc. Purification conditions, yields, and analytical data are reported below.

### Ethyl 1-benzyl-1H-indole-2-carboxylate (159 a)



Purification by flash column chromatography eluting with Petroleum Ether/EtOAc 95:5 afforded the product as a white powder (yield: 92%). <sup>1</sup>H NMR (400 MHz, DMSO-*d*<sub>6</sub>): δ 7.73 (d, *J* = 8.0 Hz, 1H); 7.58 (dd, *J* = 8.5, 0.7 Hz, 1H); 7.38 (d, *J* = 0.8 Hz, 1H); 7.34 - 7.31 (m, 1H); 7.30 - 7.18 (m, 3H); 7.17 - 7.13 (m, 1H); 7.05-7.00 (m, 2H); 5.87 (s, 2H); 4.29 (q, *J* = 7.1 Hz, 2H); 1.29 (t, *J* = 7.1 Hz, 3H).

### Ethyl 1-phenethyl-1H-indole-2-carboxylate (159 b)



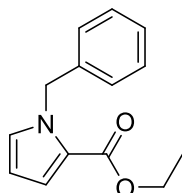
Purification by flash column chromatography eluting with Petroleum Ether/EtOAc 95:5 afforded the product as a white powder (yield: 40%). <sup>1</sup>H NMR (400 MHz, DMSO-*d*<sub>6</sub>): δ 7.70 - 7.67 (m, 1H); 7.60 - 7.57 (m, 1H); 7.34 - 7.29 (m, 1H); 7.28-7.24 (m, 3H); 7.21 - 7.16 (m, 3H); 7.14 - 7.11 (m, 1H); 4.79 - 4.75 (m, 2H); 4.31 (q, *J* = 7.1 Hz, 2H); 3.00 - 2.96 (m, 2H); 1.29 (t, *J* = 7.1 Hz, 3H).

### Synthetic procedure to obtain compounds 160 a and 160 b

Ethyl 1H-pyrrole-2-carboxylate (70 mg, 0.52 mmol) was dissolved in anhydrous DMF (3 mL/mmol) and cooled to 0 °C, then NaH (mineral oil 60%; 30 mg, 0.75 mmol) was added. The reaction mixture was left stirring for 30 minutes at room temperature. After this time, benzyl bromide or (2-bromoethyl)benzene (1.5 eq) was added, and the reaction mixture was stirred at room temperature until the consumption of starting

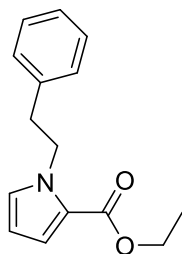
material Water was added to the reaction mixture, and it was extracted with EtOAc (X3). The organic phase was washed with brine (X3), dried over anhydrous Na<sub>2</sub>SO<sub>4</sub>, filtered, and concentrated under reduced pressure. The crude was purified by flash column chromatography eluting with Petroleum Ether/EtOAc. Purification conditions, yields, and analytical data are reported below.

#### Ethyl 1-benzyl-1H-pyrrole-2-carboxylate (160 a)



Purification by flash column chromatography eluting with Petroleum Ether/EtOAc 95:5 afforded the product as a yellow oil (yield: 84%). <sup>1</sup>H NMR (400 MHz, CDCl<sub>3</sub>): δ 7.35 – 7.29 (m, 2H); 7.28 – 7.25 (m, 1H); 7.04 (dd, *J* = 3.96, 1.76 Hz, 1H); 6.92-6.88 (m, 1H); 6.22 - 6.20 (m, 1H); 5.59 (s, 2H); 4.31 (q, *J* = 7.1 Hz, 2H); 1.31 (t, *J* = 7.1 Hz, 3H).

#### Ethyl 1-phenethyl-1H-pyrrole-2-carboxylate (160 b)



Purification by flash column chromatography eluting with Petroleum Ether/EtOAc from 97:3 to 95:5 afforded the product as a yellow oil (yield: 43%). <sup>1</sup>H NMR (400 MHz, CDCl<sub>3</sub>): δ 7.31 – 7.26 (m, 2H); 7.24 – 7.19 (m, 1H); 7.18 – 7.16 (m, 2H); 6.06 (dd, *J* = 3.92, 2.52 Hz, 2H); 4.51 - 4.46 (m, 2H); 4.23 (q, *J* = 7.1 Hz, 2H); 2.98 – 2.94 (m, 2H); 1.28 (t, *J* = 7.1 Hz, 3H).

## 4.3. Preliminary chemical investigation on 1H-benzo[d][1,2,3]triazole carboxamide (BTA) as a scaffold for a new series of cysteine biosynthesis inhibitors

### 4.3.1. Background

Our previous efforts on the research of new potential OASS inhibitors were focused on the investigation of molecules bearing a carboxylic acid portion that was discovered to be essential for the inhibition of the enzymatic activity of OASS. This evidence led to the disclosure of **UPAR415** as the hit compound of a series of cyclopropane inhibitors. Indeed, as previously reported (see 4.1), these molecules mimic the C-terminal tail of the SAT, the physiological inhibitor of OASS. After the manipulation of this scaffold and the subsequent research for a new carboxylic acid fragment to bypass the problems associated with the cyclopropane core, our interest was directed towards early evidence reported by Kredich N. *et al.*, regarding the antimicrobial activity of 1,2,4-triazole on *S. Typhimurium* OASS-A.<sup>111</sup> The authors found that OASS-A was able to catalyze a reaction between the natural substrate OAS and the 1,2,4-triazole, resulting in the formation of a false product, the 1,2,4-1-triazole-alanine (**Figure 18A**). The involvement of OAS in the formation of the false product leads to its lower intracellular concentration. OAS converts rapidly to NAS, an inducer of the enzymes involved in cysteine biosynthesis, and presumably, the inhibition of the cellular growth may be correlated to the resulting cysteine starvation caused by the lack of the L-cysteine precursors.

Moreover, the effect of an N-(phenyl)thioacetamide-linked 1,2,3-triazoles (TAT) as a disruptor of cysteine biosynthesis was recently reported by Wallace *et al.*<sup>44</sup> The authors find that the inhibition of the synthesis of cysteine by TAT is subsequent to the formation of a false product, as previously reported to Kredich Kredich N. *et al.* (**Figure 18B**). Furthermore, the TAT described in this study has been found 64 times more potent than 1,2,4-triazole.



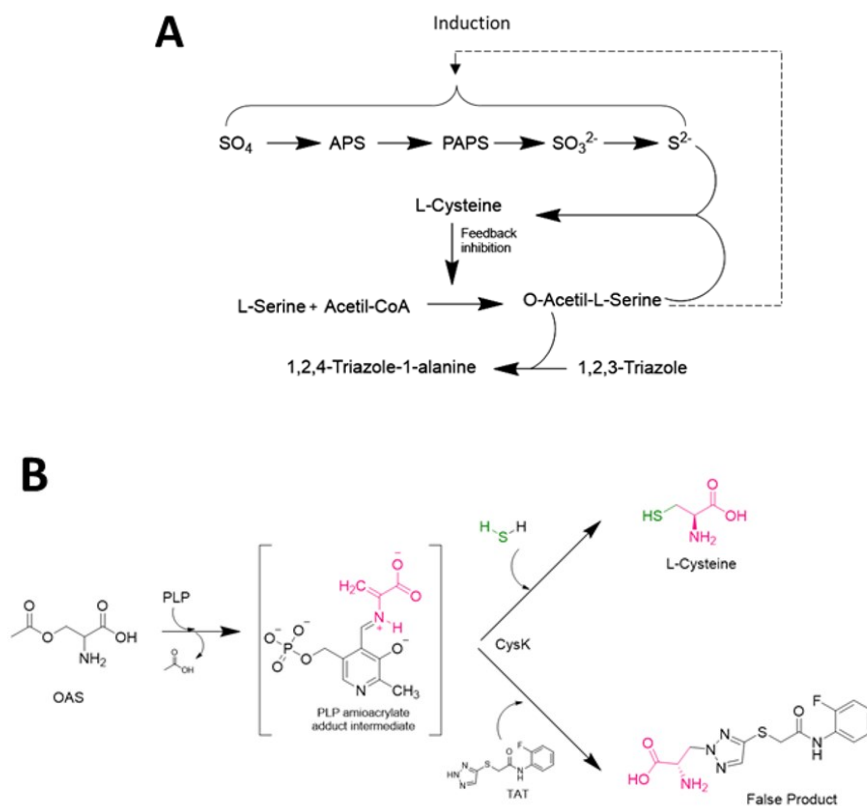


**Figure 18. A)** Effect of 1,2,4-Triazole on the cysteine biosynthetic pathway of *S. typhimurium*, adapt from ref <sup>111</sup> **B)** Putative mechanism of action for the false product, adapt from ref <sup>44</sup>

As previously reported in this thesis, compound **11** (see 3.2.1), characterized by a 1H-benzo[d][1,2,3]triazole-5-carboxamide core (**Figure 19A**), was synthesized as a potential inhibitor of SAT enzyme. The investigation of this derivative has immediately been suspended due to its low activity towards the enzyme compared to the hit compound.

Drug repurposing is a valuable tool used in drug discovery to find new applications for synthesized molecules and for which different information about their properties were collected. This approach can also be applied to academic research, wherein different potential molecules were dismissed due to their lack of activity in the enzymatic assay, as for **11**.<sup>77,112</sup> These considerations and the evidence reported in the literature regarding the ability of triazole ring to target OASS prompted us to initiate a preliminary investigation on the potential activity of the benzotriazole core (BTA) towards OASS instead of SAT enzyme. Indeed, benzotriazole is a benzo-fused azole, compound

characterized by a triazole portion, that has shown an increasing interest in pharmaceutical chemistry due to its wide potential application as medicinal drugs.<sup>113</sup>

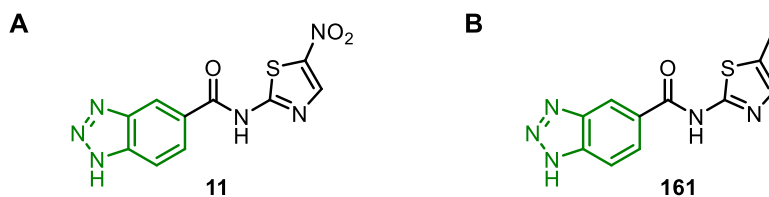


**Figure 19.** **A)** Chemical structure of compound **11**, a BTA derivate synthesized as potential SAT inhibitors. **B)** Replace the nitro group at the C-5 on the thiazole ring.

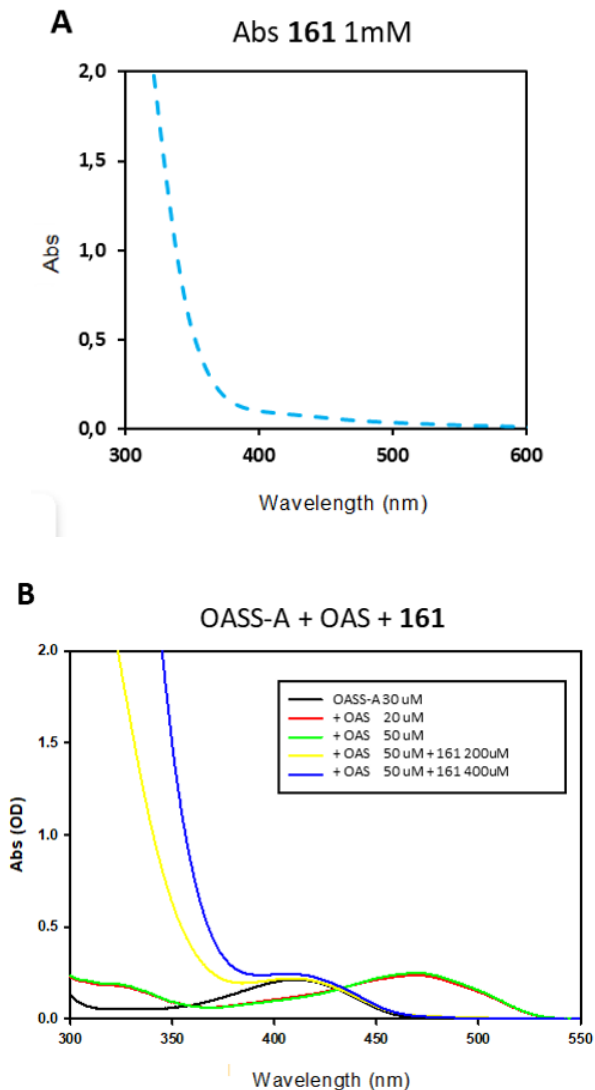
#### 4.3.2. Preliminary investigation of BTA derivatives mechanism of action (MOA) on the cysteine biosynthesis

Compound **11** belongs to a series of 2-amino-5-nitrothiazole derivatives, and in particular, it is characterized by a BTA core linked to the thiazole ring through an amide bond. The presence of the nitro group, a structural alert, is often associated with cytotoxicity issues, as previously reported for this series of derivatives. Additionally, the nitro group derivatives are often characterized by a yellow color and strong UV/Vis absorption spectra, which may represent an issue during the biological evaluation. Taken these considerations into account, a derivative of **11** was synthesized (**Figure 19B**). The nitro moiety was replaced with a methyl group, and both the derivatives were *in vitro* evaluated for their ability to interfere with the cysteine biosynthesis.

The activity of **11** was of difficult interpretation due to the formation of a yellow solution able to interfere with the spectroscopic assay. On the contrary, the analog **161** gave a colorless solution, and its absorption spectra is shown in **Figure 20A**.

OASS is a PLP enzyme that possesses a different spectroscopic profile based on the state of the aldimine intermediates (**Figure 21**). OASS-A alone has an absorption maximum of around 412 nm, corresponding to the internal aldimine (black line, **Figure 20B**). The addition of OAS and its subsequent interaction with OASS-A lead to the formation of an adduct, the  $\alpha$ -aminoacrylate, with abs of 470 nm (red or green line, **Figure 20B**). When compound **161** is tested in combination with OAS, the peak absorbance at 470 nm was not observed. The interaction between compound **161** and the  $\alpha$ -aminoacrylate led to the progressive decrease of the peak at 470 nm, and the gradual regeneration of the internal aldimine in a concentration-dependent manner.

This evidence suggests that the presence of the BTA derivative leads to the formation of a false product with OAS and the restoration of the internal aldimine (yellow and blue line, **Figure 20B**). The same result was observed when OASS-B was used (**Figure 20C**), even though higher concentrations of the compound were needed to achieve the complete shift of the equilibrium towards the internal aldimine (412 nm). Compound **11** is able to interact with both the OASS isoforms, a condition required to obtain the complete inhibition of the cysteine biosynthesis.<sup>114</sup>



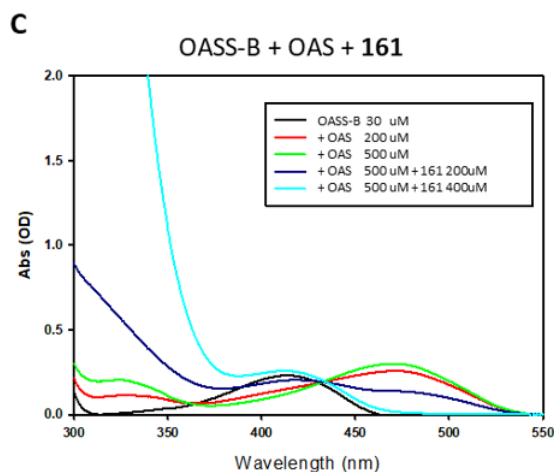


**Figure 20.** A) Spectroscopic spectra of **11** alone; B) Spectroscopic spectra of OASS-A (black line), OASS-A + OAS (red and green line); and spectroscopic interaction of OASS-A+OAS+**11** (yellow and blue line); C) Spectroscopic spectra of OASS-B (black line), OASS-B + OAS (red and green line); and spectroscopic interaction of OASS-B +OAS+**11** (blue and turquoise line).

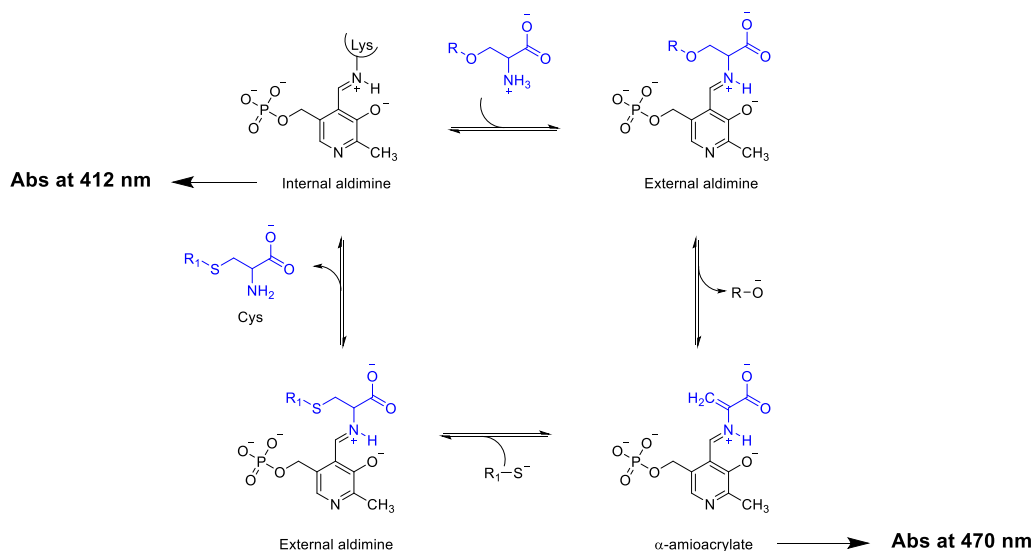


**Figure 21.** General catalytic mechanism of OASS-A/OASS-B, adapted from ref<sup>69</sup>.

### 4.3.3. Aim of the project and first round of optimization

The preliminary results obtained through the above reported *in vitro* assays regarding the BTA activity towards OASS-A and OASS-B showed a comparable MOA of those reported for the triazole scaffolds. The encouraging evidence that compound **161** may inhibit cysteine biosynthesis *via* the formation of a false product mechanism prompted us to further explore the potentiality of this scaffold. At this regard, a small series of **161** analogues were synthesized, and focused modifications, obtained through a medicinal chemistry approach, were introduced on the benzotriazole carboxamide scaffold to collect preliminary SAR information regarding the biological properties of these derivatives.

In **Figure 22** are summarized the main modifications introduced to the hit compound. Taking into account the crucial role of the BTA core for the activity, this portion was retained intact.

The thiazole core was first replaced with a phenyl ring, a moiety easy to manipulate and prone to further modifications. Indeed two phenyl derivatives were synthesized bearing EDG or EWD groups, namely methoxy and trifluoromethyl groups, respectively. Then, isosteres of the phenyl moiety, such as the thiophene and the pyridine ring,<sup>115,116</sup> were introduced. Additionally, to enlarge the set of modified derivatives, the thiazole ring was replaced with an aliphatic portion, leading to secondary and tertiary amide, and evaluate whether these substituents, with a different chemical nature, were tolerated.

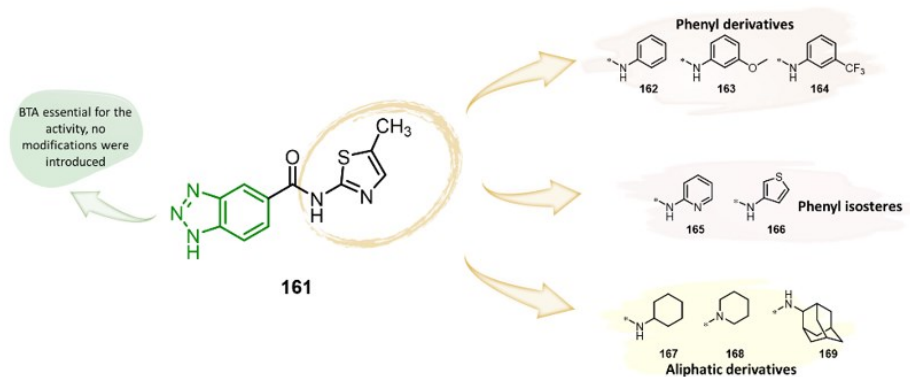


**Figure 22.** First round of modifications on the BTA scaffold.

#### 4.3.4. Biological evaluation of the first series of derivatives

##### 4.3.4.1. Antimicrobial activity

The capability of the synthesized compounds and the hit compound **161** to inhibit the bacteria growth was evaluated. The activity of each compound was assessed against three different Gram-negative bacteria strains, *E. coli*, *S. Typhimurium*, and *K. pneumoniae*, and on two different growth media. No antimicrobial activity was detected when the compounds were tested in a rich medium (Mueller Hinton broth, MH). Indeed, cysteine is largely available in this medium, and its abundance makes cysteine biosynthesis “non-essential”, and consequently, its inhibition should not affect the bacteria cell growth. On the contrary, compounds **162**, **165**, **166**, **167**, and **168** showed antimicrobial activity when tested in a minimal medium (M9), a poor medium in which precursors of cysteine are present but is deprived of preformed cysteine. Cysteine production becomes essential when the bacteria are facing harsh conditions, as in M9 broth, and inhibitors of this pathway may interfere with the bacterial growth. Surprisingly, compound **11** did not show any antimicrobial activity against *E. coli*. However, the replacement of the thiazole ring with different moieties proved to be beneficial for the activity. Indeed, compound **162**, bearing a phenyl ring instead of the thiazole moiety, showed a weak activity against *E.coli* (**162**, MIC<sub>*E. coli*</sub> = 64 µg/mL). The introduction of EDG or EWD groups at the C-3 of the phenyl ring led to a loss of activity (**163**, **164**, MIC<sub>*E. coli*</sub> > 256 µg/mL). The activity was increased 2.5 fold when the phenyl ring was replaced with 2-pyridine and 16-fold with the thiophene moiety, a remarkable achievement considering the small numbers of tested compounds (**165**, MIC<sub>*E. coli*</sub> = 26.67 µg/mL; **166**, MIC<sub>*E. coli*</sub> = 4 µg/mL). An encouraging improvement in the antimicrobial activity was also detected for the analogs bearing aliphatic groups (**167**, MIC<sub>*E. coli*</sub> = 14.67 µg/mL; **168**, MIC<sub>*E. coli*</sub> = 21.33 µg/mL). With regard to this group of derivatives, compound **169** did not show any ability to interfere with the cellular growth; likely, the increased hindrance of the adamantyl moiety is not beneficial for the biological activity (**169**, MIC<sub>*E. coli*</sub> > 256 µg/mL).

The synthesized compounds were not able to inhibit the cellular growth in *K. pneumoniae*, whereas a weak antimicrobial activity was determined for **166** and **167** against *S. Typhimurium* strain (**166**, MIC<sub>*S. Typhimurium*</sub> = 64 µg/mL; **167**, MIC<sub>*S. Typhimurium*</sub> = 106,67 µg/mL).

**Table 10.** MIC of the first series of BTA derivatives

Cpd	<i>E. coli</i> ATCC 25922		<i>S. Typhimurium</i> ATCC 14028		<i>K. pneumoniae</i> ATCC 13883	
	M9	MH	M9	MH	M9	MH
<b>161</b>	>256 µg/mL	>256 µg/mL	N/D*	N/D*	N/D*	N/D*
<b>162</b>	64 µg/mL	>256 µg/mL	N/D*	N/D*	N/D*	N/D*
<b>163</b>	>256 g/mL	>256 µg/mL	>256 µg/mL	>256 µg/mL	>256 µg/mL	>256 µg/mL
<b>164</b>	>256 µg/mL	>256 µg/mL	>256 µg/mL	>256 µg/mL	>256 µg/mL	>256 µg/mL
<b>165</b>	26.67 µg/mL	>256 µg/mL	128 µg/mL	>256 µg/mL	128 µg/mL	>256 µg/mL
<b>166</b>	4 µg/mL	>256 µg/mL	64 µg/mL	>256 µg/mL	>256 µg/mL	>256 µg/mL
<b>167</b>	14.67 µg/mL	>256 µg/mL	N/D*	>256 µg/mL	>256 µg/mL	>256 µg/mL
<b>168</b>	21.33 µg/mL	>256 µg/mL	106,67 µg/mL	>256 µg/mL	>256 µg/mL	>256 µg/mL
<b>169</b>	>256 µg/mL	>256 µg/mL	N/D*	>256 µg/mL	>256 µg/mL	>256 µg/mL

\*ND = Not determined

#### 4.3.4.2. Toxicity

Considering the encouraging activity shown to this small set of derivatives, the cytotoxicity of some compound were evaluated through the cellular viability on Human monocytes THP-I cells. 3-(4,5-dimethylthiazol-2-yl)-2,5-diphenyltetrazolium bromide (MTT) assay was performed at four different concentrations of 200, 100, 50, and 25 µM, respectively, in a triplicates experiment. All the compounds showed an excellent cytotoxicity profile, even at the highest concentrations tested (**Figure 23**).

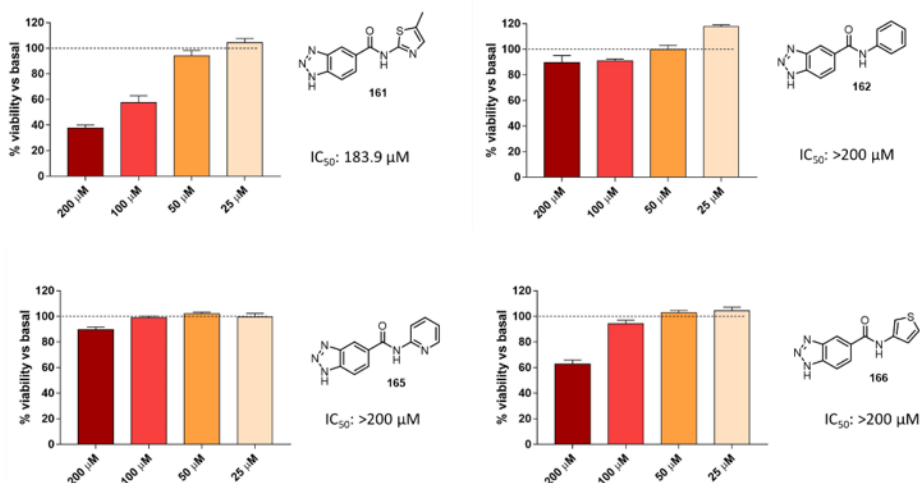


**Figure 23.** MTT charts of compounds **161**, **162**, **165**, and **166**.

#### 4.3.4.3. Spectroscopic assay of compounds **165**, **170** and **171**

To validate the mechanism of action shown to the BTA derivate **161**, compound **165**, an analogue with promising activity in the cellular assay, was evaluated for its mechanism of action. Additionally, compounds **170** and **171** (Figure 24) were synthesized and tested to prove that the BTA core is essential for the activity, and in particular, the benzotriazole NH is involved in the formation of the false product. Indeed, compounds **170** and **171**, analogues of **165** and **166**, respectively, present a BTA-NH methylated, blocking the possibility of the nitrogen forming new bounds and interacting with other substrates.

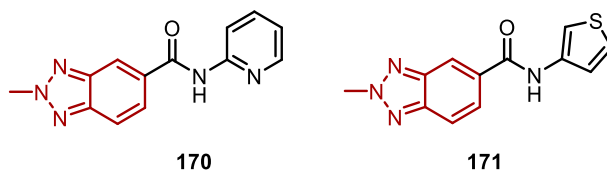


**Figure 24.** Chemical structure of compounds **170** and **171**.

As reported in Figure 25B, the analyzed compound **165** showed results comparable with those observed for the hit compound **161**. Indeed, when **165** was tested in



combination with OASS-A (or OASS-B) and OAS, the absorbance peak at 412 nm, corresponding to the internal aldimine, was observed. Rather the peak at 470 nm, corresponding to the  $\alpha$ -aminoacrylate, that can be observed in the OAS spectra (red line, **Figure 24B**), disappeared, a sign of the interaction of the compound with the  $\alpha$ -aminoacrylate.

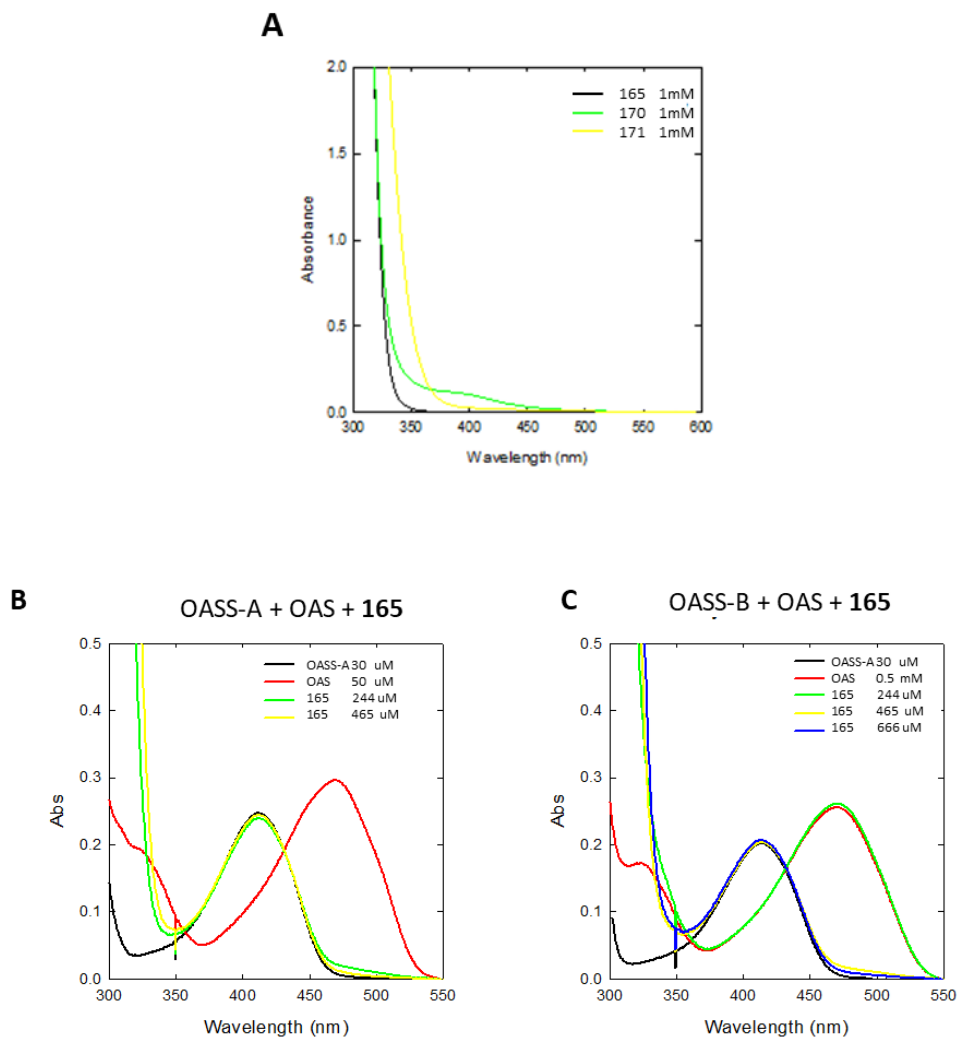


**Figure 25.** A) Absorbance spectra of compounds **165**, **170**, and **171**. B) interaction of **165** with *St*OASS-A and C) *St*OASS-B.

On the contrary, when compounds **170** and **171** were tested, the spectra corresponding to the mixture of OASS-A (or OASS-B) + OAS + BTA derivate (green, yellow, and blue line in **Figure 26**) overlap that observed for the solution without the inhibitor (OAS + OASS-

A or OASS-B, red line in **Figure 26**). Indeed, only the  $\alpha$ -aminoacrylate peak is observed, even at a high concentration of the compounds (1.12 mM or 1.3 mM, blu line, **Figure 9**). Therefore, the N-methylation of the BTA seems to prevent the interaction between the compound and the substrate, OAS.

The presence of an NH on the BTA core results crucial to interact with the  $\alpha$ -aminoacrylate to generate the false product and obtain the inhibition of the cysteine biosynthesis. Thus, it is clear that the BTA-NH should not be functionalized to preserve the activity of this potential class of inhibitors.

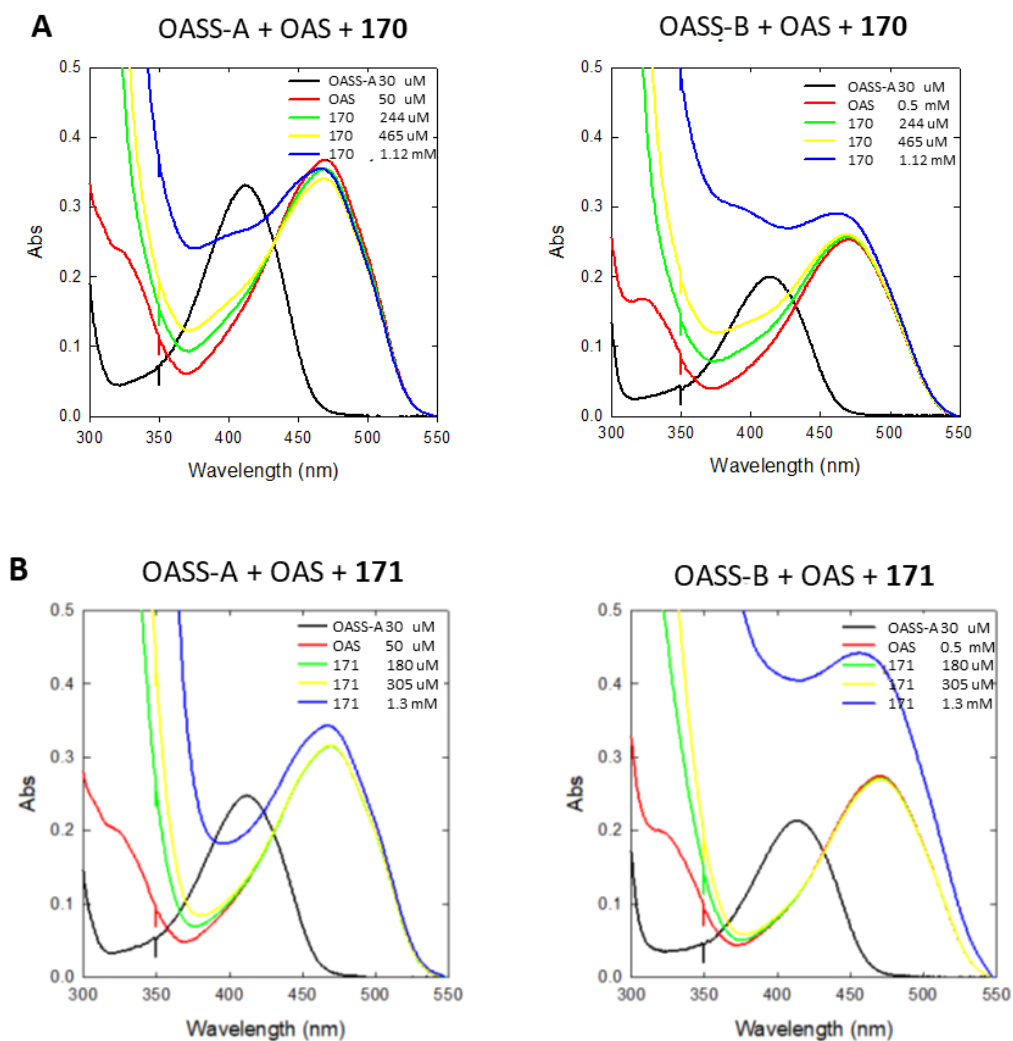


**Figure 26.** interaction of **170** (A) and **171** (B) with StOASS-A and StOASS-B.

Furthermore, the minimum inhibitory concentration (MIC) of compounds **170** and **171** was evaluated. As expected, the compound did not interfere with the bacterial growth in the minimal medium (M9) (**Table 11**). Indeed, the corresponding analogues **165** and **166** showed an encouraging activity against *E.coli*, which is not be observed when the BTA-nitrogen is methylated, further evidence of the pivotal rule of the BTA core for the inhibitory activity (**165**, MIC<sub>*E. coli*</sub> = 26.67 µg/mL; **170**, MIC<sub>*E. coli*</sub> > 256 µg/mL; **166**, MIC<sub>*E. coli*</sub> = 4 µg/mL; **171**, MIC<sub>*E. coli*</sub> > 256 µg/mL).

**Table 11.** MIC of compounds **170** and **171**.

Cpd	<i>E. coli</i> ATCC 25922		<i>S. Typhimurium</i> ATCC 14028		<i>K. pneumoniae</i> ATCC 13883	
	M9	MH	M9	MH	M9	MH
<b>170</b>	>256 µg/mL	>256 µg/mL	>256 µg/mL	>256 µg/mL	>256 µg/mL	>256 µg/mL
<b>171</b>	>256 µg/mL	>256 µg/mL	>256 µg/mL	>256 µg/mL	>256 µg/mL	>256 µg/mL

#### 4.3.5. Second series of optimization

Despite the small set of BTA derivatives synthesized, several of them were able to inhibit bacterial growth, and valuable data about the biological properties of this new series of potential cysteine inhibitors were collected. These findings prompted us to start a second cycle of hit optimization to expand the SAR information and improve the *in cell* activity of BTA analogues. At this regard, new modifications were introduced to the BTA core, which are summarized in **Figure 27**. Namely, two substitutions sites were explored: *I*) the aromatic/aliphatic portion linked to the amide bond to research the best group as a substituent of the thiazole ring, and *II*) modification of the amide bond to investigate the effect of different linkers on the activity.

*I*) Replace the thiazole moiety of the hit compound led to derivatives able to interfere with the bacterial growth. In particular, derivatives bearing pyridine or thiophene moiety showed encouraging activity (**165** and **166**), and they were considered privileged substituents for this second round of optimization.

Pyridine is a feasibility moiety that can be modified using a wide range of reactions and reagents. At this regard, to establish if the molecular structure was prone to further modification, two principal modifications were explored. Pyridine bearing an EDG or EWG group was linked to the BTA core to evaluate whether adding these groups to the structure may be detrimental to the activity, as was observed for the phenyl analogues **163** and **164**. Then, we deemed of interest to introduce a bulky group in the structure, and pyridine moiety bearing a phenyl ring at C-4 was synthesized.

Considering the good results showed to the aliphatic derivatives, six new analogues, with both secondary and tertiary amide, were synthesized to explore further the impact of these groups on the structure and the biological activity.

II) Different modifications were introduced to the amide bridge to explore the impact of the linker on the biological profile of the molecule. Firstly, four compounds were synthesized as a reverse amide, and then a spacer was introduced between the amide moiety and the aromatic substituent. In particular, ethylamino and ethoxy linkers were used. Additionally, a fluorophore probe (NBD) was introduced, with a direct bond to the amide moiety and then with an ethyl amino spacer.

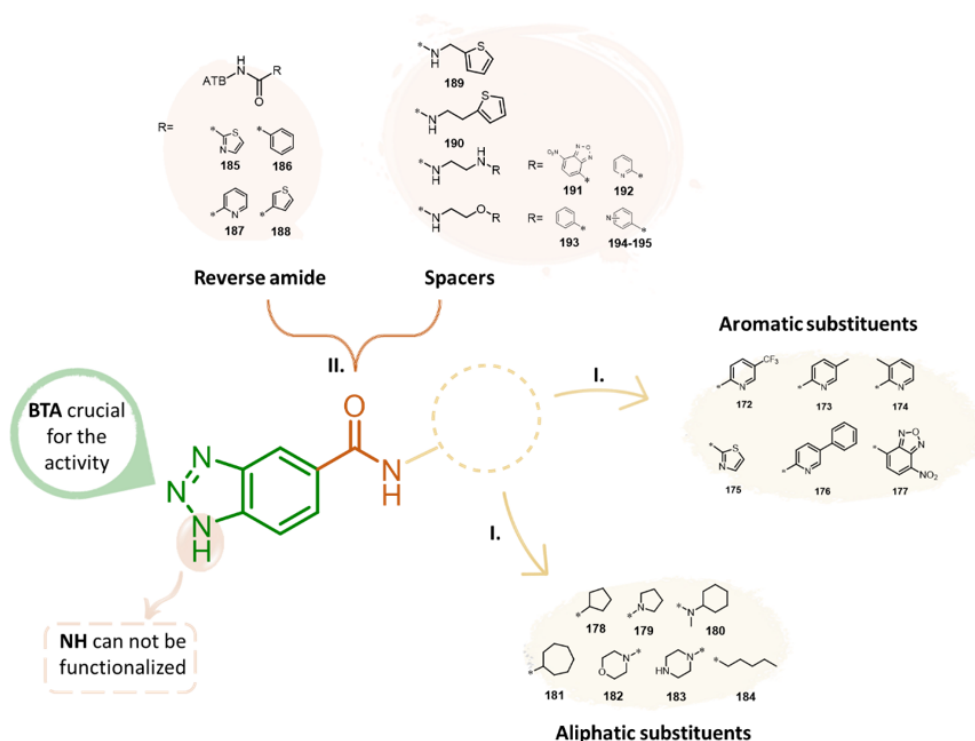
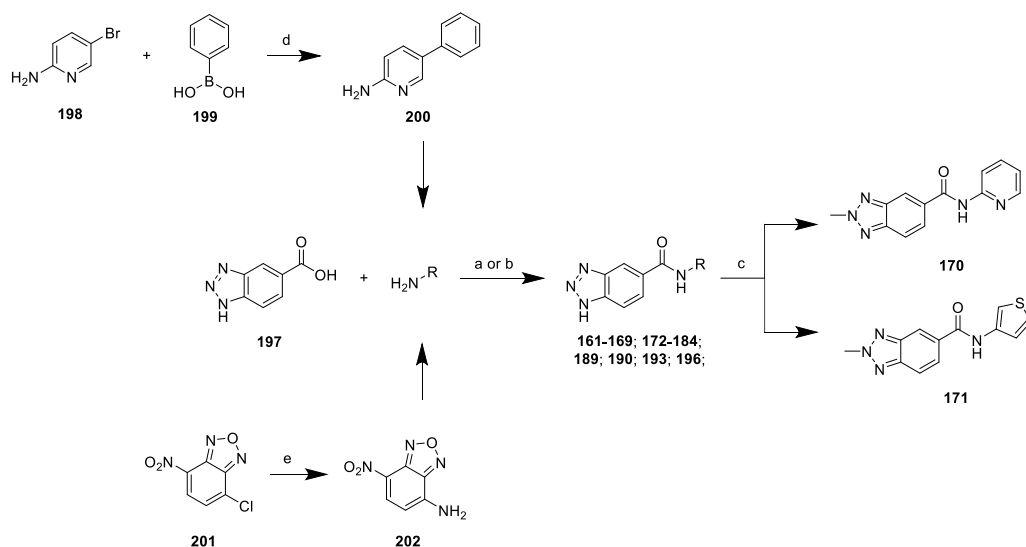


**Figure 27.** Second round of modifications.

### 4.3.6. Chemistry

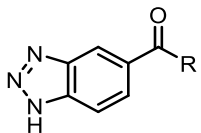
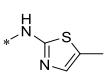
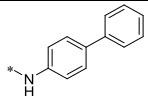
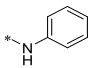
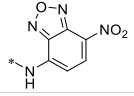
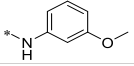
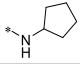
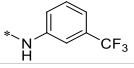
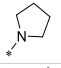
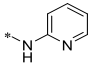
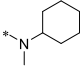
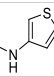
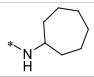
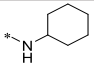
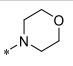
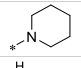
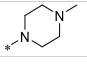
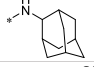
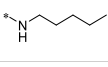
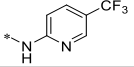
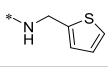
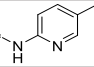
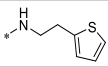
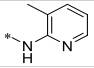
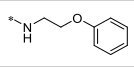
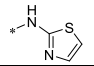
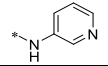
The final compounds were obtained *via* an amidation reaction between the commercially available benzotriazole-5-carboxylic acid (**197**) and an appropriate aromatic or aliphatic amine, using 1,1'-carbonyldiimidazole (CDI) as the coupling agent. The protocol used for synthesizing the final compounds was slightly different according to the nature of the amine used. DMF was used as a solvent for the aromatic amines and the aliphatic amine linked to an aromatic group through an ethyl chain, and the reaction was heated at 70 °C overnight. Instead, THF was used as a solvent for most of the other aliphatic amines, and the reaction was conducted at room temperature for 2-4 h. All the amine used were commercially available, except **200** and **202**. The synthesis of intermediate **202** was accomplished by converting 4-Chloro-7-nitrobenzofurazan (NBD-Cl; **201**) to the corresponding amine using ammonium hydroxide solution in MeOH. Amine **200** was synthesized *via* Suzuki–Miyaura cross-coupling reaction, starting from 5-bromopyridin-2-amine and phenylboronic acid, using Pd(PPh<sub>3</sub>)<sub>4</sub> as the palladium catalyst (**Scheme 9**).

**Scheme 9.**<sup>a,b</sup>



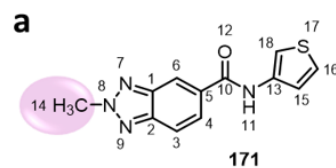
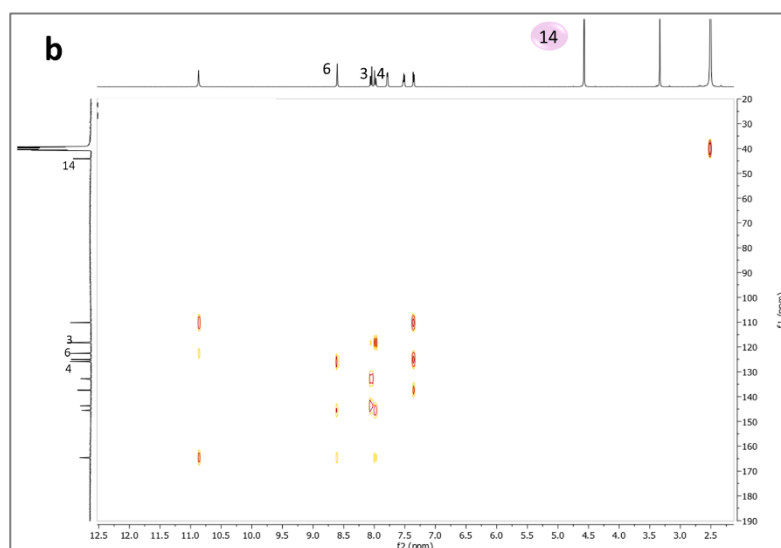
**Scheme 9.** <sup>a</sup> Reagents and conditions: a) CDI, DMF dry, 70 °C, on; b) CDI, THF dry, rt, 2-4 h; c) 1) NaH, DMF dry, r.t, 30 min; 2) MeI, rt, 20 min-on, 20%; d) NaNO<sub>3</sub>, Pd(PPh<sub>3</sub>)<sub>4</sub>; ACN/H<sub>2</sub>O (3:1); reflux, on, 50%; e) NH<sub>4</sub>OH, MeOH, r.t, on, 61%. <sup>b</sup> For complete structures, see **Table 12**.

**Table 12.** Complete structures of compounds **161-169**; **172-184**; **189**; **190**; **193** and **196**.

			
Cpd	R	Cpd	R
<b>161</b>		<b>176</b>	
<b>162</b>		<b>177</b>	
<b>163</b>		<b>178</b>	
<b>164</b>		<b>179</b>	
<b>165</b>		<b>180</b>	
<b>166</b>		<b>181</b>	
<b>167</b>		<b>182</b>	
<b>168</b>		<b>183</b>	
<b>169</b>		<b>184</b>	
<b>172</b>		<b>189</b>	
<b>173</b>		<b>190</b>	
<b>174</b>		<b>193</b>	
<b>175</b>		<b>196</b>	

The *N*-methylated benzotriazole compounds **170** and **171** were synthesized through an alkylation reaction with iodomethane in anhydrous DMF in the presence of sodium hydride (step c, **Scheme 9**). The reaction led to the formation of a mixture of isomers of benzotriazole: the 1- substituted and 2- substituted products.<sup>117,118</sup> For compound

**170** was necessary to use only 1 equivalent of iodomethane and quench the reaction after 20 min after the addition of the alkyl halide. Otherwise, the N-methylation of the amide was observed. The isomers were separated by flash column chromatography and characterized by NMR analysis. For the biological purpose of the synthesis of these compounds, only one methylated isomer was used in the biological assays and fully characterized. Regio chemistry of methyl group was confirmed by HMBC correlation study and selective 1D NOESY experiment. For the 2-substituted isomer, the methyl group should not show any correlation in the HMBC spectra with the  $^{13}\text{C}$  spectra (**Figure 28**). Even in the selective 1D NOESY experiment, the distance between the protons and the structural rigidity of the benzotriazole core render it difficult to see a correlation between the methyl group and the proton at 8.61 or 8.05 ppm (6 and 3 in **Figure 28a**). As reported in **Figure 28b** for compound **171**, the methyl group at 4.57 ppm did not show any correlation with the  $^{13}\text{C}$  spectra in the HMBC. Moreover, no correlation was observed in the selective 1D NOESY when the methyl group was irradiated. In addition, the selective 1D NOESY experiment was also performed on a different isomer of compound **171**. As reported in **Figure 29**, in this case, the irradiated methyl at 4.37 ppm showed a correlation with the doublet at 8.01 ppm (3), as is expected for 1-substituted derivative. **Figure 30** reports the HMBC and the selective NOESY spectra of compound **170**.



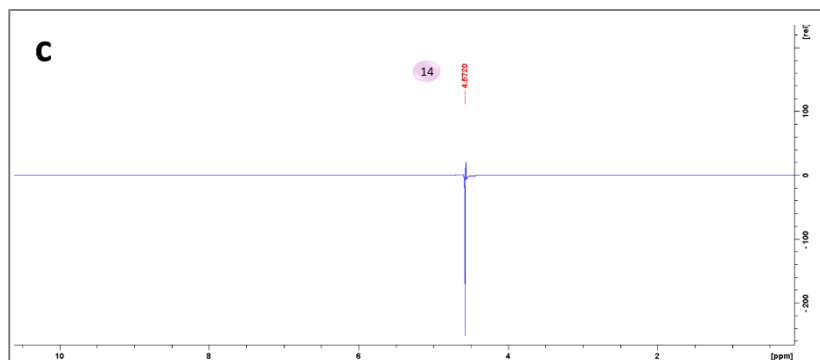


**Figure 28.** NMR spectra of **171**. a) **171** structure; b) HMBC spectra; c) selective 1D NOESY.

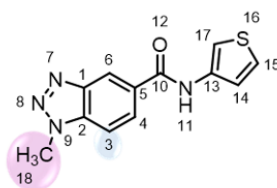
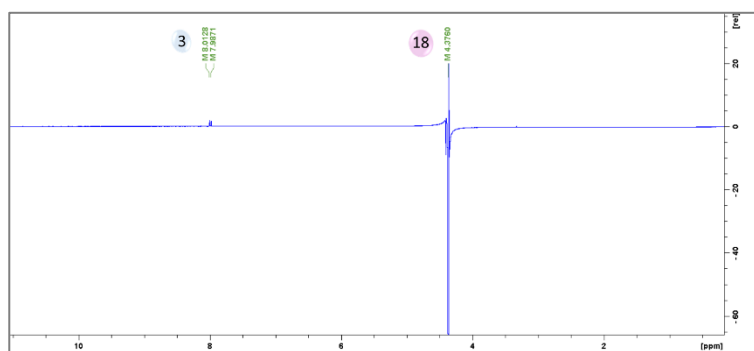


**Figure 29.** **171** isomer selective 1D NOESY.



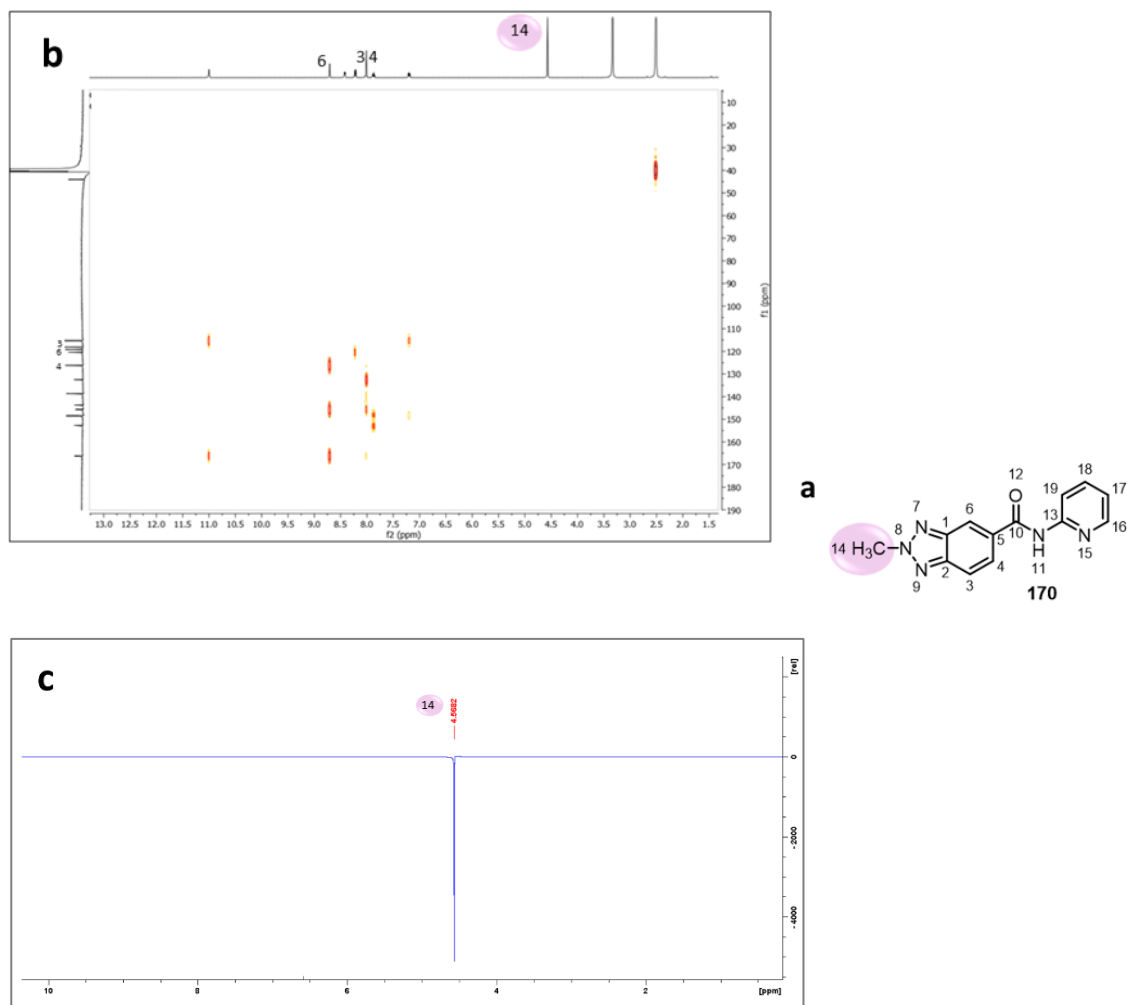
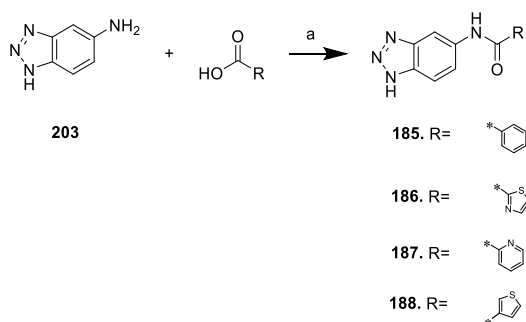


**Figure 30.** NMR spectra of **170**. a) **170** structure; b) HMBC spectra; c) selective 1D NOESY.

The reverse amides (**185**, **186**, **187**, **188**) were obtained using the commercially available 1H-1,2,3-benzotriazol-5-amine (**203**), which was reacted with the appropriate carboxylic acids through a coupling reaction, following the procedure as described above (**Scheme 10**).

### Scheme 10.<sup>a</sup>



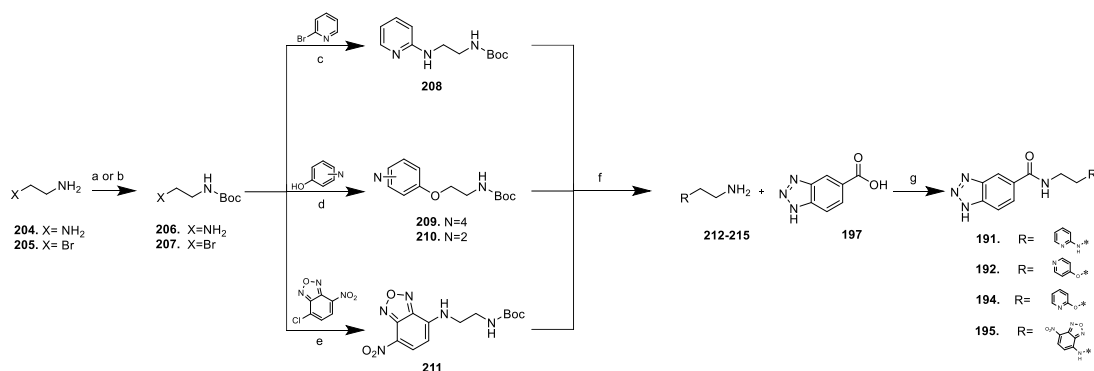
**Scheme 10.** <sup>a</sup> Reagents and conditions: a) CDI, DMF dry, 70 °C, on.

The synthesis of the compounds characterized by the presence of the ethyl chain between the benzotriazole core and the aromatic substituents (**191**, **192**, **193**, and **194**) required a protocol consisting of 4 steps (**Scheme 11**). However, the synthetic procedure followed for the second step, which allowed the introduction of the chain to the pyridine or the furazan fragments, was different for each intermediate, according to the nature of the reacted group.

The protocol starts with the protection of the primary amine of 2-bromoethylamine hydrobromide **205** or ethylenediamine **204** with  $\text{Boc}_2\text{O}$ , using TEA as the base and DCM or 1,4-dioxane as solvent. In the second step, compound **208** was synthesized *via* an Ullmann-type coupling reaction that required an  $\alpha$ -amino acid to afford the desired compound.<sup>119</sup> Intermediate **206** was reacted with 2-bromopyridine in anhydrous DMSO, using CuI as the catalyst and L-proline as a ligand. Instead, the intermediates **209**, **210**, and **211** were synthesized through a substitution reaction. For the latter, anhydrous conditions were used, with TEA and DMF in DCM. The intermediates **209** and **210**, characterized by an ether bond between the pyridine and the aminoethyl chain, required different conditions, and using  $\text{K}_2\text{CO}_3$  as a base and DMF as the solvent led to the formation of the desired intermediates. Then, the deprotection of a BOC-protected amine, simple carbamate hydrolysis in acidic conditions, was carried out to afford the primary amine, which was subsequently reacted with the benzotriazole

carboxylic acid through a coupling reaction to allow the isolation of the final compounds in the last step of this protocol.

### Scheme 11.<sup>a</sup>



**Scheme 11.** <sup>a</sup> *Reagents and conditions:* a) Boc<sub>2</sub>O, TEA, DCM, rt, on, 100%; b) Boc<sub>2</sub>O, 1,4-dioxane, rt, on, 100%; c) L-proline, CuI, K<sub>2</sub>CO<sub>3</sub>, DMSO dry, 90 °C, on, 43%; d) K<sub>2</sub>CO<sub>3</sub>, DMF, rt, on, 51-49%; e) TEA, DCM dry, DMF dry, rt, on, 77%; f) TFA, DCM dry, rt, 3h-on, 100%; g) CDI, DMF dry, 70°C, on, 30-49%.

### 4.3.7. Conclusion

In the search of novel molecules able to inhibit the cysteine biosynthetic pathway, the evidence reported in the literature regarding the ability of the triazole ring to target OASS prompted us to initiate a preliminary investigation on the potential activity of the benzotriazole core (BTA) on the cysteine pathway. Starting from an in-house benzotriazole derivative, **11**, a focused set of derivatives was synthesized. This small set of compounds allowed us to obtain preliminary hints regarding the biological properties of this new scaffold as a cysteine inhibitor.

The *in vitro* assays proved the capability of the benzotriazole derivatives to interact with both the OASS-A and OASS- B isoforms and produce a false product, leading to lower concentrations of OAS, which is the direct precursor of cysteine. This evidence was also corroborated by the lack of activity shown to the benzotriazole derivatives **170** and **171**, which present the BTA-NH methylated, preventing the possibility to interact

with OASS and producing the false product. Thus, the BTA-NH proved to be crucial for inhibitory activity. Furthermore, several compounds were also able to inhibit bacterial growth when tested against *E.coli*, allowing us to speculate about the propensity of these molecules to penetrate the Gram-negative membrane. This is a worthwhile result in the search for novel antibiotic adjuvants, often affected by poor permeability through the cell envelope.

The evidence of the ability of the BTA core to inhibit the cysteine biosynthesis in the *in vitro* assays, coupled with the growth inhibitory effects and the excellent cytotoxicity profile of the BTA derivatives, prompted us to pursue a second round of optimization to establish a SAR of this scaffold that could lead to improved inhibitory activity. Different modifications were introduced to the scaffold, such as the manipulation of the amide bridge and the investigation of the hindrance around the moiety linked to the BTA core, and a wide range of the derivatives was synthesized.

Indeed, 23 new BTA derivatives as potential cysteine inhibitors were synthesized, and the biological assays are ongoing in the laboratory of Prof. Cabassi, at the University of Parma.

## 4.3.8. Experimental Section

### 4.3.8.2. Chemistry

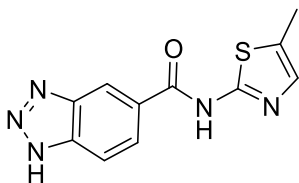
#### General procedure for the coupling reaction

**Method A:** Carbonyldiimidazole (CDI) (1.00 eq) was added to a solution of the proper carboxylic acid (1.00 eq) in dry DMF (2 mL/mmol) under N<sub>2</sub> atmosphere. The reaction mixture was left stirring for 1h at room temperature, and then the proper aromatic amine (1.00 eq) was added. The reaction mixture was heated to 70 °C. The reaction was quenched with water and extracted with EtOAc (3 x 30 mlà). The organic layers were dried over anhydrous Na<sub>2</sub>SO<sub>4</sub>, filtered, and concentrated under reduced pressure. The crude was purified by flash column chromatography eluting with DCM/MeOH or with trituration. Purification conditions, yields, and analytical data are reported below.

**Method B:** Carbonyldiimidazole (CDI) (1.00 eq) was added to a solution of the proper carboxylic acid (1.00 eq) in dry THF (2 mL/mmol) under N<sub>2</sub> atmosphere. The reaction mixture was left stirring for 1h at room temperature, and then the proper aliphatic amine (1.00 eq) was added. The reaction mixture was left stirring at room temperature

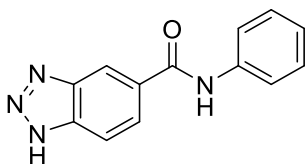
for 2 – 4 hours. After this time, the solvent was concentrated under vacuum, and the corresponding crude material was purified by flash column chromatography eluting with DCM/MeOH or with trituration. Purification conditions, yields, and analytical data are reported below.

#### **N-(5-methylthiazol-2-yl)-1H-benzo[d][1,2,3]triazole-5-carboxamide (161)**



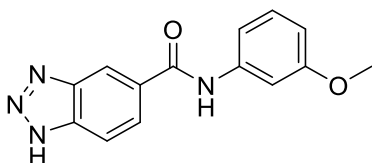
The title compound was obtained as a slightly yellow powder following the **general method A** (yield: 61%). Purification by flash chromatography eluting with DCM/MeOH from 99:1 to 90:10. <sup>1</sup>H NMR (400 MHz, DMSO-*d*<sub>6</sub>): δ 16.07 (bs, 1H); 12.63 (s, 1H); 8.77 (s, 1H); 8.14 (d, *J* = 8 Hz, 1H); 8.01 (d, *J* = 8.8 Hz, 1H); 7.25 (s, 1H); 2.40 (s, 3H). HPLC-ESI-MS analysis: calculated for C<sub>11</sub>H<sub>9</sub>N<sub>5</sub>OS: 259.05; found: 260.26 [M+H<sup>+</sup>].

#### **N-phenyl-1H-benzo[d][1,2,3]triazole-5-carboxamide (162)**



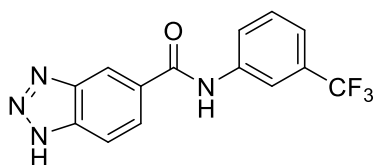
The title compound was obtained as a brown powder following the **general method A** (yield: 48%). Purification by trituration with DCM and diethyl ether. <sup>1</sup>H NMR (400 MHz, DMSO-*d*<sub>6</sub>): δ 16.04 (bs, 1H); 10.44 (s, 1H); 8.04 – 7.99 (m, 2H); 7.83 (d, *J* = 7.9 Hz, 2H); 7.40 (t, *J* = 7.7 Hz, 2H); 7.14 (t, *J* = 7.3 Hz, 1H); 2.40 (s, 3H). HPLC-ESI-MS analysis: calculated for C<sub>13</sub>H<sub>10</sub>N<sub>4</sub>O: 238.09; found: 239.32 [M+H<sup>+</sup>].

#### **N-(3-methoxyphenyl)-1H-benzo[d][1,2,3]triazole-5-carboxamide (163)**



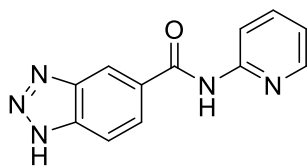
The title compound was obtained as a slightly brown powder following the **general method A** (yield: 40%). Purification by flash chromatography eluting with DCM/MeOH from 99:1 to 97:3.  $^1\text{H NMR}$  (400 MHz,  $\text{DMSO-}d_6$ ):  $\delta$  16.03 (bs, 1H); 10.4 (s, 1H); 8.62 (s, 1H); 8.04 – 7.99 (m, 2H); 7.52 – 7.51 (m, 1H); 7.42 (bd,  $J = 8.8$  Hz, 1H); 7.30 (t,  $J = 8.2$  Hz, 1H); 6.71 (dd,  $J_1=8.12$ ,  $J_2=2.2$  Hz, 1H); 3.77 (s, 3H). HPLC-ESI-MS analysis: calculated for  $\text{C}_{14}\text{H}_{12}\text{N}_4\text{O}_2$ : 268.10; found: 269.22  $[\text{M}+\text{H}^+]$ .

#### **N-(3-(trifluoromethyl)phenyl)-1H-benzo[d][1,2,3]triazole-5-carboxamide (164)**



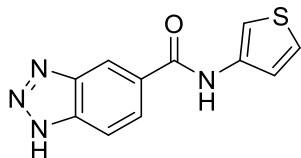
The title compound was obtained as a white powder following the **general method A** (yield: 29%). Purification by flash chromatography eluting with DCM/MeOH from 99:1 to 98:2.  $^1\text{H NMR}$  (400 MHz,  $\text{DMSO-}d_6$ ):  $\delta$  16.08 (bs, 1H); 10.73 (s, 1H); 8.68 (s, 1H); 8.30 (s, 1H); 8.11 – 8.02 (m, 3H); 7.65 (t,  $J = 7.7$  Hz, 1H); 7.49 - 7.48 (d,  $J = 7.7$  Hz, 1H). HPLC-ESI-MS analysis: calculated for  $\text{C}_{14}\text{H}_9\text{F}_3\text{N}_4\text{O}$ : 306.0; found: 307.20  $[\text{M}+\text{H}^+]$ .

#### **N-(pyridin-2-yl)-1H-benzo[d][1,2,3]triazole-5-carboxamide (165)**



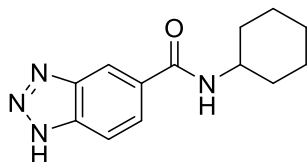
The title compound was obtained as a slightly yellow powder following the **general method A** (yield: 24%). Purification by flash chromatography eluting with DCM/MeOH from 99:1 to 98:2.  $^1\text{H NMR}$  (400 MHz,  $\text{DMSO-}d_6$ ):  $\delta$  16.04 (bs, 1H); 11.01 (s, 1H); 8.71 (s, 1H); 8.42 (d,  $J = 8.3$  Hz, 1H); 8.22 (d,  $J = 8.3$  Hz, 1H); 8.08 (d,  $J = 8.5$  Hz, 1H); 7.98 (d,  $J = 8.5$  Hz, 1H); 7.89 - 7.85 (m, 1H); 7.21 – 7.18 (m, 1H). HPLC-ESI-MS analysis: calculated for  $\text{C}_{12}\text{H}_9\text{N}_5\text{O}$ : 239.08; found: 240.15  $[\text{M}+\text{H}^+]$ .

### N-(thiophen-3-yl)-1H-benzo[d][1,2,3]triazole-5-carboxamide (166)



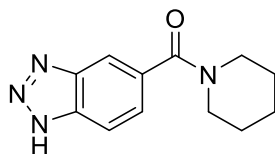
The title compound was obtained as a pink powder following the **general method A** (yield: 45%). Purification by flash chromatography eluting with DCM/MeOH 95:5.  $^1\text{H}$  NMR (400 MHz,  $\text{DMSO-}d_6$ ):  $\delta$  16.03 (bs, 1H); 10.87 (s, 1H); 8.62 (s, 1H); 8.06 – 8.02 (m, 1H); 7.78 (s, 1H); 7.52 (m, 1H); 7.37 – 7.35 (m, 1H). HPLC-ESI-MS analysis: calculated for  $\text{C}_{12}\text{H}_{14}\text{N}_4\text{O}$ : 244.27; found: 245.27  $[\text{M}+\text{H}^+]$ .

### N-cyclohexyl-1H-benzo[d][1,2,3]triazole-5-carboxamide (167)



The title compound was obtained as a brown powder following the **general method A** (yield: 33%). Purification by flash chromatography eluting with DCM/MeOH from 99:1 to 98:2.  $^1\text{H}$  NMR (400 MHz,  $\text{DMSO-}d_6$ ):  $\delta$  15.87 (bs, 1H); 8.46 (s, 1H); 8.40 (d,  $J = 7.8$  Hz, 1H); 8.22 (d,  $J = 8.3$  Hz, 1H); 7.95 – 7.91 (m, 2H); 3.83 – 7.78 (m, 1H); 1.87 – 1.85 (m, 2H); 1.77 – 1.75 (m, 2H); 1.64 – 1.61 (m, 1H); 1.40 – 1.27 (m, 4H); 1.19 – 1.11 (m, 1H). HPLC-ESI-MS analysis: calculated for  $\text{C}_{13}\text{H}_{16}\text{N}_4\text{O}$ : 244.13; found: 245.34  $[\text{M}+\text{H}^+]$ .

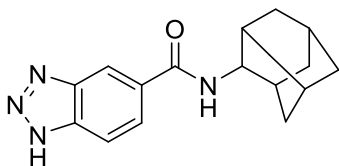
### (1H-benzo[d][1,2,3]triazol-5-yl)(piperidin-1-yl)methanone (168)



The title compound was obtained as a brown powder following the **general method B** (yield: 50%). Purification by flash chromatography eluting with DCM/MeOH from 99:1 to 98:2.  $^1\text{H}$  NMR (400 MHz,  $\text{DMSO-}d_6$ ):  $\delta$  16 (bs, 1H); 7.97 – 7.93 (m, 2H); 7.44 (d,  $J = 8.4$

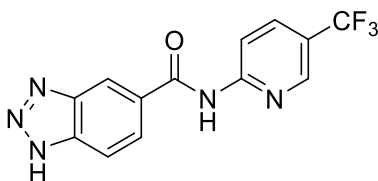
H<sub>z</sub>, 1H); 3.61 – 3.33 (m, 3H); 1.62 – 1.51 (m, 7H). HPLC-ESI-MS analysis: calculated for C<sub>12</sub>H<sub>14</sub>N<sub>4</sub>O: 230.12; found: 231.31 [M+H<sup>+</sup>].

**N-(adamantan-2-yl)-1H-benzo[d][1,2,3]triazole-5-carboxamide (169)**



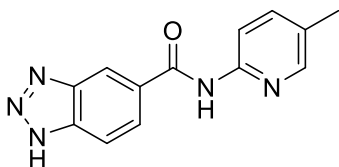
The title compound was obtained as a slightly yellow powder following the **general method B** (yield: 50%). Purification by flash chromatography eluting with DCM/MeOH from 99:1 to 93:7. <sup>1</sup>H NMR (400 MHz, DMSO-*d*<sub>6</sub>): δ 15.89 (bs, 1H); 8.42 (s, 1H); 7.88 – 7.82 (m, 3H); 2.11 – 2.08 (m, 9H); 1.68 (m, 6H). HPLC-ESI-MS analysis: calculated for C<sub>17</sub>H<sub>20</sub>N<sub>4</sub>O: 296.16; found: 297.40 [M+H<sup>+</sup>].

**N-(5-(trifluoromethyl)pyridin-2-yl)-1H-benzo[d][1,2,3]triazole-5-carboxamide (172)**



The title compound was obtained as a white powder following the **general method A** (yield: 15%). Purification by flash chromatography eluting with CHCl<sub>3</sub>/MeOH 99:1. <sup>1</sup>H NMR (400 MHz, DMSO-*d*<sub>6</sub>): δ 16.02 (bs, 1H); 11.47 (s, 1H); 8.82 (s, 1H); 8.74 (s, 1H); 8.44 (d, *J* = 8.8 Hz, 1H); 8.28 (dd, *J*<sub>1</sub> = 8.9, *J*<sub>2</sub> = 2.1 Hz, 1H); 8.08 (d, *J* = 8.7 Hz, 1H); 7.99 (d, *J* = 8.7 Hz, 1H). HPLC-ESI-MS analysis: calculated for C<sub>13</sub>H<sub>8</sub>F<sub>3</sub>N<sub>5</sub>O: 307.07; found: 308.29 [M+H<sup>+</sup>].

**N-(5-methylpyridin-2-yl)-1H-benzo[d][1,2,3]triazole-5-carboxamide (173)**

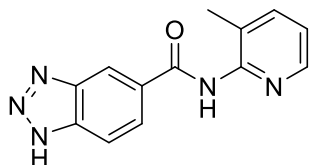


The title compound was obtained as a slightly yellow powder following the **general method A** (yield: 42%). Purification by flash chromatography eluting with CHCl<sub>3</sub>/MeOH 99:1. <sup>1</sup>H NMR (400 MHz, DMSO-*d*<sub>6</sub>): δ 16.02 (bs, 1H); 10.92 (s, 1H); 8.69 (s, 1H); 8.44 (d,



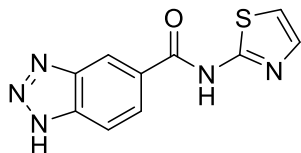
$J = 1.4$  Hz, 1H); 8.13 (d,  $J = 8.4$  Hz, 1H); 8.09 (dd,  $J_1 = 8.7$ ,  $J_2 = 1.1$  Hz, 1H); 7.98 (d,  $J = 8.7$  Hz, 1H); 7.69 (dd,  $J_1 = 8.4$ ,  $J_2 = 1.9$  Hz, 1H); 2.33 (s, 3H). HPLC-ESI-MS analysis: calculated for  $C_{13}H_{11}N_5O$ : 253.10; found: 254.30  $[M+H]^+$ .

#### N-(3-methylpyridin-2-yl)-1H-benzo[d][1,2,3]triazole-5-carboxamide (174)



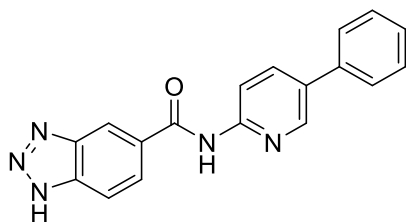
The title compound was obtained as a white powder following the **general method A** (yield: 43%). Purification by trituration with DCM and EtOAc.  $^1H$  NMR (400 MHz,  $DMSO-d_6$ ):  $\delta$  16.03 (bs, 1H); 10.71 (s, 1H); 8.67 (s, 1H); 8.34 (dd,  $J_1 = 4.8$ ,  $J_2 = 1.9$  Hz, 1H); 8.08 (d,  $J = 8.7$  Hz, 1H); 8.00 (d,  $J = 8.7$  Hz, 1H); 7.77 (dd,  $J_1 = 7.8$ ,  $J_2 = 1.9$  Hz, 1H); 7.30 – 7.27 (m, 1H); 2.24 (s, 3H). HPLC-ESI-MS analysis: calculated for  $C_{13}H_{11}N_5O$ : 253.10; found: 254.30  $[M+H]^+$ .

#### N-(thiazol-2-yl)-1H-benzo[d][1,2,3]triazole-5-carboxamide (175)



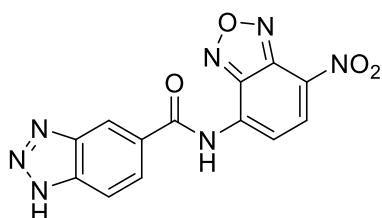
The title compound was obtained as a slightly brown powder following the **general method A** (yield: 46%). Purification by trituration with EtOAc.  $^1H$  NMR (400 MHz,  $DMSO-d_6$ ):  $\delta$  16.06 (bs, 1H); 12.83 (s, 1H); 8.80 (s, 1H); 8.15 (d,  $J = 8.5$  Hz, 1H); 8.03 (d,  $J = 8.5$  Hz, 1H); 7.60 (d,  $J = 3.5$  Hz, 1H); 7.32 (d,  $J = 3.6$  Hz, 1H). HPLC-ESI-MS analysis: calculated for  $C_{10}H_7N_5OS$ : 245.26; found: 246.23  $[M+H]^+$ .

#### N-(5-phenylpyridin-2-yl)-1H-benzo[d][1,2,3]triazole-5-carboxamide (176)



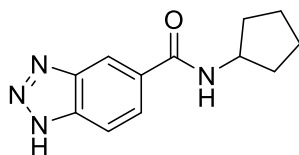
The title compound was obtained as a yellow powder following the **general method A** (yield: 25%). Purification by flash chromatography eluting with DCM/MeOH 98:2.  $^1\text{H}$  NMR (600 MHz,  $\text{DMSO-}d_6$ ):  $\delta$  11.08 (s, 1H); 8.71 (dd,  $J_1 = 2.5$ ,  $J_2 = 0.8$  Hz, 1H); 8.69 (s, 1H); 8.28 (dd,  $J_1 = 8.6$ ,  $J_2 = 0.7$  Hz, 1H); 8.15 (dd,  $J_1 = 8.6$ ,  $J_2 = 2.5$  Hz, 1H); 8.05 (dd,  $J_1 = 8.7$ ,  $J_2 = 1.4$  Hz, 1H); 7.95 (d,  $J = 8.7$  Hz, 1H); 7.73 – 7.71 (m, 2H); 7.48 – 7.46 (m, 2H); 7.39 – 7.36 (m, 1H). HPLC-ESI-MS analysis: calculated for  $\text{C}_{18}\text{H}_{13}\text{N}_5\text{O}$ : 315.11; found: 316.34  $[\text{M}+\text{H}^+]$ .

**N-(7-nitrobenzo[c][1,2,5]oxadiazol-4-yl)-1H-benzo[d][1,2,3]triazole-5-carboxamide (177)**



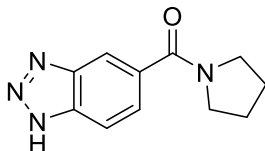
The title compound was obtained as a yellow powder following the **general method A** (yield: 43%). Purification by flash chromatography eluting with DCM/MeOH from 99:1 to 98:2 and then trituration with diethyl ether.  $^1\text{H}$  NMR (400 MHz,  $\text{DMSO-}d_6$ ):  $\delta$  11.83 (s, 1H); 8.82 (d,  $J = 8.4$  Hz, 1H); 8.76 (s, 1H); 8.35 (d,  $J = 8.1$  Hz, 1H); 8.07 (m, 2H); 7.30 – 7.27 (m, 1H); 2.24 (s, 3H). HPLC-ESI-MS analysis: calculated for  $\text{C}_{13}\text{H}_7\text{N}_7\text{O}_4$ : 325.07; found: 326.35  $[\text{M}+\text{H}^+]$ .

**N-cyclopentyl-1H-benzo[d][1,2,3]triazole-5-carboxamide (178)**



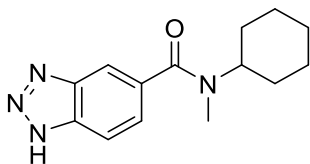
The title compound was obtained as a white powder following the **general method B** (yield: 61%). Purification by flash chromatography eluting with DCM/MeOH from 99:1 to 98:2.  $^1\text{H}$  NMR (400 MHz,  $\text{DMSO-}d_6$ ):  $\delta$  15.93 (bs, 1H); 8.47 – 8.46 (m, 2H); 7.96 – 7.93 (m, 2H); 4.32 – 4.23 (m, 1H); 1.96 – 1.88 (m, 2H); 1.77 – 1.68 (m, 2H); 1.62 – 1.54 (m, 4H). HPLC-ESI-MS analysis: calculated for  $\text{C}_{12}\text{H}_{14}\text{N}_4\text{O}$ : 230.12; found: 231.31  $[\text{M}+\text{H}^+]$ .

**(1H-benzo[d][1,2,3]triazol-5-yl)(pyrrolidin-1-yl)methanone (179)**



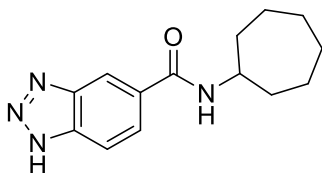
The title compound was obtained as a orange powder following the **general method B** (yield: 19%). Purification by flash chromatography eluting with DCM/MeOH 98:2.  $^1\text{H}$  NMR (400 MHz,  $\text{CDCl}_3$ ):  $\delta$  8.02 (s, 1H); 7.79 (d,  $J = 8.4$  Hz, 1H); 7.57 (dd,  $J_1 = 8.6$ ,  $J_2 = 1.1$  Hz, 1H); 3.75 (t,  $J = 6.9$  Hz, 2H); 3.51 – 3.46 (m, 2H); 2.06 – 1.99 (m, 2H); 1.95 – 1.89 (m, 2H). HPLC-ESI-MS analysis: calculated for  $\text{C}_{11}\text{H}_{12}\text{N}_4\text{O}$ : 216.10; found: 217.28[M+H $^+$ ].

**N-cyclohexyl-N-methyl-1H-benzo[d][1,2,3]triazole-5-carboxamide (180)**



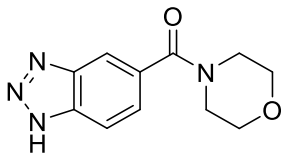
The title compound was obtained as a white powder following the **general method B** (yield: 20%). Purification by flash chromatography eluting with DCM/MeOH from 99:1 to 98:2.  $^1\text{H}$  NMR (400 MHz,  $\text{DMSO}-d_6$ ):  $\delta$  7.96 (d,  $J = 8.5$  Hz, 1H); 7.91 (s, 1H); 7.42 (d,  $J = 8.3$  Hz, 1H); 4.33 (s, 1H); 2.89 – 2.78 (m, 3H); 1.81 - 1.35 (m, 8H); 1.18 – 1.05 (m, 2H). HPLC-ESI-MS analysis: calculated for  $\text{C}_{14}\text{H}_{18}\text{N}_4\text{O}$ : 258.15; found: 259.36 [M+H $^+$ ].

**N-cycloheptyl-1H-benzo[d][1,2,3]triazole-5-carboxamide (181)**



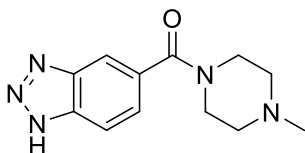
The title compound was obtained as a white powder following the **general method B** (yield: 49%). Purification by flash chromatography eluting with DCM/MeOH 98:2.  $^1\text{H}$  NMR (400 MHz,  $\text{DMSO}-d_6$ ):  $\delta$  15.91 (bs, 1H); 8.45 – 8.43 (m, 2H); 7.93 – 7.90 (m, 2H); 4.05 – 3.97 (m, 1H); 1.91 – 1.87 (m, 2H); 1.70 – 1.42 (m, 10H). HPLC-ESI-MS analysis: calculated for  $\text{C}_{14}\text{H}_{18}\text{N}_4\text{O}$ : 258.15; found: 259.23 [M+H $^+$ ].

**(1H-benzo[d][1,2,3]triazol-5-yl)(morpholino)methanone (182)**



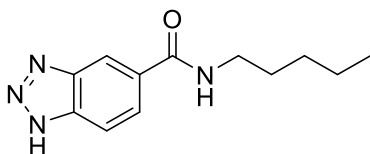
The title compound was obtained as a white powder following the **general method B** (yield: 50%). Purification by flash chromatography eluting with DCM/MeOH from 99:1 to 93:7.  $^1\text{H}$  NMR (400 MHz,  $\text{DMSO-}d_6$ ):  $\delta$  15.87 (bs, 1H); 7.99 (s, 1H); 7.98 (d,  $J = 8.5$  Hz, 1H); 7.98 (dd,  $J_1 = 8.5$ ,  $J_2 = 1.4$  Hz, 1H); 3.62 – 3.40 (m, 8H). HPLC-ESI-MS analysis: calculated for  $\text{C}_{11}\text{H}_{12}\text{N}_4\text{O}_2$ : 232.09; found: 233.17 [ $\text{M}+\text{H}^+$ ].

**(1H-benzo[d][1,2,3]triazol-5-yl)(4-methylpiperazin-1-yl)methanone (183)**



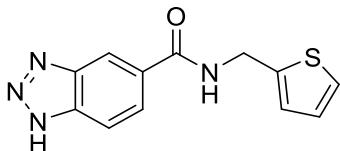
The title compound was obtained as a slightly yellow powder following the **general method B** (yield: 59%). Purification by flash chromatography eluting with DCM/MeOH from 95:5 to 93:7.  $^1\text{H}$  NMR (400 MHz,  $\text{DMSO-}d_6$ ):  $\delta$  15.84 (bs, 1H); 7.97 – 7.95 (m, 2H); 7.45 (dd,  $J_1=8.5$ ,  $J_2=1.4$  Hz, 1H); 3.62 – 3.36 (m, 4H); 2.33 (m, 4H); 2.21 (s, 3H). HPLC-ESI-MS analysis: calculated for  $\text{C}_{12}\text{H}_{15}\text{N}_5\text{O}$ : 245.13; found: 246.17 [ $\text{M}+\text{H}^+$ ].

**N-pentyl-1H-benzo[d][1,2,3]triazole-5-carboxamide (184)**



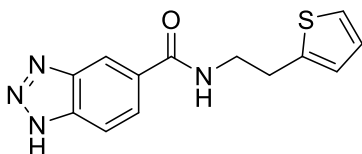
The title compound was obtained as a white powder following the **general method B** (yield: 54%). Purification by flash chromatography eluting with  $\text{CH}_3\text{Cl}/\text{MeOH}$  98:2.  $^1\text{H}$  NMR (400 MHz,  $\text{DMSO-}d_6$ ):  $\delta$  15.92 (bs, 1H); 8.63 (t,  $J = 5.2$  Hz, 1H); 8.44 (s, 1H); 8.43 (s, 1H); 7.94 (m, 2H); 3.32 – 3.27 (m, 3H); 1.60 – 1.52 (m, 2H); 1.34 – 1.30 (m, 4H); 0.90 – 0.87 (m, 3H). HPLC-ESI-MS analysis: calculated for  $\text{C}_{12}\text{H}_{16}\text{N}_4\text{O}$ : 232.13; found: 233.23 [ $\text{M}+\text{H}^+$ ].

### N-(thiophen-2-ylmethyl)-1H-benzo[d][1,2,3]triazole-5-carboxamide (189)



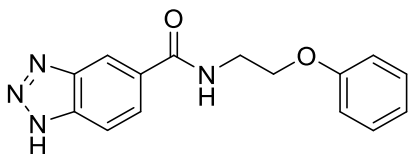
The title compound was obtained as a white powder following the **general method A** (yield: 31%). Purification by flash chromatography eluting with  $\text{CHCl}_3/\text{MeOH}$  from 99:1 to 98:2.  $^1\text{H}$  NMR (400 MHz,  $\text{DMSO}-d_6$ ):  $\delta$  15.96 (bs, 1H); 9.34 (t,  $J = 5.8$  Hz, 1H); 8.48 (s, 1H); 7.99 – 7.94 (m, 2H); 7.41 (dd,  $J_1 = 5.0$ ,  $J_2 = 1.2$  Hz, 1H); 7.06 – 7.05 (m, 1H); 6.99 – 6.97 (m, 1H); 4.69 (d,  $J = 5.8$  Hz, 2H). HPLC-ESI-MS analysis: calculated for  $\text{C}_{12}\text{H}_{10}\text{N}_5\text{OS}$ : 258.30; found: 259.30  $[\text{M}+\text{H}^+]$ .

### N-(2-(thiophen-2-yl)ethyl)-1H-benzo[d][1,2,3]triazole-5-carboxamide (190)



The title compound was obtained as a white powder following the **general method A** (yield: 33%). Purification by flash chromatography eluting with  $\text{DCM}/\text{MeOH}$  98:2.  $^1\text{H}$  NMR (400 MHz,  $\text{DMSO}-d_6$ ):  $\delta$  15.95 (bs, 1H); 8.83 (d,  $J = 5.4$  Hz, 1H); 8.44 (s, 1H); 7.94 (m, 1H); 7.35 (dd,  $J_1 = 5.0$ ,  $J_2 = 1.2$  Hz, 1H); 6.98 – 6.94 (m, 2H); 3.56 (q,  $J = 5.7$  Hz, 2H); 3.11 (t,  $J = 7.12$  Hz, 1H). HPLC-ESI-MS analysis: calculated for  $\text{C}_{13}\text{H}_{12}\text{N}_4\text{OS}$ : 272.07; found: 273.32  $[\text{M}+\text{H}^+]$ .

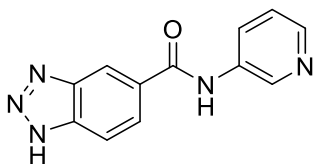
### N-(2-phenoxyethyl)-1H-benzo[d][1,2,3]triazole-5-carboxamide (193)



The title compound was obtained as a slightly pink powder following the **general method A** (yield: 80%). Purification by by flash chromatography eluting with  $\text{CH}_3\text{Cl}/\text{MeOH}$  98:2.  $^1\text{H}$  NMR (400 MHz,  $\text{DMSO}-d_6$ ):  $\delta$  15.89 (bs, 1H); 8.90 (d,  $J = 5.3$  Hz, 1H); 8.48 (s, 1H); 7.98 – 7.93 (m, 2H); 7.32 – 7.28 (m, 2H); 7.03 – 6.88 (m, 3H); 4.16 (t,  $J$

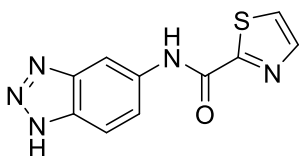
= 8.6 Hz, 2H); 3.69 (d,  $J$  = 5.8 Hz, 1H). HPLC-ESI-MS analysis: calculated for  $C_{15}H_{14}N_4O_2$ : 282.11; found: 283.38  $[M+H^+]$ .

#### N-(pyridin-3-yl)-1H-benzo[d][1,2,3]triazole-5-carboxamide (196)



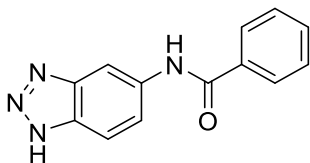
The title compound was obtained as a brown powder following the **general method A** (yield: 30%). Purification by trituration with diethyl ether.  $^1H$  NMR (400 MHz,  $DMSO-d_6$ ):  $\delta$  15.99 (bs, 1H); 10.62 (s, 1H); 8.98 (d,  $J$  = 2.3 Hz, 1H); 8.67 (s, 1H); 8.34 (dd,  $J_1$  = 4.7,  $J_2$  = 1.4 Hz, 1H); 8.25 – 8.22 (m, 1H); 8.07 – 8.01 (m, 2H); 7.43 (dd,  $J_1$  = 8.3,  $J_2$  = 4.7 Hz, 1H); 3.76 – 3.62 (m, 4H). HPLC-ESI-MS analysis: calculated for  $C_{12}H_9N_5O$ : 239.08; found: 240.28  $[M+H^+]$ .

#### N-(1H-benzo[d][1,2,3]triazol-5-yl)thiazole-2-carboxamide (185)



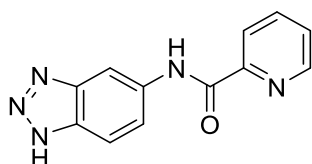
The title compound was obtained as a slightly yellow-orange powder following the **general method A** (yield: 55%). Purification by flash chromatography eluting with DCM/MeOH from 99:1 to 98:2.  $^1H$  NMR (400 MHz,  $DMSO-d_6$ ):  $\delta$  15.64 (bs, 1H); 11.08 (s, 1H); 8.50 (d,  $J$  = 1.0 Hz, 1H); 8.19 (d,  $J$  = 3.1 Hz, 1H); 8.15 (d,  $J$  = 3.1 Hz, 1H); 7.94 (d,  $J$  = 8.9 Hz, 1H); 7.87 (dd,  $J_1$  = 9,  $J_2$  = 1.7 Hz, 1H). HPLC-ESI-MS analysis: calculated for  $C_{10}H_7N_4OS$ : 245.04; found: 246.23  $[M+H^+]$ .

#### N-(1H-benzo[d][1,2,3]triazol-5-yl)benzamide (186)



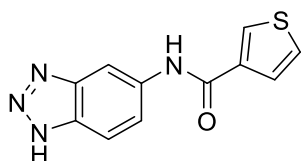
The title compound was obtained as a yellow powder following the **general method A** (yield: 8%). Purification by flash chromatography eluting with DCM/MeOH from 99:1 to 98:2.  $^1\text{H}$  NMR (400 MHz,  $\text{DMSO-}d_6$ ):  $\delta$  15.56 (bs, 1H); 10.52 (s, 1H); 8.49 (s, 1H); 8.01 – 7.98 (m, 2H); 7.95 (d,  $J = 8.8$  Hz, 1H); 7.70 (dd,  $J_1=8.9$ ,  $J_2=1.5$  Hz, 1H); 7.65 – 7.61 (m, 3H); 7.58 – 7.55 (m, 2H). HPLC-ESI-MS analysis: calculated for  $\text{C}_{13}\text{H}_{10}\text{N}_4\text{O}$ : 238.09; found: 239.25  $[\text{M}+\text{H}^+]$ .

#### **N-(1H-benzo[d][1,2,3]triazol-5-yl)picolinamide (197)**



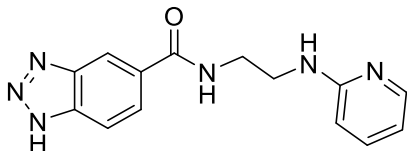
The title compound was obtained as a white powder following the **general method A** (yield: 50%). Purification by flash chromatography eluting with DCM/MeOH 99:1.  $^1\text{H}$  NMR (400 MHz,  $\text{DMSO-}d_6$ ):  $\delta$  15.61 (bs, 1H); 10.94 (s, 1H); 8.79 (d,  $J = 4.1$  Hz, 1H); 8.60 (s, 1H); 8.21 (d,  $J = 7.8$  Hz, 1H); 8.11 (td,  $J_1 = 7.7$ ,  $J_2 = 1.6$  Hz, 1H); 7.95 (d,  $J = 8.9$  Hz, 1H); 7.88 (d,  $J_1 = 8.9$ ,  $J_2 = 1.4$  Hz, 1H); 7.73 – 7.70 (m, 1H). HPLC-ESI-MS analysis: calculated for  $\text{C}_{12}\text{H}_9\text{N}_5\text{O}$ : 239.08; found: 240.28  $[\text{M}+\text{H}^+]$ .

#### **N-(1H-benzo[d][1,2,3]triazol-5-yl)thiophene-2-carboxamide (188)**



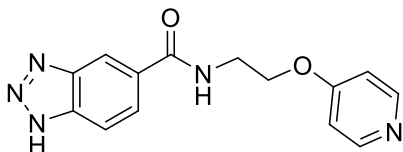
The title compound was obtained as a brown powder following the **general method A** (yield: 18%). Purification by flash chromatography eluting with DCM/MeOH from 98:2 to 97:3.  $^1\text{H}$  NMR (400 MHz,  $\text{DMSO-}d_6$ ):  $\delta$  15.57 (bs, 1H); 10.30 (s, 1H); 8.45 (s, 1H); 8.41 – 8.40 (m, 1H); 7.94 (d,  $J = 8.7$  Hz, 1H); 7.71 – 7.61 (m, 3H). HPLC-ESI-MS analysis: calculated for  $\text{C}_{11}\text{H}_8\text{N}_4\text{OS}$ : 244.04; found: 245.14  $[\text{M}+\text{H}^+]$ .

### N-(2-(pyridin-2-ylamino)ethyl)-1H-benzo[d][1,2,3]triazole-5-carboxamide (191)



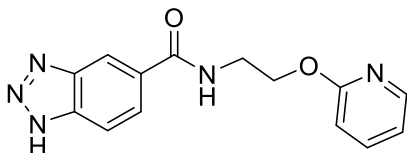
The title compound was obtained as a white powder following the **general method A** (yield: 32%). Purification by flash chromatography eluting with DCM/MeOH from 96:4 to 93:7, and then trituration with DCM and diethyl ether.  $^1\text{H}$  NMR (400 MHz, DMSO- $d_6$ ):  $\delta$  15.98 (bs, 1H); 8.82 (s, 1H); 8.47 (s, 1H); 7.99 - 7.95 (m, 3H); 7.45 - 7.40 (m, 1H); 6.86 (s, 1H); 6.56 - 6.51 (m, 2H); 3.48 (m, 4H). HPLC-ESI-MS analysis: calculated for  $\text{C}_{14}\text{H}_{14}\text{N}_6\text{O}$ : 282.13; found: 283.38  $[\text{M}+\text{H}^+]$ .

### N-(2-(pyridin-4-yloxy)ethyl)-1H-benzo[d][1,2,3]triazole-5-carboxamide (192)



The title compound was obtained as a slightly brown powder following the **general method A** (yield: 49%). Purification by trituration with DCM.  $^1\text{H}$  NMR (400 MHz, DMSO- $d_6$ ):  $\delta$  15.74 (bs, 1H); 8.79 (t,  $J = 5.2$  Hz, 1H); 8.38 (s, 1H); 7.95 (d,  $J = 7.6$  Hz, 1H); 7.87 (d,  $J = 8.5$  Hz, 1H); 7.63 (d,  $J = 7.2$  Hz, 2H); 6.05 (d,  $J = 7.2$  Hz, 2H); 4.05 (t,  $J = 5.3$  Hz, 2H); 3.63 (q,  $J = 5.3$  Hz, 2H). HPLC-ESI-MS analysis: calculated for  $\text{C}_{14}\text{H}_{13}\text{N}_5\text{O}_2$ : 283.11; found: 284.34  $[\text{M}+\text{H}^+]$ .

### N-(2-(pyridin-2-yloxy)ethyl)-1H-benzo[d][1,2,3]triazole-5-carboxamide (194)

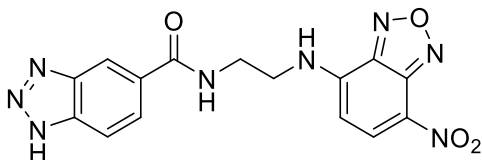


The title compound was obtained as a white powder following the **general method A** (yield: 41%). Purification by flash chromatography eluting with DCM/MeOH from 96:4 to 95:5, and then trituration with DCM and diethyl ether.  $^1\text{H}$  NMR (400 MHz, DMSO- $d_6$ ):  $\delta$  8.78 (t,  $J = 5.7$  Hz, 1H); 8.38 (s, 1H); 7.94 (d,  $J = 8.7$  Hz, 1H); 7.88 (d,  $J = 8.6$  Hz, 1H); 7.56 (dd,  $J_1 = 6.7$ ,  $J_2 = 2.1$  Hz, 1H); 7.41 (m, 1H); 6.40 (d,  $J = 9.1$  Hz, 2H); 6.16 (m, 1H);



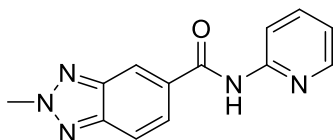
4.10 (t,  $J = 5.8$  Hz, 2H); 3.16 (q,  $J = 5.8$  Hz, 2H). HPLC-ESI-MS analysis: calculated for  $C_{14}H_{13}N_5O_2$ : 283.11; found: 284.27  $[M+H^+]$ .

**N-(2-((7-nitrobenzo[c][1,2,5]oxadiazol-4-yl)amino)ethyl)-1H-benzo[d][1,2,3]triazole-5-carboxamide (195)**



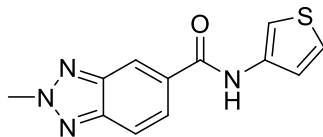
The title compound was obtained as a orange powder following the **general method A** (yield: 30%). Purification by trituration with DCM and EtOAc.  $^1H$  NMR (400 MHz,  $DMSO-d_6$ ):  $\delta$  8.90 (s, 1H); 8.52 (d,  $J = 8.7$  Hz, 1H); 8.43 (s, 1H); 7.96 – 7.90 (m, 2H); 6.53 (d,  $J = 9.0$  Hz, 1H); 3.76 – 3.62 (m, 4H). HPLC-ESI-MS analysis: calculated for  $C_{15}H_{12}N_8O$ : 368.10; found: 369.23  $[M+H^+]$ .

**2-methyl-N-(pyridin-2-yl)-2H-benzo[d][1,2,3]triazole-5-carboxamide (170)**



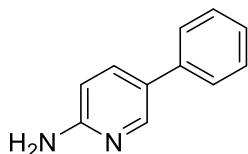
**165** (200 mg, 0.84 mmol) was dissolved in anhydrous DMF (2.40 mL/mmol), then sodium hydride 60 % dispersion in mineral oil (33 mg, 0.84 mmol) was added under  $N_2$  atmosphere at  $0^\circ C$ . The reaction mixture was left stirring for 30 min. After this time, iodomethane (52  $\mu L$ , 0.84 mmol) was added, and the reaction mixture was stirred at room temperature for 20 minutes. The reaction was quenched with water and extracted with EtOAc (3 X 30 mL). The organic layers were dried over anhydrous  $Na_2SO_4$ , filtered, and concentrated under reduced pressure. The crude was purified by flash column chromatography eluting with DCM/MeOH 99:1 to afford the title compound as a slightly yellow powder (yield: 20%).  $^1H$  NMR (400 MHz,  $DMSO-d_6$ ):  $\delta$  11.00 (s, 1H); 8.70 (s, 1H); 8.42 (dd,  $J_1 = 4.8$ ,  $J_2 = 1.0$  Hz, 1H); 8.22 (d,  $J = 8.4$  Hz, 1H); 8.04 – 7.99 (m, 2H); 7.89 – 7.85 (m, 1H); 7.21 – 7.18 (m, 1H); 4.57 (s, 3H).  $^{13}C$  NMR (100.6 MHz,  $DMSO-d_6$ ):  $\delta$  166.2; 152.7; 148.4; 145.7; 143.7; 138.6; 132.5; 126.17; 120.38; 119.19; 118.09; 115.27; 44.06. HPLC-ESI-MS analysis: calculated for  $C_{13}H_{11}N_5O$ : 253.10; found: 254.30  $[M+H^+]$ .

## 2-methyl-N-(thiophen-3-yl)-2H-benzo[d][1,2,3]triazole-5-carboxamide (171)



**166** (82 mg, 0.34 mmol) was dissolved in anhydrous DMF (2.40 mL/mmol), then sodium hydride 60 % dispersion in mineral oil (27 mg, 0.67 mmol) was added under N<sub>2</sub> atmosphere at 0°C. The reaction mixture was left stirring for 30 min. After this time, iodomethane (42 μL, 0.67 mmol) was added and the reaction mixture was stirred at room temperature overnight. The reaction was quenched with water and extracted with EtOAc (3 X 30 mL). The organic layers were dried over anhydrous Na<sub>2</sub>SO<sub>4</sub>, filtered, and concentrated under reduced pressure. The crude was purified by flash column chromatography eluting with Petroleum ether/EtOAc 7:3 to afford the title compound (yield: 20%). Purification by flash chromatography eluting with Petroleum ether/EtOAc 7:3. <sup>1</sup>H NMR (400 MHz, DMSO-*d*<sub>6</sub>): δ 10.87 (s, 1H); 8.60 (s, 1H); 8.06 (d, *J* = 8.9 Hz, 1H); 7.99 (dd, *J*<sub>1</sub> = 8.9, *J*<sub>2</sub> = 1.4 Hz, 1H); 7.79 (dd, *J*<sub>1</sub> = 3.1, *J*<sub>2</sub> = 1.1 Hz, 1H); 7.51 (m, 1H); 7.36 (dd, *J*<sub>1</sub> = 5.1, *J*<sub>2</sub> = 1.6 Hz, 1H); 4.57 (s, 3H). <sup>13</sup>C NMR (100.6 MHz, DMSO-*d*<sub>6</sub>): δ 164.6; 145.5; 145.8; 137.4; 137.4; 132.8; 125.95; 125.07; 122.59; 118.28; 118.22; 110.22; 44.09. HPLC-ESI-MS analysis: calculated for C<sub>12</sub>H<sub>10</sub>N<sub>4</sub>OS: 258.06; found: 259.14 [M+H<sup>+</sup>].

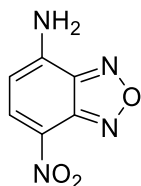
## 5-phenylpyridin-2-amine (198)



2-amino-5-bromopyridine **196** (50 mg, 0.29 mmol), phenylboronic acid **197** (49 mg, 0.41 mmol), and Na<sub>2</sub>CO<sub>3</sub> were dissolved in ACN/H<sub>2</sub>O (3:1, 7 mL/mmol), then Pd(PPh<sub>3</sub>)<sub>4</sub> (33 mg, 0.03 mmol) was added. The reaction mixture was heated at reflux overnight. After cooling to room temperature, the reaction mixture was filtered through a plug of celite. The filtrate was concentrated under reduced pressure, and the residue was extracted with EtOAc (3 X 20 mL), dried over anhydrous Na<sub>2</sub>SO<sub>4</sub>, filtered, and concentrated under reduced pressure. The crude was purified by flash column chromatography eluting with DCM/MeOH 99:1 to afford the title compound (yield:

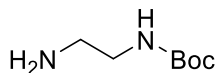
61%).  $^1\text{H}$  NMR (400 MHz,  $\text{DMSO-}d_6$ ):  $\delta$  8.25 (d,  $J = 2.0$  Hz, 1H); 7.70 (dd,  $J_1 = 8.6$ ,  $J_2 = 2.5$  Hz, 1H); 7.57 (d,  $J = 7.3$  Hz, 2H); 7.40 (d,  $J = 7.5$  Hz, 2H); 7.27 (t,  $J = 7.4$  Hz, 1H); 6.54 (d,  $J = 8.5$  Hz, 1H); 6.04 (s, 2H).

### 7-nitrobenzo[c][1,2,5]oxadiazol-4-amine (200)



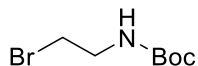
4-chloro-7-nitrobenzofurazano (**199**) (100 mg, 0.56 mmol) was dissolved in anhydrous MeOH (17 mL/mmol), then  $\text{NH}_4\text{OH}$  (2 mL) was added under  $\text{N}_2$  atmosphere. The reaction mixture was stirred at room temperature overnight. The solvent was then evaporated in vacuum, and the crude material was purified by flash column chromatography eluting with DCM/MeOH (from 99.5:0.5 to 98:2) to afford the title compound (yield: 51%).  $^1\text{H}$  NMR (400 MHz,  $\text{DMSO-}d_6$ ):  $\delta$  8.87 (s, 2H); 8.52 (d,  $J = 8.8$  Hz, 1H); 6.41 (d,  $J = 8.8$  Hz, 1H).

### Tert-butyl (2-aminoethyl)carbamate (206)



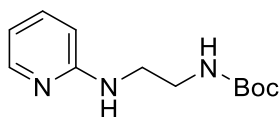
Ethylenediamine (**205**) (661 mg, 11.00 mmol) was dissolved in anhydrous 1,4-dioxane (0.350 mL/mmol), then a solution of di-tert-butylcarbonate (300 mg, 1.37 mmol) in anhydrous 1,4-dioxane (0.350 mL/mmol) was added dropwise over 1 hour under  $\text{N}_2$  atmosphere. The reaction mixture was stirred at room temperature overnight. The solvent was then evaporated in vacuum, and water was added. The insoluble material was filtered off, and the filtrate was extracted with DCM (2 X 40 mL) and Isopropanol/ $\text{CHCl}_3$  (3 X 30 mL). The collected organic layers were dried over anhydrous  $\text{Na}_2\text{SO}_4$ , filtered, and concentrated under reduced pressure. The resulting oil product was used in the next step without further purification (yield: 90%).  $^1\text{H}$  NMR (400 MHz,  $\text{CDCl}_3$ ):  $\delta$  4.98 (s, 1H); 3.21 (m, 2H); 2.84 (m, 2H); 2.14 (s, 2H); 1.46 (s, 9H).

### Tert-butyl (2-bromoethyl)carbamate (207)



2-Bromoethylamine hydrobromide (**205**) (1g, 4.9 mmol) was dissolved in DCM (6 mL/mmol), then triethylamine (0.9 mL, 6.5 mmol) was added. The reaction mixture was cooled to 0°C, and then a solution of di-tert-butylcarbonate (1 g, 5.88 mmol) in DCM was added dropwise over 15 minutes. The reaction mixture was stirred at room temperature overnight. After this time, water was added to the reaction mixture, and it was extracted with DCM (3 X 40 mL). The organic layers were dried over anhydrous Na<sub>2</sub>SO<sub>4</sub>, filtered, and concentrated under reduced pressure. The product was used in the next step without further purification (yield: 70%). <sup>1</sup>H NMR (400 MHz, CDCl<sub>3</sub>): δ 4.97 (s, 1H); 3.56 – 3.54 (m, 2H); 3.49 – 3.46 (m, 2H); 1.47 (s, 9H).

### T-butyl (2-(pyridin-2-ylamino)ethyl)carbamate (208)

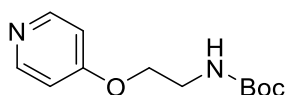


Tert-butyl (2-aminoethyl)carbamate **206** (320 mg, 1.99 mmol), L-proline (69 mg, 0.60), 2-bromopyridine (473 mg, 2.99 mmol), CuI (76 mg, 0.40 mmol) and K<sub>2</sub>CO<sub>3</sub> (550 mg, 3.98 mmol) were dissolved in anhydrous DMSO under N<sub>2</sub> atmosphere. The reaction mixture was heated at 90°C overnight. Then the reaction mixture was filtered through a plug of celite. The organic layer was washed with water (1 X 30 mL) and brine (3 X 30 mL). The collected organic layers were dried over anhydrous Na<sub>2</sub>SO<sub>4</sub>, filtered, and concentrated under reduced pressure. The crude was purified by flash column chromatography eluting with DCM/MeOH 98:2 to afford the title compound as a yellow oil (yield: 43%). <sup>1</sup>H NMR (400 MHz, CDCl<sub>3</sub>): δ 8.09 (d, *J* = 4.2 Hz, 1H); 7.44 - 7.39 (m, 1H); 6.61 – 6.57 (m, 1H); 6.43 (d, *J* = 8.4 Hz, 1H); 5.07 (s, 1H); 4.82 (s, 1H); 3.51 – 3.46 (m, 2H); 3.40 – 3.36 (m, 2H); 1.46 (s, 9H).

### Synthetic procedure to obtain compounds 209 and 210

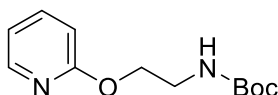
Tert-butyl (2-bromoethyl)carbamate **207** (100 mg, 0.45 mmol) was dissolved in DMF, then a solution of 4-hydroxypyridine or 2-hydroxypyridine (63 mg, 0.67 mmol) in DMF was added, followed by oven-dried  $K_2CO_3$  (93 mg, 0.67 mmol). After consumption of the starting material, a solution of NaOH 2N was added to the reaction mixture, and it was extracted with  $CH_3Cl$ /isopropanol (8:2, 3 X 20 mL). The collected organic layers were dried over anhydrous  $Na_2SO_4$ , filtered, and concentrated under reduced pressure. The crude was purified by flash column chromatography. eluting with DCM/MeOH.

#### Tert-butyl (2-(pyridin-4-yloxy)ethyl)carbamate (209)



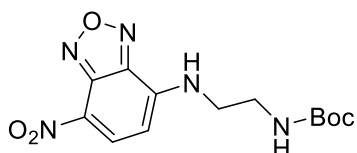
The title compound was obtained as a white powder (yield: 51%). Purification by flash chromatography eluting with DCM/MeOH from 95:5 to 80:20.  $^1H$  NMR (400 MHz,  $DMSO-d_6$ ):  $\delta$  7.53 (d,  $J = 7.5$  Hz, 2H); 6.97 (t,  $J = 5.4$  Hz, 1H); 6.05 (d,  $J = 7.5$  Hz, 2H); 3.85 (t,  $J = 5.7$  Hz, 2H); 3.23 (q,  $J = 5.8$  Hz, 2H); 1.34 (s, 9H).

#### Tert-butyl (2-(pyridin-2-yloxy)ethyl)carbamate (210)



The title compound was obtained as a white powder (yield: 49%). Purification by flash chromatography eluting with DCM/MeOH from 97:3 to 96:4.  $^1H$  NMR (400 MHz,  $CDCl_3$ ):  $\delta$  7.39 – 7.34 (m, 1H); 7.28 - 7.24 (m, 1H); 6.59 (d,  $J = 9.1$  Hz, 1H); 6.21 – 6.19 (m, 1H); 5.02 (s, 1H); 4.11 (t,  $J = 6.0$  Hz, 2H); 3.49 (q,  $J = 5.9$  Hz, 2H); 1.45 (s, 9H).

#### Tert-butyl (2-((7-nitrobenzo[c][1,2,5]oxadiazol-4-yl)amino)ethyl)carbamate (211)



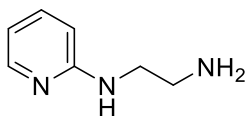
Compound **206** (60 mg, 0.38 mmol) was dissolved in anhydrous DMF (10 mL/mmol), then a solution of 4-chloro-7-nitrobenzofurazano (50 mg, 0.25 mmol) in anhydrous

DMF (3.5 mL/mmol) was added dropwise under N<sub>2</sub> atmosphere. The reaction mixture was stirred at room temperature overnight. The solvent was then evaporated in vacuum, and the crude material was purified by flash column chromatography eluting with DCM/MeOH 99:1 to afford the title compound (yield: 77%). <sup>1</sup>H NMR (400 MHz, DMSO-*d*<sub>6</sub>): δ 9.32 (s, 1H); 8.60 (d, *J* = 8.8 Hz, 1H); 6.50 (d, *J* = 8.9 Hz, 1H); 6.97 (t, *J* = 5.4 Hz, 1H); 3.86 (m, 2H); 3.20 – 3.12 (m, 2H); 1.37 (s, 9H).

### Synthetic procedure to obtain compounds **212** and **214**

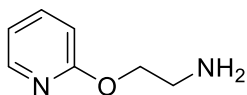
Compound **212** or **214** (1 eq) was dissolved in anhydrous DCM, and then TFA (7 eq) was added. The reaction mixture was stirred at room temperature overnight. The solvent was then evaporated in vacuum, and then 2 N aq. NaOH was added to the crude material, and it was extracted with CHCl<sub>3</sub>/isopropanol (8:2, 40 mL x 3). The organic layers were dried over anhydrous Na<sub>2</sub>SO<sub>4</sub>, filtered, and concentrated under reduced pressure. The product was used in the next step without further purification

#### N<sup>1</sup>-(pyridin-2-yl)ethane-1,2-diamine (**212**)



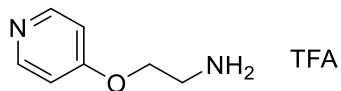
Yield: quantitative. <sup>1</sup>H NMR (400 MHz, DMSO-*d*<sub>6</sub>): δ 7.94 – 7.93 (m, 1H); 7.36 – 7.32 (m, 1H); 6.45 – 6.42 (m, 3H); 3.20 (q, *J* = 6.3 Hz, 2H); 2.67 (q, *J* = 6.4 Hz, 2H).

#### 2-(pyridin-2-yloxy)ethan-1-amine (**214**)



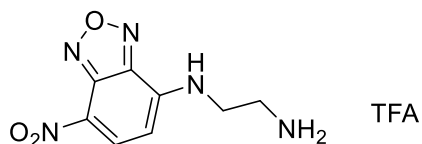
Yield: 97 %. <sup>1</sup>H NMR (400 MHz, DMSO-*d*<sub>6</sub>): δ 7.93 – 7.85 (m, 1H); 7.30 – 7.24 (m, 1H); 6.55 – 6.45 (m, 1H); 4.49 (d, *J* = 5.9 Hz, 2H); 3.34 (q, *J* = 6.0 Hz, 2H).

## 2-(pyridin-4-yloxy)ethan-1-amine (213)



Tert-butyl (2-(pyridin-4-yloxy)ethyl)carbamate **209** (45 mg, 0.19 mmol) was dissolved in anhydrous DCM, and then TFA (72  $\mu$ L, 0.94 mmol) was added. The reaction mixture was stirred at room temperature overnight. The solvent was then evaporated in vacuum, and the crude material was used in the next step without further purification (yield: quantitative).  $^1\text{H}$  NMR (400 MHz, DMSO- $d_6$ ):  $\delta$  8.44 (d,  $J$  = 7.4 Hz, 2H); 8.09 (s, 3H); 7.18 (d,  $J$  = 7.3 Hz, 2H); 4.49 (d,  $J$  = 5.9 Hz, 2H); 3.40 – 3.34 (m, 2H).

## N1-(7-nitrobenzo[c][1,2,5]oxadiazol-4-yl)ethane-1,2-diamine (215)



Compound **211** (62 mg, 0.19 mmol) was dissolved in anhydrous DCM (7 mL/mmol), then TFA (92  $\mu$ L, 1.23 mmol) was added dropwise. The reaction mixture was stirred at room temperature for 3 hours. The solvent was then evaporated in vacuum, and the crude material was used in the next step without further purification (yield: 100%).  $^1\text{H}$  NMR (400 MHz, DMSO- $d_6$ ):  $\delta$  9.32 (s, 1H); 8.60 (d,  $J$  = 8.9 Hz, 1H); 7.93 (s, 3H); 6.50 (d,  $J$  = 8.8 Hz, 1H); 3.76 (m, 2H); 3.20 – 3.12 (m, 2H).

### 4.3.8.2. Biology

#### Evaluation of Minimal Inhibitory Concentration (MIC) by broth microdilution assays

MIC values were evaluated following CLSI guidelines with some modifications (28), as referred in previous work.<sup>102</sup> Twofold dilutions 25.6-0.05 mg/mL of the tested compounds were performed in DMSO in separate 96-well microtiter U-plates (Greiner, Milan, Italy). In a different 96-well microtiter U-plate, for each well of the replicates, 49  $\mu$ L of broth medium were added. Therefore, in each well of the plate, one microliter of

each compound at variable dilution in DMSO was added. For each test, three independent experiments with three replicates each were performed.

Tested reference bacterial strains (*E. coli* ATCC25922; *S. Typhimurium* ATCC14028; *K. pneumoniae* ATCC13883) were brought to the logarithmic phase of growth in Müller Hinton medium (MHB) by incubation at 37 °C for 24 hours. After incubation, bacterial suspensions were centrifuged (2000 rpm, 4 °C for 20 minutes), and then the pellets were resuspended in phosphate buffer (pH 7, 0.1 M) to reach a final bacterial concentration of 10<sup>8</sup> CFU/mL, adjusted by spectrophotometry (OD ranged between 0.08-0.13 at 620 nm). The obtained suspensions were further diluted 1:100 in broth medium to reach a bacterial concentration of 10<sup>6</sup> CFU/mL. 50 µl of the bacterial suspension containing 10<sup>6</sup> CFU/mL were inoculated into each well within 30 minutes, to obtain a final concentration of 5x10<sup>5</sup> CFU/mL in a total volume of 100 µl. The final dilution range tested was 256-0.5 µg/mL. Growth and sterility controls were performed for each strain and for each tested compound. Plates were then incubated for 24 hours at 37 °C in aerobic atmosphere. After incubation, plates were read by unaided eye with a microtiter reading mirror and then the optical density (OD) of each well of the plates was measured spectrophotometrically at 620 nm. MIC values were calculated as the arithmetic mean ± standard deviation (SD) of the unaided eye reading and the inhibition of growth for each tested dilution was calculated from the OD values (mean ± SD). A quality control microorganism (*E. coli* ATCC 25922) was tested periodically to validate the accuracy of the procedure.

### **Cytotoxicity assay and CC<sub>50</sub> determination. Cell culture**

Human monocytes THP-1 cells were grown in suspension in RPMI 1640 (Euroclone, Italy) supplemented with 1% Sodium Pyruvate 100mM (Life Technologies, USA), 0.5% Gentamicin 10mg/mL (Sigma Aldrich, USA), 0.1% 2-Mercaptoethanol 50mM (Life Technologies, USA), Glucose (0,25 g/mL) and 10% Fetal Bovine Serum (FBS; Euroclone, Italy).

THP-1 cells were seeded in 24-well plates (Sarstedt, Germany) in the presence of 100ng/mL of phorbol 12-myristate 13-acetate (PMA; Sigma-Aldrich, USA) for 72 hours to allow the cells to differentiate into macrophages.



### **Cytotoxicity assay (MTT assay)**

MTT assay has been used to assess the cytotoxicity of synthesized compounds in THP-derived macrophages by evaluating the ability of mitochondrial succinate dehydrogenase to catalyze the enzymatic reduction of yellow water-soluble 3-[4,5-dimethylthiazole-2-yl]-2,5-diphenyltetrazolium bromide (MTT; Sigma Aldrich, USA) to insoluble purple formazan, index of cell viability. Differentiated macrophages were treated with synthesized compounds at increasing concentrations (25  $\mu$ M, 50  $\mu$ M, 100  $\mu$ M, and 200  $\mu$ M; all compounds were tested as a triplicate) for 72 hours. 20 mM compounds solutions in DMSO were prepared, and consequentially diluted to obtain a final concentration up to 200  $\mu$ M, corresponding to 1% v/v of DMSO. Afterwards, cells were incubated with a solution of 1mg/mL of MTT dissolved in RPMI 1640, supplemented with 5% FBS, at 37°C, 5% CO<sub>2</sub> for 2 hours in dark. The solution was then removed, and resulting formazan crystals were dissolved in 0,2 mL DMSO under shaking for 10 minutes. Finally, absorbance was measured on an aliquot of 0.15 mL at a wavelength of 570 nm using an absorbance microplate reader (Spark® Tecan, Switzerland).<sup>82</sup>

## Material and Methods

All the reagents were purchased from Sigma-Aldrich, Alfa-Aesar, and Fluorchem at reagent purity and, unless otherwise noted, were used without any further purification. Dry solvents used in the reactions were obtained by distillation of technical grade materials over appropriate dehydrating agents. Reactions were monitored by thin-layer chromatography on silica gel-coated aluminum foils (silica gel on Al foils, SUPELCO Analytical, Sigma-Aldrich) at 254 and 365 nm. MCRs were conducted using CEM CEM Discover Synthesis Unit (CEM Corp., Matthews, NC). Where indicated, intermediates and final products were purified through silica gel flash column chromatography (silica gel, 0.040-0.063 mm) or Combiflash® Rf 200, using appropriate solvent mixtures. <sup>1</sup>H NMR and <sup>13</sup>C NMR spectra were recorded on a BRUKER AVANCE spectrometer (<sup>1</sup>H at 300 or 400 MHz and <sup>13</sup>C at 75 or 101 MHz respectively) or a JEOL spectrometer (<sup>1</sup>H at 600 and <sup>13</sup>C at 125), with TMS as an internal standard. <sup>1</sup>H NMR spectra are reported in this order: δ ppm (multiplicity, number of protons). Standard abbreviations indicating the multiplicity were used as follows: s = singlet, d = doublet, dd = doublet of doublets, t = triplet, q = quadruplet, m = multiplet, and br = broad signal. Low-resolution mass spectrometry measurements were performed on quattromicro API tandem mass spectrometer (Waters, Milford, MA, USA) equipped with an external APCI or ESI ion source. ESI-mass spectra are reported in the form of (m/z).

## References

- (1) Hoffman, P. S. Antibacterial Discovery: 21st Century Challenges. *Antibiotics* **2020**, *9* (5). <https://doi.org/10.3390/antibiotics9050213>.
- (2) Kaufmann, S. H. E. Paul Ehrlich: Founder of Chemotherapy. *Nature Reviews Drug Discovery* **2008**, *7* (5), 373–373. <https://doi.org/10.1038/nrd2582>.
- (3) Aminov, R. I. A Brief History of the Antibiotic Era: Lessons Learned and Challenges for the Future. *Frontiers in Microbiology* **2010**, *1* (DEC). <https://doi.org/10.3389/fmicb.2010.00134>.
- (4) Chevrette, M. G.; Currie, C. R. Emerging Evolutionary Paradigms in Antibiotic Discovery. *Journal of Industrial Microbiology and Biotechnology* **2019**, *46* (3–4), 257–271. <https://doi.org/10.1007/s10295-018-2085-6>.
- (5) Hutchings, M. I.; Truman, A. W.; Wilkinson, B. Antibiotics: Past, Present and Future. *Current Opinion in Microbiology* **2019**, *51*, 72–80. <https://doi.org/10.1016/j.mib.2019.10.008>.
- (6) Durand, G. A.; Raoult, D.; Dubourg, G. Antibiotic Discovery: History, Methods and Perspectives. *International Journal of Antimicrobial Agents*. Elsevier B.V. April 1, 2019, pp 371–382. <https://doi.org/10.1016/j.ijantimicag.2018.11.010>.
- (7) Lewis, K. The Science of Antibiotic Discovery. *Cell* **2020**, *181* (1), 29–45. <https://doi.org/10.1016/j.cell.2020.02.056>.
- (8) O’Connell, K. M. G.; Hodgkinson, J. T.; Sore, H. F.; Welch, M.; Salmond, G. P. C.; Spring, D. R. Combating Multidrug-Resistant Bacteria: Current Strategies for the Discovery of Novel Antibacterials. *Angewandte Chemie International Edition* **2013**, *52* (41), 10706–10733. <https://doi.org/10.1002/anie.201209979>.
- (9) Nathan, C. Resisting Antimicrobial Resistance. *Nature Reviews Microbiology* **2020**, *18* (5), 259–260. <https://doi.org/10.1038/s41579-020-0348-5>.
- (10) Antimicrobial resistance <https://www.who.int/news-room/fact-sheets/detail/antimicrobial-resistance> (accessed 2021 -11 -30).

- (11) Pieren, M.; Tigges, M. Adjuvant Strategies for Potentiation of Antibiotics to Overcome Antimicrobial Resistance. *Current Opinion in Pharmacology* **2012**, *12* (5), 551–555. <https://doi.org/10.1016/j.coph.2012.07.005>.
- (12) Durand, G. A.; Raoult, D.; Dubourg, G. Antibiotic Discovery: History, Methods and Perspectives. *International Journal of Antimicrobial Agents* **2019**, *53* (4), 371–382. <https://doi.org/10.1016/j.ijantimicag.2018.11.010>.
- (13) Negash; Norris; Hodgkinson. Siderophore–Antibiotic Conjugate Design: New Drugs for Bad Bugs? *Molecules* **2019**, *24* (18), 3314. <https://doi.org/10.3390/molecules24183314>.
- (14) Falcó, V.; Burgos, J.; Almirante, B. An Overview of Lefamulin for the Treatment of Community Acquired Bacterial Pneumonia. *Expert Opinion on Pharmacotherapy* **2020**, *21* (6), 629–636. <https://doi.org/10.1080/14656566.2020.1714592>.
- (15) Tracking the Global Pipeline of Antibiotics in Development, March 2021 <https://www.pewtrusts.org/it/research-and-analysis/issue-briefs/2021/03/tracking-the-global-pipeline-of-antibiotics-in-development> (accessed 2022 -01 -29).
- (16) Ribeiro da Cunha; Fonseca; Calado. Antibiotic Discovery: Where Have We Come from, Where Do We Go? *Antibiotics* **2019**, *8* (2), 45. <https://doi.org/10.3390/antibiotics8020045>.
- (17) Ten threats to global health in 2019 <https://www.who.int/news-room/spotlight/ten-threats-to-global-health-in-2019> (accessed 2021 -11 -30).
- (18) WHO Publishes List of Bacteria for Which New Antibiotics Are Urgently Needed. <https://www.who.int/news/item/27-02-2017-who-publishes-list-of-bacteria-for-which-new-antibiotics-are-urgently-needed>
- (19) Duval, R. E.; Grare, M.; Demoré, B. Fight Against Antimicrobial Resistance: We Always Need New Antibacterials but for Right Bacteria. *Molecules* **2019**, *24* (17), 3152. <https://doi.org/10.3390/molecules24173152>.
- (20) EMA, Antimicrobial resistance <https://www.ema.europa.eu/en/human-regulatory/overview/public-health-threats/antimicrobial-resistance> (accessed 2022 -01 -29).

- (21) *ANTIMICROBIAL RESISTANCE Global Report on Surveillance*. <https://apps.who.int/iris/handle/10665/112642>
- (22) Rawson, T. M.; Ming, D.; Ahmad, R.; Moore, L. S. P.; Holmes, A. H. Antimicrobial Use, Drug-Resistant Infections and COVID-19. *Nature Reviews Microbiology* **2020**, *18* (8), 409–410. <https://doi.org/10.1038/s41579-020-0395-y>.
- (23) Pasero, D.; Cossu, A. P.; Terragni, P. Multi-Drug Resistance Bacterial Infections in Critically Ill Patients Admitted with COVID-19. *Microorganisms* **2021**, *9* (8), 1773. <https://doi.org/10.3390/microorganisms9081773>.
- (24) Fattorini, L.; Creti, R.; Palma, C.; Pantosti, A.; Palma, C.; Barbanti, F.; Camilli, R.; Ciervo, A.; Dattilo, R.; del Grosso, M.; Errico, G.; Fortini, D.; Fernandez, A. G.; Giannoni, F.; Giufré, M.; Imperi, M.; Lucarelli, C.; Mancini, F.; Monaco, M.; Mondello, F.; Pimentel de Araujo, F.; Ricci, M. L.; Scaturro, M.; Spigaglia, P.; Torosantucci, A.; Villa, L. Bacterial Coinfections in COVID-19: An Underestimated Adversary. *Annali dell'Istituto Superiore di Sanita* **2020**, *56* (3), 359–364. [https://doi.org/DOI: 10.4415/ANN\\_20\\_03\\_14](https://doi.org/DOI: 10.4415/ANN_20_03_14).
- (25) Mazzariol, A.; Benini, A.; Unali, I.; Nocini, R.; Smania, M.; Bertoncetti, A.; de Sanctis, F.; Ugel, S.; Donadello, K.; Polati, E.; Gibellini, D. Dynamics of SARS-CoV2 Infection and Multi-Drug Resistant Bacteria Superinfection in Patients With Assisted Mechanical Ventilation. *Frontiers in Cellular and Infection Microbiology* **2021**, *11*. <https://doi.org/10.3389/fcimb.2021.683409>.
- (26) Miethke, M.; Pieroni, M.; Weber, T.; Brönstrup, M.; Hammann, P.; Halby, L.; Arimondo, P. B.; Glaser, P.; Aigle, B.; Bode, H. B.; Moreira, R.; Li, Y.; Luzhetskyy, A.; Medema, M. H.; Pernodet, J. L.; Stadler, M.; Tormo, J. R.; Genilloud, O.; Truman, A. W.; Weissman, K. J.; Takano, E.; Sabatini, S.; Stegmann, E.; Brötz-Oesterhelt, H.; Wohlleben, W.; Seemann, M.; Empting, M.; Hirsch, A. K. H.; Loretz, B.; Lehr, C. M.; Titz, A.; Herrmann, J.; Jaeger, T.; Alt, S.; Hesterkamp, T.; Winterhalter, M.; Schiefer, A.; Pfarr, K.; Hoerauf, A.; Graz, H.; Graz, M.; Lindvall, M.; Ramurthy, S.; Karlén, A.; van Dongen, M.; Petkovic, H.; Keller, A.; Peyrane, F.; Donadio, S.; Fraise, L.; Piddock, L. J. V.; Gilbert, I. H.; Moser, H. E.; Müller, R. Towards the Sustainable Discovery and Development of New Antibiotics. *Nature Reviews Chemistry*. Nature Research October 1, 2021, pp 726–749. <https://doi.org/10.1038/s41570-021-00313-1>.

- (27) Wright, G. D. Antibiotic Adjuvants: Rescuing Antibiotics from Resistance. *Trends in Microbiology* **2016**, *24* (11), 862–871. <https://doi.org/10.1016/j.tim.2016.06.009>.
- (28) Brown, E. D.; Wright, G. D. Antibacterial Drug Discovery in the Resistance Era. *Nature* **2016**, *529* (7586), 336–343. <https://doi.org/10.1038/nature17042>.
- (29) Liu, Y.; Li, R.; Xiao, X.; Wang, Z. Antibiotic Adjuvants: An Alternative Approach to Overcome Multi-Drug Resistant Gram-Negative Bacteria. *Critical Reviews in Microbiology*. Taylor and Francis Ltd 2019, pp 301–314. <https://doi.org/10.1080/1040841X.2019.1599813>.
- (30) Liu, Y.; Li, R.; Xiao, X.; Wang, Z. Antibiotic Adjuvants: An Alternative Approach to Overcome Multi-Drug Resistant Gram-Negative Bacteria. *Critical Reviews in Microbiology* **2019**, *45* (3), 301–314. <https://doi.org/10.1080/1040841X.2019.1599813>.
- (31) González-Bello, C. Antibiotic Adjuvants – A Strategy to Unlock Bacterial Resistance to Antibiotics. *Bioorganic & Medicinal Chemistry Letters* **2017**, *27* (18), 4221–4228. <https://doi.org/10.1016/j.bmcl.2017.08.027>.
- (32) Hopkins, A. L. Network Pharmacology: The next Paradigm in Drug Discovery. *Nature Chemical Biology* **2008**, *4* (11), 682–690. <https://doi.org/10.1038/nchembio.118>.
- (33) Worthington, R. J.; Melander, C. Combination Approaches to Combat Multidrug-Resistant Bacteria. *Trends in Biotechnology* **2013**, *31* (3), 177–184. <https://doi.org/10.1016/j.tibtech.2012.12.006>.
- (34) Wildenhain, J.; Spitzer, M.; Dolma, S.; Jarvik, N.; White, R.; Roy, M.; Griffiths, E.; Bellows, D. S.; Wright, G. D.; Tyers, M. Prediction of Synergism from Chemical-Genetic Interactions by Machine Learning. *Cell Systems* **2015**, *1* (6), 383–395. <https://doi.org/10.1016/j.cels.2015.12.003>.
- (35) Annunziato. Strategies to Overcome Antimicrobial Resistance (AMR) Making Use of Non-Essential Target Inhibitors: A Review. *International Journal of Molecular Sciences* **2019**, *20* (23), 5844. <https://doi.org/10.3390/ijms20235844>.

- (36) Neu, H. C.; Fu, K. P. Clavulanic Acid, a Novel Inhibitor of  $\beta$ -Lactamases. *Antimicrobial Agents and Chemotherapy* **1978**, *14* (5), 650–655. <https://doi.org/10.1128/AAC.14.5.650>.
- (37) Bush, K. A Resurgence of  $\beta$ -Lactamase Inhibitor Combinations Effective against Multidrug-Resistant Gram-Negative Pathogens. *International Journal of Antimicrobial Agents* **2015**, *46* (5), 483–493. <https://doi.org/10.1016/j.ijantimicag.2015.08.011>.
- (38) Douafer, H.; Andrieu, V.; Phanstiel, O.; Brunel, J. M. Antibiotic Adjuvants: Make Antibiotics Great Again! *Journal of Medicinal Chemistry*. American Chemical Society October 10, 2019, pp 8665–8681. <https://doi.org/10.1021/acs.jmedchem.8b01781>.
- (39) Clatworthy, A. E.; Pierson, E.; Hung, D. T. Targeting Virulence: A New Paradigm for Antimicrobial Therapy. *Nature Chemical Biology* **2007**, *3* (9), 541–548. <https://doi.org/10.1038/nchembio.2007.24>.
- (40) Rasko, D. A.; Sperandio, V. Anti-Virulence Strategies to Combat Bacteria-Mediated Disease. *Nature Reviews Drug Discovery*. February 2010, pp 117–128. <https://doi.org/10.1038/nrd3013>.
- (41) Garland, M.; Loscher, S.; Bogyo, M. Chemical Strategies To Target Bacterial Virulence. *Chemical Reviews* **2017**, *117* (5), 4422–4461. <https://doi.org/10.1021/acs.chemrev.6b00676>.
- (42) Spyraakis, F.; Felici, P.; Bayden, A. S.; Salsi, E.; Miggiano, R.; Kellogg, G. E.; Cozzini, P.; Cook, P. F.; Mozzarelli, A.; Campanini, B. Fine Tuning of the Active Site Modulates Specificity in the Interaction of O-Acetylserine Sulfhydrylase Isozymes with Serine Acetyltransferase. *Biochimica et Biophysica Acta (BBA) - Proteins and Proteomics* **2013**, *1834* (1), 169–181. <https://doi.org/10.1016/j.bbapap.2012.09.009>.
- (43) Spyraakis, F.; Singh, R.; Cozzini, P.; Campanini, B.; Salsi, E.; Felici, P.; Raboni, S.; Benedetti, P.; Cruciani, G.; Kellogg, G. E.; Cook, P. F.; Mozzarelli, A. Isozyme-Specific Ligands for O-Acetylserine Sulfhydrylase, a Novel Antibiotic Target. *PLoS ONE* **2013**, *8* (10), e77558. <https://doi.org/10.1371/journal.pone.0077558>.
- (44) Wallace, M. J.; Dharuman, S.; Fernando, D. M.; Reeve, S. M.; Gee, C. T.; Yao, J.; Griffith, E. C.; Phelps, G. A.; Wright, W. C.; Elmore, J. M.; Lee, R. B.; Chen, T.; Lee,

- R. E. Discovery and Characterization of the Antimetabolite Action of Thioacetamide-Linked 1,2,3-Triazoles as Disruptors of Cysteine Biosynthesis in Gram-Negative Bacteria. *ACS Infectious Diseases* **2020**, *6* (3), 467–478. <https://doi.org/10.1021/acsinfecdis.9b00406>.
- (45) Annunziato, G.; Pieroni, M.; Benoni, R.; Campanini, B.; Pertinhez, T. A.; Pecchini, C.; Bruno, A.; Magalhães, J.; Bettati, S.; Franko, N.; Mozzarelli, A.; Costantino, G. Cyclopropane-1,2-Dicarboxylic Acids as New Tools for the Biophysical Investigation of O -Acetylserine Sulfhydrylases by Fluorimetric Methods and Saturation Transfer Difference (STD) NMR. *Journal of Enzyme Inhibition and Medicinal Chemistry* **2016**, *31* (sup4), 78–87. <https://doi.org/10.1080/14756366.2016.1218486>.
- (46) Palde, P. B.; Bhaskar, A.; Pedró Rosa, L. E.; Madoux, F.; Chase, P.; Gupta, V.; Spicer, T.; Scampavia, L.; Singh, A.; Carroll, K. S. First-in-Class Inhibitors of Sulfur Metabolism with Bactericidal Activity against Non-Replicating *M. Tuberculosis*. *ACS Chemical Biology* **2016**, *11* (1), 172–184. <https://doi.org/10.1021/acscchembio.5b00517>.
- (47) Turnbull, A. L.; Surette, M. G. Cysteine Biosynthesis, Oxidative Stress and Antibiotic Resistance in Salmonella Typhimurium. *Research in Microbiology* **2010**, *161* (8), 643–650. <https://doi.org/10.1016/j.resmic.2010.06.004>.
- (48) Devayani P. Bhave; Wilson B. Muse III; Kate S. Carroll. Drug Targets in Mycobacterial Sulfur Metabolism. *Infectious Disorders - Drug Targets* **2007**, *7* (2), 140–158. <https://doi.org/10.2174/187152607781001772>.
- (49) Turnbull, A. L.; Surette, M. G. L-Cysteine Is Required for Induced Antibiotic Resistance in Actively Swarming Salmonella Enterica Serovar Typhimurium. *Microbiology* **2008**, *154* (11), 3410–3419. <https://doi.org/10.1099/mic.0.2008/020347-0>.
- (50) Rosa, B.; Marchetti, M.; Paredi, G.; Amenitsch, H.; Franko, N.; Benoni, R.; Giabbai, B.; de Marino, M. G.; Mozzarelli, A.; Ronda, L.; Storici, P.; Campanini, B.; Bettati, S. Combination of SAXS and Protein Painting Discloses the Three-Dimensional Organization of the Bacterial Cysteine Synthase Complex, a Potential Target for Enhancers of Antibiotic Action. *International Journal of Molecular Sciences* **2019**, *20* (20), 5219. <https://doi.org/10.3390/ijms20205219>.



- (51) Campanini, B.; Benoni, R.; Bettati, S.; Beck, C. M.; Hayes, C. S.; Mozzarelli, A. Moonlighting O-Acetylserine Sulfhydrylase: New Functions for an Old Protein. *Biochimica et Biophysica Acta (BBA) - Proteins and Proteomics* **2015**, *1854* (9), 1184–1193. <https://doi.org/10.1016/j.bbapap.2015.02.013>.
- (52) Diner, E. J.; Beck, C. M.; Webb, J. S.; Low, D. A.; Hayes, C. S. Identification of a Target Cell Permissive Factor Required for Contact-Dependent Growth Inhibition (CDI). *Genes and Development* **2012**, *26* (5), 515–525. <https://doi.org/10.1101/gad.182345.111>.
- (53) Sturgill, G.; Toutain, C. M.; Komperda, J.; O'Toole, G. A.; Rather, P. N. Role of CysE in Production of an Extracellular Signaling Molecule in *Providencia Stuartii* and *Escherichia Coli*: Loss of CysE Enhances Biofilm Formation in *Escherichia Coli*. *Journal of Bacteriology* **2004**, *186* (22), 7610–7617. <https://doi.org/10.1128/JB.186.22.7610-7617.2004>.
- (54) Takagi, H.; Ohtsu, I. L-Cysteine Metabolism and Fermentation in Microorganisms. In *Advances in Biochemical Engineering/Biotechnology*; Springer Science and Business Media Deutschland GmbH, 2016; Vol. 159, pp 129–151. [https://doi.org/10.1007/10\\_2016\\_29](https://doi.org/10.1007/10_2016_29).
- (55) Benoni, R.; de Bei, O.; Paredi, G.; Hayes, C. S.; Franko, N.; Mozzarelli, A.; Bettati, S.; Campanini, B. Modulation of *Escherichia Coli* Serine Acetyltransferase Catalytic Activity in the Cysteine Synthase Complex. *FEBS Letters* **2017**, *591* (9), 1212–1224. <https://doi.org/10.1002/1873-3468.12630>.
- (56) Kung, H.-F.; Danchin, A. *Sulfur Metabolism in Escherichia Coli and Related Bacteria: Facts and Fiction*; 2000.
- (57) Kredich, N. M. Biosynthesis of Cysteine. *EcoSal Plus* **2008**, *3* (1), ecosalplus.3.6.1.11. <https://doi.org/10.1128/ecosalplus.3.6.1.11>.
- (58) Kredich, N. M.; Tomkins, G. M. The Enzymic Synthesis of L-Cysteine in *Escherichia Coli* and *Salmonella Typhimurium*. *Journal of Biological Chemistry* **1966**, *241* (21), 4955–4965. [https://doi.org/10.1016/S0021-9258\(18\)99657-2](https://doi.org/10.1016/S0021-9258(18)99657-2).
- (59) Feldman-Salit, A.; Wirtz, M.; Hell, R.; Wade, R. C. A Mechanistic Model of the Cysteine Synthase Complex. *Journal of Molecular Biology* **2009**, *386* (1), 37–59. <https://doi.org/10.1016/j.jmb.2008.08.075>.

- (60) Wirtz, M.; Berkowitz, O.; Droux, M.; Hell, R. The Cysteine Synthase Complex from Plants. *European Journal of Biochemistry* **2001**, *268* (3), 686–693. <https://doi.org/10.1046/j.1432-1327.2001.01920.x>.
- (61) Kredich, N. M. The Molecular Basis for Positive Regulation of Cys Promoters in Salmonella Typhimurium and Escherichia Coli. *Molecular Microbiology* **1992**, *6* (19), 2747–2753. <https://doi.org/10.1111/j.1365-2958.1992.tb01453.x>.
- (62) Gorman, J.; Shapiro, L. Structure of Serine Acetyltransferase from *Haemophilus Influenzae* Rd. *Acta Crystallographica Section D Biological Crystallography* **2004**, *60* (9), 1600–1605. <https://doi.org/10.1107/S0907444904015240>.
- (63) MINO, K.; YAMANOUE, T.; SAKIYAMA, T.; EISAKI, N.; MATSUYAMA, A.; NAKANISHI, K. Effects of Bienzyme Complex Formation of Cysteine Synthetase from *Escherichia Coli* on Some Properties and Kinetics. *Bioscience, Biotechnology, and Biochemistry* **2000**, *64* (8), 1628–1640. <https://doi.org/10.1271/bbb.64.1628>.
- (64) Huang, B.; Vetting, M. W.; Roderick, S. L. The Active Site of *O*- Acetylserine Sulfhydrylase Is the Anchor Point for Bienzyme Complex Formation with Serine Acetyltransferase. *Journal of Bacteriology* **2005**, *187* (9), 3201–3205. <https://doi.org/10.1128/JB.187.9.3201-3205.2005>.
- (65) Olsen, L. R.; Huang, B.; Vetting, M. W.; Roderick, S. L. Structure of Serine Acetyltransferase in Complexes with CoA and Its Cysteine Feedback Inhibitor . *Biochemistry* **2004**, *43* (20), 6013–6019. <https://doi.org/10.1021/bi0358521>.
- (66) Campanini, B.; Speroni, F.; Salsi, E.; Cook, P. F.; Roderick, S. L.; Huang, B.; Bettati, S.; Mozzarelli, A. Interaction of Serine Acetyltransferase with *O* -Acetylserine Sulfhydrylase Active Site: Evidence from Fluorescence Spectroscopy. *Protein Science* **2005**, *14* (8), 2115–2124. <https://doi.org/10.1110/ps.051492805>.
- (67) Kredich, N. M. Regulation of L-Cysteine Biosynthesis in Salmonella Typhimurium. *Journal of Biological Chemistry* **1971**, *246* (11), 3474–3484. [https://doi.org/10.1016/S0021-9258\(18\)62154-4](https://doi.org/10.1016/S0021-9258(18)62154-4).
- (68) Campanini, B.; Speroni, F.; Salsi, E.; Cook, P. F.; Roderick, S. L.; Huang, B.; Bettati, S.; Mozzarelli, A. Interaction of Serine Acetyltransferase with *O* -Acetylserine Sulfhydrylase Active Site: Evidence from Fluorescence Spectroscopy. *Protein Science* **2005**, *14* (8), 2115–2124. <https://doi.org/10.1110/ps.051492805>.

- (69) Campanini, B.; Pieroni, M.; Raboni, S.; Bettati, S.; Benoni, R.; Pecchini, C.; Costantino, G.; Mozzarelli, A. Inhibitors of the Sulfur Assimilation Pathway in Bacterial Pathogens as Enhancers of Antibiotic Therapy. *Current Medicinal Chemistry* **2014**, *22* (2), 187–213. <https://doi.org/10.2174/0929867321666141112122553>.
- (70) Tai, C.-H.; Cook, P. F. *O*-Acetylserine Sulfhydrylase; 2006; pp 185–234. <https://doi.org/10.1002/9780470123201.ch5>.
- (71) Feldman-Salit, A.; Wirtz, M.; Hell, R.; Wade, R. C. A Mechanistic Model of the Cysteine Synthase Complex. *Journal of Molecular Biology* **2009**, *386* (1), 37–59. <https://doi.org/10.1016/j.jmb.2008.08.075>.
- (72) Jez, J. M.; Dey, S. The Cysteine Regulatory Complex from Plants and Microbes: What Was Old Is New Again. *Current Opinion in Structural Biology* **2013**, *23* (2), 302–310. <https://doi.org/10.1016/j.sbi.2013.02.011>.
- (73) Pye, V. E.; Tingey, A. P.; Robson, R. L.; Moody, P. C. E. The Structure and Mechanism of Serine Acetyltransferase from Escherichia Coli. *Journal of Biological Chemistry* **2004**, *279* (39), 40729–40736. <https://doi.org/10.1074/jbc.M403751200>.
- (74) AGARWAL, S.; JAIN, R.; BHATTACHARYA, A.; AZAM, A. Inhibitors of Escherichia Coli Serine Acetyltransferase Block Proliferation of Entamoeba Histolytica Trophozoites. *International Journal for Parasitology* **2008**, *38* (2), 137–141. <https://doi.org/10.1016/j.ijpara.2007.09.009>.
- (75) Chen, C.; Yan, Q.; Tao, M.; Shi, H.; Han, X.; Jia, L.; Huang, Y.; Zhao, L.; Wang, C.; Ma, X.; Ma, Y. Characterization of Serine Acetyltransferase (CysE) from Methicillin-Resistant Staphylococcus Aureus and Inhibitory Effect of Two Natural Products on CysE. *Microbial Pathogenesis* **2019**, *131*, 218–226. <https://doi.org/10.1016/j.micpath.2019.04.002>.
- (76) Kontoyianni, M. Docking and Virtual Screening in Drug Discovery. In *Methods in Molecular Biology*; Humana Press Inc., 2017; Vol. 1647, pp 255–266. [https://doi.org/10.1007/978-1-4939-7201-2\\_18](https://doi.org/10.1007/978-1-4939-7201-2_18).
- (77) Begley, C. G.; Ashton, M.; Baell, J.; Bettess, M.; Brown, M. P.; Carter, B.; Charman, W. N.; Davis, C.; Fisher, S.; Frazer, I.; Gautam, A.; Jennings, M. P.; Kearney, P.; Keeffe, E.; Kelly, D.; Lopez, A. F.; McGuckin, M.; Parker, M. W.; Rayner, C.;

- Roberts, B.; Rush, J. S.; Sullivan, M. Drug Repurposing: Misconceptions, Challenges, and Opportunities for Academic Researchers. *Science Translational Medicine* **2021**, *13* (612). <https://doi.org/10.1126/scitranslmed.abd5524>.
- (78) Magalhães, J.; Franko, N.; Raboni, S.; Annunziato, G.; Tammela, P.; Bruno, A.; Bettati, S.; Armao, S.; Spadini, C.; Cabassi, C. S.; Mozzarelli, A.; Pieroni, M.; Campanini, B.; Costantino, G. Discovery of Substituted (2-Aminooxazol-4-Yl)Isoxazole-3-Carboxylic Acids as Inhibitors of Bacterial Serine Acetyltransferase in the Quest for Novel Potential Antibacterial Adjuvants. *Pharmaceuticals* **2021**, *14* (2), 174. <https://doi.org/10.3390/ph14020174>.
- (79) Eyer, P.; Worek, F.; Kiderlen, D.; Sinko, G.; Stuglin, A.; Simeon-Rudolf, V.; Reiner, E. Molar Absorption Coefficients for the Reduced Ellman Reagent: Reassessment. *Analytical Biochemistry* **2003**, *312* (2), 224–227. [https://doi.org/10.1016/S0003-2697\(02\)00506-7](https://doi.org/10.1016/S0003-2697(02)00506-7).
- (80) Nepali, K.; Lee, H.-Y.; Liou, J.-P. Nitro-Group-Containing Drugs. *Journal of Medicinal Chemistry* **2019**, *62* (6), 2851–2893. <https://doi.org/10.1021/acs.jmedchem.8b00147>.
- (81) Magalhães, J.; Franko, N.; Raboni, S.; Annunziato, G.; Tammela, P.; Bruno, A.; Bettati, S.; Mozzarelli, A.; Pieroni, M.; Campanini, B.; Costantino, G. Inhibition of Nonessential Bacterial Targets: Discovery of a Novel Serine O -Acetyltransferase Inhibitor. *ACS Medicinal Chemistry Letters* **2020**, *11* (5), 790–797. <https://doi.org/10.1021/acsmchemlett.9b00627>.
- (82) Bergonzi, C.; di Natale, A.; Zimetti, F.; Marchi, C.; Bianchera, A.; Bernini, F.; Silvestri, M.; Bettini, R.; Elviri, L. Study of 3D-Printed Chitosan Scaffold Features after Different Post-Printing Gelation Processes. *Scientific Reports* **2019**, *9* (1), 362. <https://doi.org/10.1038/s41598-018-36613-8>.
- (83) Tommasi, R.; Brown, D. G.; Walkup, G. K.; Manchester, J. I.; Miller, A. A. ESKAPEing the Labyrinth of Antibacterial Discovery. *Nature Reviews Drug Discovery* **2015**, *14* (8), 529–542. <https://doi.org/10.1038/nrd4572>.
- (84) Masi, M.; Réfregiers, M.; Pos, K. M.; Pagès, J.-M. Mechanisms of Envelope Permeability and Antibiotic Influx and Efflux in Gram-Negative Bacteria. *Nature Microbiology* **2017**, *2* (3), 17001. <https://doi.org/10.1038/nmicrobiol.2017.1>.

- (85) Brown, D. G.; May-Dracka, T. L.; Gagnon, M. M.; Tommasi, R. Trends and Exceptions of Physical Properties on Antibacterial Activity for Gram-Positive and Gram-Negative Pathogens. *Journal of Medicinal Chemistry* **2014**, *57* (23), 10144–10161. <https://doi.org/10.1021/jm501552x>.
- (86) Oliveira, W. X. C.; do Pim, W. D.; Pinheiro, C. B.; Journaux, Y.; Julve, M.; Pereira, C. L. M. Monitoring the Hydrogen Bond Net Configuration and the Dimensionality of Aniline and Phenylloxamate by Adding 1 *H* -Pyrazole and Isoxazole as Substituents for Molecular Self-Recognition. *CrystEngComm* **2019**, *21* (17), 2818–2833. <https://doi.org/10.1039/C9CE00215D>.
- (87) Eicher, T.; Hauptmann, S.; Speicher, A. *The Chemistry of Heterocycles*, second.; WILEY-VCH, Ed.; Wiley, 2003. <https://doi.org/10.1002/352760183X>.
- (88) Rishton, G. M. Nonleadlikeness and Leadlikeness in Biochemical Screening. *Drug Discovery Today* **2003**, *8* (2), 86–96. <https://doi.org/10.1016/S1359644602025722>.
- (89) Seidler, J.; McGovern, S. L.; Doman, T. N.; Shoichet, B. K. Identification and Prediction of Promiscuous Aggregating Inhibitors among Known Drugs. *Journal of Medicinal Chemistry* **2003**, *46* (21), 4477–4486. <https://doi.org/10.1021/jm030191r>.
- (90) Lor, L. A.; Schneck, J.; McNulty, D. E.; Diaz, E.; Brandt, M.; Thrall, S. H.; Schwartz, B. A Simple Assay for Detection of Small-Molecule Redox Activity. *Journal of Biomolecular Screening* **2007**, *12* (6), 881–890. <https://doi.org/10.1177/1087057107304113>.
- (91) McGovern, S. L.; Caselli, E.; Grigorieff, N.; Shoichet, B. K. A Common Mechanism Underlying Promiscuous Inhibitors from Virtual and High-Throughput Screening. *Journal of Medicinal Chemistry* **2002**, *45* (8), 1712–1722. <https://doi.org/10.1021/jm010533y>.
- (92) Rishton, G. M. Reactive Compounds and in Vitro False Positives in HTS. *Drug Discovery Today* **1997**, *2* (9), 382–384. [https://doi.org/10.1016/S1359-6446\(97\)01083-0](https://doi.org/10.1016/S1359-6446(97)01083-0).
- (93) Shoichet, B. K. Screening in a Spirit Haunted World. *Drug Discovery Today* **2006**, *11* (13–14), 607–615. <https://doi.org/10.1016/j.drudis.2006.05.014>.

- (94) Ganesh, A. N.; Donders, E. N.; Shoichet, B. K.; Shoichet, M. S. Colloidal Aggregation: From Screening Nuisance to Formulation Nuance. *Nano Today* **2018**, *19*, 188–200. <https://doi.org/10.1016/j.nantod.2018.02.011>.
- (95) Allen, S. J.; Dower, C. M.; Liu, A. X.; Lumb, K. J. Detection of Small-Molecule Aggregation with High-Throughput Microplate Biophysical Methods. *Current Protocols in Chemical Biology* **2020**, *12* (1). <https://doi.org/10.1002/cpch.78>.
- (96) Gao, R.; Liao, S.; Zhang, C.; Zhu, W.; Wang, L.; Huang, J.; Zhao, Z.; Li, H.; Qian, X.; Xu, Y. Optimization of Heterocyclic Substituted Benzenesulfonamides as Novel Carbonic Anhydrase IX Inhibitors and Their Structure Activity Relationship. *European Journal of Medicinal Chemistry* **2013**, *62*, 597–604. <https://doi.org/10.1016/j.ejmech.2013.01.030>.
- (97) Düfert, M. A.; Billingsley, K. L.; Buchwald, S. L. Suzuki-Miyaura Cross-Coupling of Unprotected, Nitrogen-Rich Heterocycles: Substrate Scope and Mechanistic Investigation. *Journal of the American Chemical Society* **2013**, *135* (34), 12877–12885. <https://doi.org/10.1021/ja4064469>.
- (98) Salsi, E.; Campanini, B.; Bettati, S.; Raboni, S.; Roderick, S. L.; Cook, P. F.; Mozzarelli, A. A Two-Step Process Controls the Formation of the Bienenzyme Cysteine Synthase Complex. *Journal of Biological Chemistry* **2010**, *285* (17), 12813–12822. <https://doi.org/10.1074/jbc.M109.075762>.
- (99) Salsi, E.; Bayden, A. S.; Spyrakis, F.; Amadasi, A.; Campanini, B.; Bettati, S.; Dodatko, T.; Cozzini, P.; Kellogg, G. E.; Cook, P. F.; Roderick, S. L.; Mozzarelli, A. Design of *O*-Acetylserine Sulfhydrylase Inhibitors by Mimicking Nature. *Journal of Medicinal Chemistry* **2010**, *53* (1), 345–356. <https://doi.org/10.1021/jm901325e>.
- (100) Amori, L.; Katkevica, S.; Bruno, A.; Campanini, B.; Felici, P.; Mozzarelli, A.; Costantino, G. Design and Synthesis of Trans-2-Substituted-Cyclopropane-1-Carboxylic Acids as the First Non-Natural Small Molecule Inhibitors of *O*-Acetylserine Sulfhydrylase. *MedChemComm* **2012**, *3* (9), 1111. <https://doi.org/10.1039/c2md20100c>.
- (101) Pieroni, M.; Annunziato, G.; Beato, C.; Wouters, R.; Benoni, R.; Campanini, B.; Pertinhez, T. A.; Bettati, S.; Mozzarelli, A.; Costantino, G. Rational Design, Synthesis, and Preliminary Structure–Activity Relationships of  $\alpha$ -Substituted-2-

- Phenylcyclopropane Carboxylic Acids as Inhibitors of *Salmonella Typhimurium* O-Acetylserine Sulfhydrylase. *Journal of Medicinal Chemistry* **2016**, *59* (6), 2567–2578. <https://doi.org/10.1021/acs.jmedchem.5b01775>.
- (102) Annunziato, G.; Spadini, C.; Franko, N.; Storici, P.; Demitri, N.; Pieroni, M.; Flisi, S.; Rosati, L.; Iannarelli, M.; Marchetti, M.; Magalhaes, J.; Bettati, S.; Mozzarelli, A.; Cabassi, C. S.; Campanini, B.; Costantino, G. Investigational Studies on a Hit Compound Cyclopropane–Carboxylic Acid Derivative Targeting O-Acetylserine Sulfhydrylase as a Colistin Adjuvant. *ACS Infectious Diseases* **2021**, *7* (2), 281–292. <https://doi.org/10.1021/acsinfecdis.0c00378>.
- (103) Marchetti, M.; de Angelis, F. S.; Annunziato, G.; Costantino, G.; Pieroni, M.; Ronda, L.; Mozzarelli, A.; Campanini, B.; Cannistraro, S.; Bizzarri, A. R.; Bettati, S. A Competitive O-Acetylserine Sulfhydrylase Inhibitor Modulates the Formation of Cysteine Synthase Complex. *Catalysts* **2021**, *11* (6), 700. <https://doi.org/10.3390/catal11060700>.
- (104) Magalhães, J.; Franko, N.; Annunziato, G.; Welch, M.; Dolan, S. K.; Bruno, A.; Mozzarelli, A.; Armao, S.; Jirgensons, A.; Pieroni, M.; Costantino, G.; Campanini, B. Discovery of Novel Fragments Inhibiting O-Acetylserine Sulphhydrylase by Combining Scaffold Hopping and Ligand–Based Drug Design. *Journal of Enzyme Inhibition and Medicinal Chemistry* **2018**, *33* (1), 1444–1452. <https://doi.org/10.1080/14756366.2018.1512596>.
- (105) st. Denis, J. D.; Hall, R. J.; Murray, C. W.; Heightman, T. D.; Rees, D. C. Fragment-Based Drug Discovery: Opportunities for Organic Synthesis. *RSC Medicinal Chemistry* **2021**, *12* (3), 321–329. <https://doi.org/10.1039/D0MD00375A>.
- (106) Li, Q. Application of Fragment-Based Drug Discovery to Versatile Targets. *Frontiers in Molecular Biosciences* **2020**, *7*. <https://doi.org/10.3389/fmolb.2020.00180>.
- (107) Murray, C. W.; Rees, D. C. The Rise of Fragment-Based Drug Discovery. *Nature Chemistry* **2009**, *1* (3), 187–192. <https://doi.org/10.1038/nchem.217>.
- (108) Ching, K.-C.; Tran, T. N. Q.; Amrun, S. N.; Kam, Y.-W.; Ng, L. F. P.; Chai, C. L. L. Structural Optimizations of Thieno[3,2-*b*]Pyrrole Derivatives for the Development of Metabolically Stable Inhibitors of Chikungunya Virus. *Journal of*

- Medicinal Chemistry* **2017**, *60* (7), 3165–3186.  
<https://doi.org/10.1021/acs.jmedchem.7b00180>.
- (109) Trost, B. M.; Dong, G. A Stereodivergent Strategy to Both Product Enantiomers from the Same Enantiomer of a Stereoinducing Catalyst: Agelastatin A. *Chemistry - A European Journal* **2009**, *15* (28), 6910–6919.  
<https://doi.org/10.1002/chem.200900794>.
- (110) Chattopadhyay, A.; Meier, M.; Ivaninskii, S.; Burkhard, P.; Speroni, F.; Campanini, B.; Bettati, S.; Mozzarelli, A.; Rabeh, W. M.; Li, L.; Cook, P. F. Structure, Mechanism, and Conformational Dynamics of O-Acetylserine Sulfhydrylase from *Salmonella Typhimurium*: Comparison of A and B Isozymes. *Biochemistry* **2007**, *46* (28), 8315–8330. <https://doi.org/10.1021/bi602603c>.
- (111) Kredich, N. M.; Foote, L. J.; Hulanicka, M. D. Studies on the Mechanism of Inhibition of *Salmonella Typhimurium* by 1,2,4-Triazole. *Journal of Biological Chemistry* **1975**, *250* (18), 7324–7331. [https://doi.org/10.1016/S0021-9258\(19\)40948-4](https://doi.org/10.1016/S0021-9258(19)40948-4).
- (112) Xue, H.; Li, J.; Xie, H.; Wang, Y. Review of Drug Repositioning Approaches and Resources. *International Journal of Biological Sciences* **2018**, *14* (10), 1232–1244.  
<https://doi.org/10.7150/ijbs.24612>.
- (113) Briguglio, I.; Piras, S.; Corona, P.; Gavini, E.; Nieddu, M.; Boatto, G.; Carta, A. Benzotriazole: An Overview on Its Versatile Biological Behavior. *European Journal of Medicinal Chemistry* **2015**, *97* (1), 612–648.  
<https://doi.org/10.1016/j.ejmech.2014.09.089>.
- (114) Hulanicka, M. D.; Hallquist, S. G.; Kredich, N. M.; Mojica-A, T. Regulation of O-Acetylserine Sulfhydrylase B by L-Cysteine in *Salmonella Typhimurium*. *Journal of Bacteriology* **1979**, *140* (1), 141–146. <https://doi.org/10.1128/jb.140.1.141-146.1979>.
- (115) Brown, N. *Bioisosteres in Medicinal Chemistry*; Brown, N., Ed.; Wiley-VCH Verlag GmbH & Co. KGaA: Weinheim, Germany, 2012.  
<https://doi.org/10.1002/9783527654307>.
- (116) Subbaiah, M. A. M.; Meanwell, N. A. Bioisosteres of the Phenyl Ring: Recent Strategic Applications in Lead Optimization and Drug Design. *Journal of Medicinal*



*Chemistry* **2021**, *64* (19), 14046–14128.  
<https://doi.org/10.1021/acs.jmedchem.1c01215>.

- (117) Singh, D.; Silakari, O. Sodium Hydrogen Exchanger Inhibitory Activity of Benzotriazole Derivatives. *European Journal of Medicinal Chemistry* **2017**, *126*, 183–189. <https://doi.org/10.1016/j.ejmech.2016.10.005>.
- (118) Le, Z.-G.; Chen, Z.-C.; Hu, Y.; Zheng, Q.-G. Organic Reactions in Ionic Liquids: An Efficient Method for the *N*-Alkylation of Benzotriazole. *Journal of Chemical Research* **2004**, *2004* (5), 344–346. <https://doi.org/10.3184/0308234041639656>.
- (119) Cai, Q.; Zhang, H.; Zou, B.; Xie, X.; Zhu, W.; He, G.; Wang, J.; Pan, X.; Chen, Y.; Yuan, Q.; Liu, F.; Lu, B.; Ma, D. Amino Acid-Promoted Ullmann-Type Coupling Reactions and Their Applications in Organic Synthesis. *Pure and Applied Chemistry* **2009**, *81* (2), 227–234. <https://doi.org/10.1351/PAC-CON-08-08-19>.